Reconstructing changes in sediment input from the Danube into the Black Sea

Adriana Maria Constantinescu

Submitted to:
Biological and Environmental Sciences
University of Stirling

December 2019

For the Degree of Doctor of Philosophy

Supervisors:
Prof. Andrew N. Tyler
Dr. Peter D. Hunter
Dr. Evangelos Spyrakos
Dr. Adrian Stănică – GeoEcoMar Romania

STATEMENT OF ORIGINALITY

I hereby confirm that this is an original piece of work conducted independently by the undersigned, and all work contained herein has not been submitted for any other degree. All research material has been duly acknowledged and cited.

Signature of Candidate:
Adriana Maria Constantinescu

Date: 14.10.2020

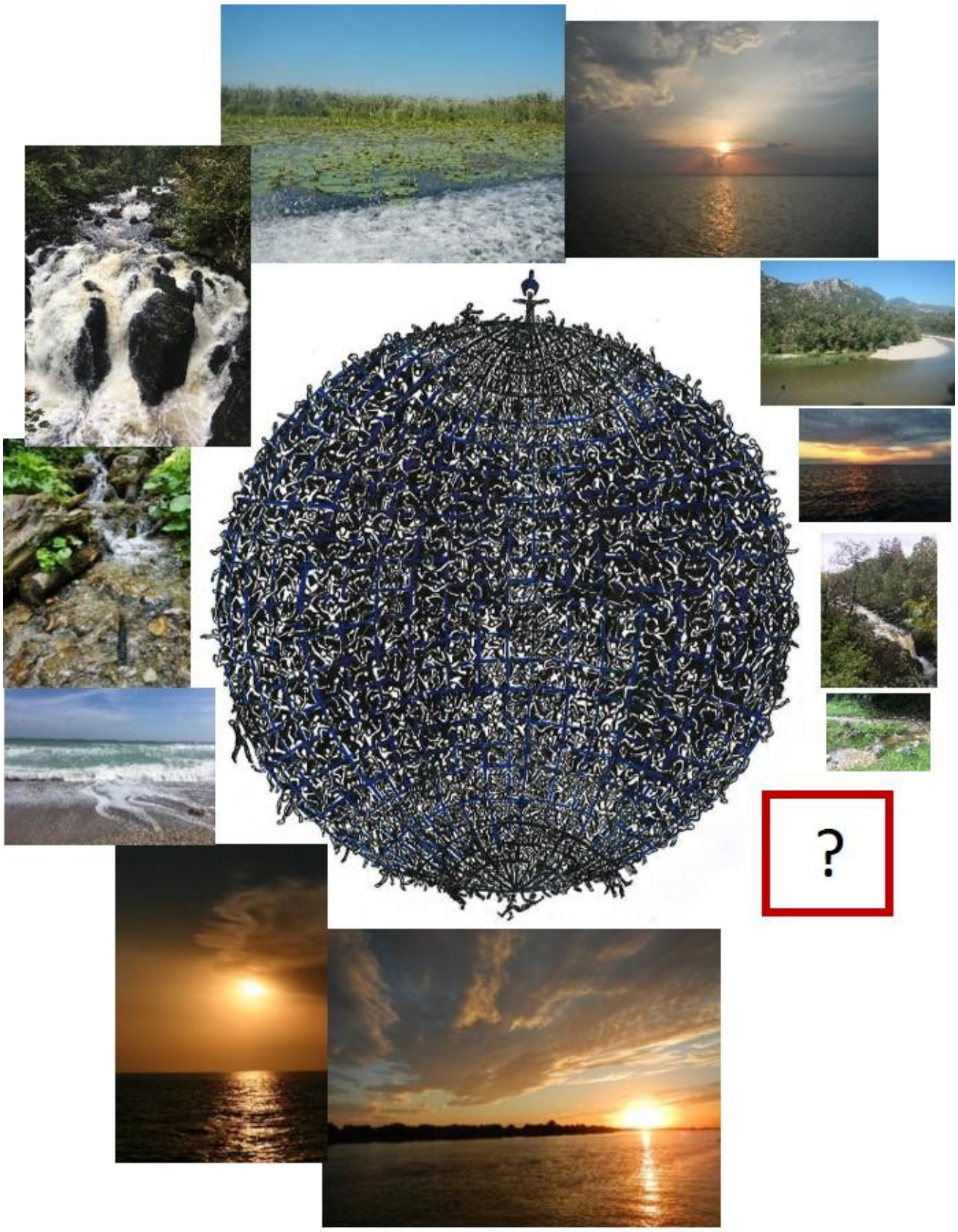

Drawing: Razvan Victor Canache
Photos: Adriana Maria Constantinescu

ACKNOWLEDGEMENTS

"In every outthrust headland, in every curving beach,
in every grain of sand there is the story of the earth."
Rachel Carson

This has been a long and rocky road. But no long, rocky road is without rewards.

I would first like to thank my four supervisor, Prof. Andrew Tyler, Dr. Peter Hunter, Dr. Evangelos Spyrakos (University of Stirling, UK) and Dr. Adrian Stanica (GeoEcoMar, Romania) for guiding and supporting me during this endeavour!

This PhD project was funded jointly by the University of Stirling (UK) and by the Romanian National Institute for Marine Geology and GeoEcology – GeoEcoMar (Romania). I would like to thank the administrative staff of these two institutions for their help in carrying out this project.

We acknowledge support from several projects: ReCoReD (Reconstructing the Changing Impact of the Danube on the Black Sea and Coastal Region), funded by EuroFleets 2; FP7 RISES-AM and H2020 DANUBIUS-PP, both funded by the European Commission; PN0302 and PN0102 – Romanian Core Program for Research, funded by the Romanian Government.

I would like to thank all my colleagues from GeoEcoMar for their continuous and great support all during my PhD, for help with field work, data and for useful discussions, and especially to: Dumitry Grosu, Irinel Caraban, Sorin Balan, Dan Secrieru, Dan Vasiliu, Mihaela Muresan, Adrian Teaca, Irina Catianis, Albert Scrieciu, Maria Ionescu, Iulian Pojar, Laura Dutu, Gabriel Iordache, Tatiana Begun. I also acknowledge the help of Andrea Losappio, Francesco Cristallo and Gianpaolo Ancona (former Master students at the University of Bari, Italy) in field sampling and giving me the chance to practice my teaching skills.

We are very grateful to the captains and crews of R/V Istros and R/V Mare Nigrum, GeoEcoMar – Romania, for their support in all the field campaigns in the Danube Delta (2015, 2016) and the Black Sea (2016).

I would like to greatly acknowledge the help and support of the technical staff of the Department of Biological and Environmental Sciences of the University of Stirling all during my PhD. I thank Stuart Bradley and Pete Smith for their great help with the dating of sediment samples, Matthew Blake, for the HPLC and spectrophotometry analysis, Jan Washbourne, for the HPLC and grain size analysis, George MacLeod for SEM analysis, Scott Jackson for IT support, James Weir for the opening of the sediment cores, Lorna English, Ronald Balfour, Sylvia Hodgson and Pauline Monteith for technical support.

Data for Chapter 2 was provided by: Danube – Romanian Institute for Marine Geology and Geo-Ecology, GeoEcoMar; Nestos – Georgios Sylaios, Democritus University of Thrace, Greece; Po – Debora Bellafiore, CNR, ISMAR-Istituto di Scienze Marine, Venice, Italy; Ebro - Confederación Hidrográfica del Ebro, with help from Prof. Vicente Gracia, LIM/UPC, Spain; Elbe – Jana Friedrich and Jens Kappenberg, Helmholz-Zentrum Geesthacht and Thomas Hoffmann, German Federal Institute of Hydrology (BfG), Germany; Thames – Mike Bowes, CEH, UK; Tay – Scottish Environment Protection Agency, UK.

Chapter 3 of this thesis was revised and improved by Acad. Nicolae Panin, GeoEcoMar and member of the Romanian Academy.

In-situ TSM data for the Black Sea in Chapter 5 was provided by the Joint Research Centre, courtesy of Giuseppe Zibordi.

I am grateful to all members of the DANUBIUS-RI onsortium of for the useful discussions and encouragements and for making by experience in the H2020 DANUBIUS-PP project so positive and inspiring.

I thank Claire, Caitlin, Adam, Shenglei and Matthew, in the 'Remote Sensing Group' for teaching and supporting me all during my PhD.

I want to thank my friends who encouraged me all during my PhD. I had the best help and support from a true friend, so thank you, Corynne !! (Corina, by your Romanian name ☺). Thank you, Aura and Dan, for all the honey, Luana and Razvan, for the fun times and interesting discussions and for always reminding me that what I do is important.

Ii multumesc familiei mele pentru tot sprijinul oferit; pentru incurajari: tusica, Magda si George. Va multumesc mult Mami, Sori si Suri!

ABSTRACT

One of global changes affecting river-sea systems is a reduction in sediment flux. This is a direct consequence of human interventions in the river basin. The delta complexes, especially, record the most striking effects, such as coastal erosion and habitat degradation.

This research assesses the change of sediment flux from the Danube Delta into the Black Sea, under the influence of dams and climate change. The effects are identified both on a long-term scale (one century) and on a short-term scale (seasonal variations).

The results show how anthropic interventions at basin level – for example, the construction of dams and local interventions in the Danube Delta complex – change sedimentary rates across the delta complex, from the delta plain to the delta front area. The results also show modifications of the hydrological regime of the Danube, as a consequence of climate change.

For the first time, the reduction in sediment deposition rates is quantified, of 46 % for the delta, 46-55 % for the delta front area and of 62 % for the prodelta. The local variations within the subaerial delta plain are controlled mainly by hydrological connectivity, while the variations within the subaqueous delta complex are controlled primarily by coastal jetties, proximity to river mouth and the character and evolution of the river plume. Seasonal variations of suspended sediment characteristics are largely controlled by the same factors, in addition to local phenomena (e.g. bottom resuspension) and the seasonality of water primary productivity.

The results of this research can be used to improve management practices of the Danube Delta and its coastal zone, for land use and remediation practices. It can also contribute to future development of methodologies for monitoring environmental changes in a collective transboundary management system of the Danube catchment, which could be applied in other river basins around the world.

GRAPHICAL ABSTRACT

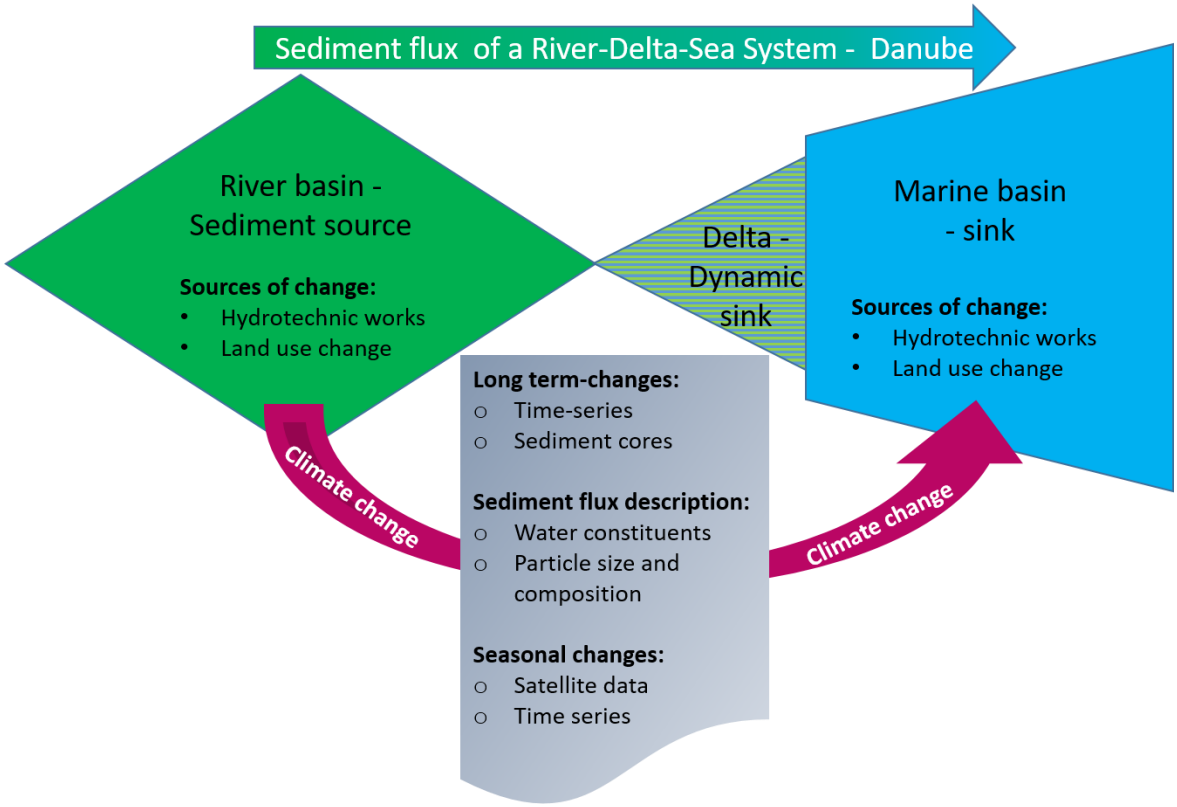

TABLE OF CONTENTS

LIST OF TABLES

LIST OF FIGURES

1. INTRODUCTION

1.1. RATIONALE. SEDIMENT FLUX CHANGES IN RIVER-SEA SYSTEMS

Among the direct impacts of human activities on a river-delta-sea system, the modification of sediment budget is one of the most important. The sediment load of rivers is a key component in river basin and coastal management, from the water way to the delta and river-sea interaction zone. It is of primary importance for: stability and function of deltas and estuaries, navigation and harbour maintenance, river and coastal fisheries, benthic ecology, water quality, and geomorphic and geochemical flux studies (Syvitski, 2011).

The sediment load of rivers varies at different time scales: short term variations are related to catchment influences (e.g. floods variability), long term variations are related to river human activities (decennial to secular time scale) and climate variability (Pont et al., 2002). The suspended sediment budget of a river, especially on long term, depends on the geomorphic/geological influences of basin area, lithology and relief; geographical influences of basin temperature, runoff and ice extent, and human activities that may accelerate or mitigate soil erosion and/or trap sediment, decreasing the hydrological connectivity of the river-sea systems (Grill et al., 2019; Petts and Gurnell, 2005; Syvitski and Milliman, 2007).

In the last two thousand years, some rivers showed an increase in their sediment loads owing to human impact (e.g. increased soil erosion due to deforestation) (Maselli and Trincardi, 2013), but have strongly decreased, since the 1950s, owing to the proliferation of dams and diversions within their drainage basins. Some of the largest rivers of the world - Yellow River (Wang et al., 2007), the Mekong (Kondolf et al., 2018), the Mississippi (Meade, 1996) and many of the European rivers - the Po (Syvitski and Kettner, 2007), Nestos (Xeidakis et al., 2010), Ebro (Ibàñez et al., 1996) as well as the Danube River (Giosan et al., 2013), are some of the most representative examples.

Most rivers (e.g. Danube, Yenisey) are carrying much less sediment, and some rivers transport virtually no sediment: Nile, Colorado, Ebro, Sao Francisco and Indus (Syvitski et al., 2005b; Vörösmarty et al., 2003). The change in sediment budgets is thus impacted by anthropic activities and has consequences on the river delta dynamics. Moreover, direct interventions by humans in deltas in aid of year-round shipping are reducing the number of distributary channels that carry floodwaters across the floodplains, (Syvitski et al. 2009). Fewer channels decrease the rate of delta-plain aggradation, locally increasing the rate of sedimentation in the coastal zone, near the channel mouths, but also increasing the rate of coastal erosion in areas that once received distributary sediment flux (Giosan et al., 2006), as it is the case for the Indus and the Nile deltas (Overeem et Syvitski, 2009) as well as for the Danube (Giosan et al., 2013).

The Danube River-Danube Delta-Black Sea is one of the largest river-delta-sea systems of Europe. The complex ecosystems in the Danube watershed provide resources and services but they are threatened by pressures that result from human activities. The transfer of sediment fluxes from along the Danube catchment to the lowlands of the Danube Delta and then to the Black Sea was severely impacted, mostly in the last 100 years as a result of the increase of direct human interventions on the Danube River and its tributaries (constructions of dams, dredging for navigation, etc.). For example, the variations of its flux or the lack of it had a major impact on the Danube Delta in general and its coastal zone in particular (Panin et Jipa, 2002; Stanica et al., 2007, 2009).

Sediment management is a key point for conservation of wetlands and transitional aquatic environments in the world. In the context of sediment starvation in deltas and sea level rise, this project aims to better understand factors controlling the spatial and temporal evolution of these areas. Seven river-sea systems of Europe (Danube, Nestos, Po, Ebro, Elbe, Thames and Tay) are chosen to analyse trends and explain controlling factors of change in water and suspended sediment discharge in their terminal areas – estuaries or lagoons. They encompass some of the most modified river-sea systems in Europe, with a long history of human occupation. They are situated in different geographical regions of Europe, form the Mediterranean in the South, to the North Sea, in the North and the Black Sea in the East. Further, the focus is on the Danube-Black Sea systems, with a detailed analysis of changes in sediment fluxes in the Danube Delta and its coastal area. The Danube-Black Sea area was chosen because of its complex catchment (19 countries), its history (continuous human induced changes from the Palaeolithic with severe consequences over the last 100 years), with a delta considered resilient to human intervention (Renaud et al., 2013), and a general scientific gap of research looking at the system as a whole, from the catchment to the sea.

This project assesses the changes in water and sediment flux of these rivers, at different time scales, depending on the availability of data, from more than 100 years for the Elbe to 30 years for the Po. The main focus of this research is on the transfer of water and sediment fluxes from the Danube basin to the Danube Delta and to the Black Sea, identifying main changes in the last century and in the present phenomena. The research is structured into two timescales, with different temporal resolutions. The first one comprises the last 100 years that represent the main period for dramatic human-induced changes in the Danube catchment and especially in the Danube Delta, with a major modification of sediment budget (Chapters 2 and 3). The second timescale, focusses on the last 20 years, based on the available satellite data and it is used to assess the present-day evolution of the sediment flux, with the short-term variability within the Danube Delta- Black Sea system, and to contribute to a better understanding of the influencing factors (Chapters 4 and 5).

1.2. STUDY SITE

The study site encompasses the so-called 'transitional area' between the Danube River and the Black Sea basin, comprising the sub-aerial delta, delta front and prodelta areas. The changes in sediment flux, driven by the changes in the Danube basin – hydrotechnical works, land use changes and climate change shape sedimentation patterns in this complex area, together with local factors. This subchapter presents the study site and the main factors which act on both water and sediment fluxes reaching the Danube Delta and the Black Sea.

1.2.1. Danube River basin

The Danube River (Fig. 1.1.) is the second longest river of Europe (2857 km), flowing from its source in the Schwarzwald Mountains in Germany eastwards to the Black Sea. The Danube has the largest drainage basin of Europe (801,463 km^2), comprising 19 countries, from Central to Eastern Europe. It is also the first in Europe for multi-annual mean discharge of 6352 m^3/s, at the delta apex (Mikhailova et al., 2012)**.** The turbid, sediment-laden waters of the Danube flow in the brackish waters of the Black Sea and mix over a large area, as the Danube splits into several distributaries in the deltaic plain – Chilia (north) with a secondary delta (situated in Ukraine), Sulina (middle) and Sfantu Gheorghe (south). The Danube Delta represents the most extended wetland area in Europe. The Danube River is the most important source of water and sediment in the Black Sea, with a discharge of about 205 km^3/year (60% of the total water runoff in the Black Sea basin) and 36.3 to 52.4 million tons per year respectively (48% of the total sediment reaching the Black Sea) (Ludwig et al., 2009; Mikhailov and Mikhailova, 2008). The north-western Black Sea also receives freshwater input from the Dnieper, Dniester and Southern Bug, in a less significant amount, 12% and 2.5%, respectively (Mikhailov and Mikhailova, 2008).

The Danube basin has several distinct regions: the Upper Danube, from the source to Devin Gate (Porta Hungarica), the Middle Danube, up the Iron Gate Gorges, the Lower Danube, between this point to the Danube Delta and the Danube Delta itself. Its present-day geomorphology expresses the interaction of the river (sediment and water discharges, flow energy, etc.) and the sea (wave and littoral currents regime, sea-level changes, etc.) over the past 12 000 years (e.g. Panin and Jipa, 2002).

The Danube is the main contributor to the sedimentation on the north-western Black Sea shelf area. The Danube influence extends far southwards, to the Bosphorous region, as well as down to the deep-sea zone (Panin and Jipa, 2002).

1.2.2. Catchment influences on the Danube water and sediment flux regime

1.2.2.1. Danube sediments

Sediment transported in fluvial environments comprises both inorganic and organic material that is transported from upstream sources to the downstream area of deposition. It is produced by weathering or erosion of rock sand soils and transported by rivers as suspended particles or bed-load material. The Danube sediments originate from its tributaries or directly from the river bed. The whole Danube basin was severely affected by human interventions so the sediment budget has changed continuously over the last century. The sediment balance of most of the rivers within the Danube Basin can be characterised as disturbed or severely altered (ICPDR 2009).

Most of the bed-load sediments are trapped by dams (80-90%) and erosion of river banks is reduced by torrent control, so a deficit of river bed load exists in most of the free-flowing sections of the Danube catchment. The grain size varies from the Upper Danube (gravel) to the Middle Danube (sand and fine gravel), due to a decreasing slope. In the Lower Danube, the suspended sediment dominates. The retention of the suspended load in the upper catchment in not very efficient (1/3 retention of the total load), and during flood events, large amounts of suspended sediment transported towards the lower catchment (ICPDR 2009).

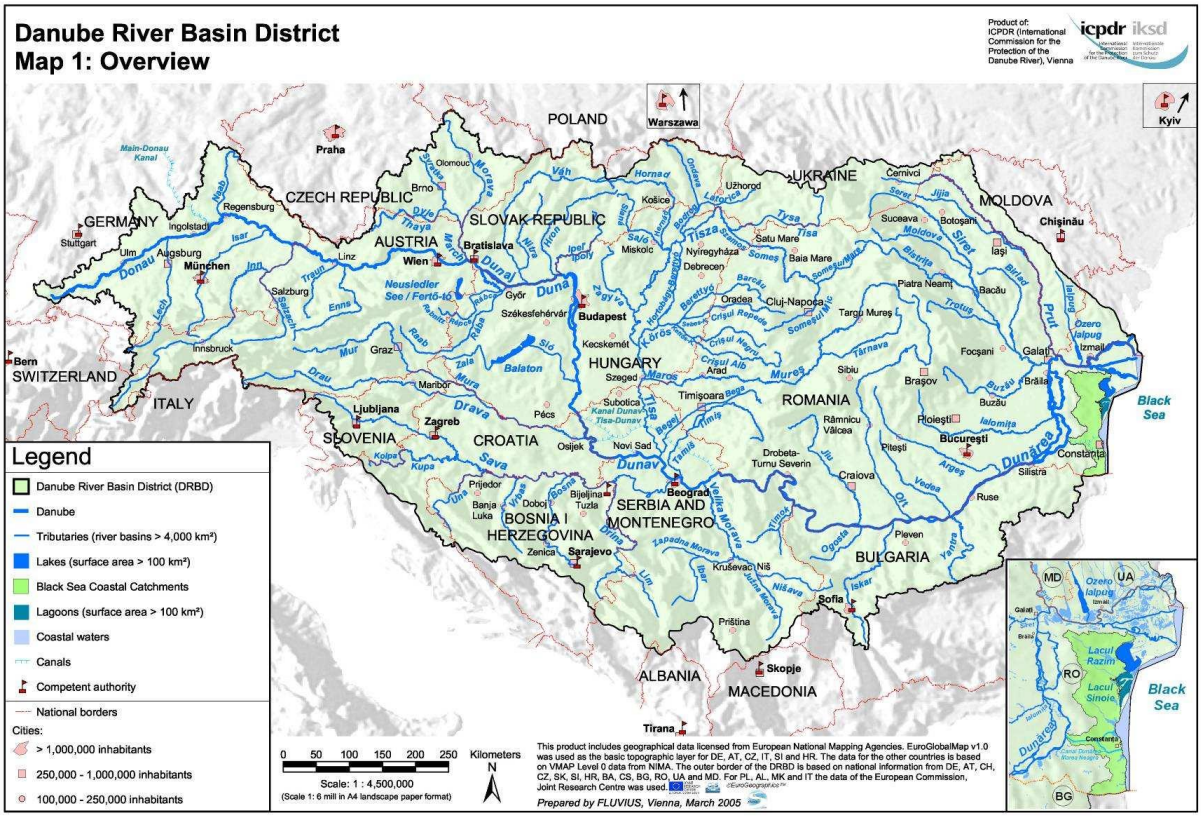

Figure 1.1. Danube Basin (source https://www.icpdr.org)

1.2.2.2. Natural Inlfuences

The Danube river basin covers several climatic zones, from the western regions with strong Atlantic influence to the eastern, dry and cold continental zones. The maximum average precipitation is 3,200 mm/y in the high mountain range of the Alps and the most arid area is the lowland at the Black Sea with an average of only 350 mm/y (Schiller and Miklós, 2010).

Extreme events like floods and droughts are not uncommon in the Danube basin. Floods have been documented (e.g. Vienna or Bratislava) since the year 1012. The main events are presented in Table 1.1, for the entire Danube basin.

The largest flood in the nineteenth century occurred in September 1899 (Pekárová, 2009), as a consequence of a flash flood on the Inn River, a tributary of Danube. The flood reached 11 200 m^3/s at the Krems station; and 10 500 m^3/ s at the Vienna station (Pekárová, 2009). The largest flood of the twentieth century occurred in July, 1954, which caused major damages in the entire Upper Danube basin. The flood peaked at Bratislava on 15 July with a stage of 984 cm (10 400 m^3/s). The other high floods (in order of peak discharge) in the second half of the 20th century were floods in 1991, 1965, and in 1975 (Pekárová, 2009).

In the Lower Danube area, absolute minimum annual discharge in Orsova was observed in 1863, 3471 m^3/s, while the absolute maximum one was in 1895, 15900 m^3/s (Bondar 2003, Pekarova et Pekar, 2006). Other major floods recorded at Orsova occurred in 1888 (15500m^3/s), 1897 (15400 m^3/s), 1940 (15100 m^3/s) and 1981 (14800 m^3/s) (World Catalogue of Maximum Observed Floods). The analysis of the data from Orsova shows that the wettest decade was in 1910–1919, while the driest one was in 1857– 1866, when the absolute maximum and minimum annual discharge was observed, respectively (Pekárová, 2009).

Climate change can influence the river runoff, as some recent results show for the last 150 years in the Danube Basin. Mikhailova et al. (2012) argue that the Danube River runoff gradually increased, indicating the prevalence of climatic factors over the human induced factors. This does not seem to influence the total discharge of the river, because no significant trend in the river mean annual discharge was identified (Pekárová et al., 2003).

Table 1.1 Major hydrological events in the Danube River basin in the last 150 years (Bondar, 2003; Bondar and Panin, 2001; Bondar and Iordache, 2012; Mikhailova et al., 2012; Pekárová et al., 2013; Pekarova and Pekar, 2006; GeoEcoMar unpublished data)

Danube Sector	Floods	Min. water levels
Upper Danube	1850, 1895, 1899, 1910, 1954, 1988, 2002, 2006, 2010, 2013	1893, 1921, 1929, 1947, 1954, 1985, 1990, 1992, 2003
Middle Danube	1850, 1876, 1880, 1883, 1888, 1890, 1897, 1899, 1910, 1915, 1923, 1940, 1942, 1947, 1954, 1956, 1965, 1970,	1863, 1921, 1929, 1947, 1954, 1985, 1990, 1992, 2003

	1975, 1979, 1981, 1988, 1991, 1994, 2002, 2006, 2010, 2013, 2014, 2016	
Lower Danube & Danube Delta	1853, 1888, 1895, 1897, 1907, 1914, 1919, 1924, 1932, 1940, 1941, 1944, 1947, 1954, 1955, 1956, 1958, 1962, 1965, 1970, 1975, 1980, 1981, 1988, 1991, 2002, 2006, 2010, 2013, 2014, 2016	1858, 1863, 1902, 1904, 1908, 1918, 1921, 1929, 1946, 1949, 1950, 1953, 1954, 1972, 1990, 1992, 2003

1.2.2.3. Anthropic influences

The history of human occupation in the Danube basin starts in the Palaeolithic. Since that time, the Danube basin was constantly modified by human activities. The last 150 years are marked by important changes in water and sediment flux due to increased anthropic pressures along the river. Both anthropic and climatic factors have acted over time to the change in sediment and water flux, but it is very difficult to separate their effects.

Schwarz (2008) identified several periods of substantial changes in sediment transport of rivers in the Danube River basin, caused by human activities. The last 150 years can be divided in:

1850-1900: “Low water regulation” (for waterway transport) and other regulation works were implemented. Also, sediments were extracted to be used as construction material for urbanisation.

1900-1950: Construction of power plant chains in the upper river stretches (the Danube and its tributaries) caused a substantial reduction of bed load as well as increased sedimentation in impoundments. Dredging was increased along the entire Danube for waterway transport and construction purposes.

1950-1990: The largest dams were built (Iron Gate I and II, Gabcikovo, Wien-Freudenau (construction began in 1992), and along with smaller dams on several tributaries, they exacerbated the sediment deficit. The amount of dredged material increased until the late 1980s (most of the pre-fabricated multi-storey buildings in “socialist” countries in the Central and Eastern Europe were built with aggregates from river beds), but decreased thereafter.

Since 1990: The political changes in Central and Eastern Europe led to a decrease in industrial production, transportation and dredging. Also, no additional large dams were built in the catchment. However since the enlargement of the European Union, economic prosperity has come back to the region, slightly increasing waterway transport. In recent years, several plans to improve navigation and to construct new power plants have been made. The European Commission also plans to improve waterway transport (TEN-T plans) and to support renewable energies, including hydropower. Dredging today is carried out for navigation reasons, the operation of hydropower plants, flood protection and commercial reasons.

The main human activities which led to substantial change are:

- *Land use changes and urbanization; population changes; vegetation changes.*

Nowadays, the Danube Basin is home of 83 million people, (103 persons/km^2), from which 20 million depend on the river for their drinking water (ICPDR 2009). Land use changes (expansion of agricultural land and deforestation) occurred in Europe and thus all around Danube basin as early as 7500 y BP (Giosan et al., 2012). These authors estimated that increased erosion of land and thus, increased sediment loads into the river, lead to an accelerated accretion of the Danube Delta, in the last two millennia. Anthropic land changes were also considered the main drivers for enhanced sediment discharges into the sea (e.g. Red river in Asia; Wan et al., 2015) and rapid growth of deltas elsewhere (Po and Rhone in Europe), in the Late Holocene (Oldfield et al., 2003; Vella et al., 2005).

The last century, particularly its second half, is characterised by important land use changes that strongly affected the extent of wetlands. In Romania (Lower Danube), in the last 60 years for example - converting the Lower Danube wetlands and Danube Delta, decreased their area to 22% and to 80%, respectively, from the initial surface (Vadineanu et al., 2003), leading to a decrease in flood attenuation capacity of 4.5 km^3 (Cristofor et al., 2003). The wetlands were mainly converted to agricultural land and fishponds. The declining of these surfaces lead to decreased aquatic plant biomass, which had an immediate effect on water quality (Vadineanu et al., 1992).

- *Dam construction*

In the Upper Danube, a total of 59 dams have been constructed on 1000 km, from the source to Gabcikovo, interrupting the free flow on the river every 16 km (Fig. 1.2). Just a few stretches can be considered as free-flowing. The second largest dam is Gabcikovo, situated downstream Bratislava (Upper Danube). It was built in 1992 near an area that represented one of the region's largest wetlands. Nowadays, the original river channel only receives 10-20% of the flow, the rest being channelled towards the power plant (ICPDR).

The largest hydropower dam and reservoir is Iron Gates. It consists of two dams, Iron Gate I and II which were constructed in 1970 and 1983 respectively. The reservoirs have a total volume of 3.2 billion m^3, and a total length of 270 km. Since their construction, they trap more than 20 M tons of sediment per year, decreasing the sediment budget downstream the dam by 50-70 **%** (McCarney-Castle et al., 2011; Panin and Jipa, 2002)**.** Dams were constructed on all major distributaries in the catchment that account for a decrease in sediment up to 60 % (McCarney-Castle et al., 2011). Sediment reduction due to damming affects river systems worldwide, with rates even higher that of the Danube, Colorado (100%) in USA and Mexico, Nile in Africa (98%), Krishna (94%) and Mahanadi

(74%) in India, Yellow River (90%) and Yangtze (70%) in China and Indus (80%) in Pakistan (Syvitski et al., 2009).

- *Flood control*

Since the 16th century dyke systems have been built along the Danube to prevent floods. Only one fifth of the flood plain area that existed in the 19th century still remains. The Danube River is regulated over 80% of its length. Floodplains were cut off from the river, so the frequency and duration of the floods were changed and floodplains were degraded in ecological terms. In the Danube Delta, an area very prone to floods, because of very low altitudes, flood protection structures were built in an area of over 100 000 hectares, but natural conditions have been restored over 15% of this area by ecological restoration since 1994 (ICPDR 2009).

- *Navigation, hydrological connectivity improvement and maintenance*

The total length of the navigable Danube is from km 2411 down to the delta, representing 87% of the river's total length. Ships can dock at 78 harbours located along the Danube between Kelheim and the Black Sea. The main pressures resulting from navigation activities are pollution and changes in the river's natural flowing regime through dredging and cutting/blocking of channels (ICPDR 2009). Dredging is common along the river and is used for waterway transport maintenance (minimum water depth), commercial extraction of sediments from riverbed, channel maintenance for flood protection, impoundment clearing for hydropower plants, fish farms. The commercial dredging is being limited in many countries along the Danube or completely prohibited. Nevertheless, the maintenance of dredging is considerable and in some parts sediments are reinserted in the river to balance the deficit (ICPDR 2009).

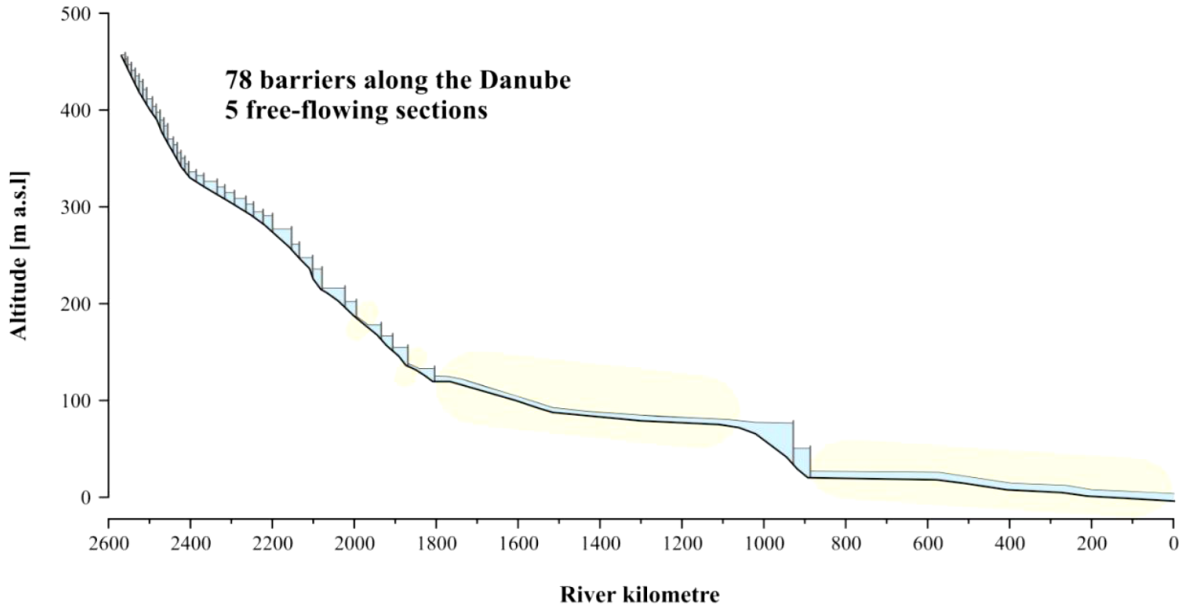

Figure 1.2. Dams along the Danube (Habersack et al., 2016)

1.2.3. Danube Delta

1.2.3.1. Water and sediment budget and distribution

The Danube Delta (Fig. 1.3) is the largest wetland in Europe and the largest delta in the European Union (second largest in Europe). Its present- day morphology is the results of the interaction between the river and sea level changes in the last 12,000 years (Panin and Jipa, 2002). The total area of the Danube Delta is 5800 km^2, of which one fifth is located in Ukraine. The delta starts at Ceatal Izmail (Mile 43 from the mouth zone, measured along Sulina distributary), where the Danube splits into 2 branches – Chilia in the north and Tulcea in the south. The Chilia branch represents the border between Romanian and Ukraine and it ends in a lobate delta with numerous distributaries (the main ones are the Oceacov flowing to NE, and Stary Stambul oriented towards S-SE).

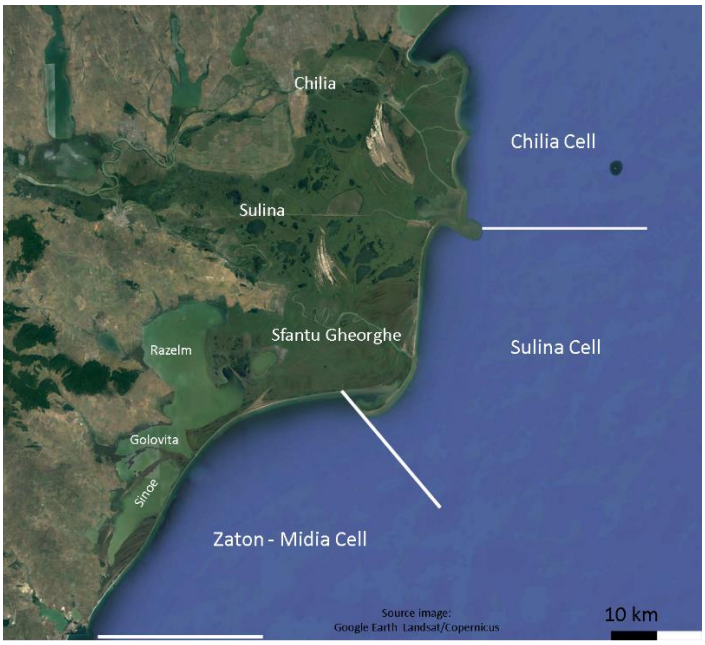

Figure 1.3. Danube Delta in the northern sector of the Romanian Black Sea littoral area (base map - Landsat 2000 image)

The Tulcea distributary flows from Ceatal Izmail, 17 km eastward and it splits in two at Ceatal Sfantu Gheorghe at Mile 33.84 (km 62.2), Sulina branch in the north and Sfantu Gheorghe in the south.

As part of the Danube Delta, in the south there is the Razelm-Golovita-Sinoe-Zmeica lagoon system, which is separated by the sea through a littoral bar. The delta is a flat zone, with an average altitude of about 0.52 m above the Black Sea mean level and with 93% of its territory under 2 m (Bondar and Panin, 2001). It has two distinct regions, separated by the Jibrieni-Letea-Raducu-Ceamurlia-Caraorman line: the fluvial delta, with a network of channel and lakes, constructed in the former Danube bay, and the marine delta, developed in the Black Sea, characterized by alongshore oriented beach ridges.

Chilia branch has a length of 111 km and transports the highest water flow, 58% of the total Danube discharge. The central branch, Sulina, which was cut for maritime navigation, is the shortest, 83 km initially and 62 km after cutting, and transports 19% of the total flow. Sfantu Gheorghe, the southern branch has a length of 108 km, 70 km after meander cutting, and has an intermediate flow - 23% (Bondar and Panin, 2001). The hydrological engineering works along the Danube distributaries have modified their water flow in the last 150 years (Fig. 1.4).

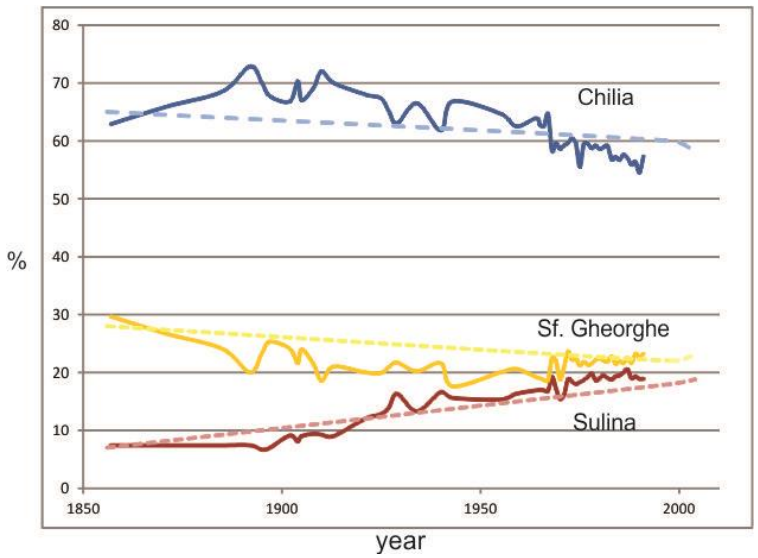

Figure 1.4. The distribution of the discharge on the arms of the Danube delta from the 19th to the 20th and 21st century (Bondar et Panin, 2001 – full lines) and (Romanescu 2013 – dashed lines).

The mean annual discharge of sediment at the delta entrance was calculated at 1737 kg/s by Bondar and Panin (2001) for the period of 1840 to 1990, with an annual volume of 54 815 551 tons, from which 2 180 000 tons were sandy alluvia. Sediment transport reveals the same seasonal variations as the water discharge, with a maximum during spring-summer and a minimum during autumn (Bondar and Panin, 2001). The total alluvial load of the river reaching the Danube Delta has decreased from the end of the 19th century, from 81 Mt in 1894 to 70 Mt in 1939 (Commission Européenne du Danube, 1894, 1934), 58.7 Mt in 1982 (Bondar, 1983; Gastescu et al., 1986), to approximately 22 Mt in the present (Romanescu, 2005). The maximum quantity of alluvium ever recorded in the Danube Delta was 178.7 Mt in 1912, and the minimum was 12.5 Mt in 1866 (Romanescu, 2013). This was also reflected in the total alluvia discharge in each distributary (Table 1.2).

Table 1.2. The quantity of alluvia in the Danube Delta arms at the end of the 19th century and the middle of the 20th century (Romanescu, 2005) for the pre-dam regime

Arm	**Quantity of alluvia Mt**	
	1894	**1958**
Chilia	56.2	48.4
Sulina	7	5.5
Sfantu Gheorghe	17.8	16.5

Chilia, the distributary with the highest water and solid discharge led to the formation and then clogging of Musura Bay. The water depth in the gulf decreased from 3.5 m in 1950 to 1.2 m in 1982 and to 1 m in 2009, with a mean rate of sedimentation of 7-10 cm/y (Romanescu, 2013).

1.2.3.2. Anthropic time line – major engineering works. Sediment budget and overall evolution in the last 150 yr

The major engineering works in the Danube Delta started in 1857, with the Sulina meander cutting programme (Table 1.3, Fig. 1.5; see Panin and Overmars, 2012, for a thorough review), with the aim of shortening the distance between the Danube harbours (Braila, Galati) and the Black Sea.

Table 1.3. Lower Danube & Danube Delta anthropic time line - last 150 years (after Bondar 2008; Panin et Overmars, 2012; Panin et Jipa, 2002)

Year	Event
1857	*Start of Sulina cut-off programme*
1860	*7-9% increase in total discharge in Sulina branch*
1902	*End of Sulina works. The construction of Ceatal-Izmail embankment*
1906	*Canal 'King Charles I' was dredged for rectifying Dunavat. Water discharge on Dunavat increased with 100-150 m3/s*
1911-1914	*Canal 'King Ferdinand' was cut to open a waterway to the Lake Dranov*
1928	*15% increase in total discharge in Sulina branch*
1901-1930	*Starting river embankment*
1959	*Sulina channel deepening from 2.5 to 9.5 m*
1970	*Iron Gates I dam was built. Sediment discharge decrease by 30-40% compared to pre-dam regime*
1983	*Iron Gates II dam was built. Sediment discharge decrease by 50-70% compared to pre-dam regime*
1931-1984	*The river embankment finished*
1983-1985	*Canal 'Mila36' was cut between Tulcea and Chilia branches*
1984-1988	*Mahmudia meander cut-off on Sfantu Gheorghe*
1985-1989	*Dunavat meander cut-off on Sfantu Gheorghe*
1986-1989	*Perivolovca meander cut-off on Sfantu Gheorghe*
1970-1990	*Harbor facilities built on the left side of Prorva distributary, Chilia delta*
1981-1992	*Ivancea meander cut-off on Sfantu Gheorghe*
1988-1992	*KM 37 meander cut-off on Sfantu Gheorghe*
1992	*5-10% increase of total run-off on Sfantu Gheorghe*
2012	*20% increase in total discharge in Sulina*

The cutting of the Danube distributaries, (Sulina and Sfantu Gheorghe) altered the hydrologic conditions (shifted the distribution of water and sediment discharge in all three distributaries – see Table 1.4) and changed the grain size and distribution of bottom sediments. Nowadays, along these two branches the bottom sediments are dominated by fine sand and silt, while on Chilia the bottom sediments are fine sand, silt and clay (Oaie et al., 2005; Opreanu et al., 2007).

Apart from the major engineering works in the delta, a constant and extensive activity was the cutting and dredging of shallow canals since the beginning of the 20th century (Fig. 1.5), but accelerated after the WWII (the total length of the canals doubled;

Gastescu et al., 1983). The main purpose was to improve access to help fishing and reed harvesting (Oosterberg et al., 2000). This network of channels influences present-day sedimentation in the fluvial delta, by increasing water and sediment delivery and overbank sediment transfer and keeping the sedimentation rates above the contemporary relative sea level rise rate in the Black Sea, i.e. 3 mm/yr (Giosan et al., 2013).

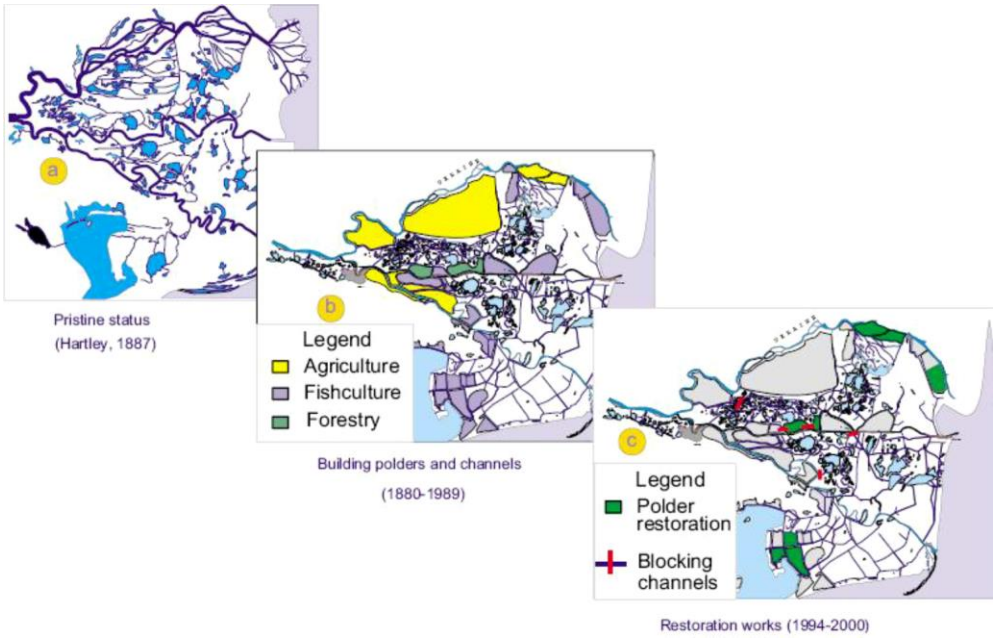

Figure 1.5 Phases in the Danube Delta recent history (Staras, 2000)

The overall sediment deficit may be attenuated by an increase in extreme floods, during which the sediment concentration increases in the whole water column, but this trend is not certain for the future, as modelling suggests an increase in droughts rather than flooding events in the Danube catchment. The sedimentation in the delta is both siliciclastic and organic, with higher organic deposition rates in the internal delta. Siliciclastic sedimentation is maximum in the vicinity of channels (natural distributaries or canals) and minimal in the distal areas, such as isolated lakes, so the finer fractions may be preferentially deposited in lakes of the delta plain that act as sinks (Giosan et al., 2013).

1.2.3.3. Sediment dynamics in the Danube Delta coastal zone

The Danube Delta littoral zone (Fig. 1.3) is one of the most dynamic parts of the Danube Delta system, being the result of the interaction of water and sediment discharge of the Danube branches and the waves and currents of the Black Sea. Damming and channel dredging have reduced the sediment input leading to delta and coast degradation and erosion (Panin and Jipa, 2002) but in the same time, intensive land use practice has had the opposite effect (McCarney-Castle et al., 2011)

During flood events, the increase in alluvial material can determine short-time changes along the shoreline. For example, the maximum recorded flood rate in the 19th century, 35,000 m^3/s (Romanescu 2013), caused the appearance of Sahalin spit at the

mouth of Sfantu Gheorghe branch in 1897 (Panin, 1997). The alluvia transported by the Danube represents mainly fine fractions (silt), most of the sandy, coarser material stops in the Iron Gates dam (Oaie et al., 2005) while the sandy material reaching the Danube delta is due to erosion of the riverbed (Romanescu, 2013). Thus, the sediment supply reaching the delta is 25–35 Mt/y, out of which 4–6 Mt/y of sandy materials are the only sediments supplying the inner shelf and littoral zone (Panin and Jipa, 2002).

The formation and transformation of the Danube Delta littoral zone has been under the influence of both natural and anthropic factors over the last 150 years (Giosan et al., 1999; Stănică et al., 2011; Stănică et al., 2007; Stănică and Panin, 2009; Ungureanu and Stanica, 2000). Panin and Overmars (2012) provide a detailed reconstruction of the littoral evolution of the delta for the last three centuries, using cartographic documents. The last 150 years are marked by the cutting of the Sulina distributary and changes in water and sediment load (7-9% in 1860) on the distributary as well as the construction of the Sulina jetties (1858-1861 – the first part), which changes the overall dynamics of the coastal current, as they were extended into the sea, reaching a length of 8 km in the present. This structure acts like a barrage, blocking alongshore drift from the secondary delta of Chilia distributary towards south completely, resulting in the clogging of Musura Bay and causing sediment starvation for the littoral areas downdrift and increased erosion in the Sulina-Sfantu Gheorghe sector (between Sulina jetties in the north and Sahalin spit in the south), as well as the dramatic decrease or even cessation of sediment supply to the southern shores of the Danube Delta (the sand bar closing the Razelm-Sinoe lagoon) (Stănică et al., 2003; 2011; Stănică and Panin, 2009). A sand bar developed in front of Sulina mouth, originating from bed-load accumulation, which is dredged periodically to maintain the water depth for navigation (8m) and the sediments are discharged offshore, so they are not part of the near-shore transport system (Giosan et al., 1999).

Sfantu Gheorghe branch developed a secondary delta, with a shallow delta front platform (Sfantu Gheorghe II). This is a wave controlled delta, formed with the sediment brought by the river and then distributed in beach ridges by the coastal current (Panin et Overmars, 2012). This delta is still prograding today and is protected by the Sahalin spit in the south (Giosan et al., 1999). The Sahalin spit grew from 1897, lengthening by 200 m/y on average and migrating by overwash towards the shore (30-70m/y), with a tendency of closing the Sahalin lagoon in the next two centuries (Dan et al., 2011; Panin and Overmars, 2012).

The Chilia secondary delta (Chilia III) developed and grew strongly beginning with the 19th century, prograding in three directions: north, east and south) and developed a shallow platform towards east and south (Panin and Overmars, 2012). The decrease in sediment delivery in the 20th century, due to the extent of the lobe in deeper water, has

slowed accretion, leading even to a general erosion trend that it can still be observed today (Filip and Giosan, 2014).

This northern sector of the Danube Delta shores (Cell Chlia & Sulina, Fig. 1.3) consists mainly of beaches with well sorted fine, quarzitic sand, locally enriched in heavy minerals, originating from the Danube (Ungureanu and Stanica, 2000) The southern sector (Cell Zaton-Midia, Fig. 1.3) is characterized by a lower proportion of mineral sand, that decrease towards south, the rest being represented by sands from mollusc shells. Most sediment is Danube alluvia, many being remobilized by erosion of previous littoral bars and rearranged by waves and currents (Stănică et al., 2011).

The sediment input from the Danube branches is reworked by waves and currents, but the tide does not have an important role, as the Black Sea has a microtidal regime (7-11 cm; Bondar et al., 1973). The longshore sediment drift is generated by wind and wave longshore current system, which transports up to 1.23 million m^3/y of sediment (Giosan et al., 1997). The wave climate in the NW part of the Black Sea is dominated by three main directions (Dan et al., 2009, 2007). The northern directions, from N to ENE, have an occurrence of 102 days/y, mostly in winter season. These waves have the largest average heights and are produced by winds with the highest speeds (34 and 40 m/s north). The eastern direction, E to SE, have the lowest average wave heights and they only occur less than 30 days/y. The Southern directions, from SSE to WSW produce medium average wave heights and occur around 90 days/year. The maximum wind speed from these directions is 30 m/s (from south-west direction) and they occur mostly in summer season (Dan et al., 2009).

Storms play an important role in the short-term dynamics of the shoreline and increase the longshore sediment transport (Stănică et al., 2011; Vespremeanu-Stroe et al., 2007). Recent results of wind data analysis (Dan et al., 2009; Stanica et al., 2011) for the time interval of 1991 to 2000, for the NW Black Sea, consider extreme events to occur 1 or 2 times in ten years (wind speeds 28-40 m/s) and milder storms which occur almost yearly (wind speeds 15-19 m/s).

1.2.4. Danube – Black Sea interaction zone

The Black Sea is a semi-enclosed basin with a surface of 432,000 km^2 and the largest anoxic basin in the world. Its present day hydrology is governed by water exchanges with the Mediterranean Sea through the Bosphorus strait and the fresh water discharges of the major rivers in the basin: the Danube, Dniester, Dnieper and Southern Bug. The water column is stratified, with a low salinity level of only 18 PSU up to 150-200 m water depth and a more saline layer of 22.5 PSU beneath, of Mediterranean origin. The upper 500 m layer is influenced by the Rim Current, with a counter clockwise circulation, with a mean velocity of 0.5-0.7 m/s. The tidal variations are small in the Black Sea, 7 to 12 cm (Bondar

et al., 1973), so the dynamics of water in the transitional zone is mostly driven by wind, waves and currents. The entire NW Black Sea shelf is very shallow [up to 110 m depth at the shelf edge (Popescu et al., 2004) and stretches across a vast area (127,000 km^2)], representing 30% of the total Black Sea basin, with a volume of water of only 6500 km^3 (only 1.2 % of the total volume of water of the Black Sea) (Panin et Jipa, 2002).

The sediment transfer from the Danube onto the shelf and into the deep basin, in close relation with the general evolution of the Black Sea basin has been thoroughly reconstructed for the last 30,000 years (Constantinescu et al., 2015; Lericolais et al., 2007, 2009, 2010, 2011; Popescu et al., 2001, 2004). These studies revealed the influence of the Danube river-borne sediments from the shelf down to the abyssal plain, up to 2200 m depth (Popescu et al., 2001). The sediment transfer was mainly controlled by climate and a Black Sea level at ~120 m lower than today (Lericolais et al., 2009).

The present-day sediment dispersal patterns are described by Panin et Jipa (2002) as grouped into two main regions with different depositional processes: the internal shelf, fed by the Danube and the sediment starved external part of the NW Black Sea shelf (Fig. 1.6). Offshore from the subaerial delta lies the delta front (no 3 in Fig. 1.7) with a total area of 1300 km^2 and the prodelta (no 4 in Fig. 1.7), at 50-60 m water depth, with an area of more than 6000 km^2. Beyond this area, the internal shelf receives clayey and siltic sediments of the Danube, which move as a plume, not reaching the outer part of the shelf, but instead, moving south, along the Romanian and Bulgarian shores and finally discharging in the deep-sea zone of the pre-Borphorus region. The mean travel time of the Danubian waters to the Bosphorus strait was calculated by Sur et al. (1996) at 1-2 months (for a mean current speed of 10-20 cm/s and a length scale of about 500 km). The external sediment starved shelf sedimentation is dominated by accumulations of relict sediments or shells and does not receive direct inputs of the Danube siliciclastic sediments (Panin et Jipa, 2002). The Danube-Black Sea interaction zone is thus restricted mainly to the internal shelf.

The dispersion patterns of the Danube water and sediment in the Black Sea NW shelf is controlled by the Danube plume. The Danube plume forms in the coastal area mainly from the three discharging arms. Using passive tracers, Bajo et al. (2014) observed the prevalence of Chilia's waters in the formation of the plume, while the waters of Sfantu Gheorghe follows the Sahalin spit and remain confined near the shores. The influence of Sulina is even more reduced, as it mixes with the waters of Chilia. The authors point out that instant patterns may be different, as the exact area and processes controlling the plumes should be investigated further. The plume extension is mainly restricted to the coast and shelf (maximum offshore extension of 70 km as estimated by Guttler et al., 2011), with a penetration depth of 15 m near the coast (Karageorgis et al., 2009), while the influence of

the Danube waters, traced through simulated inorganic N/P molar ratios at the sea surface, can extend to the Turkish coast (Tsiaras et al., 2008).

The main controlling factors for the formation and extension of the plume are hydrological (solid and liquid river discharge that varies seasonal), meteorological (wind speed and direction, and the topography of the shoreline (Karageorgis et al., 2009; Güttler et al., 2013).

Wind seems to be the primary factor for surface water direction of flow but the haline stratification can limit its influence in the deeper layers, especially near the delta (Bajo et al., 2014).

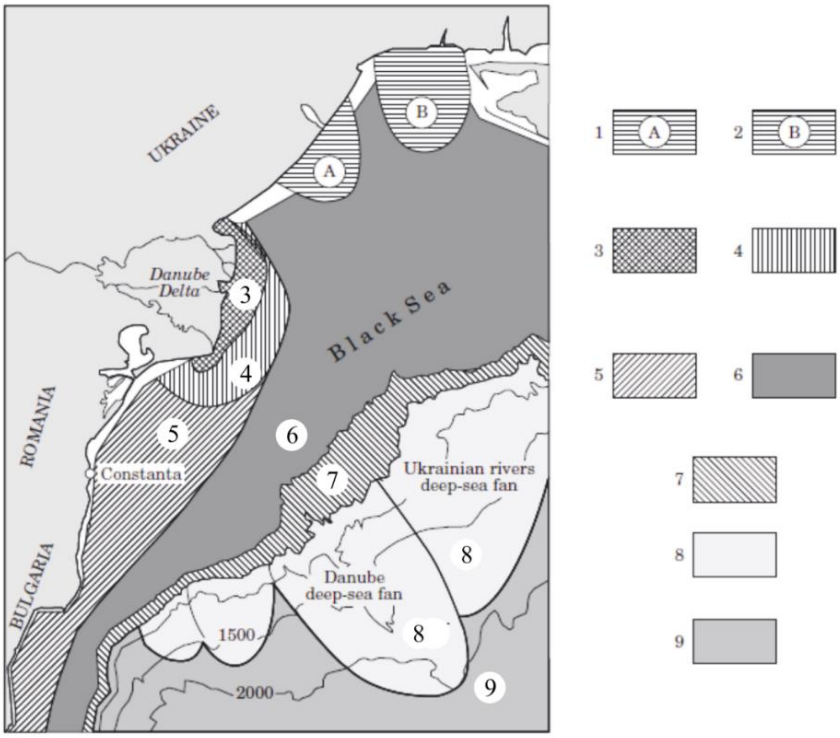

Figure 1.6. Main sedimentary environments in the north-western Black Sea. 1–2, Areas under the influence of the Ukrainian rivers (A-Dniester and B-Dnieper) sediment discharge; 3, Danube delta front area; 4, Danube prodelta area; 5–6, western Black Sea continental shelf areas; 5, area under influence of the Danube originated sediment drift; 6, sediment starved area; 7, shelf break and the uppermost continental slope zone; 8, deep-sea fans area; 9, deep sea floor area (after Panin and Jipa, 2002)

1.2.5. Water and sediment flux in the Lower Danube

Considering 130 years of hydrologic data, Bondar et al., (1991) estimated that the multiannual water discharge of the Danube has a slight increasing tendency. This reflects mostly anthropic causes as gradual damming and loss of wetlands (Panin et Jipa, 2002). While water discharge increased, sediment load reaching the delta decreased, also due to anthropic causes. While it is true that the Danube course is affected by numerous dams and hydrotechnical constructions, it is considered that the main cause for sediment

decrease and input in the delta is the emplacement of Iron Gates I and II dams (Panin et Jipa, 2002, Bondar 2008) between the Middle and Lower Danube.

The multi-annual mean discharge of the Danube is of 6352 m^3/s at the Delta apex (Mikhailova et al., 2012). From the Iron Gates to the entrance into the delta, the Danube gathers waters from Romanian and Bulgarian rivers, in total 1000 m^3/s (Mihailescu et al., 1981). The suspended sediment discharge increases along the Lower Danube, until the entrance in the delta, at Ceatal Ismail (Table 1.5), as an effect of the tributaries' contribution. Along the Romanian tributaries (Jiu, Olt, Arges, Ialomita), numerous dams were also built in the last 40 years or more, but there is no actual quantification of the effect of these dams on sediment retention and influence on the overall budget of Danube sediments. An overall decrease of 46% was calculated for all Danube tributaries (McCarney-Castle et al., 2011).

In the Lower Danube, the multiannual average suspended sediment discharges started to decrease in 1965 and the construction of the two barrages Iron Gates I and II greatly enhanced the decreasing trend due to the deposition of the sediment behind the dams (Bondar, 2008) (Table 1.4).

Table 1.4. Variation of multiannual average suspended sediment discharge along the Lower Danube (kg/s) (Bondar, 2008)

No.	Hydrometric sections	Distance km	1840-1900	1901-1930	1931-1970	1971-1984	1985-2006
1	Bazias	1072.2	1232	1191	1049	752	154
2	Orsova	957	1280	1251	1072	582	126
3	Drobeta Turnu severin	931.1	1116	1100	1117	618	142
4	Gruia	858	1390	1343	1202	635	135
5	Calafat	786.9	1699	1643	1495	989	190
6	Bechet	678.7	1588	1542	1421	1026	457
7	Corabia	624.2	1134	1101	1016	741	354
8	Turnu magurele	596.3	1605	1554	1445	969	393
9	Zimnicea	553.2	1472	1428	1317	971	440
10	Giurgiu	493.1	1630	1579	1462	1043	434
11	Oltenita	430	1722	1763	1275	701	453
12	Chiciu Calarasi	379.6	1896	1941	1690	1005	454
13	Vadu Oii	238	1761	1803	1680	1082	356
14	Braila	167	1791	1769	1638	1170	433
15	Grindu	141.3	1762	1741	1623	1236	425
16	Isaccea	101	2004	1982	1840	1526	672
17	Ceatal Ismail	80.5	1958	1808	1689	1249	650

The average annual suspended sediment discharge in the pre-damming period was 2140 kg/s (65.7 Mt/year) of which, 10% was sandy alluvia (Panin et Jipa, 2002). Bondar (2008) estimated that the coarse sediment discharge reaching the delta remained constant in time (Table 1.5), even after the construction of the two Iron Gates barrages, as the river regained much of the sediment due to riverbed scouring and contribution of the tributaries. Panin (1996) reports at present a total sediment discharge of 25-35 Mt/year, of which 4-6

tons are sandy alluvia, which means that the percentage of the coarser fraction is almost the same but its quantity decreased with the general decrease in sediment.

The marked decrease in sediment load took place in two steps, one reduction by 30-40% following the construction of Iron Gates I in 1971 and by 50-70% after Iron Gates II was finished, in 1984 (Table 1.6) (Panin et Jipa, 2002).

Table 1.5. Variation of multiannual average coarse sediment (diameter 0.1-0.5 mm – medium to coarse sand) discharge along the Lower Danube (kg/s) (Bondar, 2008)

No.	Hydrometric sections	Distance km	1840-1900	1901-1930	1931-1970	1971-1984	1985-2006
1	Bazias	1072.2	29.7	32	31	29	27
2	Orsova	957	62	67	70	3	0
3	Drobeta Turnu severin	931.1	16.3	17	17	17	14
4	Gruia	858	38.5	39	39	40	36
5	Calafat	786.9	52.7	55	33	33	31
6	Bechet	678.7	59.8	61	61	63	60
7	Corabia	624.2	118.8	123	122	125	146
8	Turnu Magurele	596.3	57.7	59	59	58	66
9	Zimnicea	553.2	74.3	74.3	73.8	73.2	69.5
10	Giurgiu	493.1	69.4	69.4	68.7	68.2	66.1
11	Oltenita	430	104.6	104.6	84.1	80.7	72.6
12	Chiciu Calarasi	379.6	112.1	112.1	119	117.4	105.0
13	Vadu Oii	238	103.2	103.2	104.6	104.7	84.3
14	Braila	167	126.8	126.8	127.1	132.7	110.9
15	Grindu	141.3	97.5	97.5	98	102.4	87.1
16	Isaccea	101	103.4	103.4	108.7	117.4	99.8
17	Ceatal Ismail	80.5	107.4	107.4	108.9	118.9	102

Table 1.6. Comparison in total sediment discharge decrease, measured in three stations along the course of the Lower Danube (Panin et Jipa, 2002)

Station	Decrease after 1971 (%)	Decrease after 1984 (%)
Zimnicea (553 km*)	30-40	60-70
Vadu Oii (247 km*)	45	60-70
Isaccea (54 km+500 m*)	10	50

*Values indicate the distance from the Sulina mouth (km 0).

1.2.6. Water and sediment flux in the Danube – Black Sea interaction zone. Controlling factors

Danube Delta

The reduction in sediment discharge greatly impacted the recent evolution of the Danube Delta, through reducing progradation rates in some parts (Chilia and Sfantu Gheorghe deltas) (Panin et Jipa, 2002) and even accelerating erosion and beach degradation in others (e.g. Sulina-Sfantu Gheorghe sector) (Stanica et al., 2007, 2009). As meander cutting and channel deepening for navigation changed the water and sediment distribution on the three delta distributaries, so the cutting of a large network of canals changed water and sediment dynamics mainly in the delta plain (Bondar, 1994).

The hydrographic network of the Danube Delta is complex, with about 3500 km of channels /canals which connect around 500 lakes (200,000 ha of water surface) (Cioaca et al., 2009). The entrance and circulation of the Danube waters in the delta has an irregular character, depending on the hydrologic regime of the river (Bondar, 1994). Thus, on the Danube distributaries, the water discharge varies on a longitudinal scale, because of the lateral channel and canals taking water but also because of overbank spilling when the water discharge at the delta apex exceeds 9100 m3/s (Bondar, 1996). Bondar (1994), calculated that the water discharge which the Danube releases in the delta plain increased from 1858 to 1980s almost four times (Table 1.7). This was caused by the cutting of deepening of canals to facilitate access in different parts of the delta.

Table 1.7. Danube water circulation and loses into the Danube Delta (Bondar, 1994)

Water discharge in m^3/s	**Time interval**			
	1858-1900	***1921-1950***	***1971-1980***	***1980-1989***
Danube	167	309	358	620

This phenomenon had a positive impact in time for the sedimentation of the delta plain, as the sediment delivery increased and sedimentation rates are maintained, at least locally, above the contemporary sea level rise (Giosan et al., 2013).

Direction and gradients of water flow regime change inside the delta, depending on the water level. The variation of water level propagates from west to east (Poncos et al., 2013). Inside the Danube Delta, alluvial sedimentation occurs when the velocity of the flow decreases under a critical value and there is a high content of suspended sediment transported in suspension. The areas where these conditions are met are mainly located at the bifurcation of bigger channel/canals in smaller branches or at the discharge point of a channel/canal into a lake. This process is very intense in the fluvial delta but it can also occur in the fluvio-maritime area (Cioaca et al., 2010a). The Danube Delta acts like a chemical and physical filter for the waters reaching the Black Sea, through its large and compact areas of reed (Cioaca et al., 2010b).

The overall sediment deficit caused by dams may be attenuated by an increase in extreme floods, during which the sediment concentration increases in the whole water column, but this trend is not certain for the future, as modelling suggests an increase in droughts rather than flooding events in the Danube catchment (Giosan et al., 2013). As the flood phenomena increased in the Danube Basin in the last decades (Mikhailova et al., 2012), one would expect to see their effects in the sediment deposition all around the delta plain and in the new delta deposits of Chilia and Sfantu Gheorghe. Also, the deposition rate should vary across the delta, depending on the connectivity of the sink to the general water circulation. Suspended sediment concentration should have increased with increasing water discharge and redistributed inside the delta. The transfer of the finer fraction inside

the shallower canals may lead to preferential deposition in the lakes of the delta plain that act as settling basins (Giosan et al., 2013).

The Danube Delta lakes are flood plain lakes (Oosterberg et al., 2000) located between the three branches of the Danube, a total of 300, with a size varying from 14 to 4350 ha (Hanganu et al., 2008). They are directly connected to the Danube through a vast network of channels and canals, as described previously. The water level is variable in a year, depending on the river pulse (Hanganu et al., 2008). Most of the lake sediments of the delta plain consist of silts (>65%), fine sand (6-15%), clay (20-30 %) and shell fragments (2-4 %) (Mihailescu et al., 1996). They are significantly bioturbated as a result of the biological activity of annelid worms, insect larvae (mainly chironomids) and molluscs (Mihailescu et al., 1982). Modern sediment fluxes in some lakes (Table 1.8) were measured by Giosan et al. (2013), using ^{137}Cs dating.

Table 1.8. Modern sediment fluxes in the internal part of the Danube Delta (from Giosan et al., 2013)

Core	Location	Depositional environment	Sedimentation rate g/cm^2/y			Bulk flux g/cm^2/y		
			1954	***1963***	***1986***	***1954***	***1963***	***1986***
KP3	Matita	Delta plain	0.66		0.52	0.53		0.31
D3	Dranov	Delta plain	0.66	0.57	0.48	0.46	0.34	0.24
FO1	Fortuna	Lake shore	0.84	0.79	0.7	0.34	0.32	0.28
GO1	Gorgova	Lake shore	0.95		0.98	0.48		0.39
HO1	Hontu	Lake shore	0.5	0.48	0.27	0.2	0.19	0.11
NE1	Nebunu	Lake shore	0.84	0.92	0.52	0.42	0.46	0.26
G1	Gorgostel	Lake	0.43		0.32	0.34		0.25
E1	Erenciuc	Lake	0.94	0.6	0.32	0.52	0.31	0.14
B1	Belciug	Lake	0.13			0.18		

One previous study (Duliu et al., 1996), also using ^{137}Cs dating, found a much smaller sediment accumulation rate for Lake Matita, 0.15±0.05 g/cm^2/y.

All delta lakes suffered from eutrophication in the recent decades, which was most intense in the 1960s to the 1980s, due to anthropogenic input of phosphorous and nitrogen (Oosterberg et al., 2000). Danube Delta lakes were classified into three main categories, taking into consideration hydrogeomorphology and water quality, composition and abundance of plankton, aquatic vegetation and the fish community. Type 1 lakes are large, characterized by a sandy-silt substratum, turbid waters (e.g. Lacul Rosu, Merhei), type 2 lakes are well connected to the channel network, have a clayey substrate and clear water (e.g. Furtuna), type 3 lakes are isolated, with organic load and clear waters (Oosterberg et al., 2000).

The water turbidity is caused by the presence of suspended solids (mineral and detritus) and phytoplankton biomass, with an equal contribution, and is subjected to a strong seasonal variation (Oosterberg et al., 2000). A supervised classification of the delta lakes was made with Landsat-TM images for July 1996 by Oosterberg et al. (2000). The resulst show that most of the large lakes (e.g. Uzlina, Furtuna, Matita, Merhei, Rosu) have turbid

waters (Table 1.9) but also that there is a gradient of turbidity, probably related to the presence/absence of vegetation (Coops et al., 1999) at local scales and the connectivity to the water network (Güttler et al., 2013). The classification cannot in fact, distinguish between mineral or algal turbidity, but it was found that there is a positive correlation between these factors (Oosterberg et al., 2000).

Table 1.9. Some ecological parameters for Lake Merhei, Matita and Rosu (Oosterberg et al., 2000).

Spring season 1997-1998					
Lakes	Chlorophyll µg/l	Secchi depth m	Water depth m		
Merhei	11	1	1.89		
Matita	9	1.25	2.92		
Rosu	10	1.25	3.90		
Summer season 1997-1998					
Lakes	Chlorophyll µg/l	Secchi depth m	Water depth m	Size ha	Aquatic vegetation cover %
Merhei	47	0.50	1.53	1368	-
Matita	52	0.60	2.54	642	-
Rosu	54	0.48	3.65	1365	18

A recent analysis on a time frame of two years (Güttler et al., 2013) revealed the seasonal variability of turbidity inside the Danube Delta and in the coastal plume. During winter high levels of turbidity characterise lakes inside the delta, even those not directly connected to the hydrographic network, due to wind-induced resuspension of bottom sediments and highly turbid plumes are generated in the coastal zone. Spring season brings the peak hydrological discharge which influences the turbidity in only the lakes directly connected to the main branches, and most lakes present clear waters. Spring represents a transition period for both the lakes inside the delta and the coastal plume – river-induced turbidity decreases and the seaward expansion of the plume increases. In the summer river-induced turbidity decreases but some lakes start to present high turbidity levels since June, coinciding with phytoplankton growth. The plume expansion decreases in the coastal area, reaching its minimum in August. During the fall, some lakes present the same turbidity patters as for summer and some others, more isolated one have higher turbidity levels. The plume extension increases compared to summer period.

Generally speaking, turbidity in Danube Delta lakes is influenced by the water discharge and hydrologic connectivity, presence/absence of macrophytes and re-suspension processes caused by wind stress (Coops et al., 1999; Güttler et al., 2013; Oosterberg et al., 2000).

Danube Delta front and prodelta

Recent studies have shown that the fate of sediments in river-mouth dominated environments depends on the relation between fluvial discharge, regional circulation and

storm events (Estournel et al., 1997; Kolker et al., 2014; Marion et al., 2010; Rong et al., 2014). The fate of the Danube sediments, discharged through its three mouths, depends on the wave regime, wind speed and direction and fluvial discharge (Bondar, 1998; Constantin et al., 2017; Güttler et al., 2013; Karageorgis et al., 2009). The coarser fraction settles near the mouths, and forms sand bars – Sahalin Island, south of the Sfantu Gheorghe mouth; the bar in front of Sulina branch, 8 km offshore the coast, which is periodically dredged to maintain the depth for navigation, the bar that closes the Musura bay in the south of the Chilia delta; a part of this fraction feeds beach sectors, while the finer fraction is transported in suspension and disperse on the shelf (Bondar 1998; Oaie et al., 1999; Panin et al., 1998; Panin et Jipa, 2002). The sediments discharged by the three branches consist of fine sand, silt and mud (Oaie et al., 1999).

The solid suspensions reaching the Black Sea (particulate organic and inorganic matter larger than 0.45 μm) were estimated at 11000 tons/day, out of which 8.9% represents phytoplankton and 0.2% zooplankton, leading to a total of $4000x10^3$ t/y of suspended solids, $35x10^3$ t/y of phytoplankton and $7x10^3$ t/y of zooplankton (Gomoiu et al., 1998). The sediment and associated particles are transported along the coast by the Rim current and across shelf-continental slope by meso-scale eddies and are deposited mainly in the Danube Delta front area and prodelta (Stanev and Kandilarov, 2012). Even if some recent studies brought insights into the water and sediment circulation and deposits characterisation of these two domains (Panin et Jipa, 2002,Oaie et al., 2004) there is no actual quantification of the recent deposition. Oaie et al. (2004) gives an average sedimentation rate of 4 cm/y for the prodelta, characterising the sedimentation as dominated by the terrigenous input of the Danube, represented mainly by well sorted silt and silty clay.

The difference in sedimentation between this area (internal shelf) and the external shelf is considerable. In a core retrieved from the shelf edge, Ayçik et al. (2004) found a sedimentary rate of 0.20±0.01 cm/y using ^{210}Pb method and 0.15±0.03 cm/y using ^{137}Cs isotope. Numerical simulations for the Black Sea, with focus on the Danube area, showed that fine sediments could cross the continental slope propagating into the deep ocean while coarser fraction has a very limited path, with a limited penetration into the deeper areas (Stanev and Kandilarov, 2012).

By comparison, the Rhone River deposits between 20 and 50cm/y of sediments in front of its mouths, and around 0.2 cm/y, southeastward from its delta (Calmet and Fernandez, 1990; Charmasson et al., 1998; Radakovitch et al., 1999; Miralles et al., 2005). The mean annual discharge of this river is almost four times smaller than that of the Danube (1700 m^3/s compared to the 6352 m^3/s), with annual peaks of 5000 m^3/s in autumn and spring (Estournel et al., 1997) compared to 9000 m^3/s for the Danube.

As there is no quantification for the modern deposition rate in front of the Danube Delta, it is difficult to assess it, but we could expect higher sediment accumulation rates than those of the Rhone River. The comparison seems possible as both rivers discharge in micro-tidal environments, where the main dispersal factors are haline stratification (buoyancy driven current), currents, wind stress, waves and topography of the shoreline**.**

1.2.7. Extreme hydrological events in the Danube-Black Sea system and their sedimentary imprint

The study of past flooding events that can be quantified with recorded data of water and sediment discharge may provide further answers on the transfer of sediments in the delta plain and to the coastal zone during these extreme events. Main indicators of floods are grain size and certain geochemical elements (e.g. Zr/Rb ratio) but they can vary depending on the event and area of deposition, as they are subject to hydrodynamic conditions, water discharge, current and waves (Schillereff et al., 2014; Drexler et Nittrouer, 2008). Also, accounting for variable sediment supply driven by land use and climatic fluctuations is critical because events of similar magnitude may deposit sequences of unequal thickness (Schillereff et al., 2014). A normal graded sequence may characterise a flood, however, it was shown for Chiangjiang (Hu et al., 2014) that while grain size is very sensitive to flood events, the evolution of the river channel or just different rhythmical fluctuation can show similar grain size trends.

In the marine environments, the properties of river flood deposits may include: presence of ^{7}Be (short-lived radionuclide, associated with terrestrial supply; $t_{1/2}$ of 53.3 days), primary physical stratification (i.e., initially little biological reworking), fine-grained sediment (high percentage of clay compared to preceding seabed sediment), and low $^{210}P_{bxs}$ activity (minimal scavenging of marine ^{210}Pb) (Sommerfield and Nittrouer, 1999; Sommerfield et al., 1999; Allison et al., 2000; Wheatcroft and Borgeld, 2000; Bentley et Nittrouer, 2003; Mullenbach et al., 2004; Palinkas et al., 2005; Wheatcroft et al., 2006, Hu et al., 2014).

The deposition of sediment during such events in marine environments is influenced by oceanic conditions (energy of waves, currents, speed of wind) (Estournel et al., 1997; Wheatcroft et Sommerfield, 2005). The oceanographic conditions in the Black Sea were studied before (Bajo et al., 2014; Dan et al., 2009; Dinu et al., 2011), but never linked to the flood deposits of the Danube. At least 28 floods were recorded in the last 150 years in the Lower Danube and the Danube Delta, so they must have created a detectable imprint in the sediment deposits of the near-mouth area of the river. To this date, there are no studies on the Danube flood deposits. What is the main deposition area, sedimentary characteristics, identifying and quantifying individual events, main factors controlling the deposition are some of the questions that need to be answered?

1.3. AIM AND OBJECTIVES

The aim and objectives of this research have been identified from the previous review. The main aim is to reconstruct changes in sediment flux in several European river-sea systems (Danube, Nestos, Po, Ebro, Elbe, Thames and Tay) with a specific focus on the Danube - Black Sea system.

The specific objectives are:

- *To understand how changes in the river basin (land use changes, dams and reservoirs, climate change) affect sediment fluxes of the Danube and the other six European rivers.*
- *To quantify the decrease in sediment flux of the Danube in the delta and the Black Sea shelf, detailing on specific environments – lakes, channels, lagoons, delta front and prodelta*
- *To describe the spatial and temporal characteristics of the sediment flux in the Danube-Black Sea interaction zone, from the sub-aerial delta to prodelta*
- *To assess the relationship between the short-term phenomena and the long-term evolution of the Danube-Black Sea interaction zone.*

1.4. THESIS STRUCTURE

The thesis is presented as a series of seven chapters. The first chapter introduces the global context of sediment flux in river-sea systems and details on the Danube basin, with a focused description of the Danube Delta and the NW Black Sea. It also identifies the knowledge gaps on the effects of the reduction of sediment flux in this area.

The long-time scale is recreated by Chapters 2 and 3. Chapter 2 analyses trends in water and suspended sediment of seven of Europe's largest rivers, including the Danube, to find possible similarities and differences. It also discusses the main acting factors on the changes of both water and suspended sediment discharge. Ninety years of water and suspended sediment data for the Danube provides an important step in recreating the long-time scale for the variation of sediment fluxes and introduces Chapter 3.

Chapter 3 recreates the variation of sediment flux in the Danube Delta and the Black Sea, providing, to date, the most complete picture of sedimentary rates across different environments of the Danube Delta, delta front and prodelta areas. The major hydrotechnical works both in the basin and locally, in the delta, are identified as main drivers of change in sediment supply and sedimentary patterns. An assessment of trapping efficiency is also done and compared with other major rivers.

The short-time scale is recreated by Chapters 4 and 5, which describe seasonal patterns of suspended sediment across the Danube Delta, delta front and prodelta areas. Chapter 4 provides a detailed analysis of suspended sediment flux from in-situ analysis of water constituents (TSM, ISM, chl-a), retrieved during different hydrological conditions and from analysis of particle size and composition. Chapter 5 analysis in more detail the seasonal variation and spatial patterns of sediment flux into the Black Sea, introducing the use of Earth Observation as an important tool in mapping complex areas and bridging the gap of both temporal and spatial availability of data.

Chapter 6 provides a general discussion of the results, summarizing the key findings of this study, showing how they can contribute to improving our understanding on global issues in river-sea systems. The thesis concludes with Chapter 7, which comprises a summary of the key conclusions of this study.

2. TRENDS IN WATER AND SUSPENDED SOLIDS DISCHARGE OF SEVERAL EUROPEAN RIVERS TO THE GLOBAL OCEAN

2.1. INTRODUCTION

There is a globally recognized need to understand the way River-Sea Systems work and particularly, the transitional areas such as deltas or estuaries, which record both local pressures and the effect of changes in the river basin. Both human direct activities and climate change and variability impact the transfer of water and sediment fluxes to transitional areas. As a consequence of direct anthropic interventions in the river basins, especially the building of dams, reservoirs and embankments, the water and sediment flow of most rivers has been changing, especially in the last 60 years, resulting in the deltas and estuaries in coastal erosion and environmental degradation (Milliman and Farnsworth, 2011; Syvitski et al., 2005b).

Routine in-situ measurements of water and suspended sediment discharge are part of the global effort to study the impact of basin drivers change on the downstream areas of River-Sea Systems across Europe and around the world (e.g. Ibàñez et al., 1996; Panin and Jipa, 2002; Syvitski et al., 2013; Walling, 2008; Xeidakis et al., 2010). A better understanding of the differential environmental controls on these areas could be achieved by undertaking an inter-comparison of river basins. However, this remains a challenge due to: (i) the inconsistency of approach to measuring liquid and solid discharge by responsible authorities within and between river basins; (ii) the lack of consistency in measuring suspended sediments discharge in space in a river basin; (iii) the frequency of measurements for both water and sediment discharge is sometimes insufficient for detecting all hydrological events (e.g. peak floods); and (iv) the time and spacing of measurements is not the same or comparable between all River-Sea Systems (it can vary from point-measurements in some cases, made only during dedicated surveys, to monthly or weekly measurements). In many river basins historical data is not available, is very scarce and/or incomplete. In many cases the length in time for the data series in not enough to assess changes. This makes difficult to: (i) assess and mitigate the effects of human interventions in River-Sea Systems; (ii) to identify the moment in time when climate change started acting as a significant hydrological driver for most river-sea systems. Therefore, there is a need for long term time-series data measured in situ, in order to understand changes in River-Sea Systems.

The effects of basin interventions or changes on fluxes of water and suspended solids of several of the rivers of this study have been documented and assessed before. For example, coastal erosion caused by reduction in sediment flux is a major problem for

the Danube, Nestos, and the Ebro deltas (Stănică et al., 2007; Xeidakis et al., 2010, Gracia et al. 2013). Here, for the first time, we analyse (i) availability of data and (ii) trends in water and suspended solids discharge in several of Europe's largest River-Sea Systems, recorded in their transitional areas, either in the deltas or at the tidal limit of their estuaries, and identify commonalities and differences in response changes in the river basin (building of major dams especially) and climate change. A statistical analysis approach is used to identify and compare trends and breaks in water and suspended solids discharge of these rivers. The river basins are located across Europe, in regions with different climatic influences, from oceanic to temperate continental and Mediterranean to transitional. The aim of the analysis is: (i) to describe differences and similarities between the systems and explore possible sources of diversity and uncertainty, with a focus on the Danube, the most international river basin in Europe; and (ii) to identify changes in water and suspended solids fluxes in the river-sea interaction areas, considering dam building and climate changes as main drivers of change and assess their impact in all river basins, with specific differences.

2.2. STUDY SITES

Seven of the Europe's largest rivers (Fig. 2.1) were chosen for this study: Danube, Nestos, Po, Elbe, Ebro, Thames and Tay. These rivers or part of the River-Sea Systems (estuaries, deltas) are designated as Supersites for the new research infrastructure DANUBIUS-RI, the International Centre for Advanced Studies on River-Sea Systems. Supersites are natural areas of high scientific importance and they will be test beds for the scientific ideas of DANUBIUS-RI.

They are located in different climatic regions of Europe and have very different catchments (in terms of size, no of riparian countries, etc). They discharge into three seas bordering Europe: the Black Sea, the Mediterranean and the North Sea (Fig. 2.1). Their main physiographic characteristics of these River-Sea Systems are presented in Table 2.1.

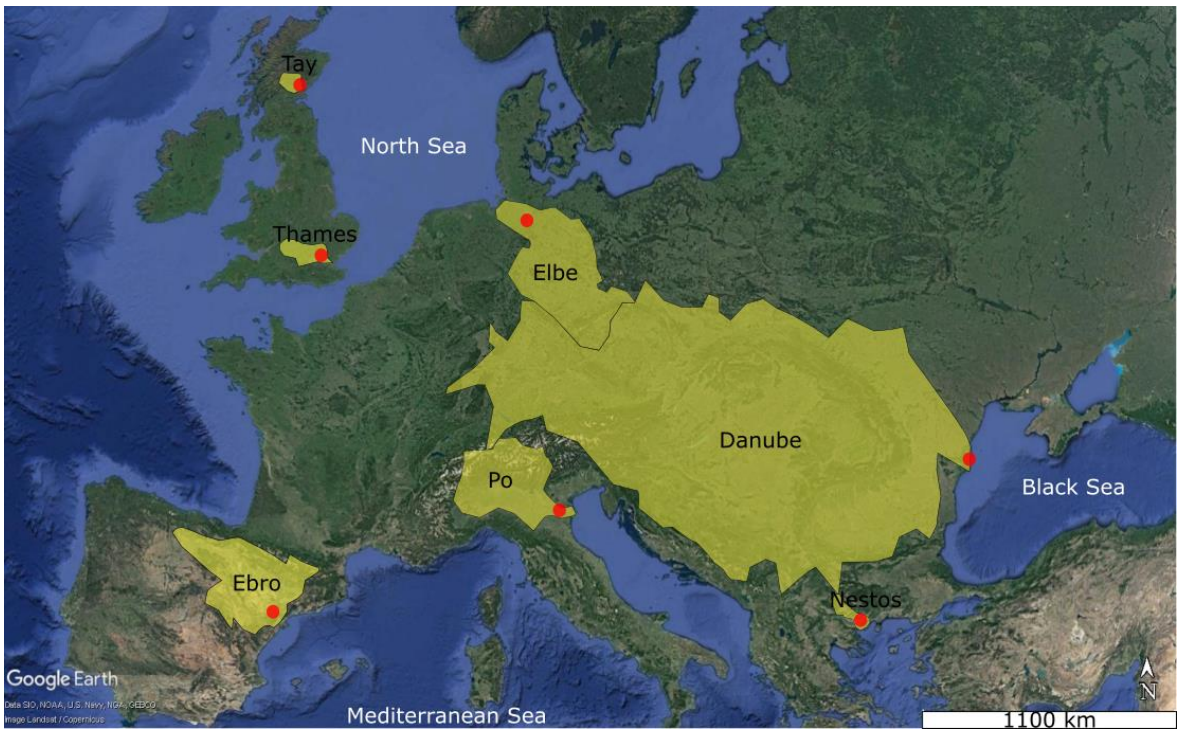

Figure 2.1 Geographical position of the river catchments of this study. The red dots represent the position of the measuring stations for each catchment.

Danube

The Danube River-Danube Delta-Black Sea is the most international river-delta-sea system in the world, with 19 countries in the river catchment. The Danube originates from the Schwarzwald Mountains in Germany and flows eastwards to the Black Sea. The history of human occupation in the Danube basin starts in the Palaeolithic. Since that time, the Danube basin was constantly modified by human activities (Giosan et al., 2012).

The transfer of sediment fluxes from along the Danube catchment to the lowlands of the Danube Delta and then to the Black Sea has been severely impacted, mostly in the last 150 years, with the increase of direct human interventions on the Danube River and its tributaries (constructions of dams, dredging for navigation, flood control, etc.) (Schwarz, 2008). There are 78 barriers along the Danube, with Iron Gates I and II, built in the 1070 and 1983, being the largest. One of the most notable impacts on the Danube Delta in general and its coastal zone in particular is accelerated coastal erosion (Panin and Jipa, 2002; Stănică et al., 2007; Stănică and Panin, 2009).

Considering 130 years of hydrologic data, Bondar et al., (1991) estimated that the multiannual water discharge of the Danube (Table 2.1) has a slight increasing tendency. This reflects mostly anthropic causes as gradual damming and loss of wetlands (Panin and Jipa, 2002), while the water discharge inside the Danube Delta has been increasing four times due to cutting and deepening of various canals (Bondar, 1994).

Mean annual discharge of sediment at the delta entrance was calculated at 1737 kg/s by Bondar and Panin (2001) for the period of 1840 to 1990, with an annual volume of

54.8 M t, from which 2.18 Mt were sandy alluvia. Sediment transport reveals the same seasonal variations as the water discharge, with a maximum during spring-summer and a minimum during autumn (Bondar and Panin, 2001). The total alluvial load of the river reaching the Danube Delta has decreased from the end of the 19th century, from 81 Mt in 1894 to 70 M t in 1939 (Commission Européenne du Danube, 1894, 1934), 58.7 Mt in 1982 (Bondar, 1983; Gastescu et al., 1986), to approximately 52 Mt in the 1990's (Panin, 1996).

Nestos

Nestos River flows through Bulgaria and Greece, and discharges its water into the Aegean Sea. It originates from Mount Rila (2,716 m) in South Bulgaria between the mountain chains of Aimos and Rodopi, where the river is called Mesta (Samaras and Koutitas, 2008). The average total physical runoff from the Rila mountain up to the Nestos/Mesta estuary is $2{,}076 \times 10^6$ m^3, based on data of the hydrological years 1965–66 to 1989–90 (Mimides et al., 2007).The Nestos forms a delta in the Aegean Sea. The river's modern delta area is almost 440 km^2 and the delta shoreline is 51 km long (Xeidakis et al., 2010).

Two dams, the Thisavros and the Platanovrysi, have already been constructed and started operating in 1997 and 1999, respectively, in Greece. Another two dams, Temenos and Arkoudorema, are under construction at present in Greece. All these four dams provide hydroelectric power and water supply for irrigation networks (Darakas, 2002).

The mean annual sediment yield before the construction of the dams was 2×10^6 t/y (or 1.08×10^6 m^3/y). Following the construction of the dams in the river course (2002 onwards) it is 0.33×10^6 t/y, meaning a reduction of 80%. This fact had as main consequence the alteration of the sediment balance in the delta area, with a dramatic impact on the washout of the river Nestos mouth and erosion of the adjacent coastline (Xeidakis et al., 2010). The construction of dams didn't affect the mean water discharge of the river but there is a smoothing of the peak discharge incidents during winter and spring (Sylaios et al., 2010).

Po

The Po valley has been populated since ancient times (Marchetti, 2002) but more marked changes happened after the Second Word War, when the river's sediment discharge decreased by 40%, due to changes in the upper basin (Manieri, 2016). Po is the most important river of Italy but also one of the main sources of sediment for the Adriatic basin. The river flows from the Alps to the Adriatic Sea, ending in a delta. The Po watershed is one of the most urbanized (260 inhabitants/km^2) and agriculturally intensive areas in Europe (Tesi et al., 2013).

The river discharge has an inter-annual variability, with two peaks, one in spring, linked to snowmelt and one in autumn, caused by rain fall (Boldrin et al., 2005). Its major sediment sources is located in both the Apennines and the Alps (Milligan et al., 2007).

Downstream of Pontelagoscuro, 90 km from the coast, Po forms a delta consisting of five major distributaries: Maestra, Pila, Tolle, Gnocca and Goro. Average suspended sediment delivery is 11.5 Mt/y, with a range of 2.9 Mt/y (1983) to 22.4 Mt/y (1937) (Syvitski et al., 2005a).

Ebro

The Ebro River is the longest river running entirely through Spain. It is located in the NE Iberian Peninsula, starting in the Pyrenes and flowing in the Mediterranean, where it forms a delta at Taragona. The Ebro Delta has an area of 320 km^2, mostly devoted to agriculture (75%) and dominated by rice cultivation. The natural areas (lagoons and wetlands) occupy only 20% of the area (Ibàñez et al., 1996).

Its mean annual discharge reduced by 30% during the last century, from 592 to 426 m^3/s. Due to reservoir trapping, the suspended sediment of the river was reduced by more than 99%, with a present value of $0.3x10^6$ Mt/y (Ibàñez et al., 1996). More recent studies (Rovira et al., 2015; Tena et al., 2011) estimates suspended sediment at 99,547 t/yr and 92,000 t/y, respectively, less than 1% of total suspended load estimated at the end of the 19th century.

Elbe

The Elbe River is one of the major rivers of Europe, flowing through the Czech Republic and Germany, where it discharges in the North Sea through an estuary.

There are 139 dams in the Upper Elbe River, with a total storage capacity of about 566 million m^3 and a flood storage of about 271 million m^3. Only two of these dams are directly built on the Elbe River, Labska dam and Les Kralovstvi dam, about 12 and 54 km beneath the Elbe spring, in the Czech Republic. Also, 28 weirs have significantly modified the character of the Upper Elbe River in the Czech Republic at a length of about 250 km. Due to the small storage capacity upstream of weirs compared with the dams, there is only a relatively small impact of those weirs on flow conditions in the Elbe River (Schmidt et al., 2008). The German section of Elbe is free-flowing, from Ústí n. L. to the impoundment weir at Geesthacht (ICPER).

Thames

River Thames is situated in the southern England and is one of the main British rivers, with a long history of human occupation in its basin (Bussi et al., 2016). It springs from the Cotswold Hills and flows eastward to the North Sea. Its basin it's densely populated,

960 people/km^2 (Merrett, 2007). The upper reaches are dedicated to agricultural use (Bussi et al., 2016; Fuller et al., 2002), while the lower reaches are intensively urbanised, containing major urban centres – London, Swindon, Oxford, Slough, Maidenhead and Reading.

The waters of the Thames are the main supply of freshwater for fourteen million people (Whitehead et al., 2013) and its nontidal section (upstream of Teddington Weir) receives treated wastewater from approximately three million inhabitants (Kinniburgh and Barnett, 2010).

Tay

River Tay is the longest river in Scotland and the river with the highest discharge in the UK (Table 2.1). Its source is situated in Western Scotland, on the slopes of Ben Lui and it flows eastward, in the North Sea, forming an estuary.

The Tay Estuary receives waters from both the Tay and Earn rivers. It is a partially-mixed, macrotidal body of water; its tidal reach extends 50 km inland the maximum depth is 30 m and tidal ranges for neap, spring and equinoctial tides are 3.5 m, 5 m and 6 m respectively (Duck, 2005). It is considered one of the cleanest major estuaries in Europe (McManus, 1998).

Land use in the catchment is primarily moorland, but there are also surfaces used for forestry (5%) and arable agriculture (8%) (Gilvear and Black, 1999). The floods are a frequent phenomenon in the Tay catchment (SEPA), usually caused by snow melt, ice blockage and heavy rain.

The river basin is drained by of 180 rivers and 27 lakes. Tay's lakes and rivers are used for a number of functions including drinking water, aquaculture, farming, recreation and fishing. Several of the lakes occur in series and are home to hydro-electric power generation schemes, the largest being Loch Dochart, Loch Lubhair and the 23 km long Loch Tay. These hydro-electric schemes also play a major part in flow regulation, as the area around Perth is flood prone with over 1,300 residential and 270 non-residential properties vulnerable to flooding. The embankment for agriculture in the lower reaches conveys water and suspended sediment more rapidly to the estuary.

Table 2.1. Main characteristics of the European River-Sea Systems and data sets analysed in this study

River	Catchment size km^2	River length km	Water discharge m^3/s	Population mil	No of countries in catchment area	Climate zones in the basin area*	Main source of change	Gauging station	River section	Data type	Observation period	Frequency of available data	Data source
Danube	801,463	2,857	6352	160	19	Temperate oceanic and continental Mediterranean	Dams	Sulina	Delta	Water discharge m^3/s Suspended solids g/m^3	01.1921-12.2010 01.1921-12.2010	Monthly averages Monthly averages	Institute for Marine Geology and Geo-Ecology – GeoEcoMar , Romania
Nestos	5,749	256	66.4	0.179	3	Temperate continental Mediterranean	Dams	Delta	Delta	Water discharge m^3/s Suspended solids g/m^3	01.1966-12.2006 -	Monthly averages -	Democritus University of Thrace, Greece No time-series data
Po	74,400	652	1525	17	4	Temperate continental Mediterranean	Land use changes Dams	Pontelagoscuro	Lower Po	Water discharge m^3/s Suspended solids g/m^3	01.1980-08.2013 -	Daily measurements -	ISMAR, Venice, Italy No available data
Ebro	85,555	928	426 s	3.2	3	Mediterranean	Dams	Tortosa	Delta	Water discharge m^3/s Suspended solids g/m^3	10.1951-09.2014 10.1980-04.2017	Monthly averages Monthly averages	Confederación Hidrográfica del Ebro
Elbe	148,000	1,091	861	25	4	Temperate transitional	Dams	Neu-Darchau Hitzacker	Lower Elbe Lower Elbe	Water discharge m^3/s Suspended solids g/m^3	11.1874-03.2017 01.1964-12.2016	Daily measurements Monthly averages	Helmholz-Zentrum Geesthacht, Germany The German Federal Institute of Hydrology (BfG)
Thames	13,000	345	67	13	1	Temperate oceanic	Land use changes	Teddington	Tidal limit	Water discharge m^3/s Suspended solids g/m^3	04.1974-12.2010 04.1974-12.2010	Weekly measurements Weekly measurements	Centre for Ecology and Hydrology, UK
Tay	4,990	193	167	~0.299	1	Temperate oceanic	Dams/Land use changes	Perth	Tidal limit	Water discharge m^3/s Suspended solids g/m^3	07.1975-12.2013 07.1975-12.2016	Weekly measurements Weekly measurements	Scottish Environment Protection Agency, UK

*Climate zones from (Schneider et al., 2013)

This study represents a first analysis in comparison of these Supersites, with a focus on the Danube, focusing on the available data on water and suspended sediment discharge. While most of these systems are changed by different land use practices and constructions of dams, the cumulative effects on their terminal areas, estuaries and deltas, are different (McManus, 1998; Panin and Jipa, 2002; Schmidt et al., 2008; Tena et al., 2011; Xeidakis et al., 2010). This study assesses the cumulative effects of these changes in the terminal areas of the River-Sea Systems, also considering the additional effect of climate change.

2.3. DATA AND METHODS

2.3.1. Data

Data used in this study consists of water (m^3/s) and suspended solids (g/m^3) discharge recorded at the gauging station located in the lower reaches of the river (delta or tidal limit – Fig. 2.1). Table 2.1 describes the availability of data (water and suspended solids discharge) and the frequency of observation for each catchment. Frequency of available data varies from daily to monthly. For the purposes of this study monthly means were calculated for all rivers.

The concept of 'hydrological year' or 'water year' was considered here. USGS defines this in relation with surface water, as the 12-month year, starting on October 1st and ending on September 30th, the next year. WaterUK defines it in relation to precipitation and ground water, as the period of time beginning on October 1, when the autumn rainfall starts, considering the hydrological cycle in balance, until April 1st the next year, when evaporation starts acting on the accumulated water reserves and then until October 1st, again, when the cycle begins again.

The positive and negative phases of the North Atlantic Oscillations Index (NAOI) were compared to the seasonal and annual trend of both water and suspended sediment discharge. The data are available from 1821 to the present date (https://crudata.uea.ac.uk/cru/data/nao/index.html, Jones et al., 1997), as monthly averages. Considering the length of the data sets for the analysed rivers, annual averages of the NAOI were used for the comparison.

2.3.2. Methods

This study employs several statistical methods to identify trends and breaks in long-time series of water and solid discharge of seven European rivers, using monthly averages calculated from the available data.

2.3.2.1. Linear trends

The data were plotted and linear trends were fitted to the data, both for the entire period of time of the time series and also for the period of time with overlapping data for all rivers (1980-2006 for water discharge and 1980-2010 for suspended solids discharge), to allow inter-comparison. Linear trends, in this case, provide a first and simple measure of changes (Walling and Fang, 2003).

The values of maximum and minimum discharge of water and suspended solids discharge were plotted for all the time series. A linear and a moving average model with a window of 5 years were used to indicate trends in the data.

2.3.2.2. Time series decomposition

The time series analysis was performed using R software (R Project for Statistical Computing). The detailed script and explanations are presented in Annex 1.

Seasonal Trend Decomposition based on Loess (Locally Weighted Regression) – STL

The method was described by (Cleveland et al., 1990) and is summarized here. STL is a filtering procedure that decomposes a time series into trend, seasonal and remainder components. The method can be used on data series with missing values.

The general model is of the form:

$$Yv = Tv + Sv + Rv \qquad (2.1)$$

where Yv, Tv, Sv and Rv are the data, the trend, the seasonal and the remainder components, respectively, for v= 1 to N.

STL consists of a sequence of smoothing operations each of which, with one exception, employs the same smoother: locally weighted regression or loess.

The loess regression curve, g(x) is a smoothing of y given x along the scale of the independent variable, where x_i and y_i, for i=1 to n are measurements of an independent and dependent variable, respectively.

STL consists of two recursive procedures, an inner loop nested in an outer loop. In each of the passes through the inner loop, the seasonal and trend components are updated once. Each pass in the inner loop consists of a seasonal smoothing that updated the seasonal component, followed by a trend smoothing that updates the trend component.

The remainder is obtained in the outer loop, as:

$$Sv = Yv - Tv + Sv \qquad (2.2)$$

STL has six parameters, n(p) – the number of observations in each cycle of the seasonal component(ex. 12 for the monthly data, 365 for daily data), n(i) – the number of

passes through the inner loop (usually 1 or 2), n(o) – the number of robustness iterations of the outer loop (from 0 to 10, depending on the degree of robustness needed in the model) , n(l) – the smoothing parameter for the low-pass filter (is taken to be the least odd integer greater than or equal to n(p)), n(t) – the smoothing parameter for the trend component (it is an odd integer that satisfies the following criteria:

$$n(t) \geq \frac{1.5\, n(p)}{1-1.5n(s)^{-1}} \qquad (2.3)$$

and n(s) - the smoothing parameter for the seasonal component (has to be at least 7 and an odd number).

We have used the STL function in R studio, with an n(s) equal to 7. This generates the maximum value of the seasonal component in the de-trending result.

Breaks for Additive Seasonal and Trend – BFAST

The BFAST method is described by Verbesselt et al. (2010a). BFAST integrates the decomposition of time series into trend, seasonal, and remainder components with methods for detecting and characterizing abrupt changes within the trend and seasonal components, without the need to select a reference period, set a threshold, or define a change trajectory. It had been used by Verbesselt et al. (2012, 2010a, 2010b) to detect trend and disturbancies on satellite images and (Wang et al., 2014) to identify regime shifts of runoff and sediment loads.

The general model is of the form:

$$Yt = Tt + St + et, \quad t = 1,2,\ldots,n, \qquad (2.4)$$

where Y_t is the observed data at time t, T_t is the trend component, S_t is the seasonal component and the remainder component et denotes the remaining variation in the data beyond that in the seasonal and trend components.

If the entire time series has l breakpoints $\tau_1,\ldots\ldots,\tau_l$ in the trend component T_t, then the slopes and intercepts are estimated within each segment. The trend component is expressed as:

$$Tt = \alpha_i + \beta_i t \qquad (\tau_{i-1}<t<\tau_i) \qquad (2.5)$$

where i=1,….,l.

The intercept α*i* and slope β*i* can be used to assess the magnitude and direction of the abrupt change and slope of the gradual change between detected breakpoints.

A season-trend model (with harmonic seasonal pattern) is used as a default in the regression modelling (Verbesselt et al., 2010b). The seasonal component is fixed between the break points in the trend component, while it can vary across break points. If the time

series has *p* seasonal break points t_1, ….t_p, then the seasonal component St can be calculated as:

$$S_t = \sum_{k=1}^{k} \gamma_k \sin(\frac{2\pi kt}{f} + \delta_k) \qquad (2.6)$$

where the parameters γ_k and δ_k, which must be estimated, represent the segment-specific amplitude and phase. The known frequency *f* is equal to 12 for the monthly observations.

The ordinary least squares (OLS) residuals-based Moving SUM (MOSUM) test is used to test if one or more breakpoints are occurring (Zeileis, 2005). If the test indicates a significant change ($p < 0.05$), then the break points are estimated using the method of Bai and Perron (2003). To determine the number and positions of breakpoints, the BFAST model parameters are estimated by the following iterative steps:

Step 1: If the OLS-MOSUM test indicates that break points occur in the trend component, then the number and positions of the break points in the trend component τ_1,……,τ_l are estimated from the seasonally adjusted data Y_t-$\check{S}_t$.

Step 2: For a specific segment, the trend coefficients αi and βi are calculated using a robust regression method based on M-estimation. The trend component for the segment can be estimated by using $Tt = \alpha_i + \beta_i t$.

Step 3: Similarly, if the OLS-MOSUM test indicates that break points occur in the seasonal component, then the number and positions of the break points in the seasonal component t1,….tp are estimated from the detrended data Y_t-$\check{S}_t$.

Step 4: The parameters γ_k and δ_k for a specific segment are calculated using a regression method based on M-estimation; then, the seasonal component in each segment can be estimated as described above.

The data analysis was run in R studio using the BFAST function, choosing the harmonic model for seasonal component and a maximum number of iterations equal to 10.

2.4. RESULTS

2.4.1. Water discharge

2.4.1.1. Linear trends

The water discharge data for all seven rivers covers different time spans, starting from 1874 for Elbe to 1980 for Po. In order to compare in between trends in the seven rivers, both linear trends for the entire data set and for the comparison period of 1980 to 2006 were plotted (Fig. 2.2). The data were represented in a logarithmic scale, in order to better represent variations in the time series.

Four of the rivers have a general decreasing trend in water discharge – Nestos, Po, Ebro, and Thames. Two rivers, Danube and Tay, present an increasing water discharge over time. There is no obvious change in the Elbe's water discharge for the time period of the data set. The trends are significant at a 95% confidence level for the Danube, Nestos and Ebro.

The trends are mostly the same for the comparison period (1980 to the end of the time series), but the slopes change. For the Nestos and Ebro, the decreasing tendency is less abrupt than for the complete time-series. For the Danube the increase is more obvious, while for the Tay the increase is less abrupt. For the Elbe, the trend is negative, indicating a decrease of water discharge. The trend is significant at a 95% confidence level only for the Danube.

The trends are very similar for the entire period of the data sets and for the comparison period. Therefore, the rest of the statistical analysis was done on the entire data available for a certain river.

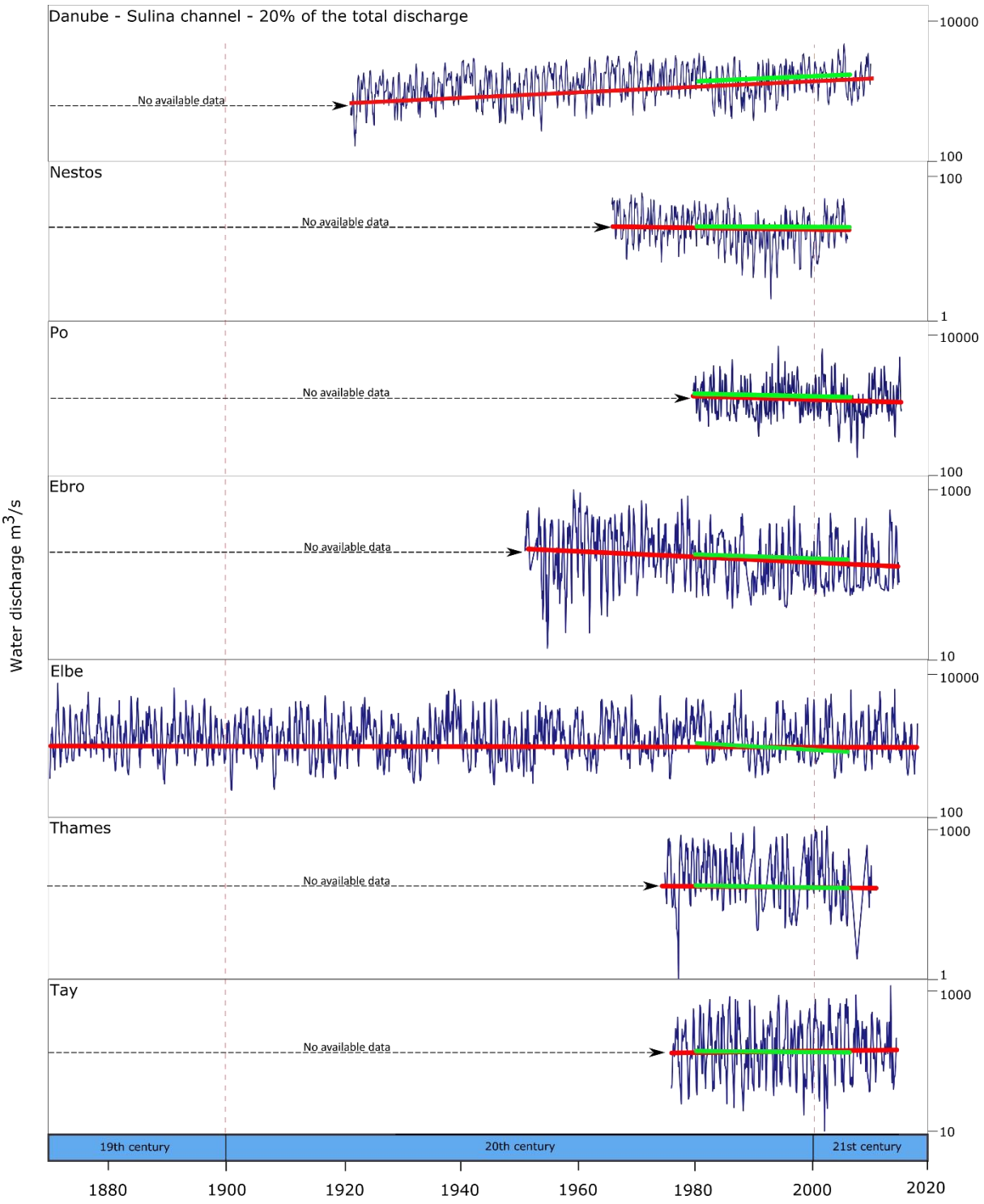

Figure 2.2 Water discharge data (in logarithmic scale) and general trends for the entire period (red line) and for the comparison period (green line). Note the different time spans and magnitudes of discharge.

Table 2.2 Summary of statistical results of the linear regression, for water discharge

River	Statistical parameters for the entire data sets			Statistical parameters for the comparison period		
	R^2	P value	Slope	R^2	P value	Slope
Danube	0.2079	0.0287	0.0135	0.036217	0.0005	0.0306
Nestos	0.0661	< 0.001	-0.0346	0.001	0.5800	-0.0002
Po	0.0011	0.5072	-0.0076	0.0034	0.2976	-0.0168
Ebro	0.0847	< 0.001	-0.0138	0.0086	0.1026	-0.0073
Elbe	0.0002	0.8532	-0.0127	0.0116	0.0529	-0.0159
Thames	0.0019	0.4209	-0.0008	0.0026	0.4085	-0.0011
Tay	0.0005	0.6960	0.0008	< 0.001	0.9269	0.0003

2.4.1.2. Evolution in time of maximum and minimum water discharge

The maximum and minimum water discharge were plotted as functions of time, for the entire time span of the data sets. This shows the seasonality of the yearly water discharge and also changes in time of the seasonality. The maxima and minima as a function of time are represented during a hydrological year, as it was defined in section 2.3.2.1. For all rivers a linear and a moving average model were fitted to the data, in order to assess such changes. For the Danube, most water discharge peaks occur in spring, from April to June. The data show a tendency of the peak occurring earlier during the year, with an offset of around month two. The trend is significant at a 95% confidence level ($p<0.05$; Table 2.3). The moving average model fitted to the data shows a periodicity of the peaks seasonality changing every 10 years, as it is shown in Fig. 2.3. In the case of Nestos, most of the peak discharges occur from February until May. The linear trend shows the tendency of this occurring later in the year, with an offset of one month, however the trend is not significant at a 95% confidence level ($p>0.05$). The moving average trend shows a periodicity of ~5 years. Po peak water discharge mostly occurs between August and October and there is no clear trend. The trend for the comparison period shows a tendency of the peak water discharge arriving earlier in the year, with a difference of two months, however, it is not significant at a 95% confidence level ($p>0.05$). The moving average trend shows a periodicity of 10 years. For Ebro, the peaks occur mostly from November until April. The trend, which is significant at a 95% confidence level, shows the peak water discharge is arriving earlier in the year, by almost 3 months. For Elbe, the peaks are grouped in the spring (February to May), with no clear trend in the data. The moving average trend shows a variation of 5 to 10 years. The trend for the comparison period shows the tendency of the peak water discharge arriving earlier with of offset of two months, however, the trend is not significant at 95% confidence level ($p>0.05$). For both Thames and Tay, the peaks do not have a clear seasonality. In the Thames, they seem to group between March and October, with no trend over the years. The moving average model shows a periodicity of 10 to 5

years. For Tay, the peak discharge can occur anytime during the year, but it seems to happen more during the intervals of January-March and October-November. There is a tendency of season shift in the peak discharge, of almost two months. The moving average model shows a variable periodicity, from 3 to 10 years.

For the Danube, most minima of water discharge occur during the October-January season. They show the tendency to arrive later in the year, but the trend is not significant at a 95% ($p>0.05$) confidence level. The moving average curve shows a general periodicity of 10 years. In the case of Nestos, most water minima occur in from July to October. They have the tendency to occur earlier, by 2 months, however the trend is not significant at a 95% confidence level ($p>0.05$). The moving average curve shows a periodicity of 5 to 10 years. For the Po, the water minima occur in the first five months of the year. They have the tendency to arrive later, however, the trend is not significant at a 95% confidence level ($p>0.05$). The moving average curve shows a periodicity of 10 years. For the Ebro, the water minima occur from July to October until the 1980's, when they start occurring more randomly during the year, January to October. This determines a tendency to arrive earlier, by two months. However, the trend is not significant at 95% confidence level ($p>0.05$). The moving average curve shows a variable periodicity, of 5 to 15 years. In the case of the Elbe, the water minima are grouped from August until January. They have the tendency to arrive later in the year, by almost 3 months. The moving average curve shoes a more obvious periodicity from the 1940's onwards, of 10 years. Both Thames and the Tay show less seasonality for the water minima. For the Thames, most water minima occurs in December and February, but the general tendency is of arriving later in the year. The trend is not significant though. The moving average trend show a more pronounced seasonality, of 5 years, compared to other rivers. For the Tay, most water minima occur in August and October. The trend shows a tendency of arriving earlier in the year, but again, it is not significant at a 95% confidence level ($p>0.05$). The moving average shows the same pronounced seasonality of 5 years.

Figure 2.3 Evolution in time of peak water discharge for the studied periods and linear trends for the entire period (red lines) and the comparison period of 1980 to 2006 (green lines)

Figure 2.4 Evolution of minimum water discharge for the studied periods and linear trends for the entire period (red lines) and the comparison period of 1980 to 2006 (green lines)

Table 2.3 Summary of statistical results of the linear regression, for peak water discharge

River	Statistical parameters for the entire data sets			Statistical parameters for the comparison period		
	R^2	P value	Slope	R^2	P value	Slope
Danube	0.0568	0.0236	-0.0184	0.0148	0.5456	-0.0305
Nestos	0.0092	0.5507	0.016	2.53E-05	0.9801	0.0012
Po	0.0066	0.6472	0.0365	0.0257	0.4240	-0.0921
Ebro	0.0844	0.0198	-0.0369	0.0308	0.3805	-0.0616
Elbe	0.0073	0.3094	0.0036	0.0390	0.3229	-0.0396
Thames	0.00001	0.9823	0.001	0.0056	0.7089	0.0311
Tay	0.0167	0.4328	0.0374	0.0116	0.5924	0.0439

Table 2.4 Summary of statistical for the linear regression, for minimum water discharge

River	Statistical parameters for the entire data sets			Statistical parameters for the comparison period		
	R^2	P value	Slope	R^2	P value	Slope
Danube	0.0227	0.1563	0.0264	0.0017	0.8382	0.0244
Nestos	0.0188	0.3925	-0.0369	0.0112	0.5977	-0.0457
Po	0.0105	0.5646	0.0231	0.0662	0.1948	0.0714
Ebro	0.0225	0.2371	-0.0254	0.0077	0.6632	-0.0329
Elbe	0.0232	0.0681	0.017	0.0019	0.8272	0.0280
Thames	0.0479	0.1929	0.0626	0.0255	0.4257	0.0659
Tay	0.0203	0.3869	-0.0472	0.0695	0.1837	-0.1233

2.4.1.3. Time-series decomposition

The seasonal trend decomposition reveals different tendencies for the seasonal variations and trends (Fig. 2.5). For the Danube, both seasonal and trend component have similar magnitudes and they are small compared to the variation in the data. There is a clear variation in the amplitude of the seasonal component every 5 years. The seasonal component shows a period of 12 months. The trend shows increasing water discharge until 1980, then a decrease from 1980 to 1990 and then another marked increase onwards. For the Nestos water discharge data, the seasonal component has greater magnitude than the trend. It exhibits amplitude variations with a time span of 10 years. The period is of 12 months. The general trend shows a decrease in water discharge over time, until the beginning of the 21st century, when there is a slight increase compared to the previous period. Also, for the Po, the seasonal component has greater magnitude than the trend. It exhibits amplitude variations with a time span of 10 years. The period of the seasonal trend is of 9 months. While the general trend indicated a decrease in water discharge, there are

three distinct peaks around 1995, 2000 and 2010 and four troughs around 1990, 1997-1998, 2007 and 2012. In the Ebro water discharge data, the seasonal component has greater magnitude than the trend, and its amplitude presents a variation every 10 years. The general period of the trend is of 12 months. The trend indicates decreasing water discharge over time, with a relative constancy from 1990 onwards. The results for the Elbe River show a greater amplitude in the seasonal component than in the trend. The seasonal amplitude displays a variation at every 5 to 10 years and a period of 12 months. The trend shows no general tendency but rather increasing variability over the studied period. There is a period of constant peaks and minima from 1874 to mid 1930's, followed by a peak around 1940. The remaining period is characterised by a regular succession of peaks and minima. For both Thames and Tay, the magnitude of the seasonal component is greater than the trend. The amplitude of the seasonality changes with a period of 5 years. Both rivers exhibit a period of the seasonal component of 6 months. For the Thames, the trend is constant from 1974 to mid-1990's, followed by a marked peak around 1995 and a minimum centred in 2000. The remaining period is characterised by a relatively constant trend. The Tay river water discharge shows a very variable trend, characterised by peaks (centred around 1982, 1990, 1996, 2008) and minima (1985, 1992, 2003, 2011).

The seasonal components and trends for all rivers were compared with the North Atlantic Oscillation Index (NAOI) (Fig. 2.6). Considering the long time period examined here, yearly averages were used to plot NAOI data. The positive phases of NAOI are associated with above-normal precipitation over northern Europe and Scandinavia and reduced precipitation over southern and central Europe. Opposite patterns of temperature and precipitation anomalies are typically observed during strong negative phases of the NAO (https://www.ncdc.noaa.gov/teleconnections/nao/).

The positive phase, marked in red, show some association with the lows of the trend component of the water discharge for the Danube, the Nestos, Po and Ebro and with the highs of the Elbe, Thames and Tay. The best fit seems to be with the Nestos and the Ebro, especially during the 20th century. The more extended positive phases seem to coincide with low water discharge for the Danube, Ebro, Po and Nestos and they mark an increase in the trend of the Elbe, Thames and Tay.

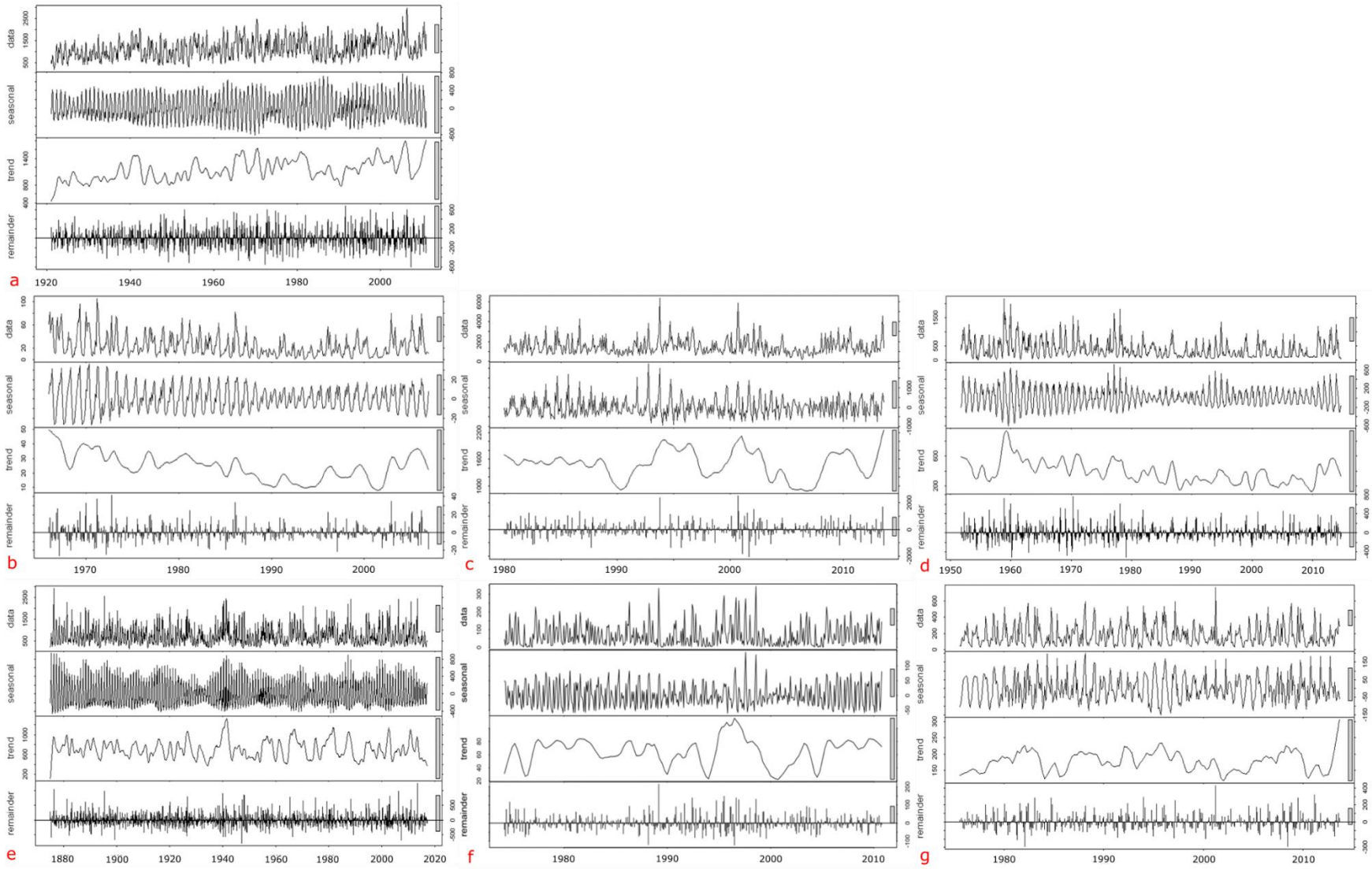

Figure 2.5 Seasonal trend decomposition (STL) analysis for water discharge. The four panel represent the original data, the seasonal component, the trend and the remainder, for the analysed period of time (years on the horisontal axis). a. Danube, b. Nestos, c. Po, d. Ebro, e. Elbe, f. Thames, g. Tay

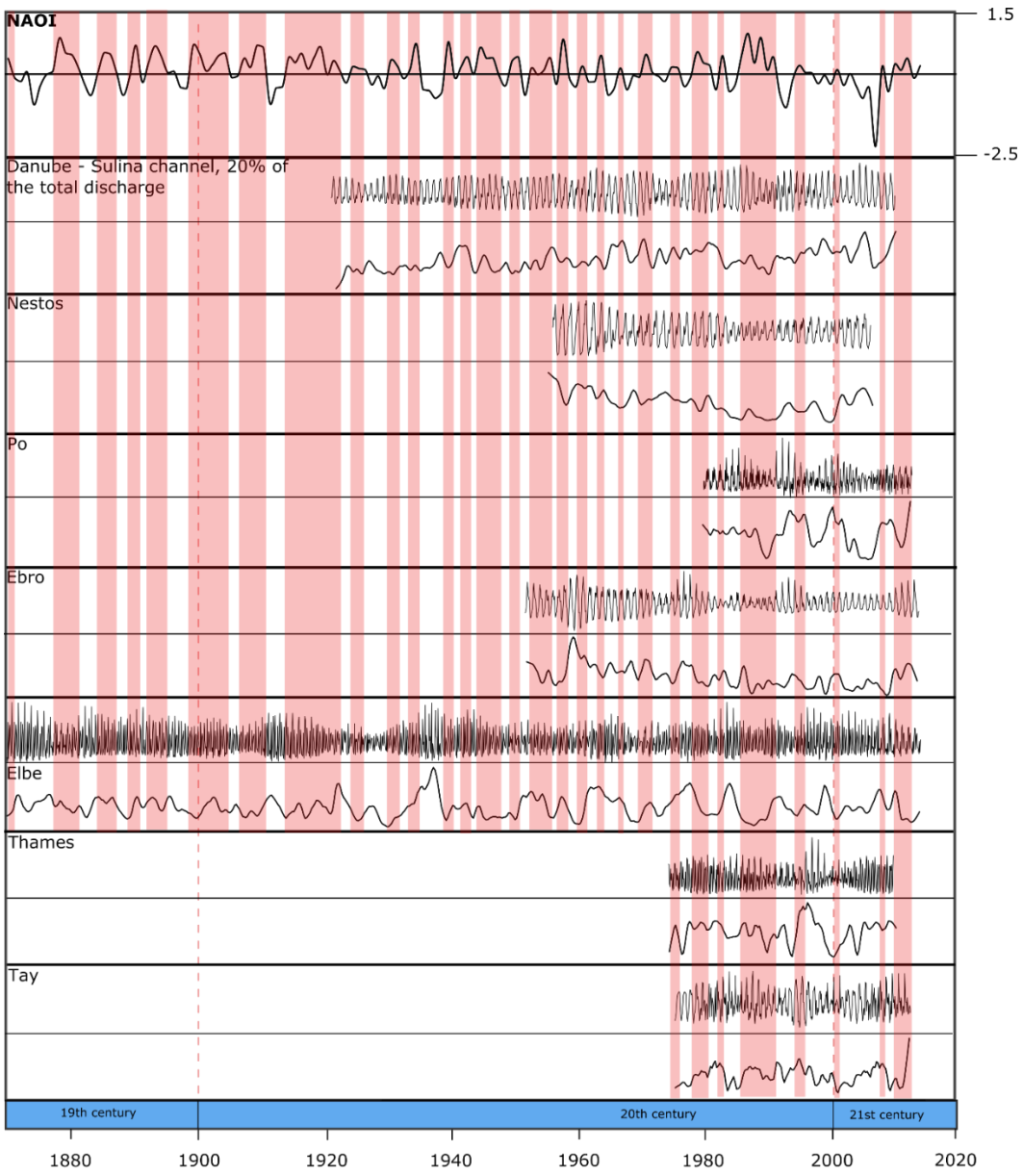

Figure 2.6 Comparison between North Atlantic Oscillation Index (yearly averages) and water discharge, seasonal component and trend for the seven rivers. The positive phases are marked in red

2.4.1.4. Identifying breaks

The BFAST method was used to detect breaks in the water discharge trend. The results are shown below (Fig. 2.7) and summarized in Table 2.4. Breakpoints were detected in the trend component of water discharge for the Danube, Nestos, Po, Ebro and Elbe and no breakpoints for the Thames and Tay. Two of the four breakpoints for the Danube decreasing trends coincide with the construction periods/operation of the two major dams built in the Lower Danube, Iron Gates I and II. There are three breakpoints for the Nestos, of which the last two are timed before and after the building of the two major dams in the Greek part of the river. However, they do not show any trend. The water discharge data for the Po spans only 33 years so it is recorded after the construction of the Isola Serafini dam. The water discharge

trend of the Ebro records two breaking points, the firsts of which can be associated with the construction period and operation of two major dams in the Lower Ebro – Mequinenza and Ribaroja (decreasing trend). The case of the Elbe is quite particular as there are no dams along its middle and lower reaches. Most major dams are built in the Upper Elbe and its tributaries (see Table 2.4). The Geesthacht weir, which is located just at the tidal limit of the Elbe, before Hamburg, was only built in 1960. The two breaking points in the trend of the Elbe water discharge cannot be correlated with the input of dams in its catchment. There are no breakpoints for the Thames and the Tay. As described before, there are no dams along the courses of the Thames and only in the very upper reaches of the Tay River.

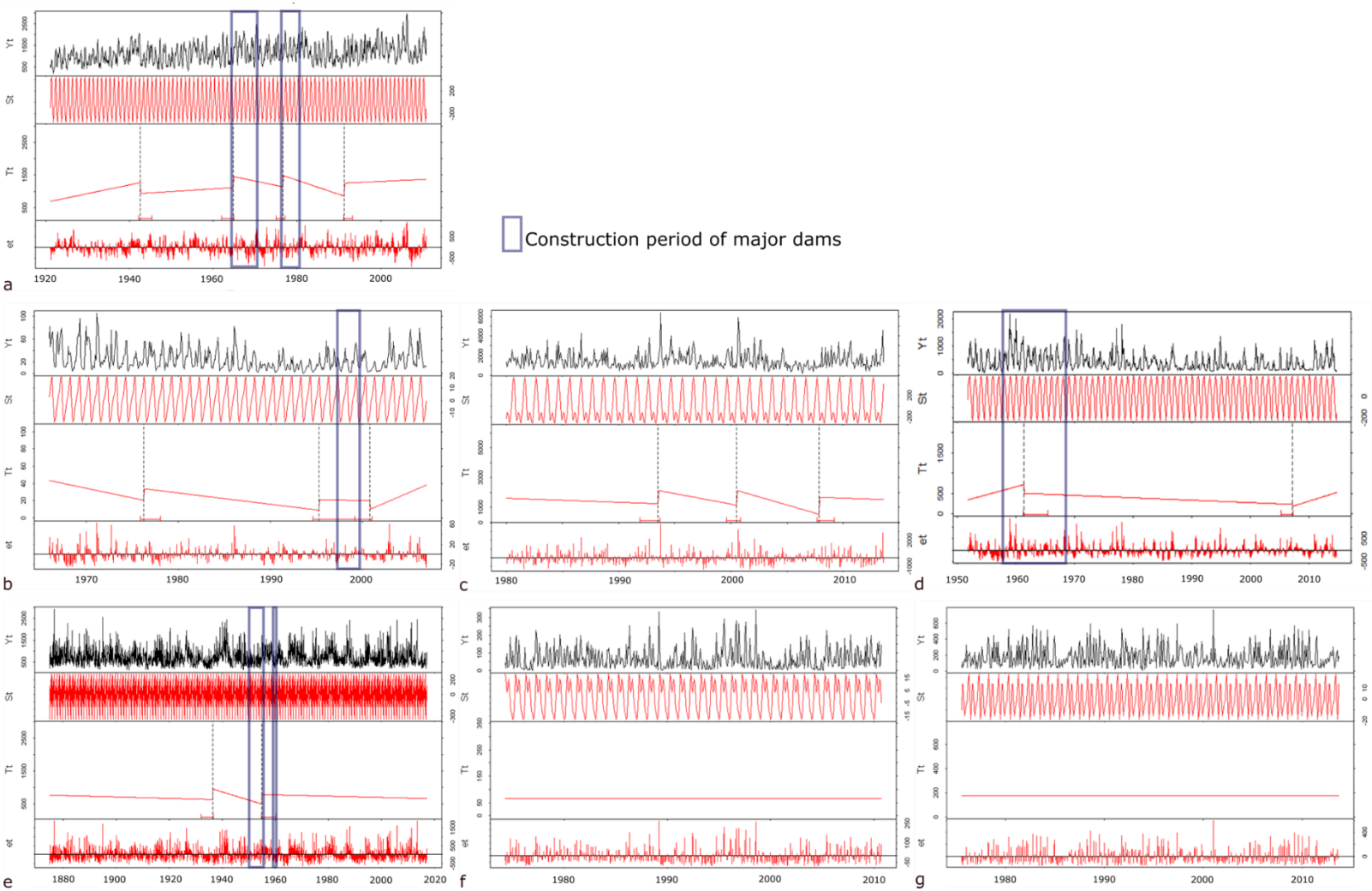

Fig. 2.7 Breaks for Additive Seasonal and Trend for (BFAST) analysis for water discharge. The four panel represent the original data (Yt), the seasonal component (St), trend with break points (Tt) and remainder (et), in the studied period of time (years on the horizontal axis). a. Danube, b. Nestos, c. Po, d. Ebro, e. Elbe, f. Thames, g. Tay . The grey squares represent the period of construction of major dams on the course of the river (Danube, Nestos, Ebro) or in the river catchment (Elbe). See table 2.4 for details

Table 2.4 Summary of statistical results of the BFAST analysis for water discharge

River	No of breakpoints	Breakpoints (with 97.5% confidence) and trend	Most significant break	Years of major dams construction/operation in the catchment
Danube	4	1942-1945 ↑ 1964↓ 1976-1977 ↓ 1991-1993↑	1991-1993	1964-1972 (Iron Gate I) 1977-1982 (Iron Gate 2)
Nestos	3	1976-1978↓ 1995-1996-- 2000↑	1976-1978	1997 (Thisavros) 1999 (Platanovrysi)
Po	3	1992-1993↓ 2000 ↓ 2007-2009 ↓	2007-2009	1955-1962 (Isola Serafini); outside the range of the time series
Ebro	2	1961-1965↓ 2007 ↑	1961-1965	1957-1965 (Meqquinenza) (?-1969) Ribarroja
Elbe	2	1937↓ 1954-1957--	1937	No dams on the Middle and Lower Elbe 1949-1955 - Slapy dam (on Valtava); Geesthacht weir – 1960 on the Lower Elbe.
Thames	0	-	-	-
Tay	0	-	-	Breadalbane Hydropower Scheme (1951-1961); outside the range of the time series

2.4.2. Suspended solids discharge

2.4.2.1. Linear trends

Suspended solids data were available for five rivers. They cover different time spans, from 1921 for the Danube to the 1980's for the Ebro. In order to compare between trends in the five rivers, both linear trends for the entire data set and for the period of 1980 to 2010, were plotted (Fig. 2.8). The data was plotted in a logarithmic scale, in order to better represent variations in the time series.

All rivers record decreasing trends for the suspended solids discharge. The trend is more abrupt for Danube and Elbe. The decrease is less marked for Ebro, Thames and Tay. All these trends are significant at a 95% confidence level ($p<0.005$).

Trends are similar for the period of direct comparison (1980-2010). The decrease is more abrupt for the Danube and the Elbe, compared to the other rivers. The trend is only significant at a 95% confidence level ($p<0.005$) for the Danube and the Thames (Table 2.5).

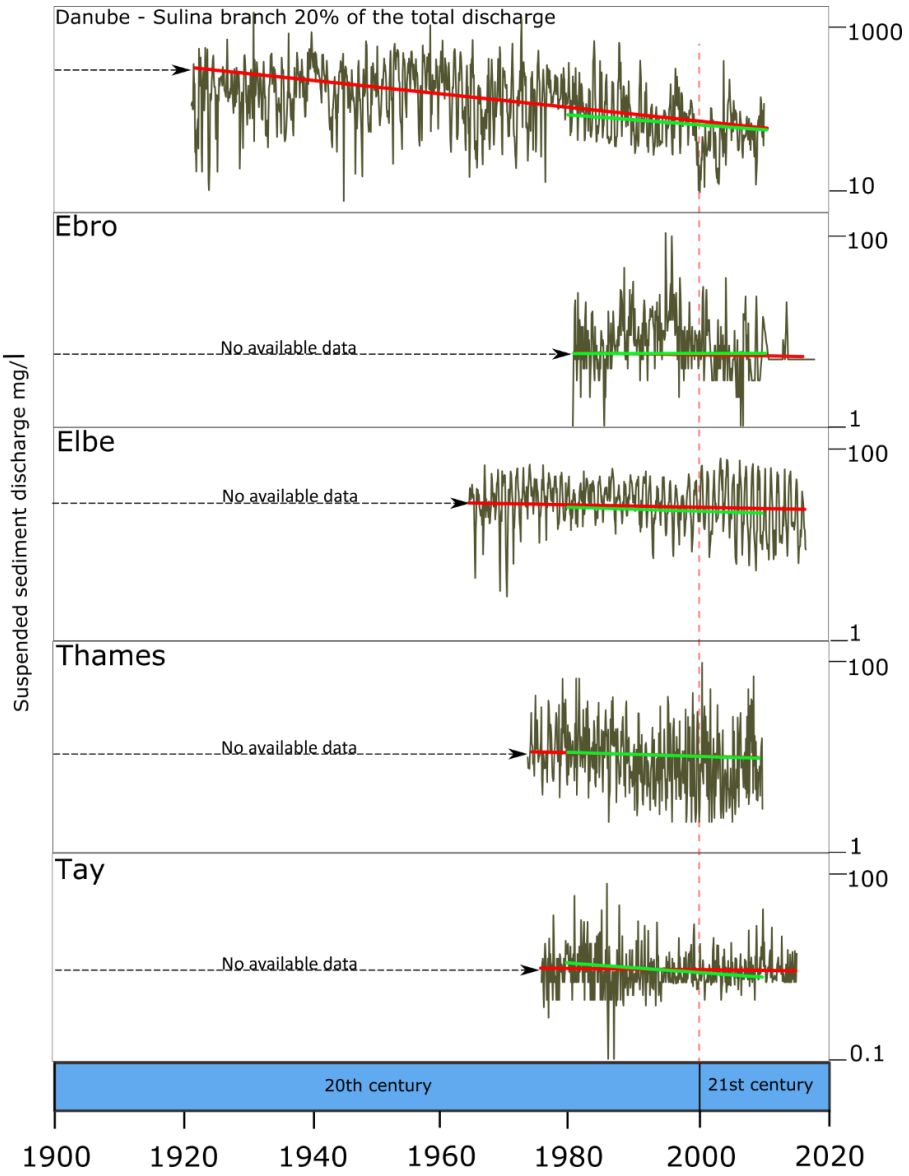

Figure 2.8 Suspended solids discharge data and general trends, for the entire length of the data sets (red line) and for the comparison period (green line). The data is in logarithmic scale. Notice the different time spans and magnitudes of solid discharge

Table 2.5 Summary of statistical results of linear regression, for suspended solids discharge

River	Statistical parameters for the entire data sets			Statistical parameters for the comparison period		
	R^2	**P value**	**Slope**	**R^2**	**P value**	**Slope**
Danube	0.1129	< 0.001	-0.0059	0.1088	< 0.001	-0.0095
Ebro	0.0115	0.0450	-0.0003	0.0028	0.3417	-0.0002
Elbe	0.0236	0.0001	-0.0004	0.0293	0.0980	-0.0007
Thames	0.0151	0.0091	-0.0178	0.0073	0.0256	-0.0006
Tay	0.01	0.0153	-0.0002	0.0095	0.0773	-0.0005

2.4.2.2. Evolution in time of the maximum and minimum suspended solids discharge

Similar to the water discharge analysis, maximum (Fig. 2.9 and Table 2.6) and minimum (Fig. 2.10 and Table 2.7) suspended solids discharge were plotted as a function of time, to assess changes in seasonality, for the periods when data was available. While the peak suspended solids discharge varies during the year for the Danube, it seems to group in the early to late spring season, coinciding with the melting season in the Danube catchment (February to June). The trend shows a tendency of the peak arriving later but is not significant at a 95% confidence level. After the 1980's most of the sediment peaks group more in the spring-summer season, with no peaks occurring October to January. The moving average model shows a periodicity of 10 years. For the Ebro, the peak of suspended solids discharge also varies greatly during the year, September being the month with the most peaks during the analysed period. The trend shows a tendency of arriving earlier, by two months. However, the trend is not significant at a 95% confidence level. The moving average model shows a periodicity of 5 to 10 years. In the case of the Elbe, the shift in peak discharge is very marked. Until the beginning of the 21st century, the peaks occur mostly from June to August, while afterwards, they occur earlier, from December to April. The linear models show a shift of 3 months and it is significant at a 95% confidence level. The moving average model shows a periodicity of 5 to 10 years for the studied period. Both Thames and Tay have peak suspended solids occurring very variably during the course of the hydrological year. There is no clear trend for these two rivers. The moving average models show a periodicity of 5 years. The trends for the comparison period of 1980 to 2010 are similar, but none are statistically significant at a 95% confidence level.

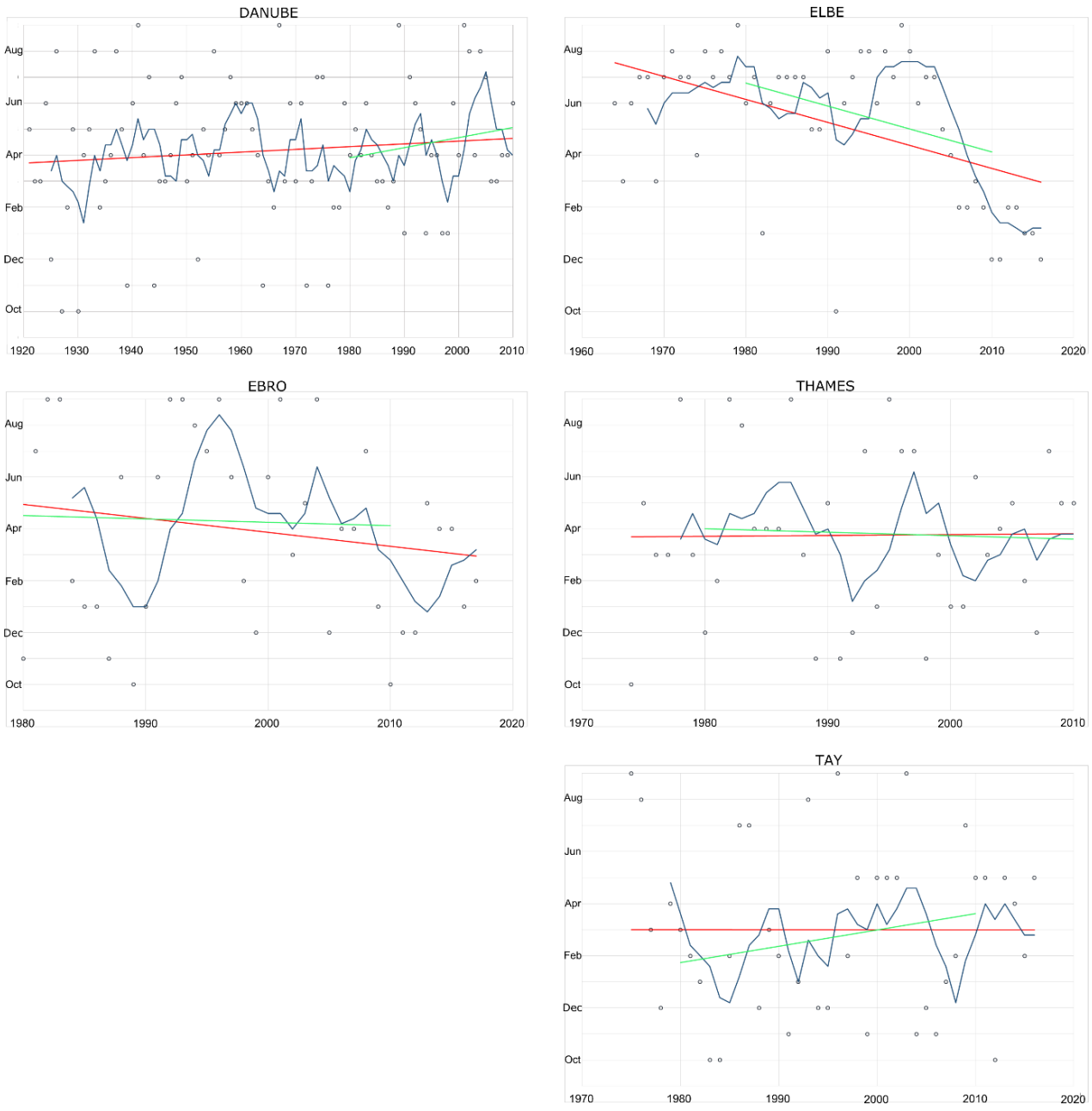

Figure 2.9 Evolution in time of the peak suspended solids discharge for the studied period and linear trends for the entire period (red lines) and the comparison period of 1980 to 2010 (green lines)

Table 2.6 Summary of statistical results of linear regression, for peak suspended solids discharge

River	Statistical parameters for the entire data sets			Statistical parameters for the comparison period		
	R^2	P value	Slope	R^2	P value	Slope
Danube	0.0109	0.3284	0.0105	0.0238	0.4067	0.0387
Ebro	0.0278	0.3168	-0.0541	0.0010	0.8646	-0.0133
Elbe	0.2394	0.0002	-0.0881	0.0880	0.1050	-0.0879
Thames	0.0001	0.9467	0.0033	0.0014	0.8366	-0.0133
Tay	4E-07	0.9969	-0.0002	0.0294	0.3558	0.0625

The suspended solids minima for the Danube can occur at any time during the year, however, most occur from August until January. The trend shows the tendency of the suspended solids minima occurring later in the year, by two months, however it is not significant at a 95% confidence level. The trend for the comparison period of 1980 to 2010, however, shows the opposite tendency, with more suspended solids minima occurring in the winter rather than late summer and autumn. This trend is only significant at a 92% confidence level. The moving average curve shows a periodicity of 5-10 years, marking a shift around the 1970's. After this time, more suspended solids minima occur in August-September rather than October to December. For the Ebro, also, the suspended solids minima can occur at any time during the year. They tend to occur more often from December until May. There is a tendency of later occurrence, while the trend is not significant at a 95% confidence level. The trend of the comparison period shows the opposite tendency, with suspended solids minima happening earlier in the year. The moving average curve shows a seasonality of 5 to 10 years. In the case of the Elbe, there is a clear shift of season for minimum suspended solids discharge, indicated by a trend, which is significant at a 95% confidence level. Until the beginning of the 21st century, the suspended solids minima occur mostly from December until March. Afterwards, they mostly occur from April to September. The trend of the comparison period is similar. The moving average curve does not show any seasonality during the studied period. For the Thames River most of the suspended solids minima occur in November, March and July, but there's no clear seasonality to it. Interestingly, the trend, which is significant at a 95% confidence level, shows a shift in the minima from winter to summer season. The trend remains the same for the comparison period. The moving average shows a seasonality of 5 years. The Tay River shows no clear trend for the minima of suspended solids discharge, but they tend to occur more often from September until February. The moving average model shows a variation in the season at every 5 years.

Figure 2.10 Evolution in time of the minimum suspended solids discharge for the studied period and linear trends for the entire period (red lines) and the comparison period of 1980 to 2010 (green lines)

Table 2.7 Summary of statistical results of linear regression, for minimum suspended solids discharge

River	Statistical parameters for the entire data sets			Statistical parameters for the comparison period		
	R^2	P value	Slope	R^2	P value	Slope
Danube	0.0204	0.1795	0.0233	0.1043	0.0763	-0.1532
Ebro	0.0504	0.1756	0.0557	0.0051	0.7006	-0.2564
Elbe	0.2947	< 0.001	0.1061	0.2789	0.0022	0.1866
Thames	0.1117	0.0431	0.1136	0.1460	0.0338	0.1568
Tay	0.0029	0.7326	0.0149	0.0004	0.9086	-0.0080

2.4.2.3. Time-series decomposition

The seasonal trend decomposition reveals different tendencies for the seasonal variations and trends of the suspended load (Fig. 2.11). For all rivers, the seasonal component has a greater magnitude in the data compared to the trend. In the case of the Danube, the amplitude of the seasonal component varies at a time interval between 4 to 10 years. Its period is of 11 months. The trend shows a decrease in solid load over time, with more variability until mid-1970's. There are three periods of higher suspended solids discharge, until 1975, centred on 1930, 1940 and 1960 and three periods of low discharge, centred around 1938, 1944 and 1966. For the Ebro, the interval of variation for the seasonal component is around 5 years. The period is of 8 months. The trend shows an increase in suspended solids discharge from the 1980's until 1995 and then a marked reduction. In the Elbe's suspended load discharge, the amplitude of the seasonal component varies with a time interval of 5 to 15 years. The period of the seasonal component is of 12 months. The trends show a decrease in solid load, with a clear variability over time. There are several periods of increase in solid load, centred around 1973, 1987, 2003 and several of relative decrease, centred around 1980, 1997 and after 2010. The amplitude of the seasonal component of the Thames data varies at every 5 years. The period is of 12 months or greater. The trend displays a variable pattern, with period of relative increased solid flux, centred on 1980, 1995, 2000, 2003 and periods of lower solids flux, centred around 1992, 1997 and 2002. There's a similar variation of the amplitude of the seasonal component in the case of the Tay. The period is of 6 months. The trends show a general decrease in solids flux over time. The period on 1975 to 1988 is characterized by relatively high solid discharge but this starts decreasing afterwards. There is a relative increase afterwards, around 2011.

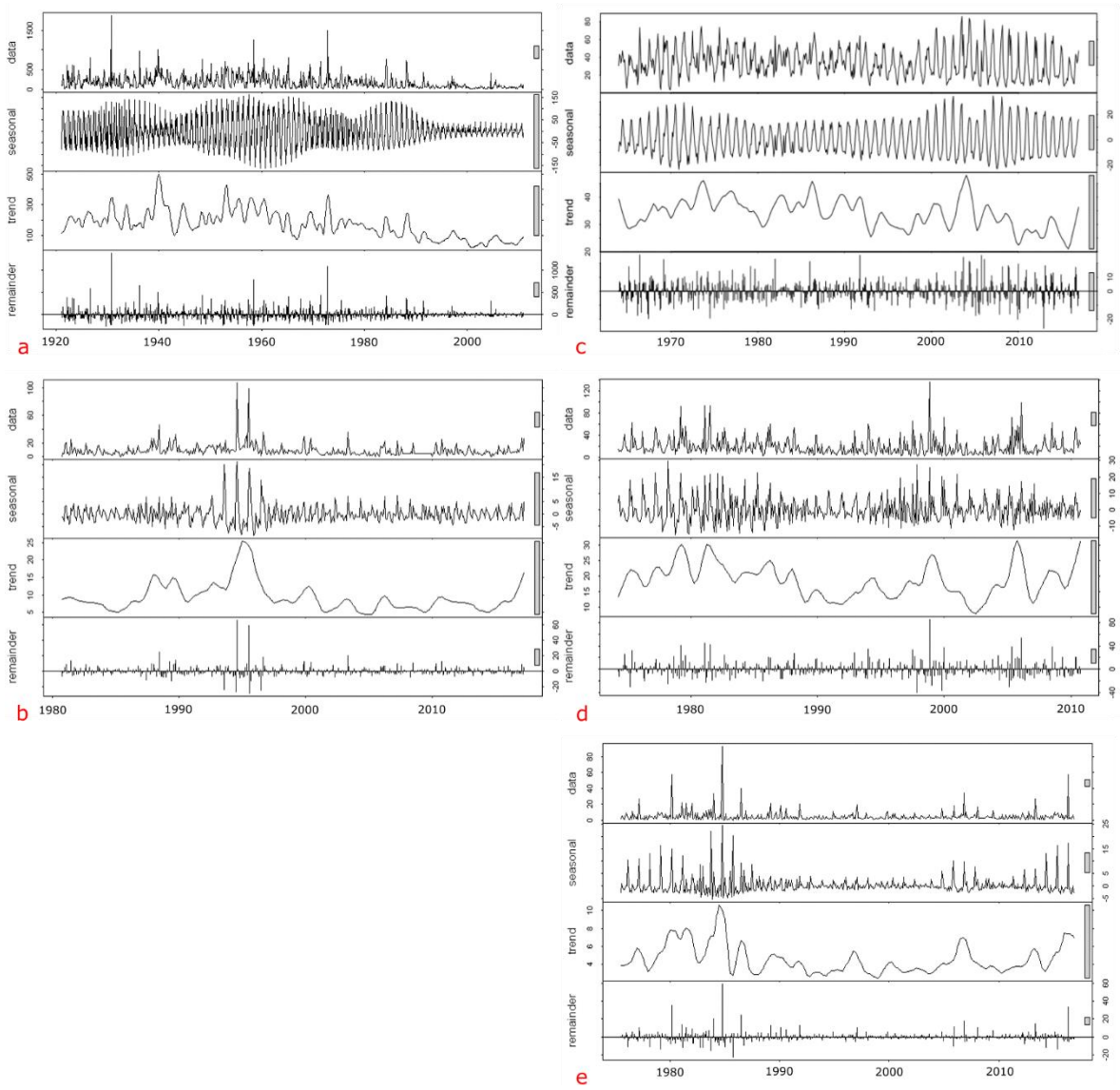

Figure 2.11 Seasonal trend decomposition (STL) analysis for suspended solids discharge (g/m^3). The four panel represent the original data, the seasonal component, the trend and the remainder. a. Danube b. Ebro c. Elbe d. Thames f. Tay

The seasonal and trend components of the suspended solids data was associated with the NAOI (Fig 2.12). Assuming that solid discharge in rivers is controlled to a certain extent by precipitation, the positive/negative phases of the NAOI could potentially modify the quantity of suspended solids across Europe. While some positive phases seem to be associated with some of the peaks for the Danube, Elbe, Thames and Tay, and with the beginning of a marked peak in the Ebro, the most extended positive phases coincide more with low solid discharge or they mark a downward trend.

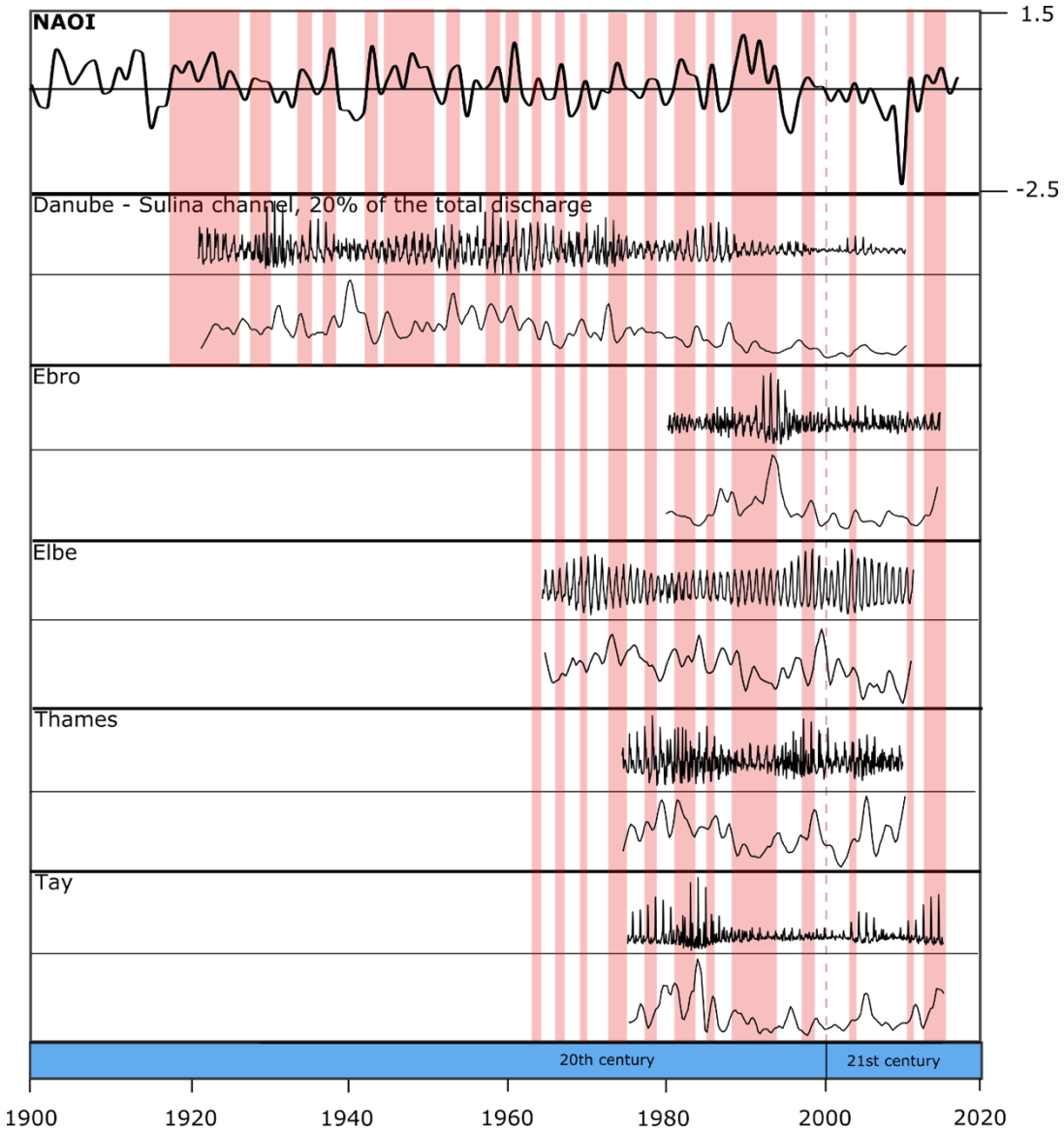

Figure 2.12 Comparison between North Atlantic Oscillation Index (yearly averages) and suspended solids discharge, seasonal component and trend for the seven rivers. The positive phases are marked in red.

2.4.2.4. Identifying breaks

The BFAST method was used to detect breaks in the water discharge trend. The results are shown below (Fig. 2.13) and summarized in Table 2.8. Breakpoints were detected in the trend component of the suspended solids discharge of the Danube and the Ebro and no breaking points were detected for the Elbe, Thames and Tay. There are three breaking points identified for the Danube. The last one (decreasing trend) of them, coincides with the construction phase of the Iron Gate I dam, the largest dams built on the Lower Danube and it precedes the construction of Iron Gate II (Table 2.6). The data set for the Ebro only spans 34 years. The two breaking points (decreasing trend) could not be associated with the onset of dams along the river. The two major dams, Mequinenza and Ribaroja (Table 2.6), were built before the data was recorded. In the case of the Elbe and Tay, there are no dams in their Middle and Lower reaches. Also, the data used for the

analysis war recorded after the completion of the dams built in their basins, which are located in the upper reaches of these two rivers. There are no dams built on the Thames and also the results do not show any breaking point.

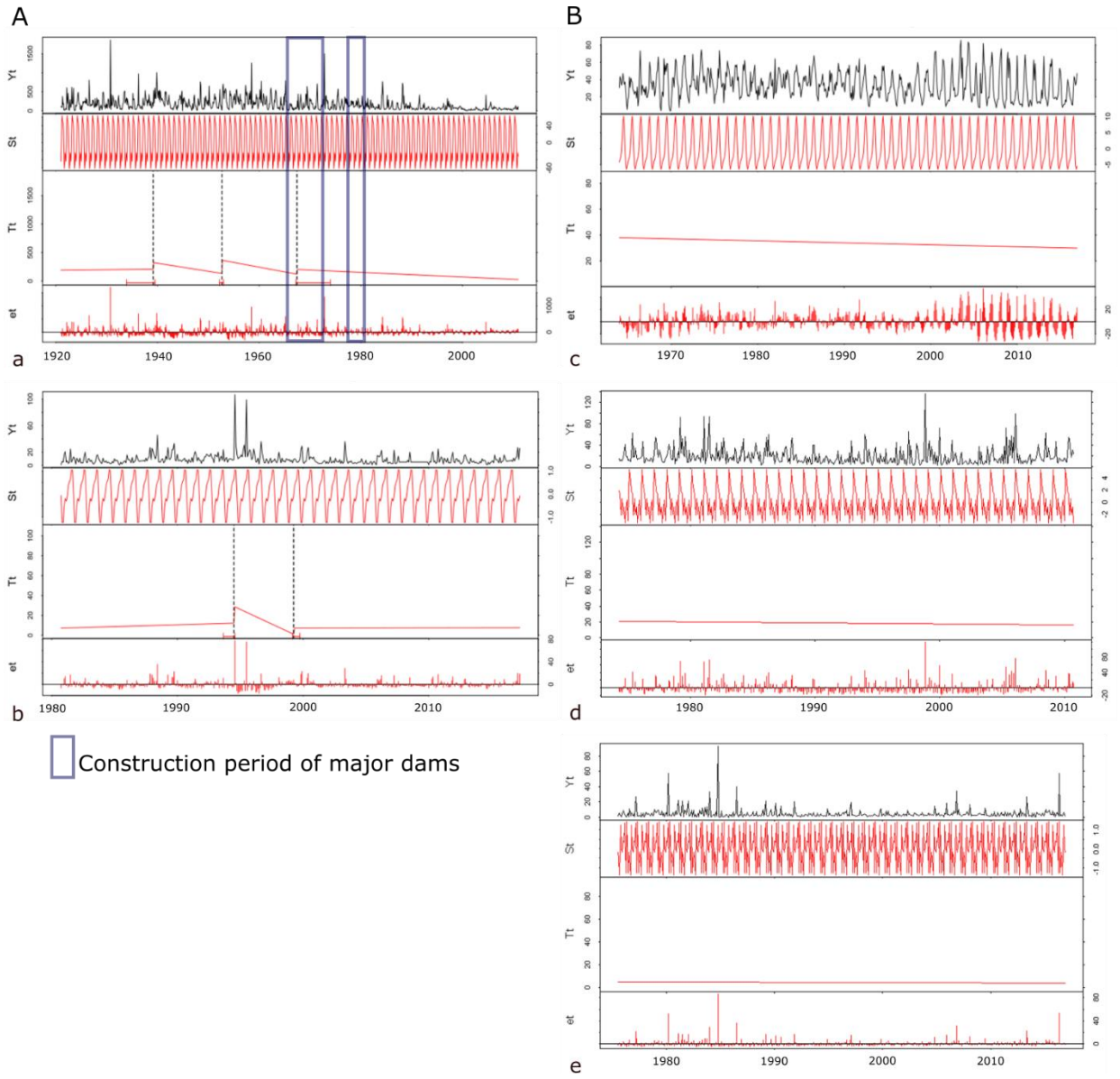

Figure 2.13 Breaks for Additive Seasonal and Trend (BFAST) for suspended solid discharge (g/m^{3}l). A. Rivers with breakpoints. A. Rivers with no breakpoints. The four panel represent the original data, the seasonal component, trend with break points and remainder. a. Danube b. Ebro c. Elbe d. Thames f. Tay. The rectangles mark the construction period of the main dams (see Table 2.6 for details).

Table 2.8 Summary of statistical results of the BFAST analysis for solids discharge

River	No of breakpoints	Breakpoints (with 97.5% confidence) and trend	Most significant change	Years of major dams construction/operation
Danube	2	1939↓ 1952-1953↓ 1967-1974↓	1952-1953	1964-1972 (Iron Gate I) 1977-1982 (Iron Gate 2)
Ebro	2	1994↓ 1999--	1994	1957-1965 (Meqquinenza) (?-1969) Ribarroja outside the range of the time series
Elbe	0			No dams on the Middle and Lower course 1949-1955 - Slapy dam (on Valtava). 1960 - Geesthacht weir on the Lower Elbe; outside the range of the time series
Thames	0	-	-	-
Tay	0	-	-	Breadalbane Hydropower Scheme (1951-1961); outside the range of the time series

2.5. DISCUSSION

2.5.1. Water and suspended solids discharge data

For this study, both water and suspended solids discharge data, available from stations located in the terminal zones of the river basins (delta, estuary), were gathered for seven European rivers (Danube, Nestos, Po, Ebro, Elbe, Thames and Tay). A statistical analysis approach was used to identify and compare trends in the data for all rivers. This posed several challenges.

For the analysis of suspended solids, the data available were either measured as suspended sediment or total suspended solids. While in some rivers, only one of these parameters are routinely measured, being considered synonyms, this is not necessarily the case. Comparison was made between the two analytical methods for measuring the mass of solid phase material in natural-water samples — suspended sediment concentrations (SSC), and total suspended solids (TSS) (Gray et al., 2000; Qizhong Guo, 2006). Results show that usually, methods used to measure TSS underestimates the amount of sand. This may not be a problem for certain rivers, where most of the suspended sediment consist of finer fraction (<50 µm). In the case of the Danube and other similar systems, where the suspended solid discharge consists of a wide range of particle sizes (from clay to sand, 0.4 to >125 µm), the two methods should not be used inter-changeable. In some river basins there is no data on suspended sediment or solids, gathered regularly. For example, suspended solids data sets were not available for the Nestos, because this is not routinely being measured in the basins (Gyorgyos Sylaios, personal communication).

Data sets cover different timespans so direct inter-comparison is only possible for a certain period of time (1980-2006 for water discharge and 1980-2010 for suspended solids

discharge). Also, the data from before the construction of major dams is not available in certain river basins, which is the case for Ebro, Elbe and Tay in this study.

The frequency of available data differs from monthly to weekly and to daily for different rivers. Also, some of the data series are incomplete. For this study, monthly averaged were calculated for all rivers. Using incomplete data sets and monthly averaged instead of more frequently measured data may fail to capture the natural variability of rivers, flattening the magnitude of extreme events, such as floods. One example is the Tay River. The 'Great Tay Flood' of January 1993 is not detected in the data set, because the measurements for this month are missing and overall, the frequency of measurements is 2-4 times a month.

The statistical analysis is applied to monthly data and the results should only be interpreted as such. This time interval might be enough for the present study, to understand change at decadal to century time scale, however, they have to be interpreted with caution.

2.5.2. Water and suspended solids discharge trends and main factors of change

Both water and suspended solids discharge of the all rivers changed over the analysed period. Generally, linear trends show an increase in the water discharge of the Danube and the Tay. The overall increase in water discharge of the Danube was previously shown by Bondar et al. (1991), and considered a consequence of gradual damming and especially of loss of wetlands in the basin (Panin and Jipa, 2002) by 68% (Hein et al., 2016). In this case, the evolution of water discharge, measured in the port of Sulina, reflects also the local effect of cutting and deepening of Sulina channel for maritime navigation. The water flow of Sulina increased from 7%, of the total flow of the Danube, in 1850's to 20% in the present (Bondar and Panin, 2001). In the case of Tay, increase in water discharge is not an effect of the land-use changes in the basin, as for the Danube, but as an effect of climate change, reflected in an increase winter runoff, already documented in the United Kingdom (Schneider et al., 2013).

Four rivers show decreasing trends in water discharge for the analysed period: Nestos, Po, Ebro and Thames, with significant trends for the Ebro and Nestos. A decrease in Nestos mean water discharge has not been documented before. The apparent decrease in water flow for the Po river is more likely caused by the water use practices in the basin (hydropower generation and agriculture), which is one of the most urbanised (260 habitant/km^2) and agriculturally intensive areas in Europe (Tesi et al., 2013). The decrease in water discharge in the lower Ebro was already estimated at almost 30%, during the last century (Ibàñez et al., 1996) and was attributed to increase of water use and evaporation from reservoirs. The apparent decrease in Thames water discharge may be due to the water use practices in the basin (water storage for domestic use), as the Thames is the main

supply of freshwater for fourteen million people (Whitehead et al., 2013). There is no clear trend for the Elbe's water discharge for the entire data set but there is an apparent decreasing trend for the comparison period of the last 30 years.

The seasonal evolution of high-water (analysed as water maxima) and low-water (analysed as minima) levels shows changes for all rivers. The high waters of the Danube, the spring peak, arrives earlier, with a shift from late spring to early spring. The seasonality of minimum water discharge also shows evidence of change, with the drought season shifting towards autumn, however, most minima are grouped from late summer to late winter. The evolution of high and low water discharge may reflect the size of the Danube basin and its various climate zones. The influence of changes in both precipitation patterns and seasonal temperature was observed in rivers discharge in Romania (Croitoru and Minea, 2015). Shifts in the melting season and reduced ice cover was documented in the Lower Danube, as a result of an increasing mean winter temperature (Ionita et al., 2018). Elbe's water maximum and minimum show a similar evolution with the Danube, with a tendency of the peak arriving earlier in the spring (this trend is shown for the comparison period of 1980 to 2006) and a shift in the dry season towards autumn.

The Ebro shows the same significant shift of water peaks. A clear shift in the seasonality of low water levels happens in the beginning of the 1980's, when they start happening more randomly during the year. There is a clear seasonality for Nestos, from late summer to early autumn, with a tendency of happening earlier in the summer. Generally, rivers in the Mediterranean region and NE Europe are primary climate change hot-spots – so it is more likely that the rivers in those areas will be more impacted in the future. From the studied rivers, the Danube and the Mediterranean rivers (Ebro, Po, Nestos) are more prone to climate change effects (Schneider et al., 2013; Giorgi, 2006).

For the Po, the Thames and Tay, water minima are more distributed during the year, with a tendency of arriving later in the year for the Po and Thames and earlier for the Tay. The Thames and Tay rivers, while situated in the same climatic zones, show different behaviour. Tay has a more evident shift of high-water discharge towards the spring time. This might be an effect of the increased precipitation during the spring season, in addition to snow melting in the Highlands. The increase of the water discharge of the Tay river, recorded in the middle reaches, at Bridge Kenmore, was observed by Black and Hardie (2000) and Gilvear and Black (1999), beginning with the late 1950's to the 1990's. They found an increase in extreme floods over the studied period (with three major floods occurring in the 1990'), and especially in the spring and winter flows, reflecting climate change effects in Scotland. Black (1996) has documented an increased flood frequency in Scotland since 1988, attributed to climate change, and noted a similar change in western Scandinavia (Hisdal et al., 1995). Smith & Bennett (1994) have shown that this increase is

concentrated in the winter half-year, and has led to increases in winter runoff of approximately 40% in the Tay catchment. An increase in the magnitudes of maximum flows in the United Kingdom and winter precipitation has already been described by Schneider et al. (2013). For the temperate oceanic zone, flow regimes are more uniform in a year, with broad winter peak or autumn peak in Scotland and summer low (Haines et al., 1988); generally, winter precipitation is increasing and summer precipitation is decreasing. The shift of the Thames water low levels towards the summer season is a direct consequence of the dry summers in the south of the UK.

Therefore, changes in seasonality of discharge for different rivers is the result of the size of the basin and the spatial patterns of climatic influences and changes over the basin. Water discharge of all rivers shows a strong seasonal component. The amplitude of the seasonal component varies between 5 to 10 years, and its period varies from 6 to more than 12 months. Rivers with large basins, such as the Danube, have the flow regulated by more than one dominant climate variable. The trend of the water discharge of the Danube shows some comparison with the negative and positive phases of the NAO index over Europe. Precipitations and the melting seasons in the Alps and the Carpathians have a combined effect both on water trend and seasonality. Nestos and Ebro and potentially other Mediterranean rivers show a dominant effect of precipitation patterns. The data for the Po shows it is less sensitive to changes in the NAOI, probably because it gets most of its waters from the Alps, where the seasonality of the runoff is controlled by snow and ice cover (Boldrin et al., 2005).

Breaking points were identified in the trend component for several rivers and correlated with the input of dams in the river basins, as main factors of trend change. The results show dams can create marked changes, in both water and suspended solids discharges. The analysis encompassed rivers with dams along their ways, in the middle or lower reaches (Danube, Nestos, Ebro), rivers with dams in the upper basin (Tay, Elbe) and rivers with no dams in the basin (Thames). The data set for the Po is too short to link breaking points with the input of dams. The Danube data sets provided the advantage of containing the same time span for both water and suspended solids discharge. The onset of the Iron Gate I and II dams (1964-1972 and 1977-1982, respectively) in its lower course, produces breaks in both water and suspended solids. Even if the water discharge increases over time, this method shows breaks in water discharge coinciding with the input of dams that look like temporary disturbance. For the suspended sediment, dams create breakpoints that mark a decrease in total concentration, as also identified by the linear trend analysis. Dams also create changes in water discharge trends for the Nestos, Ebro and the Elbe, marking decreases for all these rivers. The suspended solids data set for the Ebro is too short to correlate changes with input of dams, while there is no change in the trend

component of the Elbe data set. The Thames and Tay provide a distinct example, as the data sets for both water and suspended solids have the same length in time so they can be easily compared but they do not show any breaks in the trend component for water or suspended sediment discharge.

The amount of the suspended solids carried by rivers in their terminal zone – deltas and estuaries depend on a series of factors. Generally, they vary at different time scales: seasonal variations are related to catchment influence and type of climate, long term variations are related to river human activities (decennial to secular time scale) and climate variability (Pont et al., 2002). The suspended solids of a river, especially on long term, depends on the geomorphic/geological influences of basin area, lithology and relief; geographical influences of basin temperature, runoff and ice extent, and human activities that may accelerate or mitigate soil erosion and/or trap sediment (Sytvinski et Millimann, 2007). Dams and reservoir are the main traps of sediment (Dunn, 2017) but loss of natural wetlands also alters the flux of both water and suspended solids in rivers (Hein et al., 2016; Hudson and Hans Middelkoop, 2015).

For the analysed rivers it is interesting to notice an overall decrease in suspended solids discharge, which is significant, even for those rivers with no dams (Thames) in the basin, or with dams situated only on tributaries or in the upper catchment (Elbe and Tay). An important decrease in sediment discharge reaching the terminal areas of the Danube (50-70 **%** - McCarney-Castle et al., 2012; Panin and Jipa, 2002) and the Ebro (99% - Ibàñez et al., 1996; Rovira et al., 2015; Tena et al., 2011) river-sea systems has already been documented.

For the Danube, both suspended solids peaks and minima arrive slightly later in the years, however the minima show a shift after the mid-1970's, with a short-term tendency of arriving earlier. The peak is characteristic for the spring, when, after the melting season, precipitation enhances soil erosion and transport to the river and the high-water discharge probably helps dislocating higher volumes of sediments from the river valley, which arrive in the delta with a certain delay. It is interesting to notice that, beginning with this period, during winter, even with a scarce vegetation cover and increased soil erosion there are no maxima of suspended sediment discharge, even with a slight increase in the water discharge due to lack of ice cover (Ionita et al., 2018). In the same time, the trend component of the Danube suspended solids discharge shows a decrease after the 1970's. The increase in sediment due to soil erosion might not be high enough to surpass the dam barriers and the increase in water discharge during winter might not be high enough to remobilise sediment from the river valley and transport it to the end of the delta. As another contributing factor and indicator of climate change in Eastern Europe, winter precipitation

has decreased in the last 57 years (Croitoru et al., 2016; Croitoru and Minea, 2015), which could mean a decrease in surface erosion in this region.

The peak of suspended solids discharge of the Elbe River arrives mostly during the summer season (April-August), until the years 2000, when a marked shift is observed. The peaks start arriving in the winter-spring season (December-March), while the minima shift to the summer. The summer peaks have a high organic component that was documented by Hillebrand et al. (2018). Changes in soil erosion in Germany were previously attributed to climate change which causes changes in vegetation phenology and rainfall patterns (Routschek et al., 2014).

While the Ebro shows less seasonality of suspended solids discharge in general, there is a tendency for the peaks of arriving earlier, shifting from summer to spring and for the minima of arriving latter in the year, changing from winter to spring.

The Thames only shows a clear trend for the minima, a shift from the winter to the summer season. This shift towards summer season may be associated with the overall decrease in the summer precipitation in this region (Schneider et al., 2013), simultaneously with the peak of the vegetation growing season. The Tay does not show any tendency for the peak and a slight tendency for the minima of arriving latter in the year.

Suspended solids discharge of the analysed rivers also shows changes in seasonality but not as marked as the water discharge. The period of the seasonal component seems to vary more for the suspended solids discharge, compared to water discharge, probably because there are more factors controlling it, from basic activities in the basin like agriculture to natural variability related to soil erosion and primary production in the river (ex. Hillebrand et al., 2018; McCarney-Castle et al., 2012; Walling, 2008). Most of them have the same length as the hydrological year, with the exception of the Ebro (8 months). The trend components show similar general tendencies as the linear trends, while also revealing periods of change. Some of the periods of increased suspended sediment coincide or are marked by periods of above normal precipitation in Northern Europe.

All these results reveal the climate control over suspended solids discharge. The decrease is visible for all rivers with dams like the Danube, Ebro, Elbe. It is interesting to note that the suspended solid in the Danube Sulina branch are decreasing significantly after the input of the two dams, while the local works of transforming the branch into a maritime channel has no significant influence on this. From the present results, the seasonality of water and suspended solids discharge of the Danube seems to be affected by dam construction.

2.5.3. The implications of changes in water and suspended solids flows to the terminal areas of River-Sea Systems.

Deltas and estuaries are dynamic systems, which makes them important climate hot spots. The changes in water and suspended solids (and more specifically, sediments) are already causing severe consequences in these areas (e.g. Day et al., 2016; Yang et al., 2015), combined with sea level rise and storm surges. The most known examples include coastal erosion (see the examples of the deltas of Danube, Nestos, Ebro (Stanica et al., 2007; Xeidakis et al., 2010; Rovira et al., 2015) and degradation of habitats (Merchand and Guchte, 2010).

As shown in the previous sections, both water and suspended solids discharge of the analysed rivers change in time. Long-term trends show a decrease in suspended solids but also changes in seasonality. The decrease in sediment flux that feeds deltas and estuaries, due to the presence of dams in the river basin, and a change in seasonality of the sediment discharge, acting as joint factors, together with increased storminess during certain periods (ex. winter), might increase erosion during certain times of the year. Depending on the case, there is the question if this trend can be counteracted/ attenuated by increased spring flows and if the amount of the spring sediment peak might be enough to replace the sediment that is taken out of the system.

The sedimentation rate in the Danube Delta is still considered to remain above sea level rise in the Black Sea, in the next decades (Giosan et al., 2013). However, there is not much information on the overall change in sedimentary processes at the whole scale of the delta complex. The next chapter (Chapter 3) will try to answer this question, presenting the distribution of the sediment accumulation rates in various environments inside the delta plain, marine delta, front and prodelta.

Seasonality of suspended solids discharge is a key factor in understanding the functioning of ecosystems in river-sea systems. They feed the terminal areas of the systems as sediment supply and source of nutrients. Modified water and sediment flow equally influence ecological functioning of deltas and estuaries. The changes in transfer of water and associated particles from the basins to the sea will potentially impact the transfer of organic matter and nutrients (Engström et al., 2005), pollutants and other man-made particles (e.g. macro- and micro-plastics) (Chapman and Wang, 2001; Lechner et al., 2014) and the natural cycles of carbon and iron and other elements (Haywood et al., 2018; Wu et al., 2018).

Under current climate change scenarios, river runoff will change, increasing in norther Europe and decreasing in Central Europe and the Mediterranean region (Arnell and Gosling, 2013). Sediment fluxes will be modified by future hydrotechnical works and land-use practices. As deltas and estuaries are areas of particular sensitivity to change,

measuring just water and sediment fluxes might not be enough, especially if they are not routinely and systematically done. Moreover, previous studies have shown that a good estimate of the relation between the suspended solids and water discharge requires measurements over several decades (Eisma, 1993) and in all part of the basin, for a better basin management. For the deltas and estuaries, in particular, a better temporal and spatial resolution and a deeper understanding of the interplay between river, substrate and biota will be necessary. One of the tools that is currently being developed is Earth Observation, especially through the latest generations of satellites of the European Space Agency (Sentinel missions). Their use has already been proven efficient in retrieving concentrations of suspended particles (TSM – Total Suspended Matter), chlorophyll, and changes in land use and erosion/accretion and some studies show its uses at basin scale (Tyler et al., 2016). Chapter 5 will address EO uses in the Danube Delta coastal zone.

2.6. CONCLUSIONS

This study undertakes a comparison of water and suspended solids discharge of seven rivers, measured in their terminal areas, deltas and estuaries. The need for comparable and complete data sets, as well as an improved temporal and spatial frequency of data is identified. More and more studies on river-sea systems show the importance of using reliable and appropriate methods for measuring environmental parameters. To understand changing river-sea systems, at a global level, inter-comparable data sets are essential. The magnitude and frequency of more extreme events, as manifestations of climate change, call for an adequate frequency of measurements that will capture these phenomena, especially where early-warning systems might by necessary to avoid loss of human life or industrial accidents. Depending on the size and complexity of the river basin, a certain number of measuring station with appropriate temporal frequency might be necessary to capture the natural conditions of the system and to identify changes. As management strategies are based on the measured data from these systems, an incomplete or non-representative data input might lead to inappropriate decisions.

For all the analysed rivers, changes in trends of both water and suspended solids were identified. These changes depend on: the size of the catchment, the degree of the sensitivity of the river basin to climate changes, the number and placement of the dams in the catchment, the natural variability of the hydrological cycle in a year. A decrease in sediment discharge to deltas and estuaries was identified for all the analysed rivers, even for those rivers where major dams are not present or they are placed in the upper reaches of the catchment. Dams have also effects on the water discharge, either reducing the overall discharge to the sea or flattening the seasonal variations. Some of the controls of these changes are not well understood. Climate change affects both the total water discharge,

especially in the warmer climate areas, and modifies seasonal variability of high and low-waters, as well as total suspended sediment discharge.

Apart from the obvious effects of coastal erosion, other effects are not yet well described in the transitional environments of the analysed rivers. While it is easier to quantify long term changes in water and suspended solids pre and after dam input, the understanding of seasonal changes, as effects of climate change, need a more refined temporal and spatial investigation.

Understanding change in river-sea transition zone is very important for the long term-sustainability of use of such areas. The next chapters will explore the changes in sediment fluxes of the Danube in the Danube Delta and Black Sea area and will focus on the past 100 years (Chapter 3). The long term (Chapter 3) and short-term variation (Chapter 5) will be quantified, as well as the nature of the sediment flux (Chapter 4).

3. A CENTURY OF SEDIMENT FLUX VARIATIONS IN THE DANUBE-BLACK SEA SYSTEM

3.1. INTRODUCTION

The sediment flux of many of the world rivers has been substantially modified by anthropic interventions, such as by the building of upstream dams (Milliman and Farnsworth, 2011). The river-sea transitions zones, such as deltas, which are fed by the water and sediment fluxes, are very vulnerable to any changes occurring in their regime. Climate change, evidenced through changes in hydrological conditions, increased storminess and sea level rise, add to the impact and potential loss of sediment (Giosan et al., 2014; Syvitski et al., 2009; Tessler et al., 2015).

The Danube-Black Sea interaction zone is a vast and complex environment, from the apex of the Danube Delta to the NW Black Sea shelf. Humans have lived in the basin and the delta area for thousands of years (Giosan et al., 2012), as the Danube, as many world rivers, has been a favourable place for people settlements to thrive. It is considered that agriculture and deforestation have contributed to soil erosion and thus, to the growth of the delta complex (McCarney-Castle et al., 2011).

The last century has been marked by extensive anthropic interventions in the Danube basin with the extent of agricultural lands, embankment for flood protection (Constantinescu et al., 2015; Hein et al., 2016), construction of dams and reservoirs (Habersack et al., 2016) as well as direct interventions in the delta complex (Panin and Overmars, 2012). These interventions modify the flux of sediment that arrives and it is distributed in this area.

The Danube drains a large area of Europe and is interrupted in its way to the Black Sea by 78 dams and reservoirs (Habersack et al., 2016). It is estimated that the building of the major dams at Iron Gates I and II reduced the sediment flux reaching the Danube Delta by 50 to70% (McCarney-Castle et al., 2011; Panin and Jipa, 2002).

Chapter 2 shows how water and sediment fluxes are impacted by these upstream interventions, both in term of overall quantity but also regarding natural seasonality. The distribution of the sediment fluxes on this large and complex area is not known in detail. In this study we show results from 12 cores, gathered from selected areas of the Danube Delta complex (lakes, lagoons, channels, delta front and prodelta) of distributions and timely variations of sediment accumulation rates (SAR) and grain size. The timeline used for the SAR is based on ^{210}Pb dating and validated by ^{137}Cs profiles.

We want to explore the footprint of these marked changes in the basin, in a complex area such as the Danube Delta and the Black Sea shelf, looking at sediment flux

variations, as an indicator of marked change in its internal dynamics. Looking at a century scale gives us the opportunity to understand the effects of the most marked changes in the basin in the present and future evolution of the delta complex and the adaptive behaviour of this environment.

The main questions we address are:

I. What is the relation between sediment flux (water and sediment discharge, transport and dynamics) and sedimentation patterns (grain size, bulk flux, spatial distribution) in the Danube Delta and the Black Sea?

II. Is the impact of sediment starvation equal over different environments – lakes, lagoons, Black Sea shelf)?

III. What is the influence of extreme hydrological events on the delta-sea system? Can individual events be traced in the sedimentary records?

IV. What is the main deposition area, sedimentary characteristics, and main acting factors?

3.2. REGIONAL SETTING

3.2.1. The Danube – Black Sea interaction zone

The Danube River (Fig. 3.1) is the second longest river of Europe (2857 km), flowing from the Schwarzwald Mountains, in Germany, eastwards to the Black Sea, in Romani and Ukraine. The Danube has the largest drainage basin of Europe (801,463 km²), comprising 19 countries.

The Danube River is the largest source of source of water and sediment in the Black Sea, with a water discharge of about 205 km^3/y (60% of the total water runoff in the Black Sea basin) and 36.3 to 52.4 million tons of sediment per year respectively (48% of the total sediment reaching the Black Sea) (Ludwig et al., 2009; Mikhailov et Mikhailova , 2008). The NW Black Sea also receives freshwater input from the Dnieper, Dniester and Southern Bug, in a less significant amount, 12% and 2.5%, respectively (Mikhailov and Mikhailova, 2008). The Danube waters can be traces far southwards, to the Bosphorous region, as well as down to the deep-sea zone (Panin and Jipa, 2002).

The turbid, sediment-laden waters of the Danube flow in the brackish waters of the Black Sea and mix over a large area, as the Danube splits into several distributaries in the deltaic plain – Chilia (north) with a secondary delta (situated in Ukraine), Sulina (middle) and Sfantu Gheorghe (south).

The Danube Delta (Fig. 3.1) is the largest wetland in Europe and the largest delta in the European Union (second largest in Europe). Its present-day morphology is the results

of the interaction between the river and sea level changes in the last 10,000 years (Panin and Jipa, 2002). The total area of the Danube Delta is 5800 km^2, of which one fifth is located in Ukraine. The delta starts at Ceatal Izmail (Mile 43 from the mouth zone, measured along Sulina distributary), where the Danube splits into 2 branches – Chilia in the north and Tulcea in the south. The Chilia branch represents the border between Romania and Ukraine and it ends in a lobate delta with numerous distributaries (the main ones are the Oceacov flowing to NE, Stary Stambul oriented towards S-SE and Bastroe, oriented W to E). The Tulcea distributary flows from Ceatal Izmail, 17 km eastward and it splits in two at Ceatal Sfantu Gheorghe at Mile 33.84 (km 62.2), Sulina branch in the north and Sfantu Gheorghe in the south. As part of the Danube Delta, in the south there is the Razelm-Golovita-Zmeica-Sinoe lagoon system, which is separated by the sea through a littoral bar.

The delta is a flat zone, with an average altitude of about 0.52 m above the Black Sea mean level and with 93% of its territory under 2 m (Bondar and Panin, 2001). It has two distinct regions, separated by the Jibrieni-Letea-Raducu-Ceamurlia-Caraorman line: the fluvial delta, with a network of channel and lakes, constructed in the former Danube bay, and the marine delta, developed in the Black Sea, characterized by alongshore oriented beach ridges.

Chilia branch has a length of 111 km and transports the highest water flow, <50% of the total Danube discharge. The central branch, Sulina, which was cut for maritime navigation, is the shortest, 83 km initially and 62 km after cutting, and transports 19-20 % of the total flow. Sfantu Gheorghe, the southern branch has a length of 108 km, 70 km after meander cutting, and has an intermediate flow - 30% (Bondar and Panin, 2001). The hydrological engineering works along the Danube distributaries have modified their water flow in the last 150 years (Jugaru Tiron et al., 2009; Panin and Overmars, 2012).The cutting of Sulina and Sfantu Gheorghe branches meander loops altered the hydrologic conditions, shifting the distribution of water and sediment discharge in all three distributaries and changed bottom sediments grain size and distribution. Nowadays, along these two branches the bottom sediments are dominated by fine sand and silt, while on Chilia the bottom sediments are fine sand, silt and clay (Oaie et al., 2005, Opreanu et al., 2007).

The hydrographic network of the Danube Delta is complex, with about 3500 km of channels /canals which connect around 500 lakes (200,000 ha of water surface) (Cioaca et al., 2009). They are directly connected to the Danube through a vast network of channels and canals. The water level is variable in a year, depending on the river discharge (Hanganu et al., 2008).

The circulation of the Danube waters in the delta depends on the hydrologic regime of the river (Bondar, 1994). Thus, on the Danube distributaries, the water discharge varies on a longitudinal scale, because of the lateral channel and canals taking water but

also because of overbank spilling when the water discharge at the delta apex exceeds 9100 m^3/s (Bondar, 1996). Bondar (1994), calculated that the water discharge which the Danube releases in the delta plain increased from 1858 to 1980s almost four times. This was caused by the cutting and deepening of canals to facilitate access in different parts of the delta. This phenomenon is considered to have a positive impact in time for the sedimentation of the delta plain, as the sediment delivery increased and sedimentation rates are maintained, at least locally, above the contemporary sea level rise (Giosan et al., 2013) .Direction and gradients of water flow regime change inside the delta, depending on the water level. The variation of water level propagates from west to east (Poncos et al., 2013). Inside the delta alluvial sedimentation occurs mainly at the discharge point of a channel/canal into a lake. This process is very intense in the fluvial delta but it can also occur in the fluvio-maritime area. The Danube Delta is considered to act like a chemical and physical filter for the waters reaching the Black Sea, through its large and compact areas of reed (Cioaca et al., 2010b).

Most of the lake sediments of the delta plain consist of clay (20-30 %), silts (>65%), fine sand (6-15%), and shell fragments (2-4 %) (Mihailescu et al., 1996). They are significantly bioturbated as a result of the biological activity of annelid worms, insect larvae (mainly chironomids) and molluscs (Mihailescu et al., 1982).

The sediment transfer from the Danube onto the shelf and into the deep basin, in close relation with the general evolution of the Black Sea basin has been thoroughly reconstructed for the last 30,000 years (Constantinescu et al., 2015; Lericolais et al., 2007, 2009, 2010, 2011; Popescu et al., 2001, 2004). These studies revealed the influence of the Danube river-borne sediments from the shelf down to the abyssal plain, up to 2200 m depth (Popescu et al., 2001). The sediment transfer was mainly controlled by climate and a Black Sea level at ~120 m lower than today (Lericolais et al., 2009).

The present-day sediment dispersal patterns are described by Panin and Jipa (2002), as grouped into two main regions with different depositional processes: the internal shelf, fed by the Danube and the sediment starved external part of the NW Black Sea shelf (Fig. 3.1). Offshore from the subaerial delta lies the delta front (Fig. 3.1) with a total area of 1300 km^2 and the prodelta (Fig.3.1), at 50-60 m water depth, with an area of more than 6000 km^2. Beyond this area, the internal shelf receives clayey and silty sediments of the Danube, which move as a plume, not reaching the outer part of the shelf, but instead, moving south, along the Romanian and Bulgarian shores and finally discharging in the deep-sea zone of the pre-Borphorus region. The mean travel time of the Danubian waters to the Bosphorus strait was calculated by Sur et al. (1996) at 1-2 months (for a mean current speed of 10-20 cm/s and a distance of about 500 km). The external sediment starved shelf sedimentation is dominated by relict sediments or shells and does not receive direct inputs

of the Danube siliciclastic sediments (Panin and Jipa, 2002). The Danube-Black Sea interaction zone is thus largely restricted mainly to the internal shelf.

Using passive tracers, Bajo et al. (2014) observed the prevalence of Chilia's waters in the formation of the plume, while the waters of Sfantu Gheorghe follows the Sahalin spit and remain confined near the shores. The influence of Sulina is even more reduced, as it mixes with the waters of Chilia. The authors point out that instant patterns may be different, and the exact area and processes controlling the plumes should be investigated further. The plume extension is mainly restricted to the coast and shelf (maximum offshore extension of 70 km as estimated by Güttler et al., 2013), with a penetration depth of 15 m near the coast (Karageorgis et al., 2009), while the influence of the Danube waters, traced through simulated inorganic N/P molar ratios at the sea surface, can extend to the Turkish coast (Tsiaras et al., 2008). The main controlling factors for the formation and extension of the plume are hydrological (solid and liquid river discharge that varies seasonally), meteorological (wind speed and direction) and the topography of the shoreline (Güttler et al., 2013; Karageorgis et al., 2009). Wind seems to be the primary factor for surface water direction of flow but the haline stratification can limit its influence in the deeper layers, especially near the delta (Bajo et al., 2014).

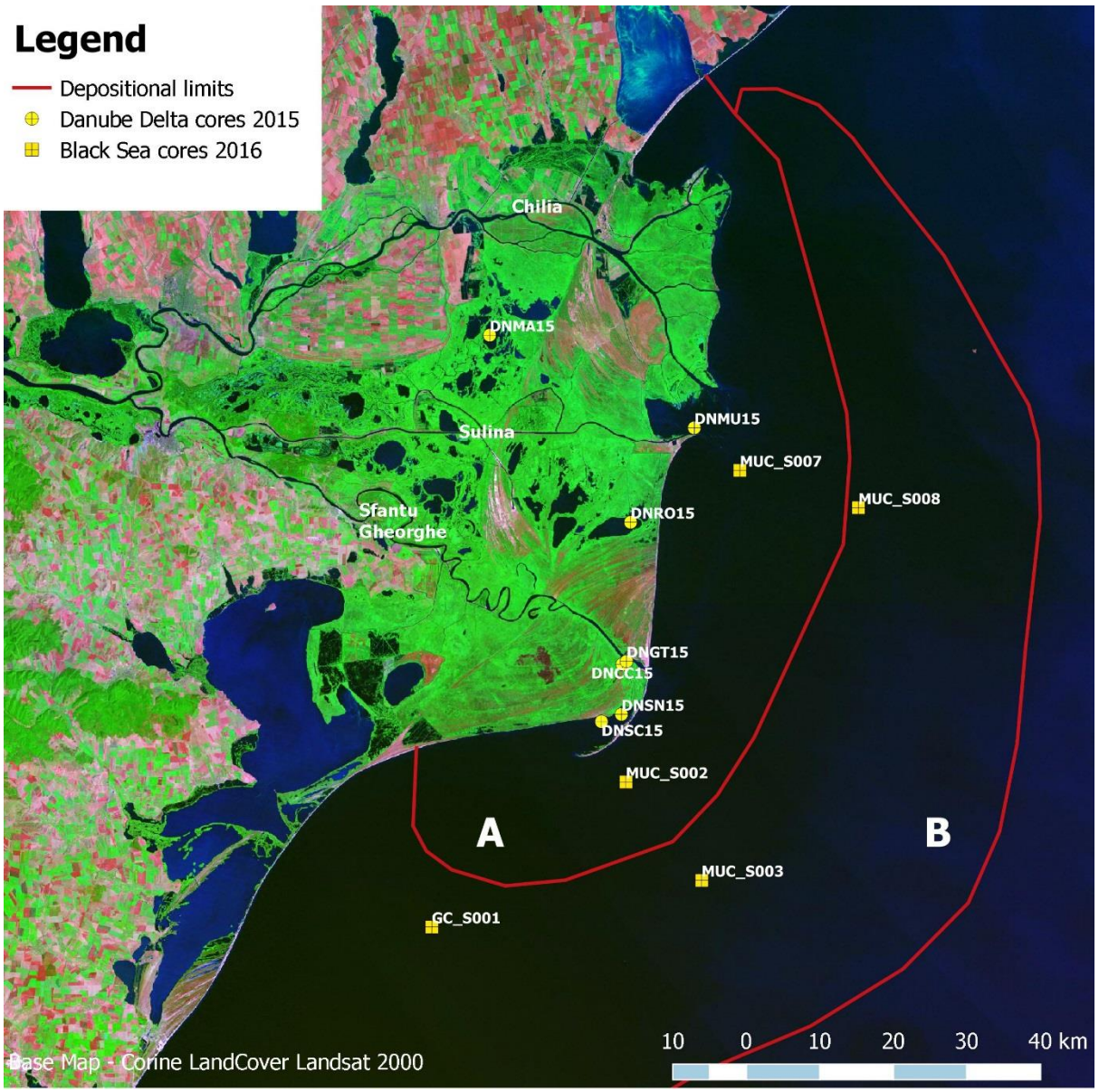

Figure 3.1. The Danube Delta and the NW Black Sea shelf (base map Corine LandCover Landsat 2000) with the locations all cores used for this study. The red lines represent the depositional limits of the delta front (A) and prodelta (B) from (Panin and Jipa, 2002). The exact location of all cores are presented in table 3.1 and 3.2. Detailed locations of the cores retrieved in the Danube Delta are presented in Figure 3.2.

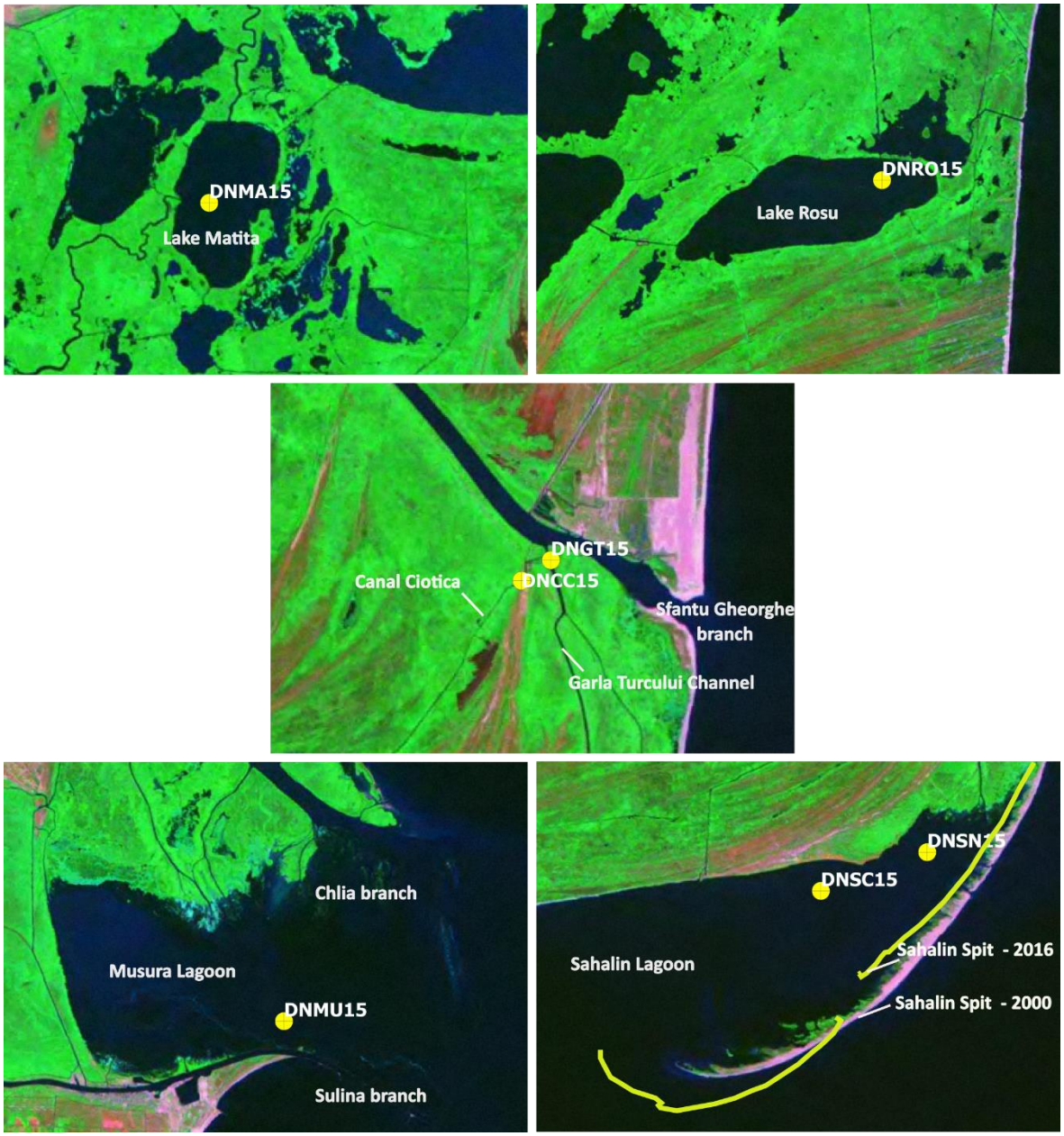

Figure 3.2. Detailed locations of the cores in the different environments of the Danube Delta (base map Corine LandCover Landsat 2000). Notice movement of the Sahalin Spit from 2000 to 2016 (source data: GeoEcoMar, PN0302 report 2016).

3.2.2. Sediment fluxes in the Danube-Black Sea area. Controlling factors

The sediment balance of most of the rivers within the Danube Basin can be characterized as disturbed or severely altered (ICPDR 2009). Most of the bed-load sediments are trapped by dams (80-90%) and erosion of riverbanks is reduced by torrent control. As a result, there is a deficit of riverbed load in most of the free-flowing sections of the Danube catchment. The grain size varies from the Upper Danube (gravel) to the Middle Danube (sand and fine gravel), as might be expected by the decreasing slope.

There are 78 barriers along the course of the Danube and its main tributaries (Habersack et al., 2016), among which the Iron Gate I and II are the largest. Together with

all the dams on the Romanian tributaries of the Danube, determined a reduction of the sediment budget downstream of the dam by 50 to 70 **%** (McCarney-Castle et al., 2011; Panin and Jipa, 2002, 1998), with immediate consequences in the Danube Delta – decrease progradation rates in the active areas, Sahalin and Chilia deltas (Panin and Overmars, 2012) and coastal erosion (Stănică et al., 2007; Stănică and Panin, 2009; Ungureanu and Stanica, 2000)**.**

The alluvia transported by the Danube represents mainly fine fractions (silt), most of the sandy, coarser material stops in the Iron Gates dam (Oaie et al., 2005) while the sandy material reaching the Danube delta is due to erosion of the riverbed (Romanescu, 2013). Thus, the sediment supply reaching the delta is 25–35 million t/y, out of which 4–6 million t/y of sandy materials are the only sediments supplying the inner shelf and littoral zone (Panin and Jipa, 2002).

Damming and channel dredging have reduced the sediment input leading to delta and coast degradation and erosion (Panin and Jipa, 2002) but in the same time, intensive land use practice has had the opposite effect (McCarney-Castle et al., 2011). The cutting and dredging of shallow canals was a constant and extensive activity in the delta, since the beginning of the 20th century, but accelerated after the WWII (the total length of the canals doubled; Gastescu et al., 1983). The main purpose was to improve access to help fishing and reed harvesting (Oosterberg et al., 2000). This network of channels is considered to play a role in present-day sedimentation in the fluvial delta, by increasing water and sediment delivery and overbank sediment transfer and keeping the sedimentation rates above the contemporary relative sea level rise rate in the Black Sea, i.e. 3 mm/y (Giosan et al., 2013).

The formation and transformation of the Danube Delta coastal zone, including the three mouth areas of the main branches, has been under the influence of both natural and anthropic factors over the last 150 years (Giosan et al., 1999; Stănică et al., 2011; Stănică et al., 2007; Stănică and Panin, 2009; Ungureanu and Stanica, 2000). The last 150 years are marked by the cutting of the Sulina distributary and changes in water and sediment load (7-9% in 1860) on the distributary as well as the construction of the Sulina jetties (1858-1861 – the first part), which changes the overall dynamics of the coastal current, when they were extended into the sea, reaching a length of 8 km in the present (Panin and Overmars, 2012). This structure acts like a barrage, blocking most of the alongshore drift from the secondary delta of Chilia distributary towards south, resulting in the clogging of Musura Bay and causing sediment starvation for the littoral areas downdrift and increased erosion in the Sulina - Sfantu Gheorghe sector (between Sulina jetties in the north and Sfantu Gheorghe mouth in the south), as well as the dramatic decrease or even cessation of sediment supply to the southern shores of the Danube Delta (the sand bar closing the Razelm-Sinoe lagoon)

(Stanica et al., 2003, Stănică et al., 2011; Stănică and Panin, 2009). A sand spit developed in front of Sulina mouth, originating from bed-load accumulation, which is dredged periodically to maintain the water depth for navigation (8 m) and the sediments are discharged offshore, so they are not part of the near-shore transport system (Giosan et al., 1999; Stănică et al., 2007).

The Chilia secondary delta (Chilia III) developed and grew strongly beginning with the 19th century, prograding in three directions: north, east and south and developed a shallow platform towards east and south (Panin and Overmars, 2012). The decrease in sediment delivery in the 20th century, due to the extent of the lobe in deeper water, has slowed accretion, leading even to a general erosion trend that it can still be observed today (Filip and Giosan, 2014).

Sfantu Gheorghe branch developed a secondary delta, with a shallow delta front platform (Sfantu Gheorghe II). This is a wave controlled delta, formed with the sediment brought by the river and then distributed in beach ridges by the coastal current (Panin and Overmars, 2012). This delta is still prograding today and is protected by the Sahalin spit in the south. The Sahalin spit grew from 1897, lengthening by 200 m/year on average and migrating by overwash towards the shore (30-70m/year), with a tendency of closing the Sahalin lagoon in the next two centuries (Dan et al., 2011; Panin and Overmars, 2012).

The sediment input from the Danube branches is reworked by waves and currents, but the tide does not play a crucial role, the Black Sea having a microtidal regime (7-11 cm; Bondar et al., 1973). The longshore sediment drift is generated by wind and wave longshore current system, which transports different volumes on sediment per sector: 0.72 Mm^3/y in front of the Chlia delta, 0.81 Mm^3/y between the Sulina jetties and Sfantu Gheorghe mouth, up to 1.23 Mm^3/y at Sfantu Gheorghe mouth, along the Sahalin spit, 0.22 Mm^3/y, between the tip of Sahalin and Perisor, 0 between Perison and Periteasca and 0.66 Mm^3/y between Periteasca and the jetties of Midia harbor (Giosan et al., 1997; Panin, 1999).

The main deposition areas are identified in the Danube Delta itself and the immediate vicinity of the three discharging arms. Offshore this area, including the southern prodelta area, the sedimentation related to the Danube discharge is considered to occur only in exceptional circumstances. This study will assess the sedimentation process over all these environments.

3.3. MATERIAL AND METHODS

3.3.1. Material Sedimentary cores

3.3.1.1. Danube Delta cores

Seven sediment cores were retrieved from various environments in the Danube Delta in August 2015, on Board R/V Istros (Table 3.1, Fig.3.2). In order to assess the impact of sediment flux changes over the Danube Delta, different sedimentary environments have been chosen, with different connection to the hydrographic network. Hence, one core was collected from the fluvial delta (DNMA15), one from the marine delta (DNRO15), both in lakes connected to the main branches through channels; two cores (DNGT15, DNCC15) from active channels in the active delta of Sfantu Gheorghe; three in the terminal lagoons Musura and Sahalin, (DNMU15, DNSN15, DNSC15), representing the active deltas of Chilia and Sfantu Gheorghe. All cores were collected with a manual corer with 0.5 cm liners to reduce compaction.

Table. 3.1 Parameters of the Danube Delta cores analyzed in this study

Core	Latitude	Longitude	Location	Environment	Water depth m	Length cm
DNMA15	45°17'39.7'' N	29°21'52.5'' E	Lake Matita	lake	2	65.5
DNRO15	45°03'36.9'' N	29°35'54.44'' E	Lake Rosu	lake	2.3	55
DNGT15	44°53'25.2'' N	29°35'01.8'' E	Garla Turcului	channel	2.1	60
DNCC15	44°53'12.6'' N	29°34'34.7'' E	Ciotica Canal	canal	1.4	46.5
DNMU15	45°10'23.5'' N	29°42'50.2'' E	Musura Bay	lagoon	2	119
DNSN15	44°49'32.1'' N	29°34'19.7'' E	Sahalin Lagoon	lagoon	1	59
DNSC15	44°49'02.9'' N	29°32'14.9'' E	Sahalin Lagoon	lagoon	1	99

The cored lakes are Type 1 lakes, according to Oosterberg et al. (2000). They are large and turbid (Coops et al., 1999), have a sandy-silt substratum, have high phytoplankton abundance and low abundance of macrophytes.

Lake Matita is situated in the delta plain, between Chilia and Sulina distributaries and is connected with these main branches through other lakes and channels. The connecting channels have a sinuous path so a considerable fraction of the transported sediments does not reach Lake Matita (Duliu et al., 1996). In Lake Matita, bottom sediments consist of three categories: lacustrine (first 50cm, 3500 years BP), brackish (50-120 cm, 3500-7200 years BP) and leossoide deposits, continental (>120 cm) (Noakes et Hertz, 1983).

Lake Rosu, situated between Sulina and Sfantu Gheorghe branches is connected to both through several channels and canals. Many dredging works were performed for the maintenance of the connection between the town of Sulina and the village of Sfantu

Gheorghe, increasing water and sediment input in all the lakes in the area, silting-up Lake Rosu, among others (Munteanu, 1996).

Channel Garla Turcului is one of the distributaries of the Sfantu Gheorghe Delta II and it is shown as an active channel on a 1918 Austrian map (Panin and Overmars, 2012). Canal Ciotica is directly connected to Garla Turcului and is a shallow canal dug in the sand bars of Sfantu Gheorghe Delta II, in the early 1950's to provide access for fisherman to the south of the Danube Delta (Bondar and Panin, 2001).

Musura lagoon was formed as a consequence of anthropic interventions on both Chilia and Sulina branches. The construction and continuous elongation of Sulina jetties trapped most of the sedimentary load of Chilia in the north, leading to the formation of a barrier island - Musura since the 1980s (Stanica et al., 2003, Stănică et al., 2011; Stănică and Panin, 2009). The main effect is the clogging of Musura. In the recent years, the redistribution of water and sediment inside the secondary delta of Chilia, with a shift of the bulk water and sediment from the Stari Stambul channel which reaches Musura lagoon, to Bastroe, which discharges in the Black Sea, has led to a decrease of water circulation and sediment supply in this area.

Sahalin lagoon lies behind the Sahalin spit. This feature emerged at the mouth of Sfantu Gheorghe branch in 1897 (Panin, 1996). It grew from 1897, lengthening with 200 m/year in average and migrating by overwash towards the shore (30-70m/year), with a tendency of closing the lagoon in the next two centuries (Dan et al., 2011).

3.3.1.2. Black Sea cores

Five cores were retrieved from the NW Black Sea shelf, in the delta front and prodelta of the Danube in May 2016, during the ReCoReD research cruise on board R/V Mare Nigrum (Table 3.2, Fig. 3.1). The cores were collected with a Mark II Octopus Multicorer, equipped with 8 perspex tubes of 60 cm in length and 10 cm in diameter, and a gravity corer, available on board the RV. The short cores were sampled on board and the samples were frozen. The long cores were only taken where the substrate allowed it and the cores were cut in 1 m sections and kept in the cold room.

Two of the cores were sampled in the delta front, one in front of the Sulina branch, south from the jetties (S007) and one in front of the Sfantu Gheorghe branch, south from the Sahalin spit (S002). Three cores were retrieved from the prodelta, outside the main area of sediment deposition of the Danube, east from Sulina (S008) and south from Sfantu Gheorghe (S003) and one south from the main discharging branches, in the area of deposition for the sediments of the Danube drift (S001).

Table. 3.2. Parameters of the Black Sea cores analysed in this study

Core name	Latitude	Longitude	Location	Environment	Water depth m	Length cm
S007	45.1194	29.78937	Sulina mouth	Delta front	18.9	35
S002	44.74274	29.57613	Sfantu Gheorghe mouth	Delta front	24.6	39
S008	45.06834	29.99259	Offshore Sulina	Prodelta	33.7	18
S003	44.6195	29.7006	Offshore Sfantu Gheorghe	Prodelta	44.8	27
S001	44.57236	29.23605	Offshore Gura Portitei	Prodelta	30	40

3.3.2. Methods

3.3.2.1. Sedimentological analysis

All cores were photographed and described. All cores were sub-sampled at 1 to 3 cm, depending on the lithology. For each sample wet and dry weight and water content were determined (samples were dried in ovens at 55°C for 48h). In addition, the shell content was measured by weighing the shell fraction for each sample. Up to 25 grams of sample were grinded and made into cylindrical pellets, with known geometry, for ^{210}Pb and ^{137}Cs dating. The rest of the sample was sieved with a 2 mm sieve and prepared for grain size analysis.

The grain size analysis was done using a Coulter Counter LS 230, in the laboratories of the University of Stirling. The instrument measures the size distributions of particles with a size range of 0.04 to 2000 µm. Control samples were used at the beginning of each working day, to make sure that the distribution of particle sizes is correct. Measurements were repeated for those samples were the distribution curves were noisy.

3.3.2.2. Radiogenic dating

Radionuclides, coming from both natural and anthropogenic sources are being successfully used as tracers for assessing sedimentary processes in lakes and the marine environment (Broecker and Peng, 1983; Santschi, 1988). Sediment accumulation rates in these areas, as a result of: rapid deposition, resuspension, molecular diffusion, and bioturbation are processes that can exert an influence on the formation of the sedimentary record and produce uncertainty in calculating accumulation rates from radiotracer activity-depth profiles (Frignani et al., 2004).

^{210}Pb dating is a method of dating recent sediment deposition and accumulation using down-core profiles of short-lived radioactive ^{210}Pb (Swarzenski, 2014) in a time scale up to 130 years (Appleby, 2008).

The naturally occurring ^{210}Pb radionuclide is part of the ^{238}U radioactive decay series, with a half-life of 22.23 years. ^{210}Pb is involved in the sedimentary processes through a chain of natural events: the noble gas nuclide ^{222}Rn (T1/2 = 3.82 d), a daughter of ^{226}Ra and part of the ^{238}U decay series, diffuses out of the Earth's crust to the atmosphere from the soils, sediments and bedrock geology. Radon remains in the atmosphere until it decays. Decay products of ^{222}Rn, including ^{210}Pb, are removed from the atmosphere by dry gravitational settling, usually attached to dust particles and through precipitation scavenging. Thus, a relatively continuous flux of ^{210}Pb is provided to land and water surfaces. The ^{210}Pb, which is precipitated from the atmosphere, is defined as 'unsupported' ^{210}Pb, compared to the 'supported' component that grows in situ within the sediment, soil or bedrock. In aquatic environments ^{210}Pb is absorbed by suspended particulate matter (clay fraction and organic matter) and deposited in the sediments. Both the 'unsupported' and 'supported' ^{210}Pb components will be present in the sediments. It is the 'unsupported' or 'excess' ^{210}Pb component which provides the chronological component as it decays with the half-life of 22.23 years, and allows for geochronology investigations of lacustrine, estuarine and marine environments (Appleby, 2008; Appleby and Oldfield, 1978; Goldberg, 1963). The 'excess' ^{210}Pb component can be estimated by subtracting the 'supported' component by allowing samples to reach equilibrium with the parent ^{226}Ra, which is readily estimated from the ^{214}Bi and ^{214}Pb concentrations.

Here the ^{210}Pb dates are validated by ^{137}Cs profiles. The distribution pattern of ^{137}Cs (T1/2 = 30.14 y) found in sediments represent time markers for the last 50 years. The introduction of ^{137}Cs into the atmosphere occurred as a result of nuclear tests after 1960s (with a peak in 1961) (Fig. 3.3) and in 1986 as a result of Chernobyl accident (Buesseler and Livingston, 1996).

In the Black Sea basin, the main source of anthropogenic radioactivity (Gulin et al., 2013) was the global fallout from the atmospheric large-scale nuclear weapon tests, which were carried out between 1954–1958 and 1961–1962 (Buesseler and Livingston, 1996). In addition, the Black Sea basin and its large catchment area has received substantial amount of the long-lived artificial radionuclides, ^{90}Sr, ^{137}Cs, and plutonium isotopes, released into the atmosphere from the Chernobyl nuclear reactor accident in 1986, which was delivered via air masses moving south- and westward from the accident area in the Ukraine and through the Dnieper directly draining the contaminated Chernobyl exclusion zone, as well as the Danube river water discharge itself (Livingston et al., 1988; Polikarpov et Egorov, 2009; Gulin et al., 2002).

All cores were analyzed for ^{210}Pb and ^{137}Cs, for a *ca.* 100 years chronology of the sedimentary processes and their magnitude across the delta and the shelf.

All sediment samples were ground after drying and made into pellets of known geometry and weight. They were put in plastic containers and left to sit for up to 3 weeks, for the radon concentration in the sample achieve an equilibrium with the natural occurring radon in the outside atmosphere.

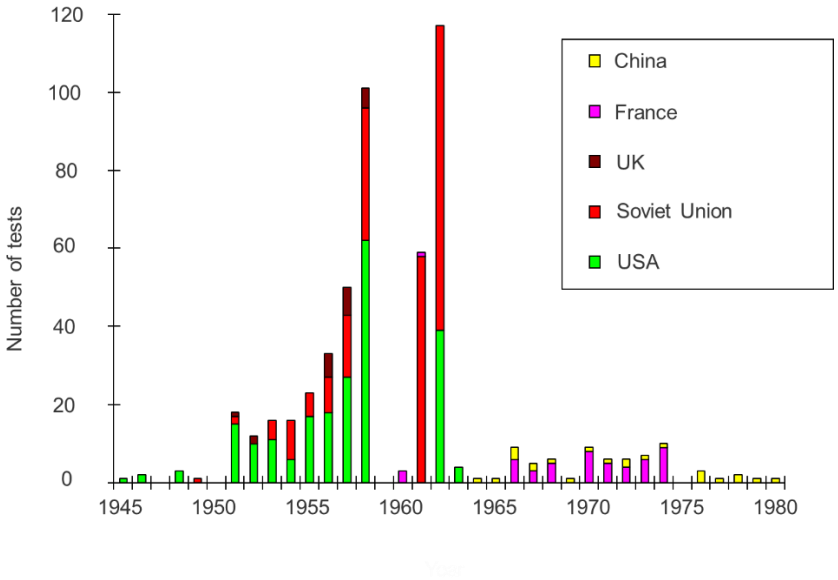

Figure 3.3. Atmospheric Nuclear Weapons Tests in the world.

All samples were analysed in the ERL (Environmental Radioactivity Laboratory) of the University of Stirling, in two high purity-Germanium, low ^{210}Pb background GEM HPGe detectors. Each sample was counted for 48h. Weekly checks were performed for each detector, consistency in detector performance including energy calibration, energy resolution, efficiency calibration and traceability to international reference materials as part of the ISO 17025:2005 accreditation.

The CRS model (Appleby and Oldfield, 1978; Swarzenski, 2014) was used to calculate sediment accumulation rates. This model assumes that the down-core excess of ^{210}Pb activity, integrated vertically to a depth, x, or a cumulative dry mass, m, will equal the flux of ^{210}Pb, integrated over the corresponding time interval. Integrating to either x or m,

$$A(x,m) = A_0^{(-\lambda t)} \qquad (3.1)$$

where A(x, m) is the cumulative residual unsupported or excess 210Pb activity beneath sediment of depth x, or mass m, A_0 is the total unsupported 210Pb activity in the sediment column, l is the 210Pb decay constant, 0.03114 year^{-1}, and t represents time. The age of sediment at depth x, m is then described by:

$$t = \frac{1}{\lambda} \ln \left[\frac{A_0}{A_{(x,m)}}\right] \qquad (3.2)$$

This will establish for the first time an age model for the Danube Delta and the NW Black Sea Shelf, for the last century, in an integrated way.

3.4. RESULTS

3.4.1. Danube Delta

3.4.1.1. Sedimentary facies

The following description of the cores comprises the entire core, as it was retrieved from a specific environment, while the grain size, time frame and sedimentation rates will only focus on the last century (1916-2016).

Danube Delta

Lakes (see Figure 3.2)

CoreDNMA15 consists of brown silt and sandy silt in the top (0-25 cm), with plant remains and abundant whole freshwater shells and fragments. It is followed downwards by black silty clay (25-50 cm), with an abundance of fragments of marine shells at the base, and a light-grey clay with distinct silt laminae (50-65.5 cm) (Fig 3.4 and 3.5). This same succession of lithological horizons was previously described in Lake Matita by Catianis et al. (2014).

Core DNRO15 has a similar brown silt level at the top (0-26 cm), very rich in plant and fragments of freshwater shells. Next level (26-40.5 cm) consists of a light-grey, finely laminated sandy silt, very rich in the remains of vegetation and shell fragments. The bottom layer of the core is a dark-grey, finning upwards silty sand to medium sand, with shell and vegetation fragments and two distinct sand laminae (Fig. 3.3 and 3.4).

Channels (see Figure 3.2)

Core DNGT15 presents an alternation of grey, finely laminated clayey and sandy silt, with coarser levels towards the base. The core has no fauna or plant remains, with the exception of a whole and perfectly conserved half shell of at 30 cm depth (Fig. 3.4 and 3.5).

Core DNCC15 has a finer level at the top (0-6 cm), of grey sandy silt. It is followed by a succession of grey silty sand levels, with different proportions of sand, with scarce carbonized wood fragments (17-22). The level in the base is coarser, grey sand with shell remains, delimited by the upper levels through an erosional contact (Fig. 3.4 and 3.5).

Lagoons (see Figure 3.2)

Core DNMU15 consists mainly of black silt, very homogenous in both colour and texture, with no internal structure. The sediment changed colour after the opening of the

core in the presence of air, from black to light brown (Fig. 3.4 and 3.5). Plant remains were found in the first 35 cm.

Core DNSN15 presents a coarser top layer (0-13cm) of grey and black silty sand. There is a distinct horizon of freshwater shell fragments at 7 to 11 cm. the rest of the core is an alternation of finely laminated grey and black sandy silt, with black streaks and spots that appears light brown on the image in Fig. 3.4. The surface of the sediment changed colour after the opening of the core.

Core DNSC15 consists in an alternation of grey or light brown sandy silt and silty sand, with distinct coarser levels and laminations (Fig. 3.4 and 3.5). The core is rich in plant remains especially, with recent vegetal debris at the top and two distinct level of very-rich carbonized plant fine fragments that alternate with silty sand (63-65 and 80-91 cm) (Fig. 3.4). The shells and shell fragments are from marine specimens.

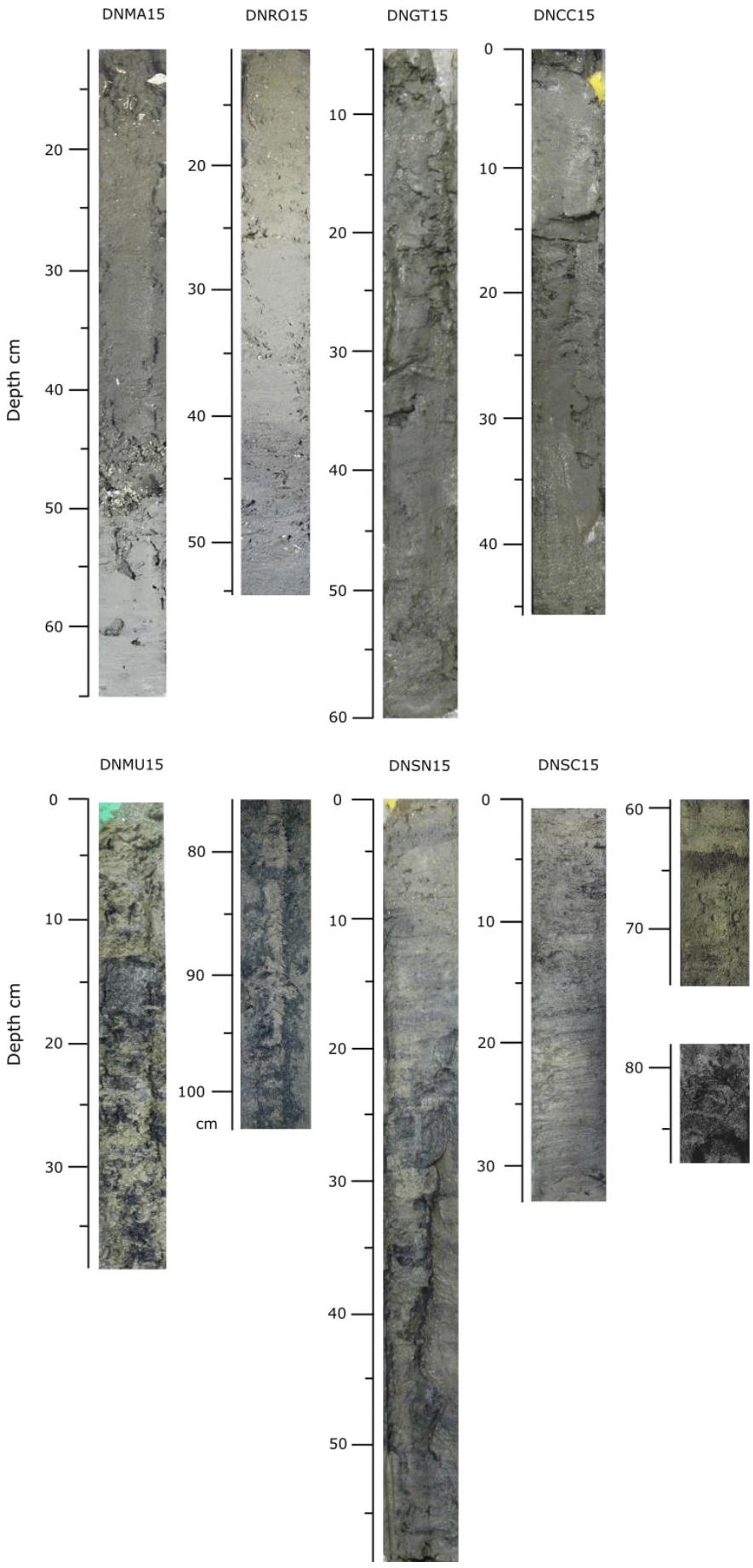

Figure 3.4. Photographs of sedimentary facies in the split cores sampled in the Danube Delta. See text for detailed description.

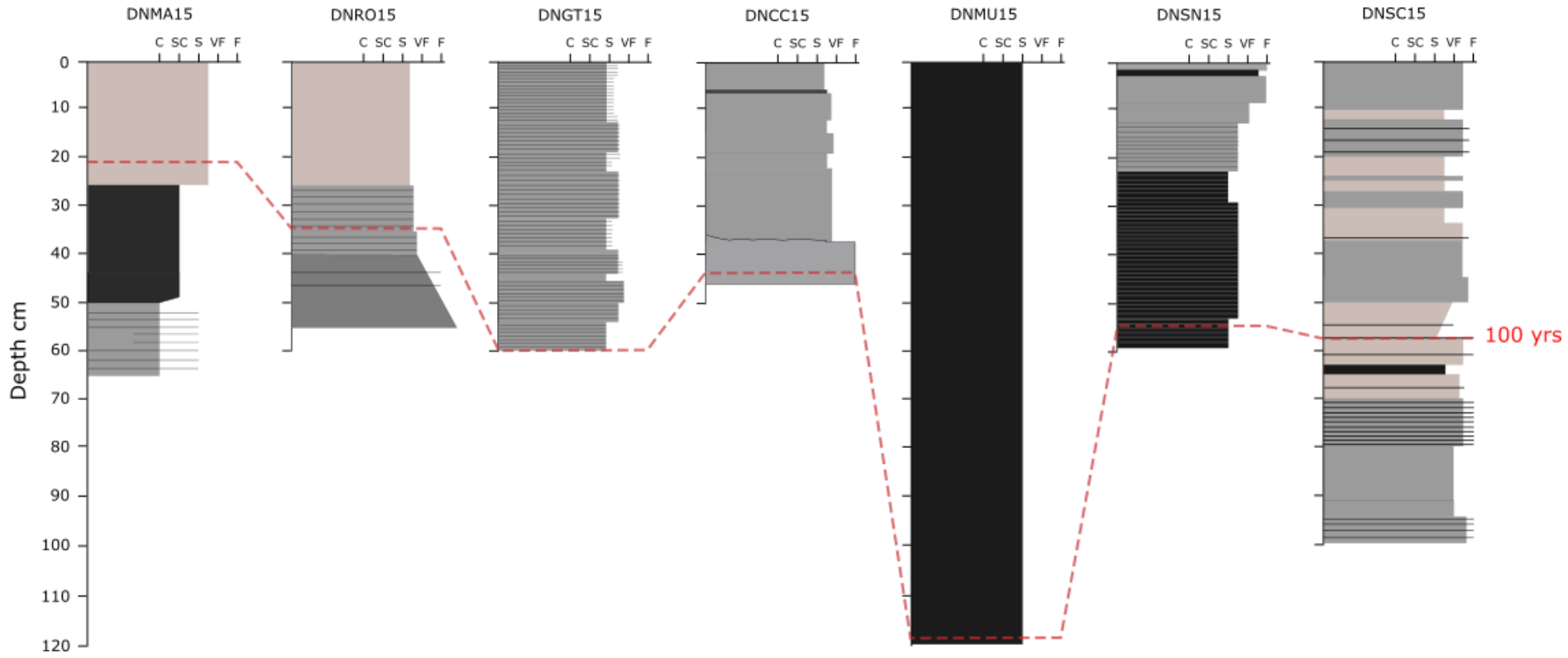

Figure 3.5. Sedimentary logs of the Danube Delta cores from lakes (DNMA15, DNRO15), channels (DNGT15, DNCC15), lagoons (DNMU15, DNSN15, DNSC15). C – Clay, SC – Silty Clay, S – Silt, VF – Very Fine Sand, F – Fine Sand. The red dotted line represents one century. The exact location of the cores is presented in Fig. 3.1 and Table 3

3.4.1.2. Chronostratigraphic framework

The chronostratigraphic framework for all cores is based on ^{210}Pb and ^{137}Cs dating.

The CRS (Constant Rate of Supply) model was considered to be appropriate for obtaining the real ages for all cores. This model has been previously used by Begy et al. (2018) to date sediments from the Danube Delta lakes. ^{210}Pb obtained ages were compared with the ^{137}Cs activity, for the initial and second rise (1954 and 1961-1963) and the Chernobyl event (1986).

Lakes

The CRS age model as a function of depth shows quiet sedimentation conditions in the two lakes (Fig. 3.6 and 3.7).

The ^{137}Cs peaks have a good fit with the CRS age model. The sediment column of Lake Matita has one ^{137}Cs peak, at ~1986, which could be an overlap of the two peaks of 1963 and 1986, as previously observed by Duliu et al. (1996), while there is no earlier peak for 1954 (Fig. 3.6). . The sediment record of Lake Rosu has two distinct ^{137}Cs peaks, of similar magnitude, one centred at ~1994 and the second one at ~2011. The difference between these two lakes in term of recording ^{137}Cs activity is the location of cores in the sediment sinks. While the Matita core is retrieved from the centre of the lake, the Rosu core is taken from an area with continuous exchange of water and suspended matter between Lake Rosu and Lake Rosulet in the north which may reflect a more complex ^{137}Cs profile.

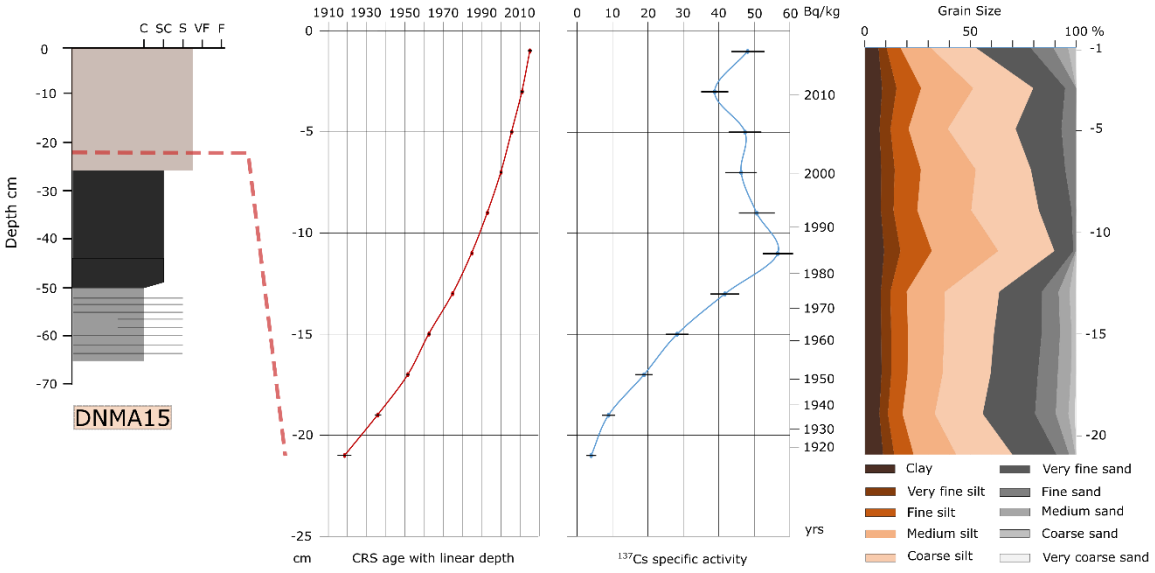

Figure 3.6. Summary figure of core DNMA15. Sedimentary log, ^{210}Pb derived CRS age model with linear depth for the one century time period, ^{137}Cs activity with depth, compared with the CRS age model, grain size in percentages of fractions using the Udden-Wentworth scale.

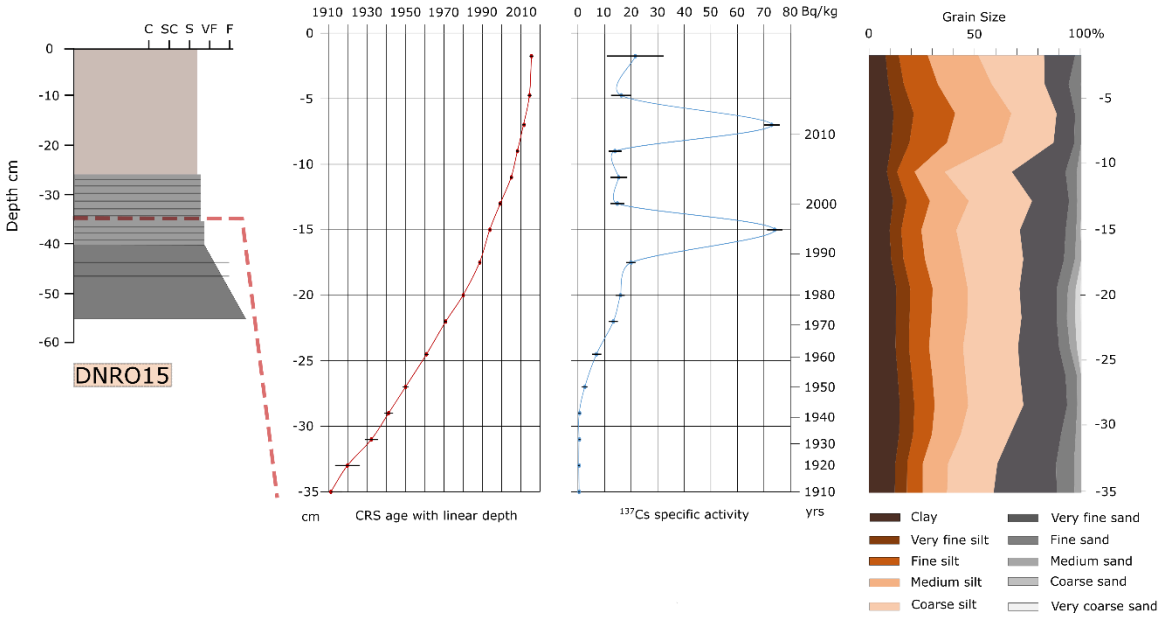

Figure 3.7. Summary figure of core DNRO15. Sedimentary log, ^{210}Pb derived CRS age model with linear depth for the one century time period, ^{137}Cs activity with depth, compared with the CRS age model, grain size in percentages of fractions using the Udden-Wentworth scale.

Channels

The two channels, Garla Turcului (Fig. 3.8) and Canal Ciotica (Fig. 3.9) show different patterns of CRS age model and ^{137}Cs activity variation. The CRS model for Garla Turcului shows a rather mixed profile, with a very rapid accumulation, while Canal Ciotica shows quitter conditions of sedimentation. While they both show very low ^{137}Cs activity values overall, typical of a profile dominated by nuclear weapons test fallout (<10 Bq/kg), Garla Turcului shows one high ^{137}Cs peak ~100 Bq/kg, centred at 1949 (CRS age), almost 5 years earlier than the first rise (1954) and very low values afterwards, while the values for Canal Ciotica are very low overall, not exceeding 8 Bq/kg, very close to the natural background. The records show just one ^{137}Cs peak, of 7.83±1.63 Bq/kg, from 1954 to 1968 (CRS age), and a constant decrease afterwards. These results have to be interpreted with care, due to an incomplete ^{210}Pb profile, where there is still excess ^{210}Pb profile at the base of the cores, so the mismatch of the ^{137}Cs peaks and CRS age are generated by an underestimate of the age at the base of the core.

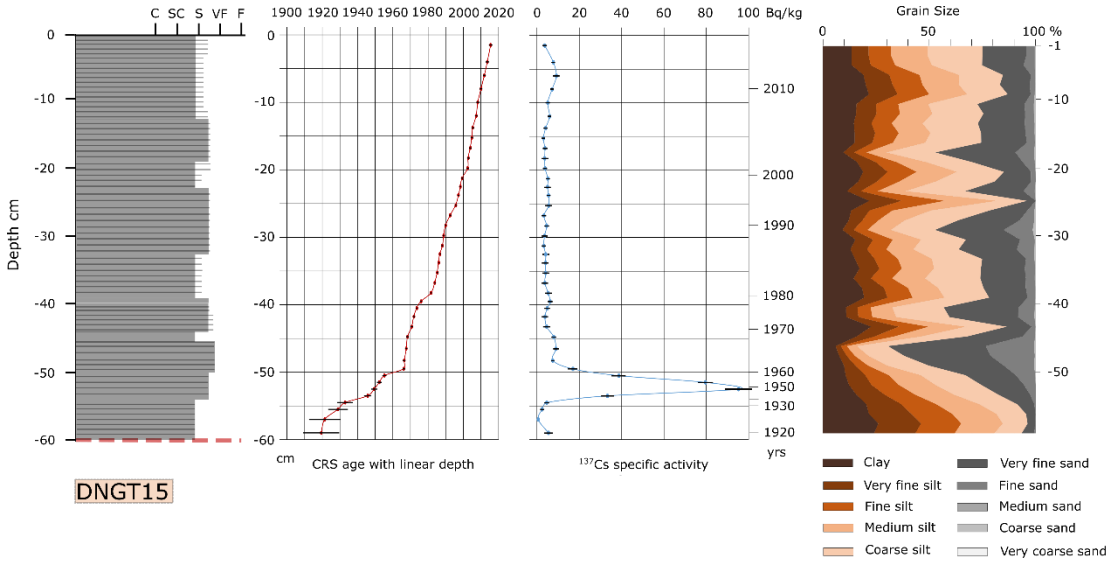

Figure 3.8. Summary figure of core DNGT15. Sedimentary log, ^{210}Pb derived CRS age model with linear depth for the one century time period, ^{137}Cs activity with depth, compared with the CRS age model, grain size in percentages of fractions using the Udden-Wentworth scale.

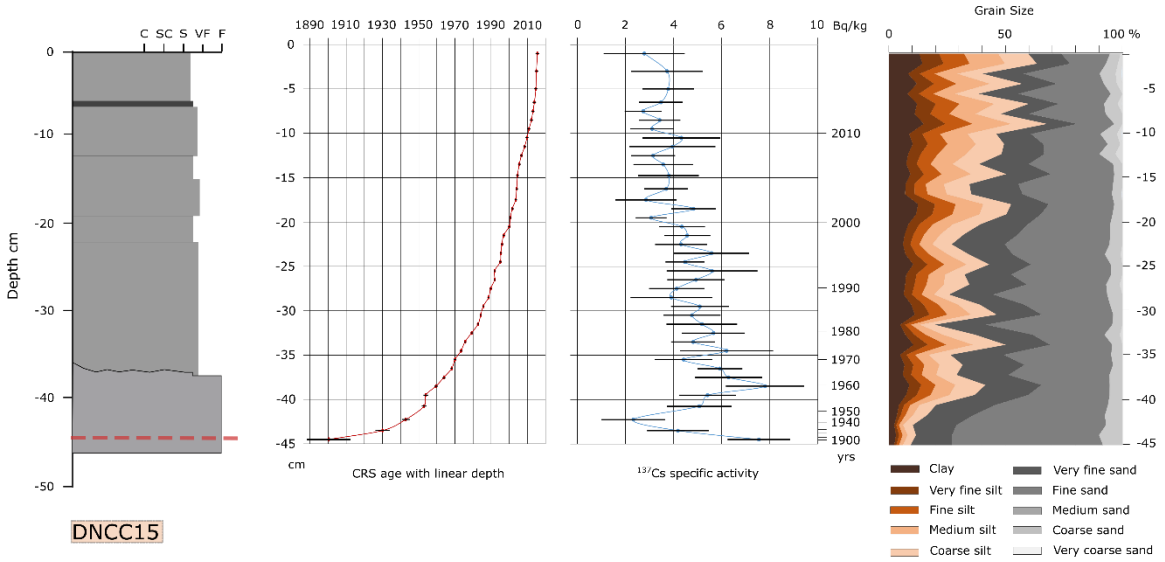

Figure 3.9. Summary figure of core DNCC15. Sedimentary log, ^{210}Pb derived CRS age model with linear depth for the one century time period, ^{137}Cs activity with depth, compared with the CRS age model, grain size in percentages of fractions using the Udden-Wentworth scale.

Lagoons

The two lagoons, Musura (Fig. 3.10) and Sahalin (Fig. 3.11 and 3.12) show different behaviors in terms on sedimentation patterns. The CRS model with linear depth shows calm sedimentation conditions in Musura, while the profiles are both disturbed for Sahalin, in the north, DNSN15 (Fig. 3.11) and in the centre, DNSC15 (Fig. 3.12). The ^{137}Cs activity in Musura has values between 20 and 140 Bq/kg, with one distinct peak centred in the early 1980s. Considering the very high accumulation rates in this region (Giosan et al., 2013; Stănică et al., 2007) it is very likely that the ^{137}Cs activity peak represents the 1986 event. Also, there is still excess ^{210}Pb profile at the base of the core, which indicated that the one century limit might be lower in the sediment succession than the one indicated here.

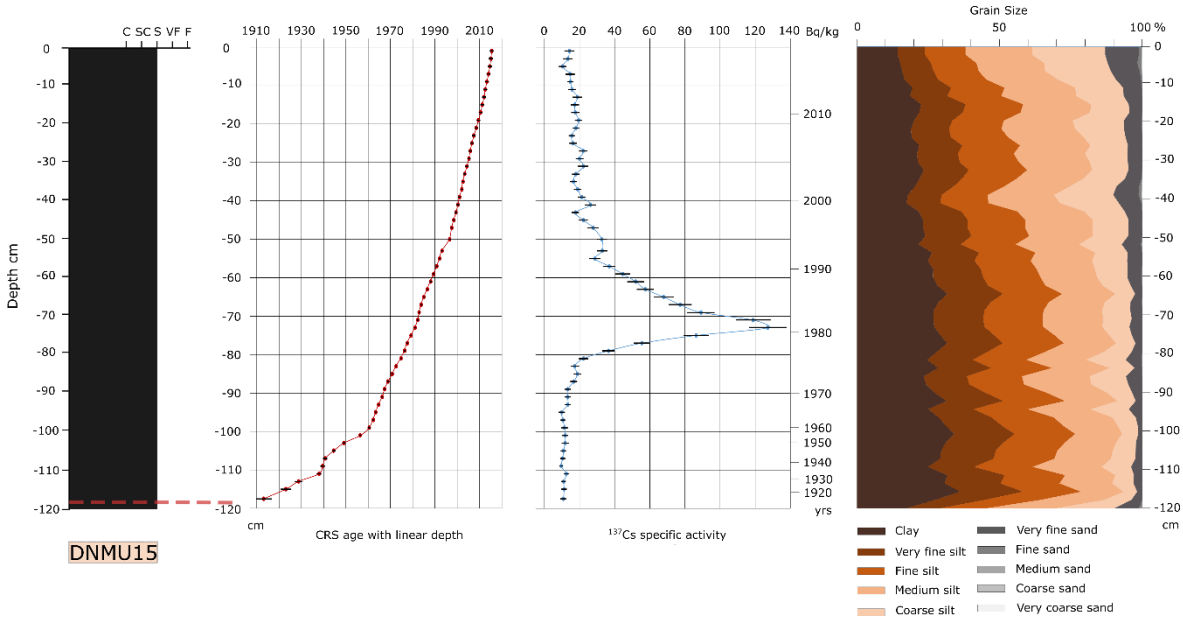

Figure 3.10. Summary figure of core DNMU15. Sedimentary log, ^{210}Pb derived CRS age model with linear depth for the one century time period, ^{137}Cs activity with depth, compared with the CRS age model, grain size in percentages of fractions using the Udden-Wentworth scale.

The CRS models for both DNSN15 and DNSC15 show disturbance in sedimentation patterns, with mixing and erosion. DNSN15 has calmer sedimentation conditions due to its position, in the inner part on the Sahalin lagoon, very close to Garla Turcului. The ^{137}Cs activity shows similar values for both cores overall, not exceeding 25 Bq/kg. DNSN15 shows a first peak from 1930 to 1960 CRS time, of 13 Bq/kg and another marked peak of ~24 Bq/kg, centred around 1986. Values decrease afterwards, getting close to zero after 2010. DNSC15 shows very low values of ^{137}Cs activity, with a peak between 2000 and 2010. The rest of the values are low, very close to values for the natural background. In these two cores, ^{137}Cs activity varies also with the content in clay and the finer fraction (Figs. 3.11 and 3.12), so the results should be interpreted with care.

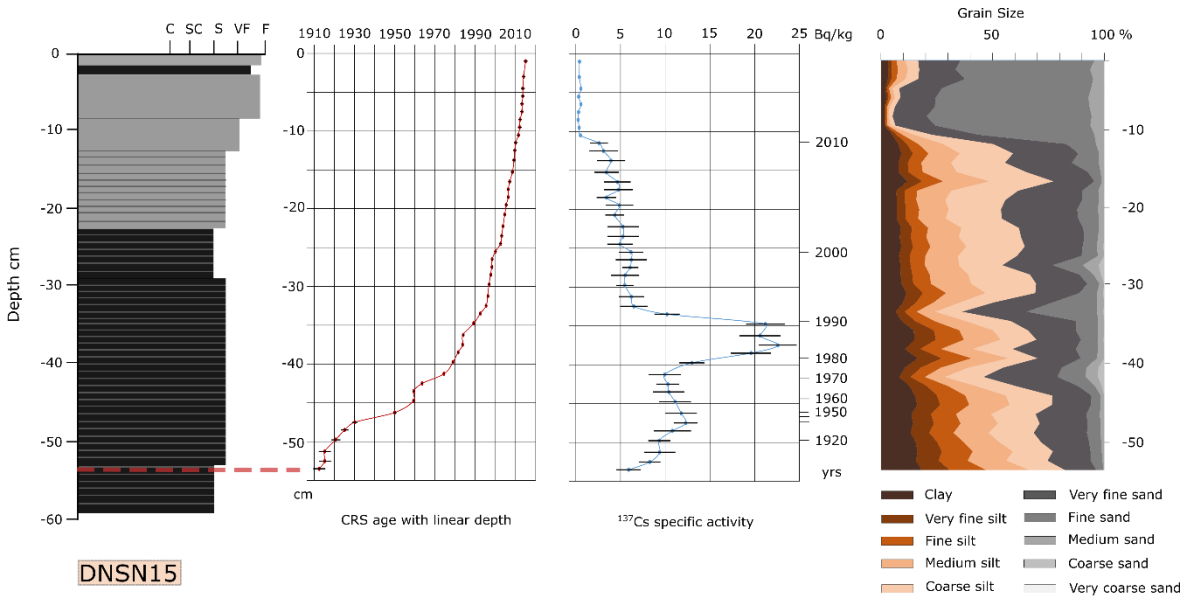

Figure 3.11. Summary figure of core DNSN15. Sedimentary log, ^{210}Pb derived CRS age model with linear depth for the one century time period, ^{137}Cs activity with depth, compared with the CRS age model, grain size in percentages of fractions using the Udden-Wentworth scale.

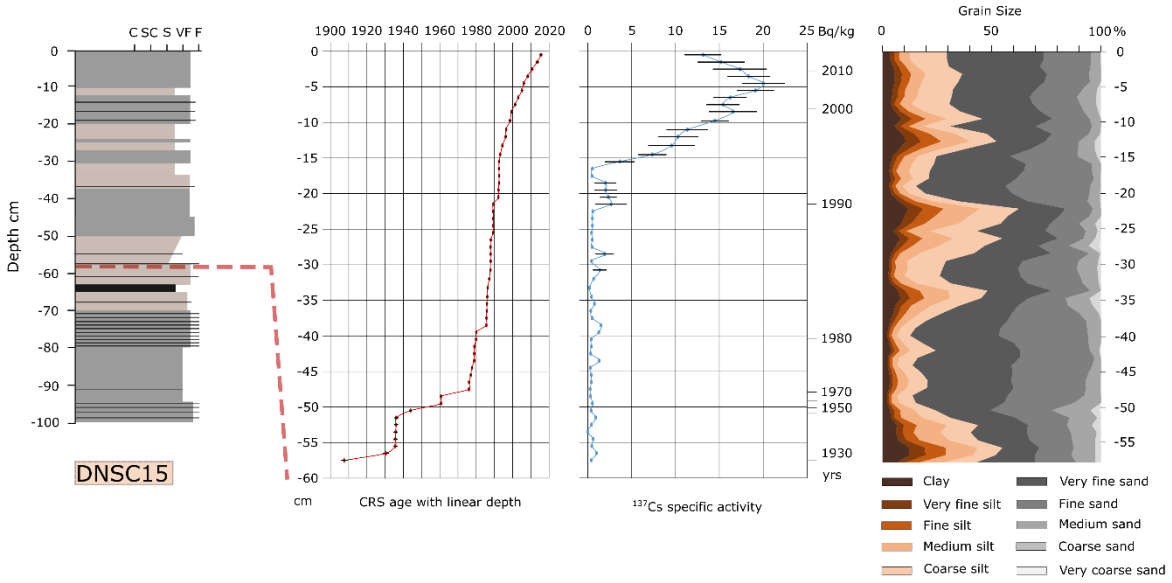

Figure 3.12. Summary figure of core DNSC15. Sedimentary log, ^{210}Pb derived CRS age model with linear depth for the one century time period, ^{137}Cs activity with depth, compared with the CRS age model, grain size in percentages of fractions using the Udden-Wentworth scale.

3.4.1.3. Sediment flux variations

Mass accumulation rates (MAR) were calculated for all cores (Table 3.3), based on the ^{210}Pb CRS age model (Fig. 3.13) and using mass depth, that expresses the variation of sediment mass with depth and dry density. MAR are described for the periods pre- and post-dams (before and after 1982). Sediment accumulation rates (SAR) (cm/y) were also computed pre- and post-dams, to be compared with previously published data (Table 3.3). The ^{137}Cs was used to validate and check the ^{210}Pb CRS age model. MAR and SAR are also calculated using the 1963- and 1986-time horizons. The year 1986 can be considered the limit between the pre- and post-dam periods, so the MAR at 1963 is comparable with the pre-dams value, while the one calculated at 1986 can be compared with the post-dam value. They are presented for comparison in Table 3.3.

For the two analysed **lakes**, the MAR shows a decrease in the last century (Fig. 3.13). For Lake Matita, in DNMA15, MAR ranges from 0.04±0.012 g/cm^2/y to 0.3±0.05 g/cm^2/y. The pre-dams average is 0.25±0.052 g/cm^2/y and 0.17±0.04 g/cm^2/y, post-dams, marking a decrease of 33%. The MAR values obtained using the ^{137}Cs dating are similar (Table 3.3). The second value is very close to the one found by Duliu et al. (1996), using ^{137}Cs dating, of 0.15±0.05 g/cm^2/y, but both values are half of the ones found by Giosan et al., (2013), of 0.53 and 0.31 g/cm^2/y, respectively. In Lake Rosu, DNRO15 shows a MAR ranging from 0.04±0.04 g/cm^2/y to 0.93±0.16 g/cm^2/y, with a pre-dams average of 0.57±0.11 g/cm^2/y and a post-dams average of 0.24±0.08 g/cm^2/y, marking a decrease of 57%. MAR values obtained with the ^{137}Cs dating are lower, 0.13±0.05 and 0.03±0.015. The grain size in the two lakes is predominantly represented by silt, for the last century. There is a change in grain size in both lakes, post-dams, from almost 40-50% sand fraction to less than 30%, and an increase in silt content of 10-15%, which replaces the sand.

The two **channels**, Garla Turcului and Canal Ciotica, show an increase of MAR over the last century. DNGT15 shows MAR values ranging from 3.4±0.26 g/cm^2/y to 176.18±1.14 g/cm^2/y, with a pre-dams average of 62.63±1.7 g/cm^2/y and post-dams average of 60.08±o.96 g/cm^2/y, marking an decrease of 4%. DNCC15 has MAR values ranging from 1.26±0.1 g/cm^2/y to 33.32±2.40 g/cm^2/y, with a pre-dam average of 13.48±0.97 g/cm^2/y and an average post-dam of 15.59±1.09 g/cm^2/y, marking an increase of 13.5%. For comparison, the MAR values obtained with ^{137}Cs dating are two times higher for the both pre- and post-dam periods. In Garla Turcului and Ciotica, the grain size varies, with sand representing up to 70% in DNGT15 and 90% in DNCC15, but decreasing over time. Sand decreases to 30-40 % in DNGT15 being replaced by silt, especially after the Iron Gates I and II dams input, and not exceeding 50% in laminae. DNCC15 shows a constant decrease of sand in time, from 90 to 40 %.

In the two sampled **lagoons**, because of their formation and evolution, MAR varies spatially and depicts different processes (Fig. 3.13). In Musura, MAR decreases in the last century, DNMU15 showing MAR values ranging from 0.47±0.13 g/cm^2/y to 50.32±0.51 g/cm^2/y. The pre-dams average is of 22.91±2.23 g/cm^2/y and the post-dams average is 15.17±1.77 g/cm^2/y, marking a decrease of 34%. The ^{137}Cs derived MAR value of ~19.76±2.23 g/cm^2/y is closer to the pre-dam value, indicating a very rapid sedimentation in this area. However, this core was taken in the distal part of the lagoon and considering the evolution of the lagoon in the last century (Giosan et al., 2013; Stănică et al., 2007), this is probably an area inside the Musura lagoon where the sedimentation rate is one of the lowest. Another argument is the grain size of the core, which consist in 90% silt and with a very good sorting of the grain size classes, suggesting that this is the tip of the sediment plume in the area, where the energy of the water and sediment current slows down enough to deposit the finer fractions. There is an increase in sand content to almost 10%, around 2010.

The two cores in the Sahalin lagoon show different evolutions in the last century. DNSN15, taken in the north of the lagoon, shows MAR values ranging from 1.03±0.05 g/cm^2/y to 62.23±3.92 g/cm^2/y, with a pre-dams average of 9.44±0.63 g/cm^2/y and a post-dams average of 26.45±1.64 g/cm^2/y, marking an increase of 65%. The ^{137}Cs derived MAR values are very different, the 1963 one is more than twice higher than the pre-dams CRS value, while the 1986 one is closer to the post-dam value, indicating rapid sedimentation in this area. DNSC15, sampled towards the centre of the lagoon, shows a decreasing MAR over the 100 years' time. The MAR ranges from 0.13±0.02 g/cm^2/y to 614.89±2.79 g/cm^2/y. The pre-dams average is of 225.22±1.01 g/cm^2/y and the post-dams average is of 71.93±0.88 g/cm^2/y, with a decrease of 68%. The variation of grain size in time in the north of the Sahalin lagoon shows an increase in sand content and a decrease in silt and clay contents over time. From 2010 there is a marked increase in sand content from 50 to 80-90%. This shows most probably the migration of the spit through overwash (see Fig. 3.2 which shows the shoreline of Sahalin in 2016) and its tendency to get closer to the shore.

The input of dams does not seem to change the distribution of grain size fractions in this area. The centre of the Sahalin lagoon, as shown in DNSC15 is dominated by sand, 50-90% of the sediment. There is a slight decrease in sand content after the input of dams but this core reflects more probably the local evolution of the lagoon rather than the evolution of overall sediment flux.

Table 3.3. Average mass accumulation rates (MAR) and sedimentation rates for the Danube Delta cores

Core	CRS Mass Accumulation Rate g/cm^2/y		CRS Sediment Accumulation Rate cm/y	^{137}Cs Mass Accumulation Rate g/cm^2/y		^{137}Cs Sediment Accumulation Rate cm/y	
	Pre-dam	Post dam		1963	1986	1963	1986
DNMA15	0.25±0.052	0.17±0.04	0.24	0.27±0.57	0.25±0.06	0.28	0.37
DNRO15	0.57±0.11	0.24±0.08	0.36	0.13±0.05	0.03±0.015	0.29	0.24
DNGT15	62.63±1.70	60.08±0.96	1.32	-	99.1±2.08	-	1.77
DNCC15	13.48±0.97	15.59±1.09	1.18	22.45±1.77	29.3±2.1	0.87	1.3
DNMU15	22.91±2.23	15.17±1.77	1.90	32.63±3.31	19.76±2.23	-	2.52
DNSN15	9±0.6	26.45±1.64	1.62	23.63±1.6	27.4±1.76	0.9	1.27
DNSC15	225.22±1.01	71.93±0.87	1.98	-	-	-	-

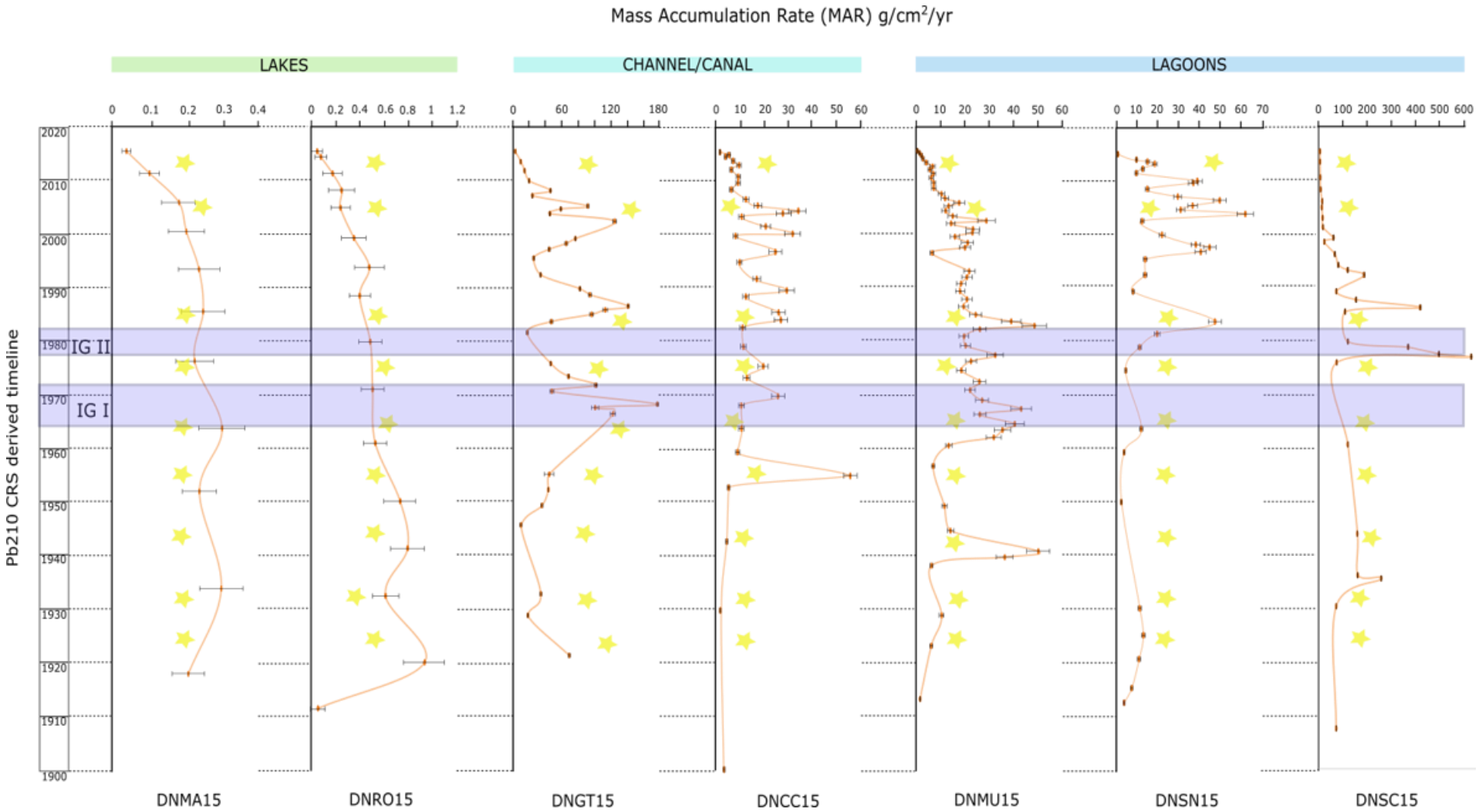

Figure 3.13. Mass accumulation rates in g/cm²/y for lakes, channels and lagoons of the Danube Delta, based on the time line obtained from ^{210}Pb dating, using the CRS (Constant Rate of Supply) model. The input of dams on the time line (Iron Gate I – 1964-1972 and Iron Gate II – 1978-1982) is marked by the purple squares. The stars mark periods of floods in the Lower Danube (1924, 1932, 1940-1947, 1954-1958, 1960-1970, 1975, 1980-1988, 2005-2006, 2010-2016).

3.4.2. Black Sea shelf

3.4.2.1 Sedimentary facies

Danube Delta front

Core S007 (Fig. 3.15) consists of a brown layer of silt at the top (0-11 cm) with a few laminae of sandy silt at 6-8 cm and 10-11 cm. The next layer (11-26 cm) is a dark grey clayey silt with several coarser levels of sandy silt at 14-17 and 22-24 cm. The bottom layer is a black clayey silt with silty sand levels at 28 and 20-35 cm. This layer contains shell and plant fragments and lime concretions.

Core S002 (Fig. 3.14 and 3.15) starts with a light brown-grey silt layer (0-8 cm), similar to S007. The next layer consists of a grey sandy silt (8-23 cm) (point A in Fig. 3.14). The bottom layer is a black clayey silt, similar to the one in S007, that contains shell and plant fragments.

Danube Prodelta

Core S008 (Fig. 3.14 and 3.15) consists of three layers of different colours, dark brown (0-6 cm), grey (6-13.5 cm) and dark grey (13.5-18.5) of sandy silt and silty sands, very rich in whole shells and shell fragments, starting with colonies of live mussels at the top of the core (point B in Fig. 3.14).

Core S003 consists of three layers of silty sand, with different colours, a brown layer (0-5 cm), very rich in whole shells, a dark grey layer (5-10 cm) and a grey layer (10-30 cm) (Fig. 3.15).

Most of the sediment in these cores is biogenic, with 15-80% from the weight of the samples being shell content, especially sand like grains, which are fine fragments of shells.

S001 starts with a brown layer of clayey silt at the top (0-3 cm) (Fig. 3.1 and 3.15). The rest of the analysed core consists of an alternation of light and dark grey clayey silt, which changed colour after the opening of the core (Fig. 3.14). This core has a very low content of shell fragments, compared to the other two from the prodelta (<5%).

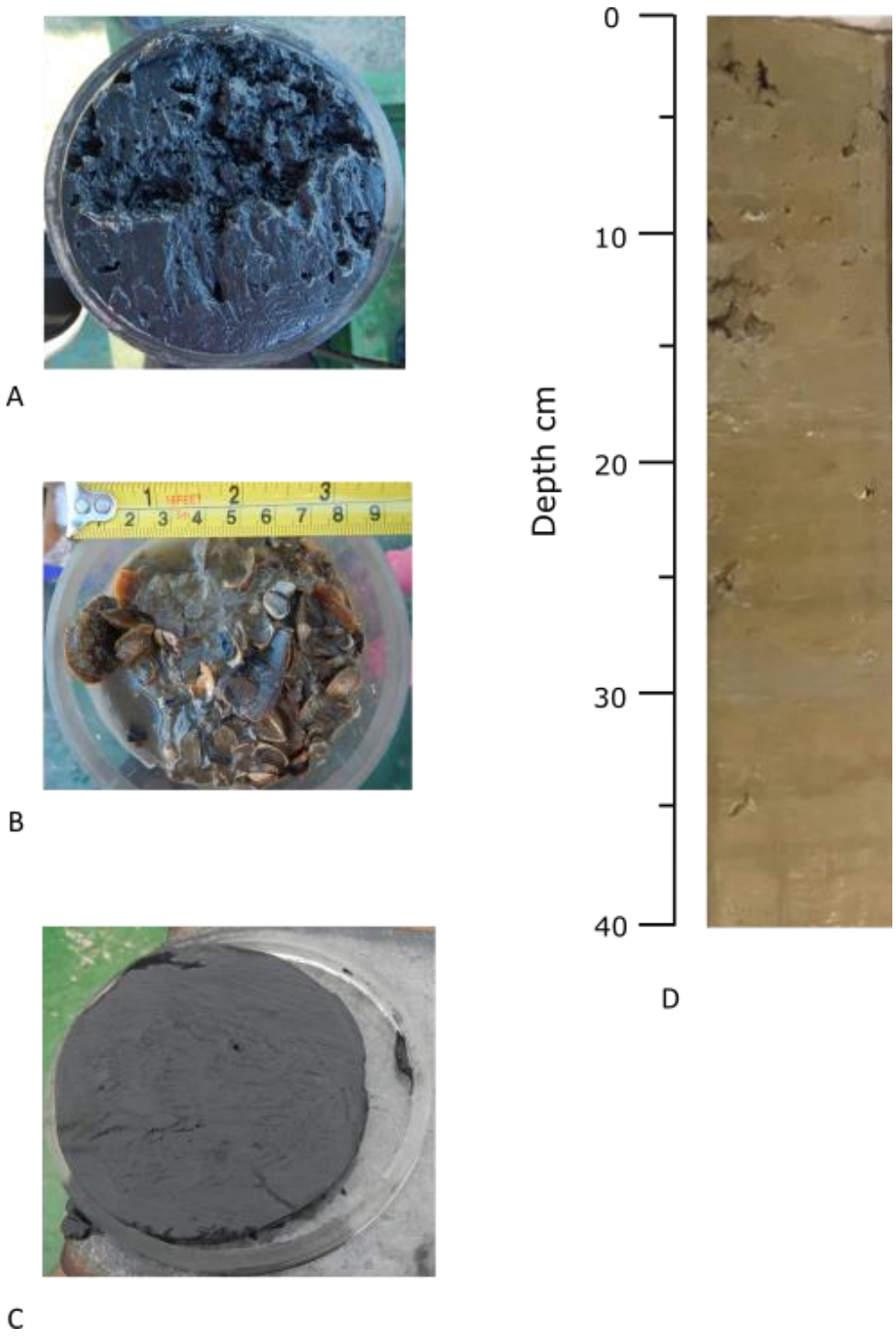

Figure 3.14. Photos of sedimentary facies in the multicorer samples. A. core S002; B. core S008. C. Core S001 at the time of the opening (multicorer sample). D. First 40 cm of the gravity core S001, which was used for this study. Notice change in colour from C to D, due to air exposure.

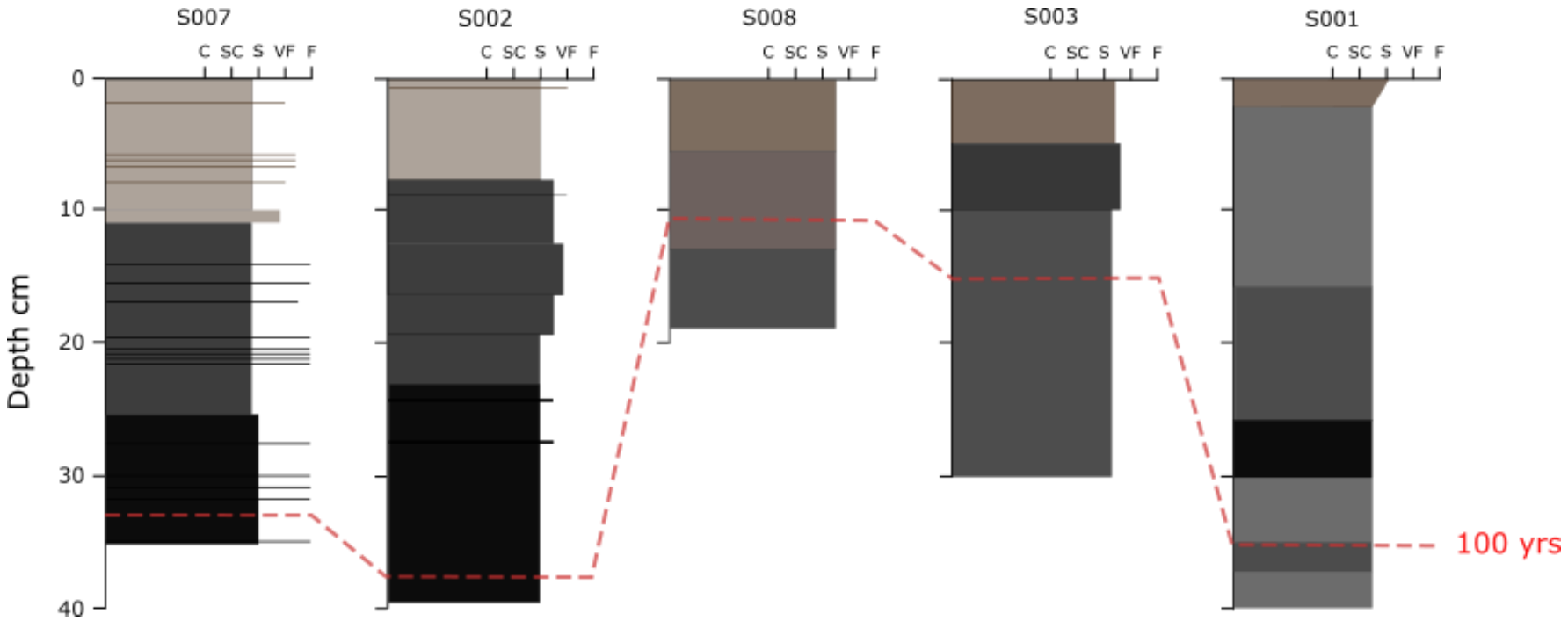

Figure 3.15. Sedimentary logs of the Danube delta front (S007 and S002) and prodelta (S008, S003, S001). C – Clay, SC – Silty Clay, S – Silt, VF – Very Fine Sand, F – Fine Sand. The red dotted line represents one century. The exact location of the cores is presented in Fig. 3.1 and Table 3.2.

3.4.2.2. Chronostratigraphic framework

The chronostratigraphic framework for all cores is based on ^{210}Pb and ^{137}Cs dating.

The CRS (Constant Rate of Supply) model was considered to be appropriate for obtaining the real ages for all cores. This model has been previously used by Begy et al. (2018) to date sediments from the Danube Delta lakes. ^{210}Pb obtained ages were compared with the ^{137}Cs activity, for the initial and second rise (1954 and 1961-1963) and the Chernobyl event (1986). To our knowledge, this is the first time sediments from both the Danube Delta front and prodelta areas are dated using these methods.

Danube Delta Front

The cores of the delta front (S007 and S002, Fig. 3.16 and 3.17) show very similar results for the CRS age model, with rather undisturbed profiles. The ^{137}Cs activity shows a similar pattern, reaching values of 80 Bq/kg in S007 and 70 Bq/kg in S002. Core S007 shows a first peak centred around 1970 and three smaller peaks, around 2000, 2010 and 2015. Core S002 shows the same peak centred in 1970 and another two, one centred at 2000 and 2015. The extent of the first peak suggests an overlap of the 1963 and 1986 events marked by rises in ^{137}Cs activity. The later peaks of ^{137}Cs activity may be due to recent contamination of the Black Sea waters (starting in 1995-1999) with Chernobyl-derived ^{137}Cs and ^{90}Sr, as recently documented by Gulin et al. (2013). Their ^{137}Cs activity peaks mimic very well the variation in clay and silt content, corresponding to the highest content of these grain classes.

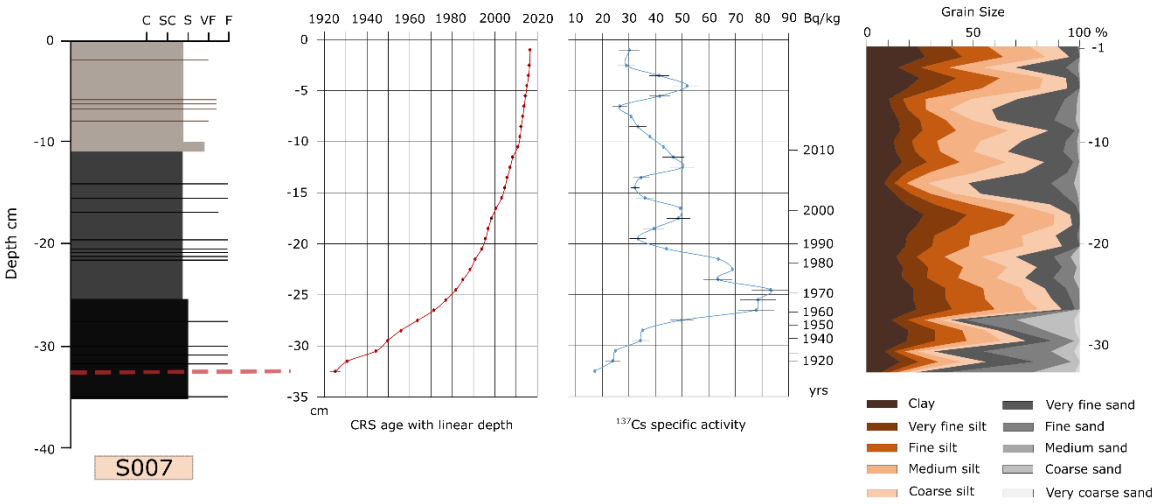

Figure 3.16. Summary figure of core S007. Sedimentary log, ^{210}Pb derived CRS age model with linear depth for the one century time period, ^{137}Cs activity with depth, compared with the CRS age model, grain size in percentages of fractions using Udden-Wentworth scale.

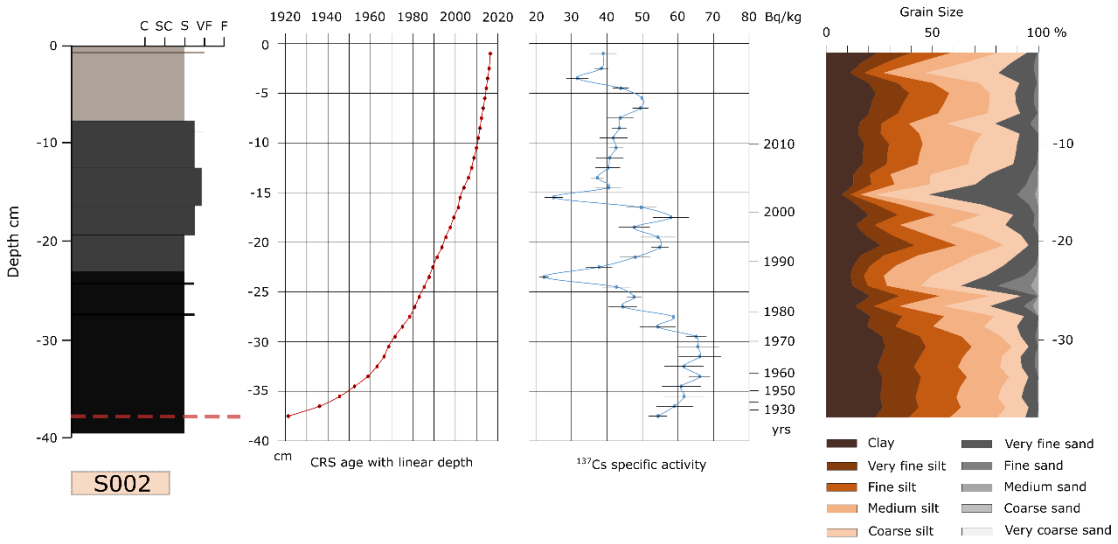

Figure 3.17. Summary figure of core S002. Sedimentary log, ^{210}Pb derived CRS age model with linear depth for the one century time period, ^{137}Cs activity with depth, compared with the CRS age model, grain size in percentages of fractions using the Udden-Wentworth scale.

Danube prodelta

For the prodelta, there is a clear difference in both CRS age model and ^{137}Cs activity between the two cores situated offshore the Danube mouths (S008 – Fig. 3.18 and S003 – Fig. 3.19) and core S001 (Fig. 3.20), located in the southern area of the prodelta, offshore the Razelm-Sinoe lagoon (Fig. 3.1). The first two cores show a very mixed ^{210}Pb age profile, suggesting a mixed sediment pattern. ^{137}Cs activity shows similar values, up to 40 Bq/kg, with a peak for S008, centred in 2000 and an increase for S003, starting around 1960's. These results suggest on overlap of the 1963, 1986 events and probably, a contribution from the recent secondary contamination of the Black Sea waters in 1995-1999 (Gulin et al., 2013). The ^{137}Cs activity peaks also reflect the variation in the finer sediment fraction, corresponding to the highest content of clay and silt.

Core S001 shows an undisturbed ^{210}Pb profile and two distinct peaks in ^{137}Cs activity. The first one is centred in 1963, while the second is a broad peak (1986-2015) that overlaps the 1986 Chernobyl event and the more recent secondary contamination from 1995-1999.

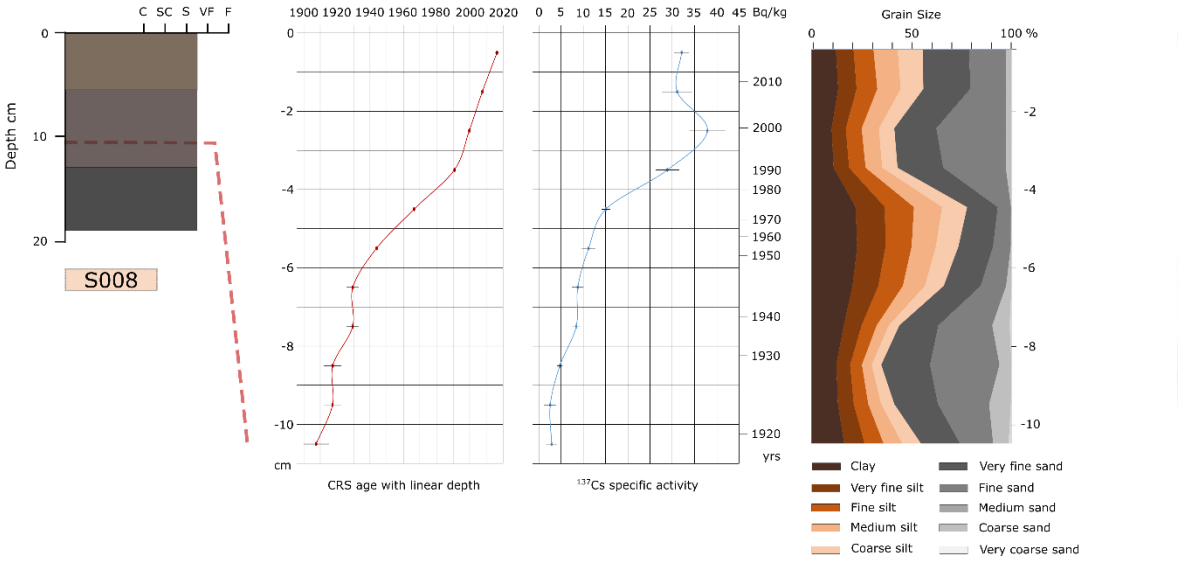

Figure 3.18. Summary figure of core S008. Sedimentary log, ^{210}Pb derived CRS age model with linear depth for the one century time period, ^{137}Cs activity with depth, compared with the CRS age model, grain size in percentages of fractions using the Udden-Wentworth scale.

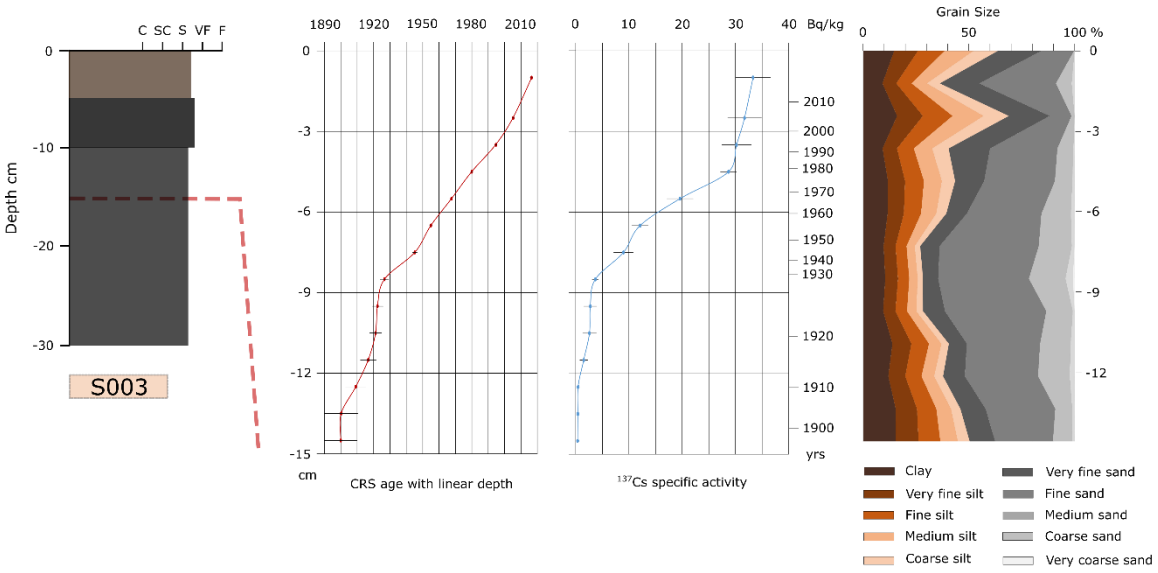

Figure 3.19. Summary figure of core S003. Sedimentary log, ^{210}Pb derived CRS age model with linear depth for the one century time period, ^{137}Cs activity with depth, compared with the CRS age model, grain size in percentages of fractions using the Udden-Wentworth scale.

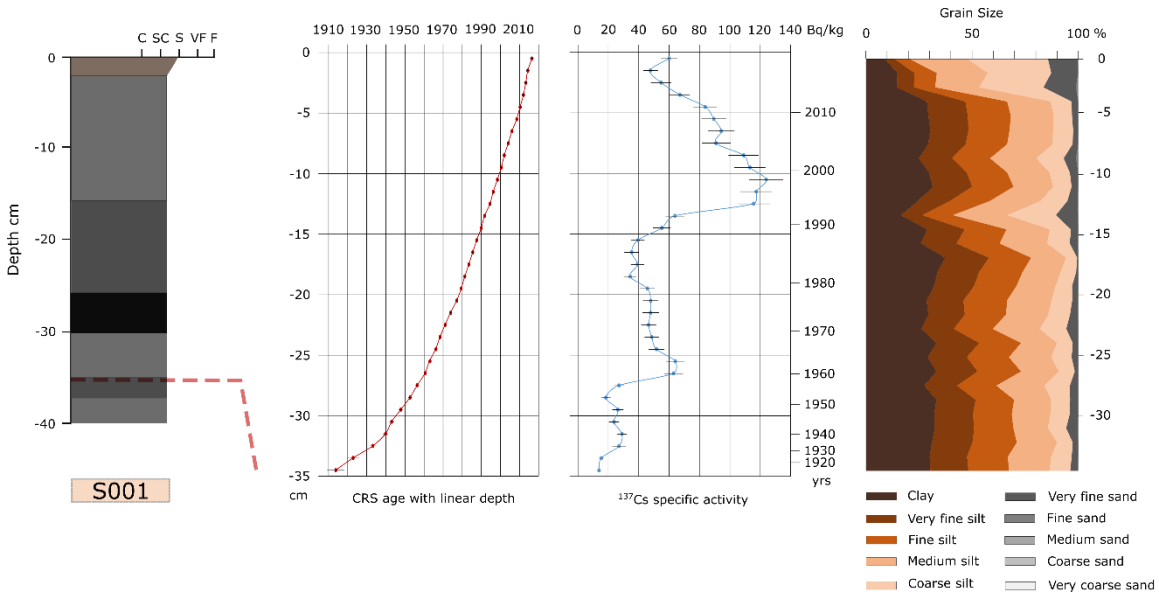

Figure 3.20. Summary figure of core S001. Sedimentary log, ^{210}Pb derived CRS age model with linear depth for the one century time period, ^{137}Cs activity with depth, compared with the CRS age model, grain size in percentages of fractions using the Udden-Wentworth scale.

3.4.2.3. Sediment flux variations

Mass accumulation rates (MAR), using mass depth, that express the variation of sediment mass with depth and dry density, and sediment accumulation rates (SAR) (cm/y) were calculated for all cores (Table 3.4), based on the ^{210}Pb CRS age model (Fig. 3.21). SAR are described for the periods pre- and post-dams (before and after 1982). MAR were also computed pre- and post-dams, to be compared with previously published data (Table 3.4). The ^{137}Cs was used to validate and check the ^{210}Pb CRS age model. ^{137}Cs derived MAR and SAR were also calculated using the 1963- and 1986-time horizons. The year 1986 can be considered the limit between the pre- and post-dam periods, so the MAR at 1963 is comparable with the pre-dams value, while the one calculated at 1986 can be compared with the post-dam value. They are presented for comparison in Table 3.4.

On the **delta front**, the two cores, S007 and S002 show different evolution of the MAR in the last century.

S007, which records the sediment discharge of Sulina and to a certain extent of Chilia branch as well, shows MAR values ranging from 0.40±0.16 g/cm^2/y to 7.95±1.4 g/cm^2/y, with a pre-dams average of 2.27±0.38 g/cm^2/y and post-dams average of 4.02±0.77 g/cm^2/y, marking an increase of MAR of 43%. The ^{137}Cs derived MAR shows similar values to the post-dam average, of 5.24±0.94. However, this core has an incomplete ^{210}Pb profile, having excess ^{210}Pb in the base. This could underestimate any MAR or SAR calculated for this area. There is a marked decrease of grain size after year 1965 CRS, sand content decreasing from <60% to ~20%, being replaced mainly by silt. Sand content increases again after 2000, up to 30-50% but it is mainly present in fine (1-2 mm) laminae.

S002, which records mainly the sediment discharge of Sfantu Gheorghe branch, shows MAR values ranging from 0.18±0.09 g/cm2/y to 120.83±1.42 g/cm^2/y. The pre-dams average is 60.84±0.73 g/cm^2/y and the post-dams average is 29.84±0.81 g/cm^2/y, showing a decrease of 51%. The ^{137}Cs derived MAR values are slightly higher, with a higher difference for the pre-dams values and the same value for post-dams. Considering that this core has also an incomplete ^{210}Pb profile, with excess ^{210}Pb in the base, the CRS derived MAR could be underestimated. The grain size is mainly represented by silt, ~60%, and sand only represents >20%. Sand content increases after 1980's but is only presented on certain intervals and fine (1-2 mm) laminae. It increases up to 50% between 2000 and 2006, marking a 4 cm interval (13-17 cm depth in the core).

In the **prodelta** area, the three cores show different MAR values, with a marked difference between the core in the north, S008 and the two cores in the south, S003 and S001 (Fig. 3.21).

Core S008, which records the contribution of Sulina and Chilia branches, has MAR values ranging from 0.005±0.0009 g/cm^2/y to 0.62±0.02 g/cm^2/y, with a pre-dams average of 0.42±0.013 g/cm^2/y and a post-dams average of 0.12±0.01 g/cm^2/y, marking a decrease in MAR of 72%. The ^{137}Cs MAR values are comparable but slightly lower. Grain size varies throughout the core, with sand representing ~50% of the sediment. Sand content decreases after 1950's, but increases again between 1990 and 2010.

Core S003 records mainly the Sfantu Gheorghe sediment discharge but, to some extent, also the contribution of the two other branches, Sulina and Chilia. The CRS derived MAR values range from 0.003±0.0009 g/cm^2/y to 3.48±0.14 g/cm^2/y, with a pre-dams average of 1.21±0.08 g/cm^2/y and a post-dams average of 0.04±0.007 g/cm^2/y, meaning a decrease of 96%. The ^{137}Cs MAR value at 1963 is almost five times lower than the CRS derived pre-dams value, while the one at 1986 is very similar to the post-dams value. Grain size is dominated by sands, with a content of <50%. Sand content, however, decreases after 1990.

Core S001 records the overall contribution of all branches, being located in the distal part of the prodelta, south from the Danube estuaries. The CRS derived MAR values range from 0.17±0.02 g/cm^2/y to 2.62±1.07 g/cm^2/y, with a pre-dams average of 1.68±0.28 g/cm^2/y and a post-dams average of 1.12±0.45 g/cm^2/y, showing a decrease of 33%. The MAR values calculated using ^{137}Cs dating are comparable, but lower, with a pre-dam value of 1.65±0.68 g/cm^2/y and a post-dams value of 0.71±0.23 g/cm^2/y. Grain size is dominated by the silt fraction, ~80%. There is a slight increase of sand content, on certain intervals, just after 1990 and after 2010, up to 10%.

Table 3.4. Average mass accumulation rates (MAR) and sediment accumulation rates (SAR) for the delta front and prodelta

Core	CRS Mass Accumulation Rate g/cm^2/y		CRS Sediment Accumulation Rate cm/y	^{137}Cs Mass Accumulation Rate g/cm^2/y		^{137}Cs Sediment Accumulation Rate cm/y	
	Pre-dam	Post dam		**1963**	**1986**	**1963**	**1986**
S007	2.27±0.38	4.02±0.77	0.80	4.11±0.73	5.24±0.94	0.50	0.80
S002	60.84±0.73	29.84±0.81	0.70	74.85±0.89	23.0±0.65	0.66	0.67
S008	0.42±0.01	0.12±0.01	0.42	0.3±0.01	0.08±0.007	0.10	0.08
S003	1.21±0.08	0.04±0.007	0.29	0.27±0.21	0.05±0.07	0.12	0.11
S001	1.68±0.28	1.12±0.45	0.42	1.65±0.68	0.71±0.23	0.50	0.40

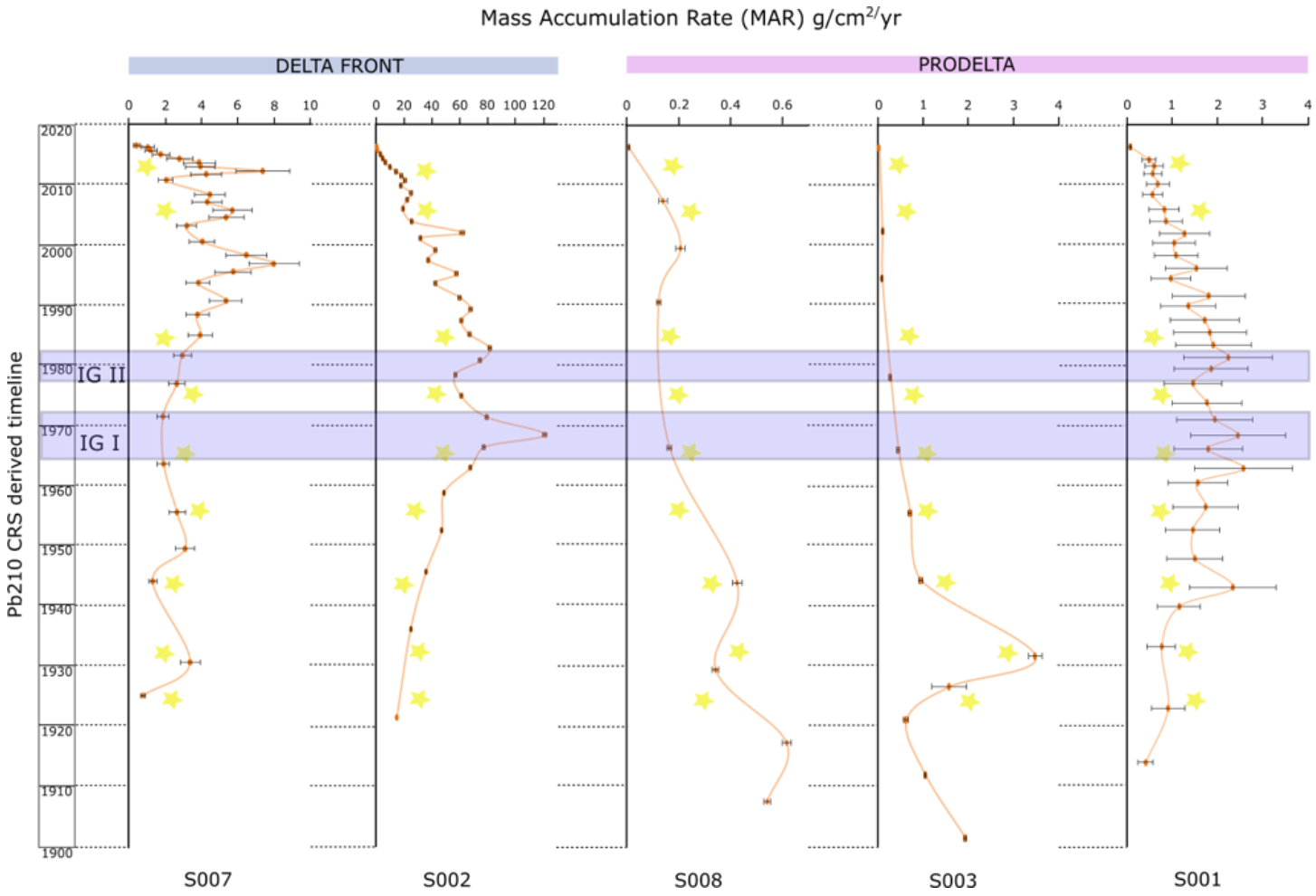

Figure 3.21. Mass accumulation rates in g/cm²/y for the Danube delta front and the prodelta, based on the time line obtained from ^{210}Pb dating, using the CRS (Constant Rate of Supply) model. The input of dams on the time line (Iron Gate I – 1964-1972 and Iron Gate II – 1978-1982) is marked by the purple square. The stars mark periods of floods in the Lower Danube (1924, 1932, 1940-1947, 1954-1958, 1960-1970, 1975, 1980-1988, 2005-2006, 2010-2016)

3.5. DISCUSSION

3.5.2. Methods for assessing sediment flux variations in the Danube Delta – Black Sea area

Very few studies have used sediment cores to assess fluxes in the Danube Delta area (Begy et al., 2018; Duliu et al., 1996; Giosan et al., 2013). Their results, based on ^{137}Cs or ^{210}Pb dating, or both, report mass accumulation rates from cores sampled mainly in lakes. While the results of lake cores are easier to interpret, they do not provide a complete picture of the distribution of sediment fluxes inside the delta complex. Published data on sedimentation rates for the Black Sea is even scarcer, with one value published for the area close to the Danube mouths (Oaie et al., 2004), who obtained a sedimentation rate of 4 cm/y, using the ^{137}Cs isotope, and one for the far shelf (Ayçik et al., 2004), who obtained 0.20±0.01 cm/y using ^{210}Pb method and 0.15±0.03 cm/y using the ^{137}Cs isotope. The first value is five times higher than the one obtained for the Delta front in this study (Table 3.3), but it can be a good approximation for sedimentation rates very close to the Danube mouths. The second values are lower than the ones obtained for the prodelta area in this study (Table 3.4), due to the location of the sampling area, outside the influence area of the Danube plume.

Other estimations of sediment fluxes for the delta especially, come from measuring solid discharge in hydrological stations and calculating averages for each year. Previous study give values of 51.7 Mt (Bondar, 1991, Panin, 1996) to approximately 25-35 Mt in the present (Panin and Jipa, 2002). However, they do not provide an idea of how much sediment is actually being deposited inside the delta or on the shelf.

Here we propose a rough estimation of sediment fluxes which are being deposited in different areas of the Danube-Black Sea zone, using the values of mass accumulation rates (MAR) from the studies cores (Table 3.5) and using the values for areas from Panin et al (1998).

Our method shows a decrease in overall sediment flux of 46%, with very similar values for the Danube Delta and the delta front area, and of 62% for the prodelta. The values for the delta front and prodelta derived from ^{137}Cs dating are similar, with a slightly higher reduction for the delta front, of 55%. However, these values may be underestimated, due to the methods used. Some of the cores did not sample a complete ^{210}Pb profile, which leads to an underestimation of MAR. For ^{137}Cs sedimentary process (clay and organic matter content, bioturbation and anoxia) can modify the value of ^{137}Cs activity in the sediment column (Corcoran and Kelley, 2006).

Table 3.5. Sediment flux calculated from MAR data for the morphological regions of the Danube Delta

Zone	Area Km^2	Pre-dams sediment load Mt/y	Post-dams sediment load Mt/y	Reduction %	1963 ^{137}Cs derived sediment load Mt/y	1986 ^{137}Cs derived sediment load Mt/y	Reduction %
Danube Delta	5800	30.71	16.65	45.75	-	16.99	-
Delta Front	1300	4.10	2.20	46.35	5.13	2.35	54.2
Prodelta	6000	0.60	0.22	61.70	0.36	0.14	59.58
Total	*13.100*	*35.41*	*19.08*	*46*	-	-	-

Considering that the available sediment flux that enters the Danube Delta has dropped by 50 to 70% (McCarney-Castle et al., 2011; Panin and Jipa, 2002), the difference calculated in this study may be explained by local bank erosion and redistribution of available sources of sediment (erosion and re-suspension of bed sediment at high-waters, overwash, littoral erosion and redistribution on the marine shelf), as well as by the amount of organic sedimentation, which is usually not quantified (see also Giosan et al., 2013).

3.5.3. Sediment flux in the Danube Delta – Black Sea area.

3.5.3.1. General evolution

This study provides the most complete picture, to date, of sediment flux variations in the Danube Delta – Black Sea interaction zone. The variation of mass accumulation rates over different environments of the delta shows changes in local depocentre in time, due to the anthropic interventions in the basin or at local level but also due to natural variability.

The results show a sediment load of 35 Mt/y being deposited in the delta complex, before the input of dams. If we compare it with the value of pre-dam sediment load, of 51.7 Mt/y (Panin and Jipa, 2002), the results seem possible. The value obtained for post-dams sediment load, of 19.08 Mt is much closer to the present estimates of 25-35 Mt. This would mean a trapping efficiency for the delta complex of 63% (pre-dams) and 60% (post-dams), and of the subaerial delta of 54% (pre-dams) and 52% (post-dams), which is comparable with deltas of Asian rivers (Liu et al., 2009).

Danube Delta

In lakes, sediment delivery decreases overall, but before the two main dams Iron Gate I and II are in place, it responds to natural variability, increasing during flood pulses (Fig. 3. 13.). Floods of the last 10 years (2006 and 2010) do not seem to mark an important increase in sediment flux in these areas.

The active sedimentation in the two analysed channels, Garla Turcului and Canal Ciotica that increases after 1970's, shows a shift of the depocentre towards the secondary delta of Sfantu Gheorghe. Garla Turcului is one of the most active channels of the Sfantu Gheorghe secondary delta, delivering water and sediment in the Sahalin lagoon. Interestingly, the grain size in this area decreases, sand being replaced by silt. It is debatable if this is a reflection of an overall process in the Danube Delta or the so-called 'silting' process that occurs naturally in a channel or canal. It is gradually being filled with sediment so the speed and volume of water decreases or stagnates, and the coarser sediment does not reach this area.

The sedimentation in Garla Turcului is particularly sensitive to flood pulses, recording most of them in fine laminae. Canal Ciotica represents a very good example of a canal dug in the early 1950's, for access to more remote areas of the delta, for fishing and reed harvesting. This actions increased sedimentation locally, as it was described by Giosan et al. (2013), but as is gradually being filled with sediment, the water and sediment fluxes arriving in this area decrease and it can finally become clogged. Low water level and siltation lead, in time to the over-growth of macrophytes.

According to Panin and Jipa (2002), the percentage of sandy alluvia in the Danube remains the same, at 10%, even after the construction of dams. This is confirmed in all the analysed cores, from the lakes and channels, which record a sand percentage of over 10%.

The two analysed lagoons, Musura and Sahalin, reflect the sedimentation patterns of the two active depocentres, the secondary deltas of Chilia in the north and Sfantu Gheorghe in the south. Sediment flux decreases in Musura, with the input of the dams, but most flood pulses are recorded in the active sedimentation. This particular area of the lagoon records the end of the Chilia plume, being protected by the barrier spit and far enough from the mixing zone with the sea, resulting in a thick layer of silt and a regional anoxia. The same sedimentary pattern and anoxia is present in the north of the Sahalin lagoon. The main difference between these two areas is given by the proximity to the main water and sediment plume, which translates in different amounts of sand, higher in Sahalin, and the record of most of the flood pulses in sand laminae. While the spit moves closer to the shore, thus closing the lagoon, and the distribution of sediment changes inside the lagoon, the overall sediment flux decreases. The movement

of the spit is well visible in the northern core, marked by a sharp increase in sand of 40%, around 2010.

Delta front and prodelta

On the delta front, the evolution of depocentres change from south to north, around 1960. In Chapter 2 the overall decrease of sediment transported by the Sulina arm is shown, under the changes in the Danube basin, including dams and the changes in natural variability due to climate change. In 1859, the Sulina channel was deepened for navigation from 2.5 to 9.5 m, resulting, in the century, in an increase of water discharge on Sulina up to 20% (Panin and Overmars, 2012). Afterwards, the mouth of the channel, as well as the navigation way between the two jetties was constantly dredged to maintain navigation, and the sediment (sand mostly) was discharged at more than 20 m depth on the Black sea shelf (Stănică et al., 2007). The very active sedimentation in front of Sulina, especially after 1970, reflects thus the local anthropic changes on the Sulina channel. However, it also records the natural variability of flood pulses, which are well visible in the sediment, in sand laminae. The Sfantu Gheorghe depocentre reacts to the overall deficit of sediment and only seems to record just some of the flood pulses. The main difference of these two areas, in the near shore domain, is that while on Sulina, most of the water and sediment is concentrated in the navigation channel, between the jetties, the Sfantu Gheorghe branch flows in fairly natural conditions and feeds a secondary delta, on a much wider area than the Sulina depocentre. The main consequence is that most of the sediment on Sulina is taken out of the coastal circulation (Stănică et al., 2007), resulting in an erosive trend of the coastal strip between Sulina and Sfantu Gheorghe, while the sediment carried by Sfantu Gheorghe branch is kept closer to the coast, feeding the Sahalin lagoon and a small area south of it.

The prodelta area records a decrease in sedimentation beginning with the 1940's in the eastern part. The south part of the prodelta, south of the main three estuaries of the Danube shows an increasing trend in sediment flux from the beginning of the century until mid 1960's, and a marked decrease afterwards, following the general decreasing trend of sediment flux, due to the input of dams. Direct observations in cores show that the eastern part of the prodelta is dominated by the presence of coquina, a thick layer of dead shells of various species, which represent most of the sediment source. In the southern part of the prodelta, the shell content is much lower, and most of the sediment is detrital, of the finer fraction (clay and silt), as shown in core S001. This part records most likely the resulting Danube plume, as it is moving southward.

3.5.3.2. What next?

Danube Delta

It was considered that the overall deficit of sediment supply, caused by dams, may be attenuated by an increase in extreme floods, during which the sediment concentration increases in the whole water column, but this trend is not certain for the future, as modelling suggests an increase in droughts rather than flooding events in the Danube catchment (Giosan et al., 2013). Recent analysis on hydrological data shows that the flood phenomena increased in the Danube Basin in the last decades (Mikhailova et al., 2012). One would expect to see their effects in the sediment deposition all around the delta plain and in the new delta deposits of Chilia and Sfantu Gheorghe. However, the effect is not obvious in the analysed areas. As shown in Chapter 2, natural variability of water and sediment pulses that arrive in the Danube Delta are attenuated, beginning with the mid 1970's, which coincides with the input of Iron Gate I. The results of this study show that only areas that are directly connected to the main branches (larger channel, some areas of the terminal lagoons and mouths of the main branches) record these pulses, depending on the degree of connection.

The question remains if the present sediment flux is enough to maintain the aggradation process in the future, in the Danube Delta, above mean local sea level rise of 3 mm/yr, and especially, if there will be enough sand in the system to feed the coastal zone. The sedimentation rates in all the analysed area appear close or exceeding this value. For the moment, our results suggest that the two active depocentres, Chilia and Sfantu Gheorghe deltas, concentrate most of the sediment flux in the Danube Delta. However, the question still remains: Will the reduction of sediment flux be constant or will it grow?

Delta front and prodelta

The accumulation of sediment on the delta front seems to depend not only on the overall sediment flux variations but also on the flow regime of the main branches and the anthropic interventions on the coast. The Sulina jetties determine a relative increase in sediment flux close to this branch, and they probably concentrate sediment flux in front of Chilia Delta as well. To our knowledge, there is no published data on sediment accumulation rates from the Ukrainian waters, for comparison. The prodelta records the highest decrease in sediment flux, with the southern part concentrating most of the sediments brought by the Danube plume. The largest quantity of sediments is deposited in the main direction of flow, as the plume usually travels from north to south, with the coastal current, while its lateral extent depends very much on wind conditions (Güttler et al., 2013).

3.6. CONCLUSIONS

This study provides, for the first time, values of sedimentation rates in the Danube-Black Sea interaction zone, from the Danube Delta to the prodelta area. Based on the sedimentary rates calculated for the last century, a reduction of sediment flux is estimated for the Danube-Black Sea interaction area, following the input of the Iron Gate I and II dams. This reduction is of around 46% for the sub-aerial delta, 46-65% for the delta front area and of 65% for the prodelta. This leads to an estimation of the retention capacity of the sub-aerial delta to 54-52 % for the last century.

The impact of the overall reduction of sediment flux brought and discharges by the Danube, over the various environments of the delta – lakes, channels and lagoons, delta front and prodelta is different. The overall reduction in sediment flux does not produce major changes in the depocentre. The changes are mainly represented by a general decrease of sedimentation rates, while the general evolution of the delta stays the same. This is mainly controlled by the degree of connectivity to the main branches or by local anthropic interventions in the area. The changes of water and sediment flux on the Sulina channel, for example, and a channelling effect of the jetties increase sediment supply locally, in this area of the delta front. Also, the extreme hydrological events, such as the major floods of the last century can only be traced in certain areas – larger channels, terminal lagoons and delta front, which are directly connected to the main hydrologic network, represented by the three discharging branches. Changes in grain size are not significant, though the lakes and smaller channels record lower sand content after the input of dams. This could also be a secondary effect of the natural siltation process, and not necessarily linked to sediment sources in the Danube basin.

The findings of this study show the importance in continuity and quantity in sediment flux for delta complexes in general, but also in maintaining a good hydrological connectivity of the sub-aerial deltas in particular, for an efficient aggradation process.

Some questions still remain. Is this sediment deficit low enough to allow the aggradation and progradation process to continue and maintain the Danube Delta above sea level rise? What will be the tipping point for its coastal area, which is the most affected by the decrease of sediment supply?

For deltas which are not heavily managed, as it is the case of the Danube Delta, ensuring an efficient hydrological connectivity is of primary importance for the delivering of sediment in the buffer areas, such as the terminal lagoons, where progradation happens, but also for ensuring efficient water circulation and mitigating eutrophication.

An improvement in understanding sediment flux in this area would be obtaining more sedimentation rates, from all parts of the delta, together with a better quantification of suspended and bed-load distribution in the complex of channels and canals. A quantification of the organic component of sedimentation in all environments would be necessary. The distribution and variation in time of the total sediment flux would improve our understanding of the interactions between hydrology, geology and ecology in such a complex area. The nature and seasonal distribution of sediment flux in the Danube Delta, delta front and prodelta will be explored further in the next two chapters.

4. PROPERTIES OF SUSPENDED SEDIMENT FLUX IN THE DANUBE-BLACK SEA INTERACTION ZONE

4.1. INTRODUCTION

Sediments are an intricate part of all water bodies. Knowing more about their physical and chemical properties provides useful information about if and how the state of these environments is changing and about the acting factors of these changes. Sediment particle size, distribution and composition in water bodies is important for understanding, to a certain extent, the behaviour of light scattering (Risović, 2002), phytoplankton and zooplankton dynamics, biogeochemical cycling (Quéré et al., 2005), the transportation of particulate reactive pollutants and also, the dynamics of sediment fluxes (Mikkelsen and Pejrup, 2001).

Chapter 3 focused on creating an image of the effects of decreased sediment flux in the different environments of the Danube Delta and the NW Black Sea, from sediment cores. This study aims to investigate the quality of suspended sediment particles, comprising particle concentration, size and composition in the Danube Delta and the NW Black Sea shelf area, using in-situ measurements of water constituents – TSM, ISM and Chl-a and direct analysis of particles from Scanning electron Microscope, coupled with an XRF detector. It is for the first time that this kind of a study is done in this area, on such a large scale. This contributes both to understanding the ecological status of these environments but also to link sedimentary processes which happen in the water column, distribution of sediment flux in a complex river-se transition zone, with the use of remote sensing techniques for mapping sediment fluxes. This last part will be addressed in the next chapter.

While the information provided by sedimentary cores, as is described in Chapter 3, describes the changes in timing and dynamics of sediment flux, with implications for both aggradation and progradation of the Danube Delta, this chapter is painting the image of these environments at a seasonal scale, focusing on the relation between water and sediment fluxes and the ecological status and current evolution of these environments.

In this context, suspended sediment is defined by all particles, of any nature – of natural or anthropic origin, either of mineral or organic composition, allogenic or autogenic, present in the water, in suspension, at a certain movement in time.

4.2. MAIN SOURCES OF SUSPENDED SEDIMENT AND CONTROLLING FACTORS

The Danube basin and interaction zone, comprising the Danube Delta and the marine shelf around it have been described in detail in Chapter 1. In this chapter we will focus on the

description of suspended sediment (concentration in water, particle size, particle composition) in this complex area.

The main source of sediment in the Danube Delta and the marine shelf around it is the Danube River. In the Danube Delta, the main three branches transport most of the alluvia. The mean annual discharge of sediment at the delta entrance was calculated at 1737 kg/s by Bondar and Panin (2001), which translates into 14 695 t/day, for the period of 1840 to 1990, with a mean volume of 54 815 551 or 54 815.5x10^3 t/year, from which 2 180 000 tons were sandy alluvia. Sediment transport reveals the same seasonal variations as the water discharge, with a maximum during spring-summer and a minimum during autumn (Bondar and Panin, 2001). Inside the Danube Delta, alluvial sedimentation occurs when the velocity of the flow decreases under a critical value and there is a high content of suspended sediment transported in suspension. The areas where these conditions are met are mainly located at the bifurcation of bigger channel/canals in smaller branches or at the discharge point of a channel/canal into a lake. This process is very intense in the fluvial delta but it can also occur in the fluvial-maritime area (Cioaca et al., 2010). The Danube Delta acts like a chemical and physical filter for the waters reaching the Black Sea, through its large and compact areas of reed (Cioaca et al., 2010).

The hydrographic network of the Danube Delta is complex, with about 3500 km of channels /canals which connect around 500 lakes (200,000 ha of water surface) (Cioaca et al., 2009). The active secondary deltas of Chilia and Sfantu Gheorghe end in lagoons, Musura and Sahalin, where most of the sediment carried by these two branches is deposited and reworked by waves and currents. The water circulation of the Danube in the delta has an irregular character, depending on the hydrologic regime of the river (Bondar, 1994). Water discharge varies on a longitudinal scale, on the Danube distributaries. The lateral channels and canals take water overbank spilling happens when the water discharge at the delta apex exceeds 9100 m3/s (Bondar, 1996). Direction and gradients of water flow regime change inside the delta, depending on the water level, from west to east (Poncos et al., 2013). Bondar (1994), calculated that the water discharge which the Danube releases in the delta plain increased from 1858 to 1980s almost four times. This was caused by the cutting of deepening of canals to facilitate access in different parts of the delta.

The Danube Delta lakes are directly connected to the Danube through a vast network of channels and canals, as described previously. They are flood plain lakes (Oosterberg et al., 2000), located between the three branches of the Danube, with a size varying from 14 to 4350 ha (Hanganu et al., 2008). Their water level is variable in a year, depending on the river pulse (Hanganu et al., 2008). Most of the lake sediments of the delta plain consist of silts (>65%),

fine sand (6-15%), clay (20-30 %) and shell fragments (2-4 %) (Mihailescu et al., 1996). All delta lakes suffered from eutrophication in the recent decades, which was most intense in the 1960s to the 1980s, due to anthropogenic input of phosphorous and nitrogen (Oosterberg et al., 2000). Danube Delta lakes were classified into three main categories, taking into consideration hydrogeomorphology and water quality, composition and abundance of plankton, aquatic vegetation and the fish community. Type 1 lakes are large, characterized by a sandy-silt substratum, turbid waters (e.g. Lacul Rosu, Merhei), type 2 lakes are well connected to the channel network, have a clayey substrate and clear water (e.g. Furtuna), type 3 lakes are isolated, with organic load and clear waters (Oosterberg et al., 2000).

The particles present in the water column are suspended solids (mineral and detritus) and phytoplankton biomass, with an equal contribution, and they are subjected to a strong seasonal variation (Oosterberg et al., 2000). Turbidity varies in the lakes (Güttler et al., 2013; Oosterberg et al., 2000), depending on the connectivity to the water network and the presence/absence of vegetation (Coops et al., 1999).

A recent analysis on a time frame of two years (Güttler et al., 2013), revealed a seasonal variability of turbidity inside the Danube Delta and in the coastal plume:

- During winter high levels of turbidity characterize lakes inside the delta, even those not directly connected to the hydrographic network, due to wind-induced resuspension of bottom sediments and highly turbid plumes are generated in the coastal zone;
- Spring season brings the peak hydrological discharge which influences the turbidity in only the lakes directly connected to the main branches, and most lakes present clear waters. Spring represents a transition period for both the lakes inside the delta and the coastal plume – river-induced turbidity decreases and the seaward expansion of the plume increases;
- In the summer, river-induced turbidity decreases but some lakes start to present high turbidity levels since June, coinciding with phytoplankton growth. The plume expansion decreases in the coastal area, reaching its minimum in August.
- During the fall, some lakes present the same turbidity patters as for summer and some others, more isolated one have higher turbidity levels. The plume extension increases compared to summer period.

The solid suspensions reaching the Black Sea (particulate organic and inorganic matter larger than 0.45 µm) were estimated at 11000 tons/day, out of which 8.9% represents phytoplankton and 0.2% zooplankton, leading to a total of 4000x103 t/y of suspended solids,

35x103 t/y of phytoplankton and 7x103 t/y of zooplankton (Gomoiu et al., 1997). The sediment and associated particles are transported along the coast by the Rim current and across shelf-continental slope by meso-scale eddies and are deposited mainly in the Danube Delta front area and prodelta (Stanev and Kandilarov, 2012).

Previous studies have described the spatial dispersion patterns of the Danube plume, which forms through the main discharging arms, and assessed the main influencing factors. Using passive tracers, Bajo et al. (2014) observed the prevalence of Chilia's waters in the formation of the plume, while the waters of Sfantu Gheorghe follows the Sahalin spit and remain confined near the shores. The influence of Sulina is even more reduced, as it mixes with the waters of Chilia. Bajo et al. point out that instant patterns may be different, as the exact area and processes controlling the plumes should be investigated further. The plume extension is mainly restricted to the coast and shelf (maximum offshore extension of 70 km as estimated by Güttler et al., 2013), with a penetration depth of 15 m near the coast (Karageorgis et al., 2009), while the influence of the Danube waters, traced through simulated inorganic N/P molar ratios at the sea surface, can extend to the Turkish coast (Tsiaras et al., 2008). The main controlling factors for the formation and extension of the plume are hydrological (solid and liquid river discharge that varies seasonally; meteorological (wind speed and direction) and the topography of the shoreline (Güttler et al., 2013; Karageorgis et al., 2009). Wind seems to be the primary factor for surface water direction of flow but the haline stratification can limit its influence in the deeper layers, especially near the delta (Bajo et al., 2014).

While the distribution of suspended sediment fluxes has been described in more detail for the Danube Delta and for the Black Sea, these two areas should be studied together. The transfer and distribution of both size, concentration and composition of suspended particles through the delta and onto the marine shelf determines sedimentary patterns and gives indications on environmental changes.

4.3. METHODS

4.3.1. Field surveys

Danube Delta

Two field surveys were carried out in 2015 and 2016 (27.07-03.08.2015 and 23.05-03.06.2016), on board RV Istros, in different seasons and hydrological conditions, low water discharge in the late summer of 2015 and high-water discharge in the late spring of 2016 (Fig. 4.1). Water samples were collected from all the areas of the Danube Delta, from the main branches to lakes and lagoons (coded DNstation_no in Fig. 4.2 and Table in Annex 2). The

locations in the Danube Delta were chosen to sample: the main channels (Sulina and Sfantu Ghoerghe), cut meanders (Old Danube on Sulina, Mahmudia and Dunavat), secondary channels or canals, lakes of different sizes and different degree of connectivity to the main hydrographyc network (Matita, Fortuna, Rosu and Rosulet), and lagoons (Musura, Sahalin, Razelm and Golovita).

Black Sea

The Black Sea marine cruise was carried out in May 2016 (4-12.05.2016), on board RV Mare Nigrum, as part of the EuroFleets 2 funded project ReCoReD (Reconstructing the Changing Impact of the Danube on the Black Sea and Coastal Region). During the cruise the water discharge of the Danube was close to annul average (normal water level in Tulcea, Fig. 4.1), wind conditions were stable, with dominant direction from N-NE or N-NW, with a low average speed (<10 m/s). Surface samples were collected from all stations (T or S stations). Water at different depth were collected in all S stations (Fig. 4.2, Table in Annex 2). The locations in the Black Sea were chosen to sample the Danube plume, both its lateral and longitudinal extent to the east and south, respectively, and the extent in depth, from the surface, down to -80 m.

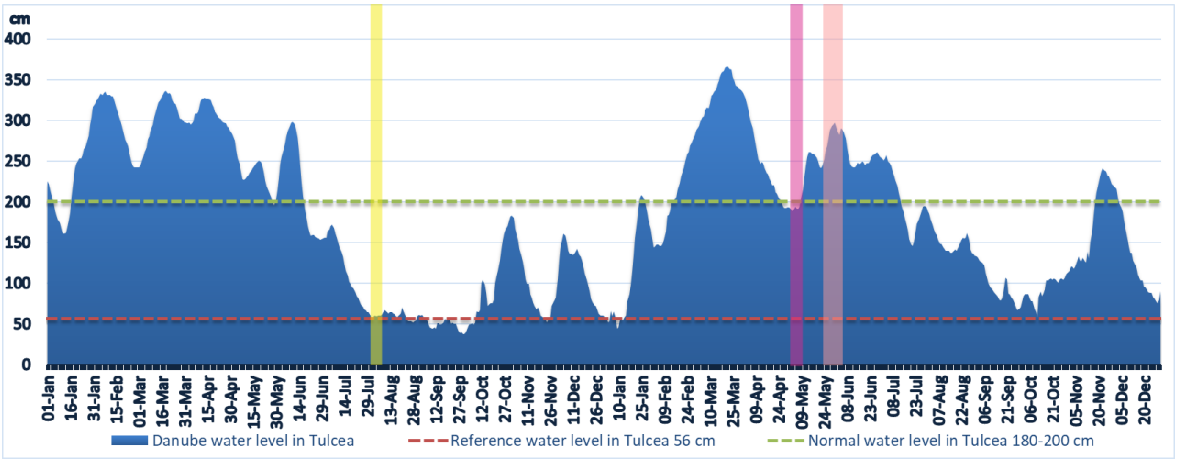

Figure 4.1. Danube water levels in the port of Tulcea (blue curve) and the sampling periods in the Danube Delta in 2015 (yellow square) and 2016 (pink square) and in the Black Sea in 2016 (purple square) (these colours correspond with the colours of the sampling points in Fig. 4.2).

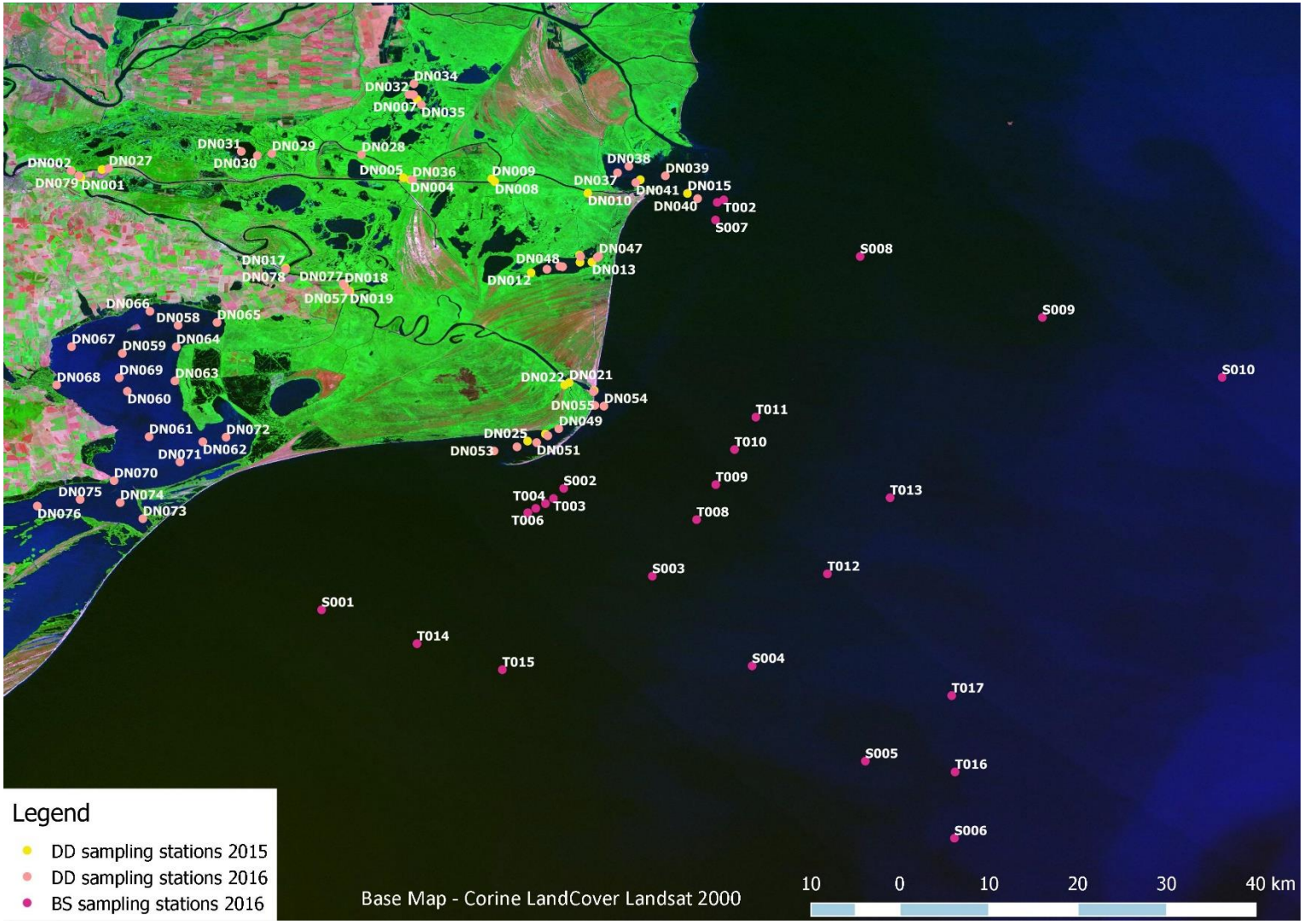

Figure 4.2. Sampling stations for water constituents in the Danube Delta and on the Black Sea shelf, for 2015 and 2016. Color code for sampling stations corresponds with the squares in Fig. 4.1. All S stations in the Black Sea depth profiles were sampled

4.3.2. In-situ water constituents

4.3.2.1. Sample collection and preparation

In the Danube Delta, the surface water was sampled from the boats, directly into plastic bottles and filtered right away. Water sampling from the Black sea was done with 5 l Niskin bottle system, equipped with a CDT, at depths were the chl-a and turbidity values were changing.

Sub-samples were then filtered for Total Suspended Matter (TSM), chlorophyll-a and particle size. All samples were preserved at appropriate temperatures for analysis.

4.3.2.2. Analysis

Total Suspended Matter (TSM)

For the Danube Delta samples, between 200 and 1500 ml of water were filtered through pre-weight glass fibre filters. For the Black Sea samples, between 1000 and 2500 ml of water were filtered. They were then packed in petri dishes and refrigerated. Before weighing, the filters were dried at 60°C for 24h. TSM was measured from three replicates per sampling point, using an electronic balance with a 10^{-5} accuracy. The filters were then ashed in an oven at 450°C for 5h to remove the organic fraction. They were re-weighted to determine the inorganic fraction of suspended matter (ISM).

Chlorophyll-a

For the Danube Delta samples, between 25 150 ml of water were filtered through glass fibre filters. For the Black Sea samples, between 50 and 1500 ml of water were filtered. The samples were packed and frozen for analysis at -80°C, before analysis.

Chlorophyll-a was determined using two methods. All samples of 2015 were analysed using the spectrometric method, based on ISO 10260 (1992). All samples were grinded until the filter fibres were separated and 10 ml of boiling ethanol was added. After centrifugation, they were stored in darkness at approximately 2°C for 24h. After decanting the clear supernatant, all samples were analysed using a CARY 100 dual beam spectrometer. A blank with 90 per cent ethanol solution was used at each wavelength. Three replicates per sampling point were used for the analysis.

For the samples where the chlorophyll concentration was expected to be lower, such as turbid water or the Black Sea and the Danube Delta, the HPLC (High Performance Liquid Chromatography) method was used. A DIONEX (Ultimate 300) system equipped with DPA and vacuum degasser was used. The samples were kept at 4°C prior injection. Dionex Chromeleon software is used to control the HPLC, manage the files and identify the peaks.

4.3.3. Scanning Electron Microscope analysis

4.3.3.1. Sample collection and analysis

All samples were analysed with a Zeiss EVO MA-15 variable pressure SEM fitted with an Oxford Instruments X-Max 80 mm2 SDD EDX detector, in the laboratories of the University of Stirling. The instrument was used in the variable pressure mode, with the chamber pressure at 60 Pa, an accelerating voltage of 20kV, the filament current at 2.770 A and the beam current at 50 µA. The working distance was kept between 8.5 and 10 mm, and the magnification was x10-x200, depending on the loading on the filter.

The X-ray acquisition rate was 8.5-10 kcps, spot size of 530 and filament current ~2.573A to increase scan speed.

As guideline for this analysis we have used the method described in Groundwater et al. (2012).

Filtering and preparation. Samples were collected in 2016, from both the Danube delta and the Black Sea area, in the same sampling points with the other water constituents.

They were filtered on Whatman polycarbonate filters of 0.2 µm pore, immediately after collection or within a few hours after collection. Filters were rinsed with distilled water for the marine samples to clear salts. They were then frozen in Petri dishes and dried before analysis for at least 24 h @35°C. TSM values for each sampling point were measured separately as previously described.

Standard preparation. The standard test was conceived so it would simulate a similar situation with the natural environment sampled, the waters of the different environments of the Danube Delta and the NW Black Sea. The results of grain size analysis of the sediment cores, as well as information from literature show that most the Danube sediments are in a range of 0.06 µm (clays) to 125 µm (fine sands). The two main parameters to check in the experiment were particle size and size range or distribution.

To check accurate measurement of particle sizes we used a standard of 8 µm, provided by Sigma-Aldrich, consisting of micro particles based on polystyrene in aqueous suspension, concentration 10%, 8 µm std dev <0.2 µm, coeff var <2%, 1.05 g/cm^3 density. Several images of the standard were taken and the analysis was done on 136 particles. An example image is Fig. 4.10.

In order to determine the number of measurements to capture the relevant particle size range we used a standard with particle sizes in the range of 10-50 µm, tested previously with a Coulter Counter. An analytical blank was also prepared by filtering Milli-Q.

Standards test. Ten random, non-overlapping images were acquired with the SEM, for each filter. We have found that this number of images is enough to have a correct distribution of particle sizes for the sample (also see Groundwater et al., 2012). The scanning of the analytical blank revealed no particles on the filter. Particles representing all size categories were scanned with the EDS-XRF. The particles had similar compositions. For the actual samples, where we expected more variation in composition, we have used two transects on the two diagonals of the image, to acquire the data, on ten random particles per filter. As we have scanned individual particles, we assume that the O and C in the results show the particle composition and not the effect of the filter.

Field samples. Ten random images were acquired for each sample. For each image, an XRF scan was done on single particles, chosen so their size would be easy to determine at the scale of the image. Ten such scans were done for each image, in a cross pattern. This method was considered to be more time effective but to also provide statistically significant data, so at least 100 scans were done for each sample.

4.3.3.2. Image analysis

All images acquired with the SEM were analysed in Image J. This software provides a tool for particle size measurements and counting.

For each image, the scale was calibrated with the scale bar. Then, an area with even illumination was selected and duplicated for analysis. Then, a bandpass filter was applied in order to highlight the particles from the filter. This method has, in addition, the possibility to adjust a threshold to delineate the darker areas of the image, the particles in this case, from the background. The disadvantage is that the filter can sometimes cause the appearance of fake particles of very small diameter but a manual sorting of the results can identify them. Then, the automatic particle analysis is done, that provides each identified particle with a number and calculates the area.

4.3.3.3. Particle size

The area obtained with Image J was used to calculate the equivalent spherical diameter using the formula:

$$D = 2\sqrt{\frac{A}{\pi}} \qquad (4.1)$$

Then, the number of particles in a size bin per unit volume was calculated from the particle frequency (v) –number of particles within a bin size, normalized by the total volume of water filtered multiplied by the volume correction:

$$dN = \frac{\nu}{VfiltrVcorr} \quad (4.2)$$

The volume correction factor was calculated because only a portion of the filter was imaged. For each sample, images were taken at different magnifications so, an average area imaged was determined and then the volume correction factor was:

$$Vcorr = \frac{10Ai}{A\ filter} \quad (4.3)$$

The particle size data was divided into bins corresponding to the categories of grain size, according to the Udden-Wentworth scale. The dimensions range from 0.4 to 200 µm (the 0.2 µm is the pore size of the filters), so the actual lower limit for clay sized particles is 0.4 and not 0.06. The results are presented for each environment: lakes, channels, lagoons, delta front and prodelta, in percentages of the total number of particles.

4.3.3.4. Particle composition

Around 100 particles (between 80 and 130) per sampled site were scanned with the EDS-XRF detector. The results of the scanning are reported in percentages for the main elements: C, O, Fe, Ca, Si, Al, Mg, Na, etc.

4.3.3.5. Statistical analysis

Variations of the percentage of these elements were analysed as a function of particle size, for each of the environments sampled, using correlation. Correlation coefficients are presented in the graphs, for all elements (R^2).

4.4. RESULTS

4.4.1. Standard test results for particle size

The polystyrene standard (Fig. 4.3) was used to check the accuracy of the method of obtaining particle diameter using image analysis in ImageJ. The test results show an average value for particle size of 7.8 µm (calculated as equivalent spherical diameter), with a minimum of 6.06 µm and a maximum of 9.65 µm, with a standard deviation of 0.65 µm, which is very close to the dimensions provided by the manufacturer (8 µm std dev <0.2 µm, coeff var <2%).

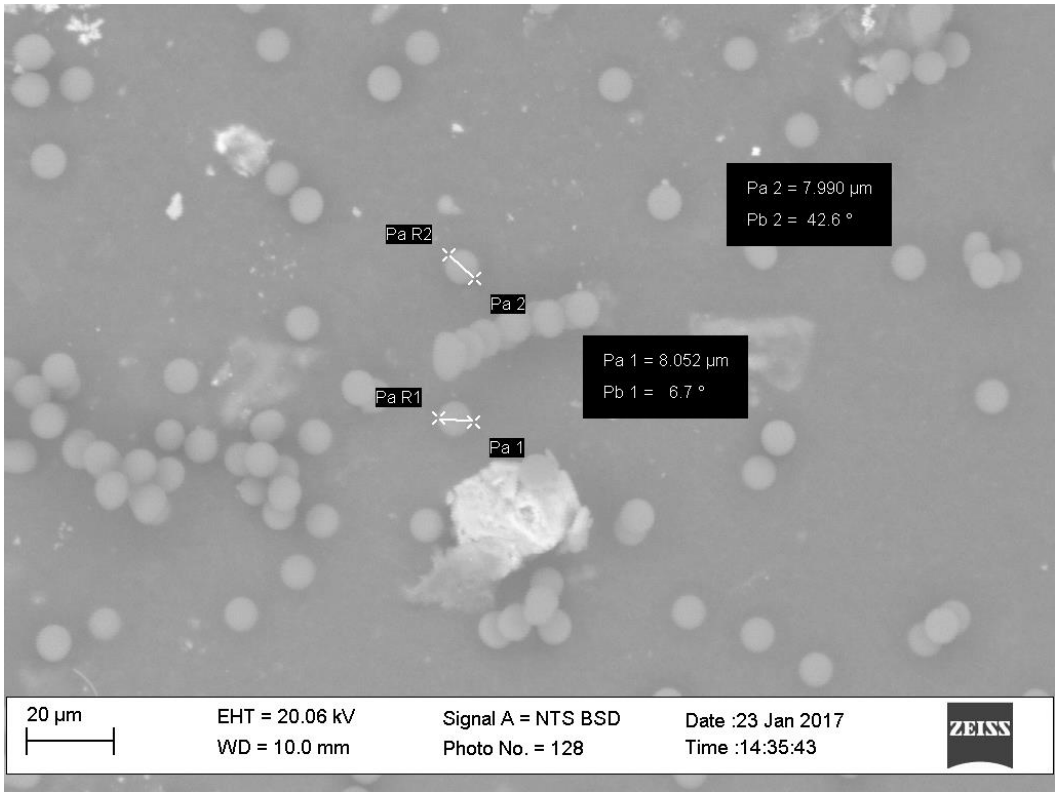

Figure. 4.3. SEM image of the polystyrene standard used to check particle size accuracy

The test for particle size range, from image analysis, revealed values of particle size between 5 to 65 µm, with the highest frequency of particles with diameters between 20 and 60 µm (Fig. 4.4), which agrees well with the results provided by the Coulter Counter, of 10 to 50 µm.

The determination of equivalent spherical diameter was done on 152 particles. The mean value of particle size was 29.86 µm, with a standard deviation 8.6, skewness of 1.04 and a kurtosis of 1.92. The Kolmogorov-Smirnov Test of Normality reveals a value of 0.1141 and a p value of 0.03541, showing that the particle size distribution does not follow a normal distribution. As expected in these experiments, the distribution of values is skewed, in this case towards values <35 µm. The source of errors in these experiments depend on the size and mass of filtered particles on the filtered, which was found to be up to 30 % for particles greater than 2-6 µm (Groundwater et al., 2012). The precision of the method can be improved by analysing more images, however, for this experiment, the results of the standard test for particle size distribution was found adequate. Considering that the aim of this experiment is to analyse classes, rather than individual sizes, and assuming that suspended particles from the Danube Delta and the Black Sea range from 0.6 to 125 µm, the errors are negligible in respect to the size range.

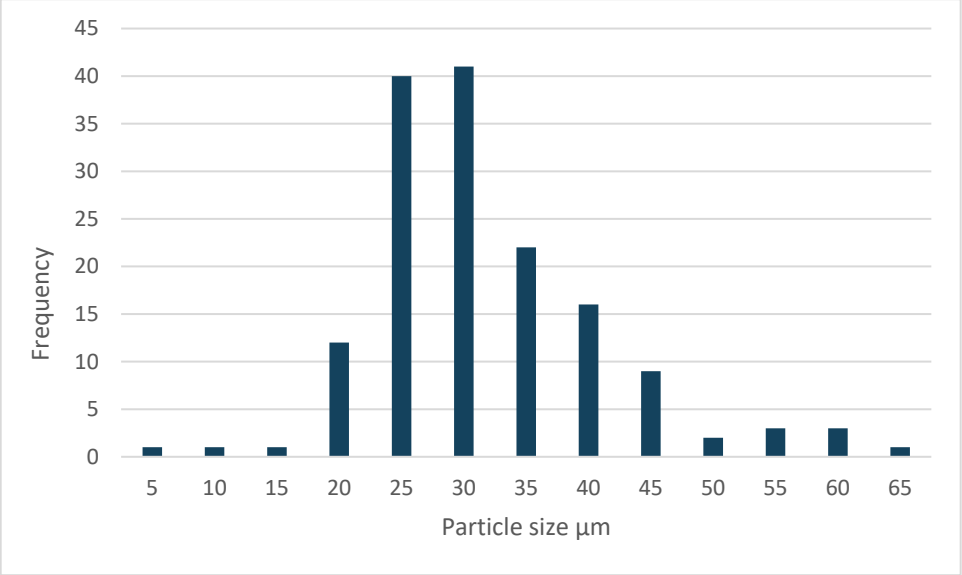

Figure 4.4. Particle size distribution for the standard test

4.4.2. Danube Delta

4.4.2.1. In-situ water constituents

Total and Inorganic Suspended Matter

A total number of 79 sampling sites were visited during the field campaigns in 2015 (low water discharge) and 2016 high water discharge).

In lakes, TSM values range from 12 to 26 g/m^3 in 2015 (low water discharge), with an average of 15.7±1.3 g/m^3 and from 1 to 5 g/m^3 in 2016 (high water discharge), with an average of 2.5±0.6, while the inorganic fraction, ISM (Inorganic Suspended Matter), ranges from 2.5 to 5 g/m^3 in 2015, with an average of 3.5±1.4 and from 0.5 to 2.5 g/m^3 in 2016, with an average of 1±0.4 (Fig. 4.5). The greatest difference between TSM and ISM values is in lakes, in both years, where ISM is less than 50% from TSM and even <20% in some cases.

On channels, TSM values range from 5 to 25±20 g/m^3 in 2015 (low water discharge), with an average of 15.5±6.3 and from 2 to 205±33 g/m^3 in 2016 (high water discharge), with an average of 67.9±6.9, while the inorganic fraction, ISM, ranges from 1 to 20±19 g/m^3 in 2015 (low waters), with an average value of 11.2±4 and from 0.5 to 190±31.5 g/m^3 in 2016 (high waters), with an average of 62.9±6.4. The highest values of both TSM and ISM are on the Danube branches, Sulina and Sfantu Gheorghe >30 g/m^3, with the highest value of 205 g/m^3 measured in the Sfantu Gheorghe mouth area, after an episode of heavy rain (Fig. 4.6).

In the sampled lagoons, TSM values range from 12 to 40 g/m^3 in 2015 (low waters), with an average value of 24.4±2.2 and from 2 to 77±42 g/m^3 in 2016 (high water discharge), with an average of 19.7±3.1 while the inorganic fraction, ISM, ranges from 7.7 to 32 g/m^3 in

2015 (low water discharge), with an average of 17.1±1.7 and from 0.7 to 71±42 g/m^3 in 2016 (high water discharge), with an average of 13.7±3 (Fig. 4.7).

Thirteen points in the Danube Delta were visited during both campaigns of 2015 and 2016 and they are presented in comparison (Fig. 4.8). In lakes (Fig. 4.8 B) TSM values are much lower in 2016 compared to the previous year and most of the suspended matter is organic in nature. The ISM values are very low in both years, not exceeding 5 g/m^3. For all channels (Fig. 4.6. A) and the Musura lagoon (Fig. 4.8. B), the TSM and ISM values are higher in 2016, during high-water discharge, compared to 2015, during low water discharge, 5 to 20 times higher (with the extreme case of the Sfantu Gheorghe mouth). It is interesting to notice how the proportion between TSM and ISM is similar in both years, with ISM representing most of the suspended fraction in water. The Sahalin lagoon (Fig. 4.8. B) shows a particular case. In both low and high waters, the ISM is the dominant suspended fraction. The values of TSM and ISM are very similar in both years, in the sampled point in the north of the lagoon, while in the centre, TSM and ISM are 50% lower in the in 2016 (high water discharge) compared to 2015 (low water discharge).

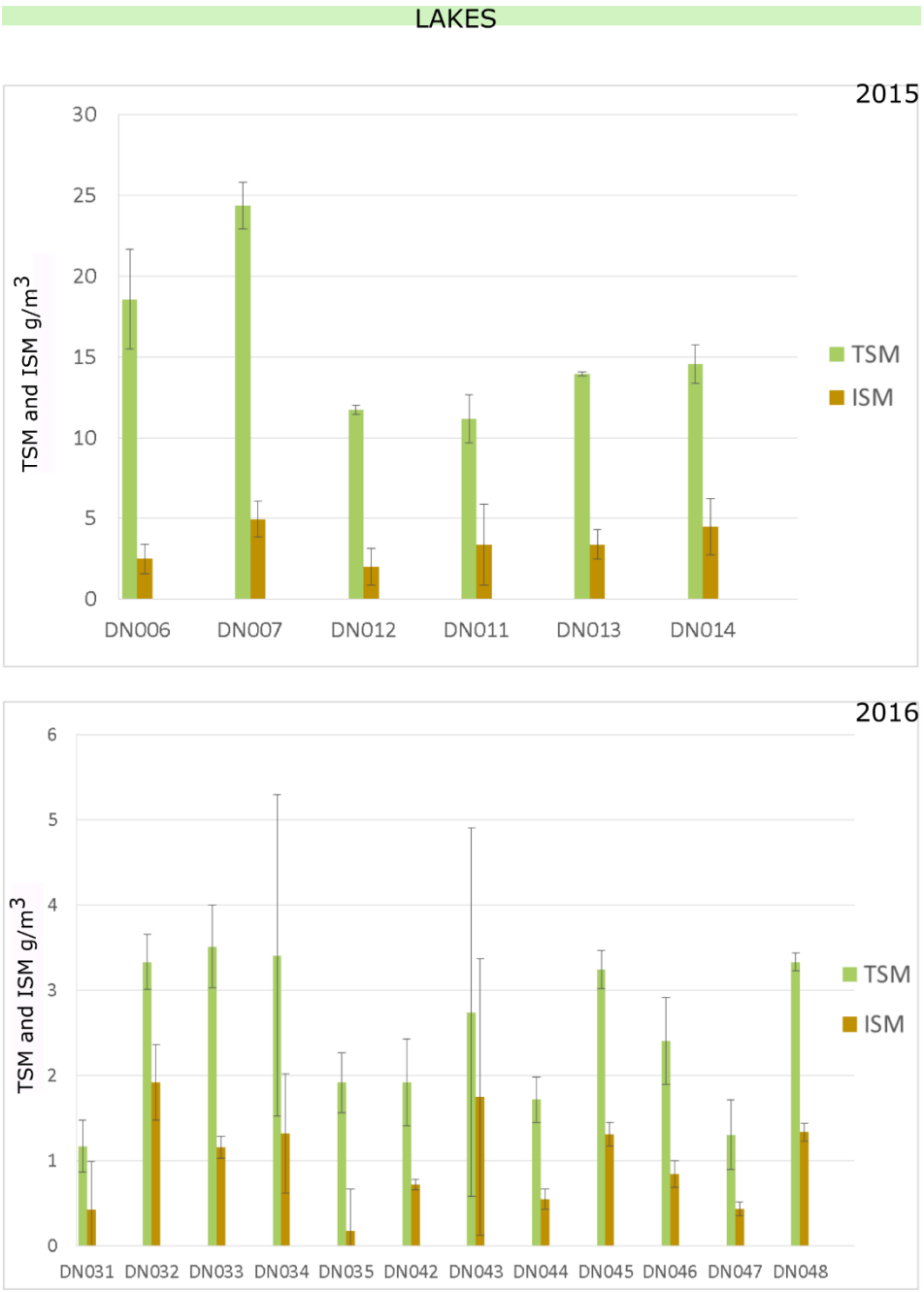

Figure 4.5. TSM and ISM values measured in lakes, in 2015 (low water discharge) and 2016 (high water discharge)

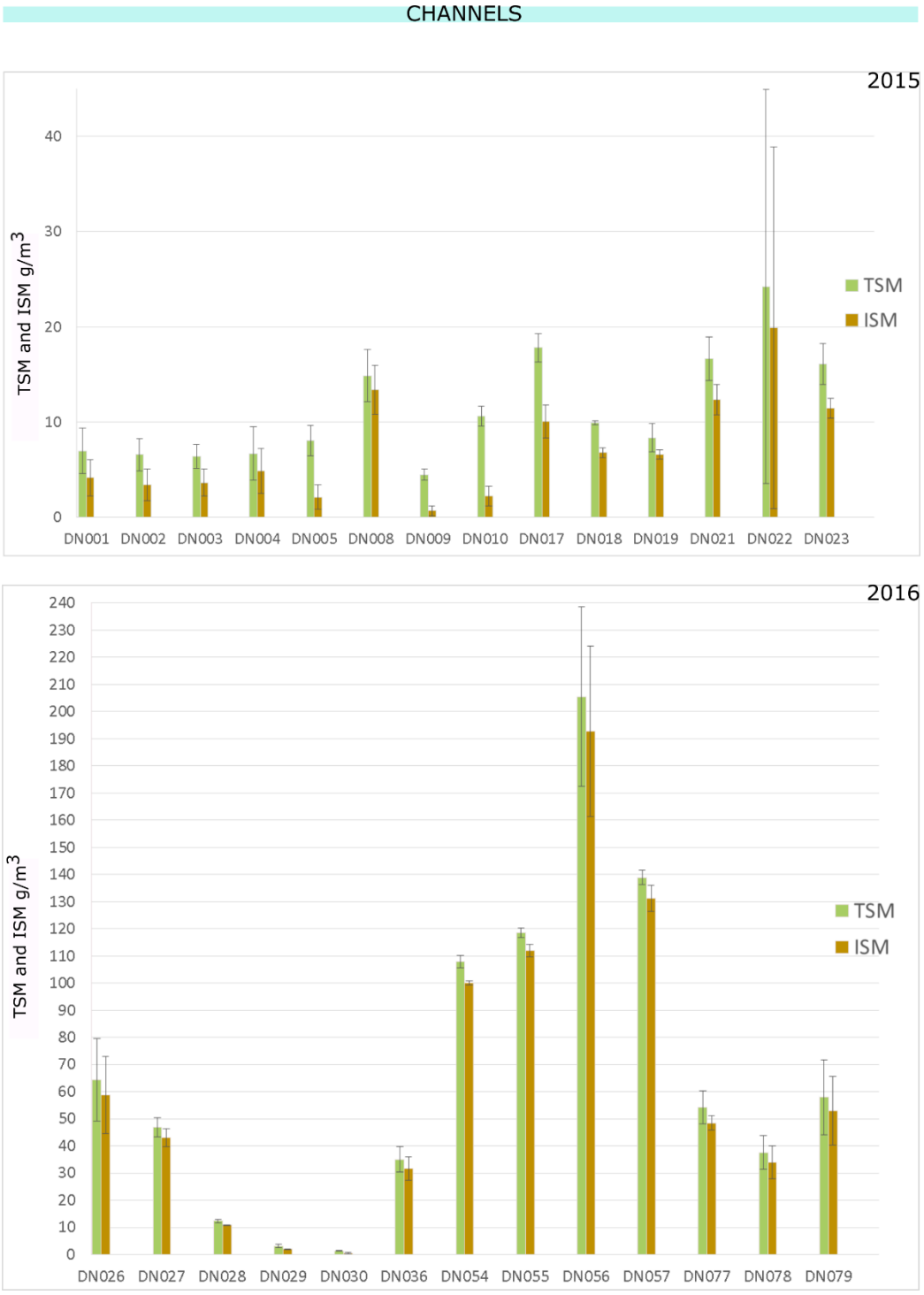

Figure 4.6. TSM and ISM values measured on channels, in 2015 (low water discharge) and 2016 (high water discharge)

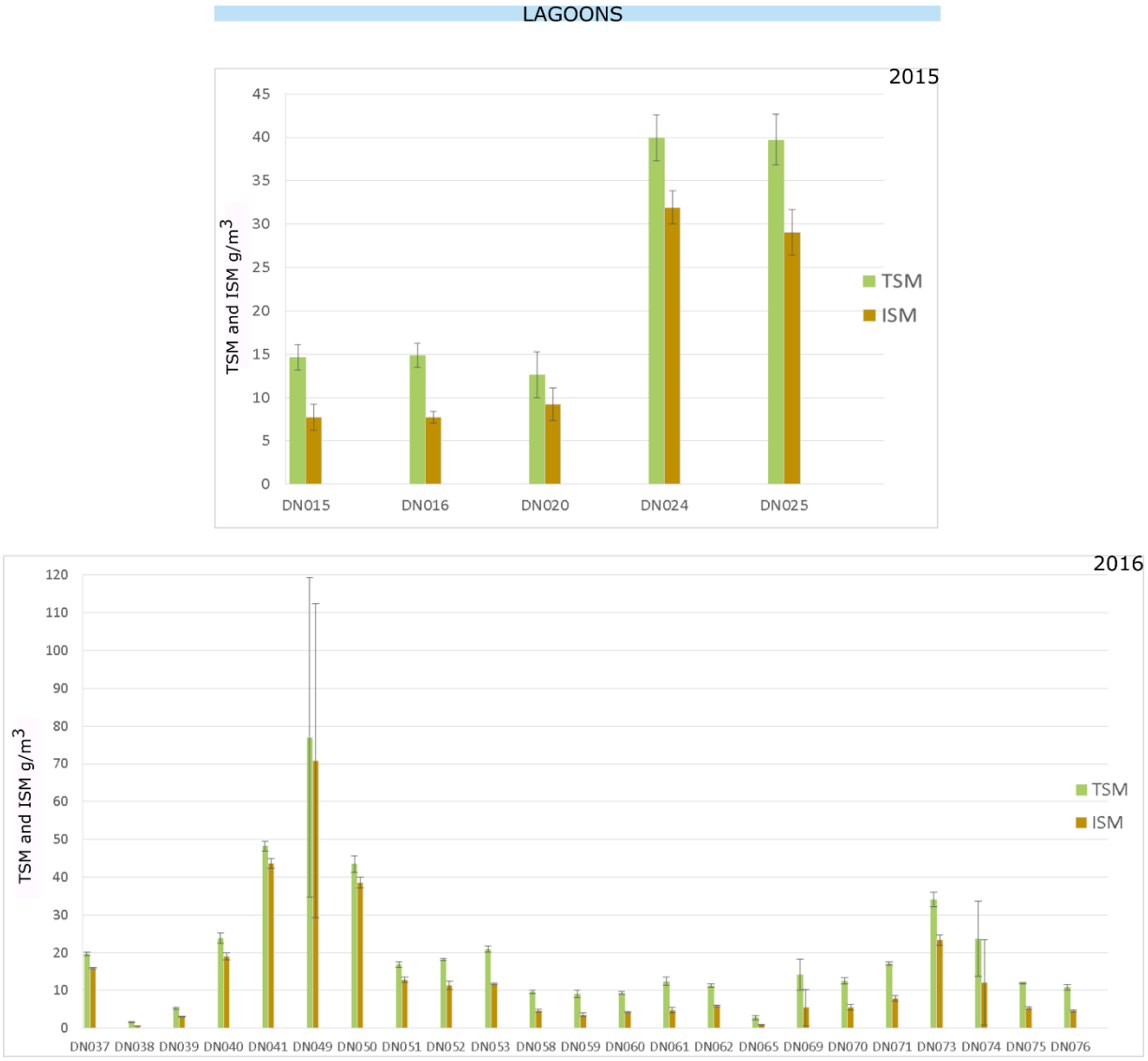

Figure 4.7. TSM and ISM values measured in lagoons, in 2015 (low water discharge) and 2016 (high water discharge)

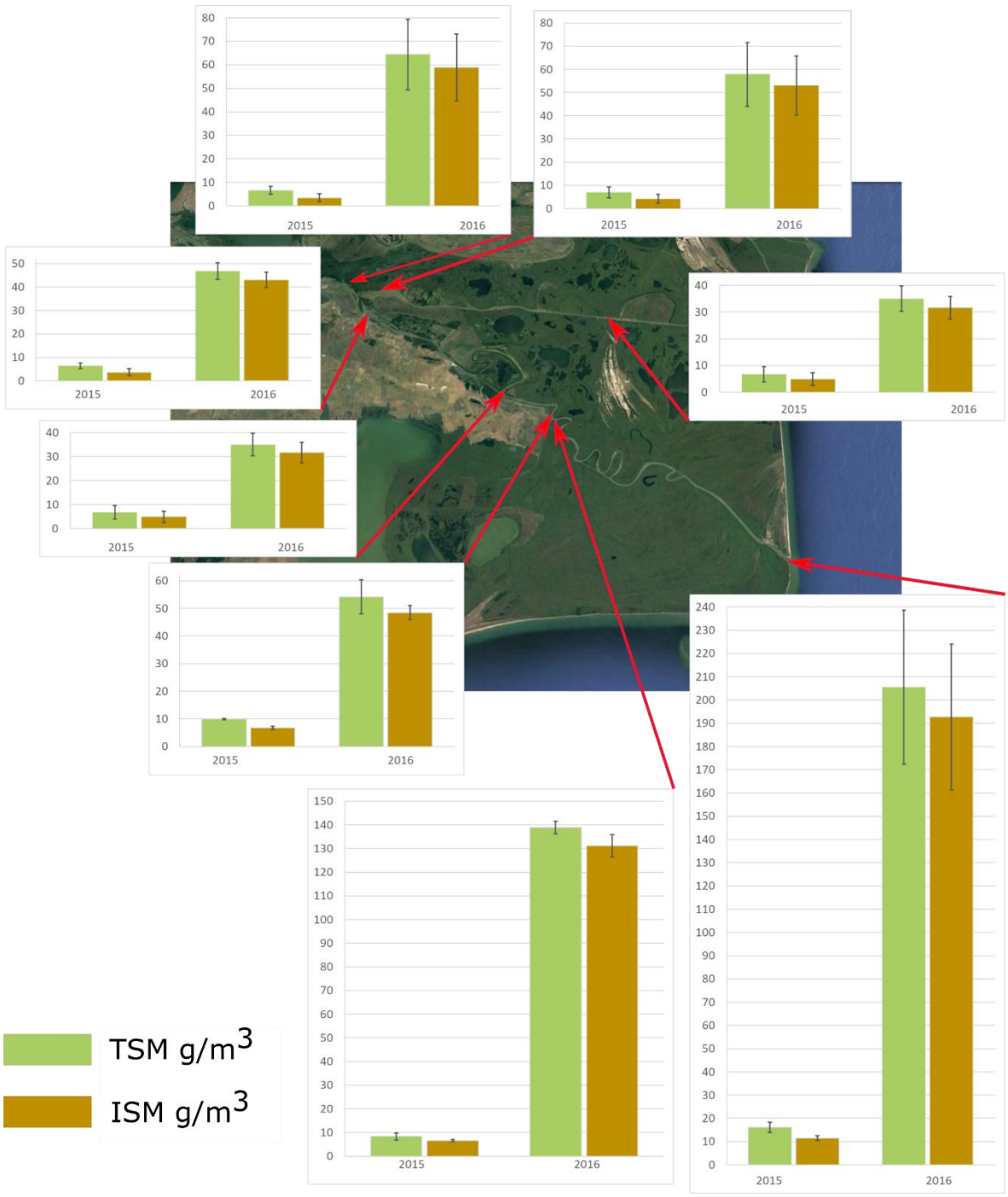

A.

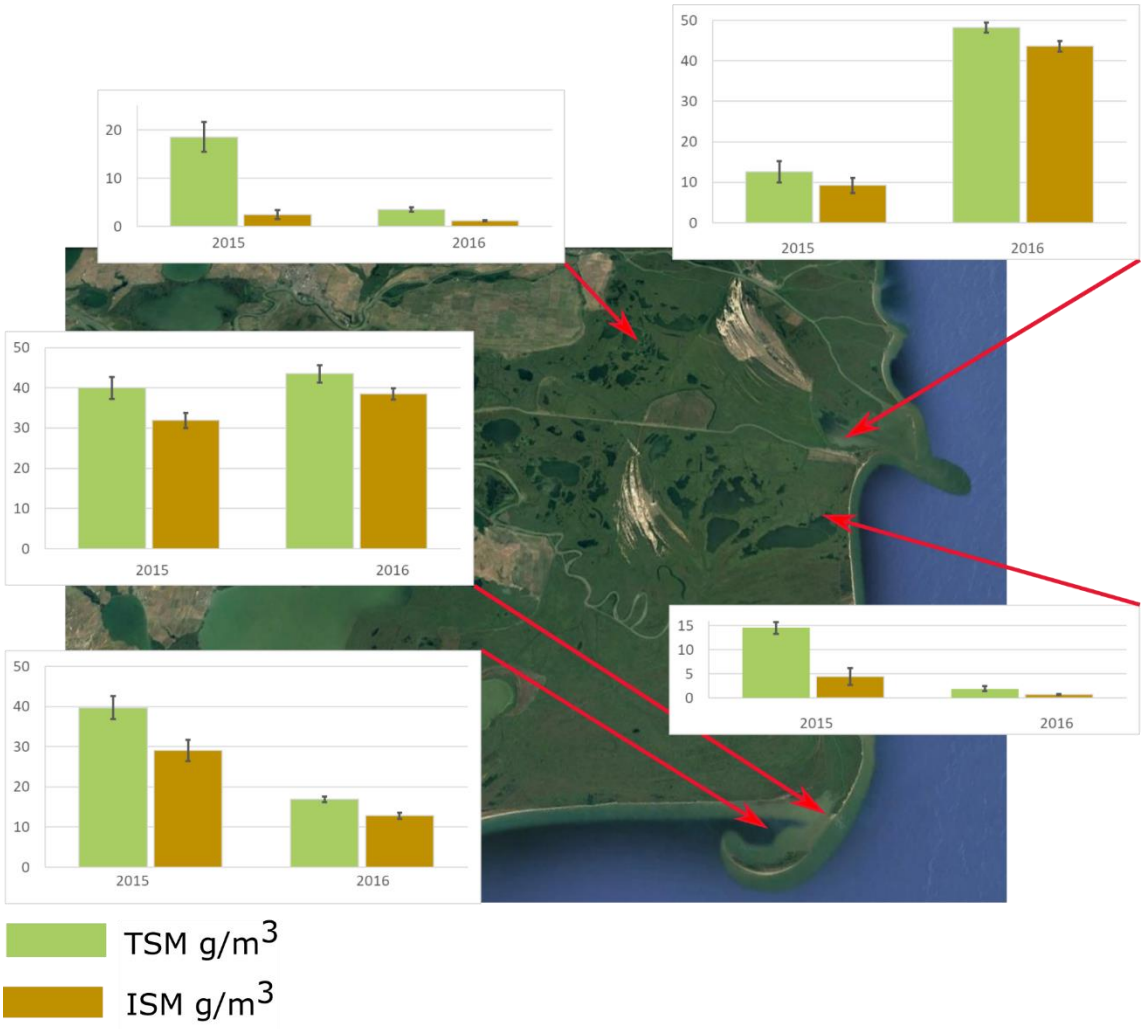

B.

Figure 4.8. TSM and ISM values of the revisited points in the sampled channels (A), lakes and lagoons (B), in the Danube Delta in 2015 (low water discharge) and 2016 (high water discharge), presented in comparison.

Chlorophyll-a

Chlorophyll-a was sampled from various environments of the Danube Delta in late summer in 2015 (low waters) and late spring in 2016 (high waters). A total number of 79 sampling sites were visited during the field campaigns in 2015 and 2016. The results of 2015 are the averaged value from three replicates while the ones of 2016 were obtained from analysing just one sample in the HPLC machine.

In lakes, chlorophyll-a values range from 50 to 99 mg/m^3 in 2015, with an average of 68.7±8, and 0.8 to 7 mg/m^3 in 2016, with an average of 3.85 (Fig. 4.9). The same three lakes were sampled in both years, Lake Rosulet, Lake Rosu and Matita. Overall, Lake Rosulet has the lowest chl-a values, in both seasons, while Lake Rosu and Matita have more similar and higher values. These results are comparable with the values found by (Oosterberg et al., 2000)

for the year 1997-1998, for lakes Matita and Rosu, of 9 and 10 mg/m^3 (spring season) and of 52 and 54 mg/m^3 (summer season).

On the channels, the chl-a values range from 20 to 120 mg/m^3 in 2015, with an average of 25.7±4.7 and from 0.2 to 23 mg/m^3 in 2016, with an average of 4.9 (Fig. 4.10). For the summer season of 2015, the lowest chl-a values are on the main branches of Sulina and Sfantu Gheorghe and the highest on the old meanders of Sulina (the 'Old Danube, Big M') and Sfantu Gheorghe (Mahmudia meander). The highest chl-a values in 2016, in the late spring season, are found in or around the meanders of Sfantu Gheorghe (Mahmudia and Dunavat meanders) (Fig. 4.10).

In the sampled lagoons, chlorophyll-a values range from 10 to 45 mg/m^3 in 2015, with an average value of 21.5±2.7 and from 1 to 33.5 mg/m^3 in 2016, with an average of 9.7 (Fig. 4.11). In the late summer season, Musura lagoon records the highest chl-a values while Sahalin lagoon records the lowest. In the late spring, Sahalin lagoon records both the highest and the lowest chl-a values, with the lower values in the vicinity of the Garla Turcului channel and the highest ones in the open waters (center and south) of the lagoon. The Musura lagoon records similar values with the Razelm - Golovita lagoon system.

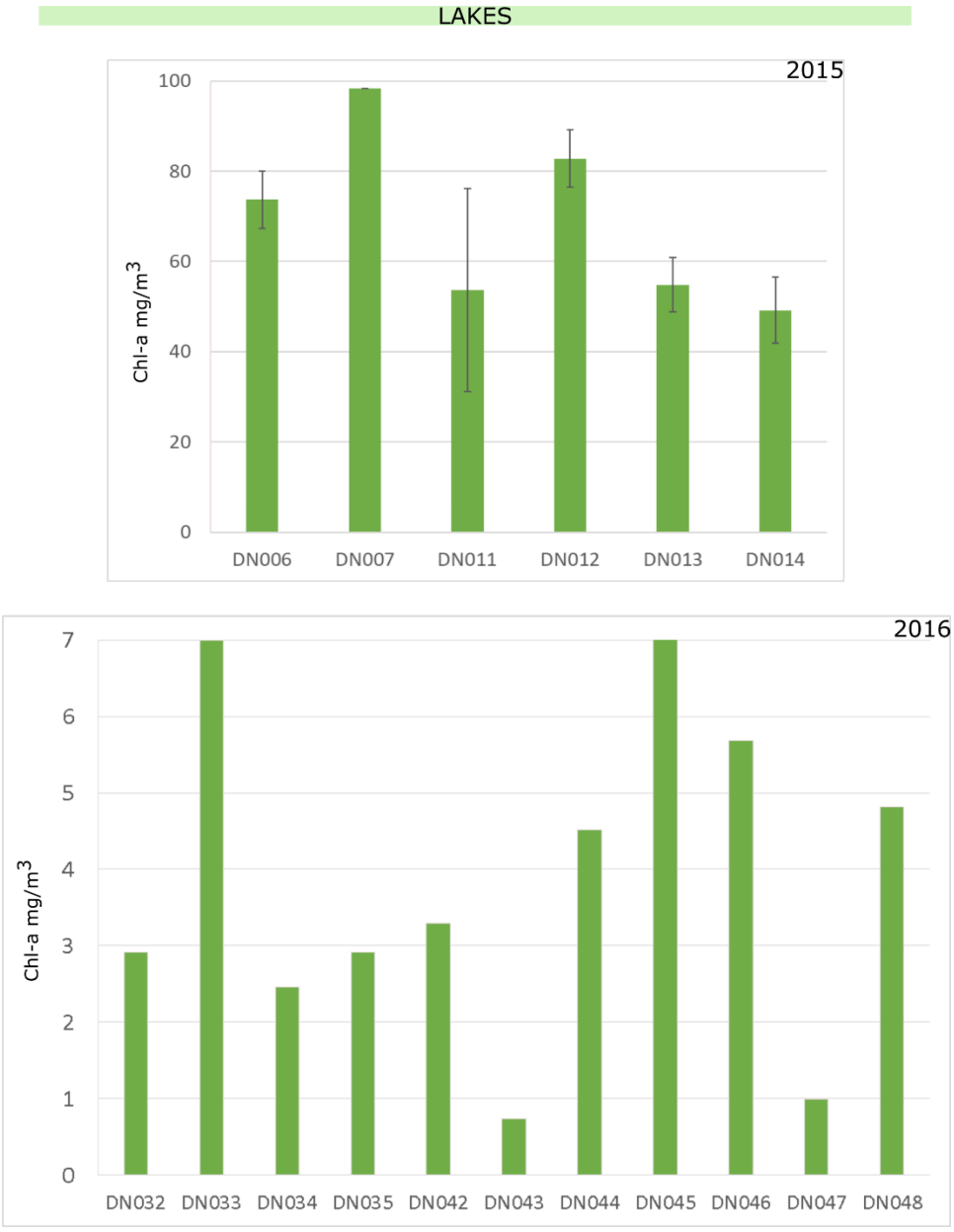

Figure 4.9. Chlorophyll-a values for the sampled lakes in the Danube Delta, in 2015 (late summer) and 2016 (late spring). For details on the sampling points see table in Annex 2 and Fig. 4.1

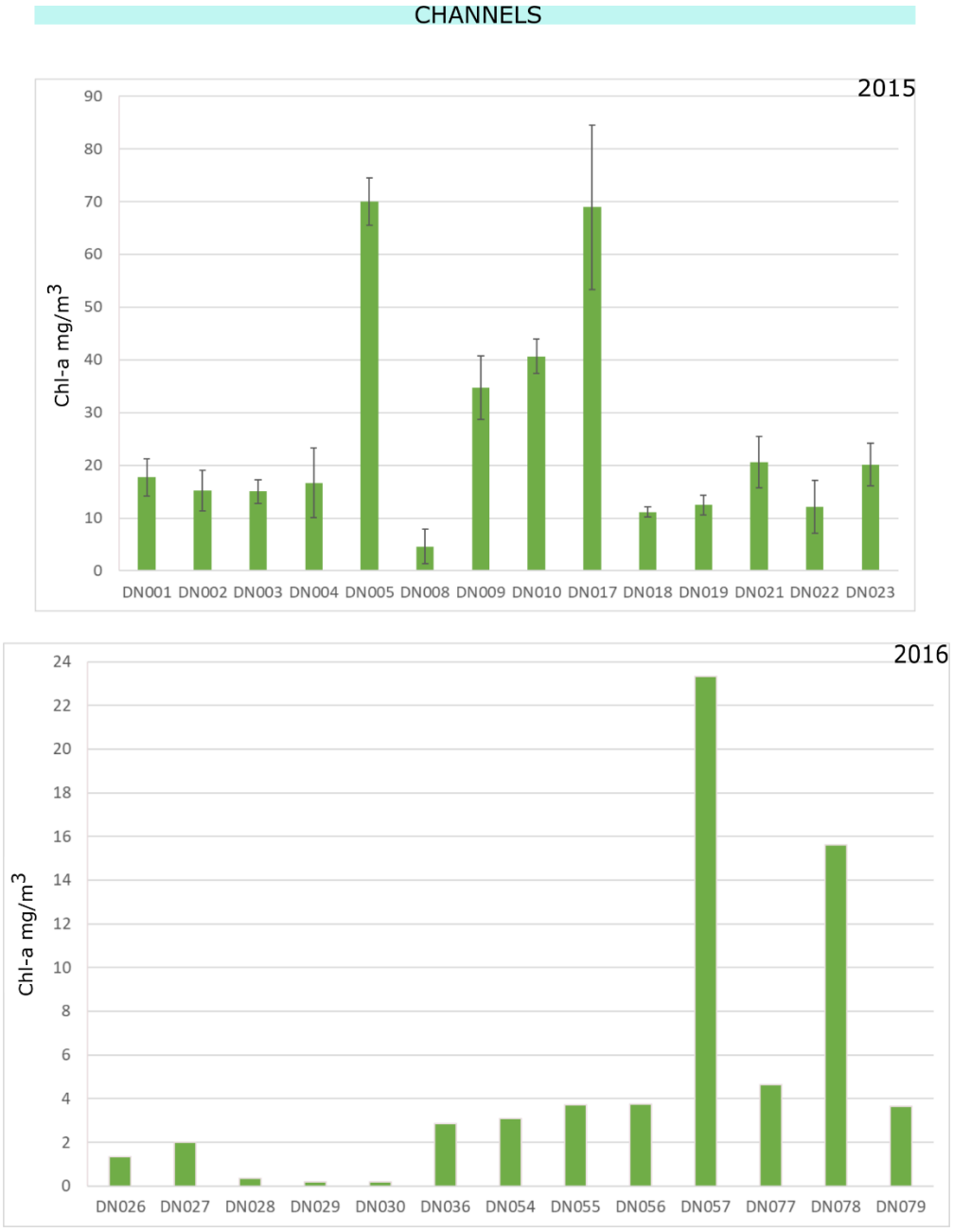

Figure 4.10. Chlorophyll-a values for the sampled channels in the Danube Delta, in 2015 (late summer) and 2016 (late spring). For details on the sampling points see table in Annex 2 and Fig. 4.1

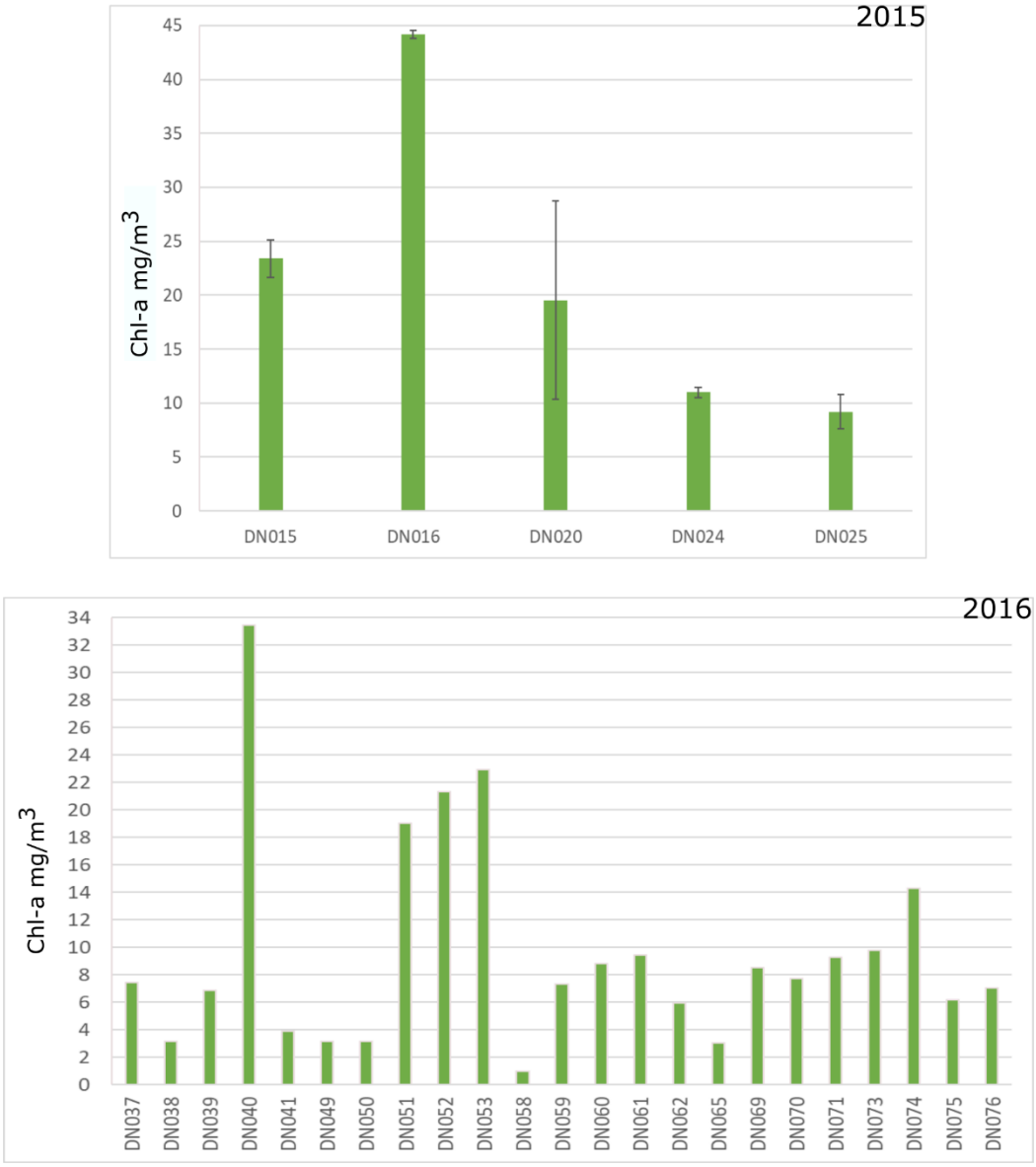

Figure 4.11. Chlorophyll-a values for the sampled lagoons in the Danube Delta, in 2015 (late summer) and 2016 (late spring). For details on the sampling points see table in Annex 2 and Fig. 4.1

4.4.2.2. Particle size

All the samples of this experiment were collected in May-June of 2016, during high water discharge conditions (+1 m over the normal water level, as recorded in Tulcea).

In all the sampled environments of the Danube Delta, lakes, channels and lagoons (Fig. 4.12), over 80% of the analysed suspended particles are in the size range of clays (0.06 – 3.9 µmm, according to the Udden-Wentworth scale). The highest percentage is in lakes, ~92 %. Channels and lagoons have similar percentages, 82 % and 87 %, respectively. Very fine (3.9 – 7.8 µm) and fine silt (7.8 – 15.6 µm) sized particles represent 8% of the analysed particles in lakes, 15 % in channels and 12 % in lagoons. The rest of the particles, not exceeding

1%, are represented by medium (15.6 – 31 µm) and coarse silt (31 – 63 µm) and very fine sand (63 – 125 µm) sized particles.

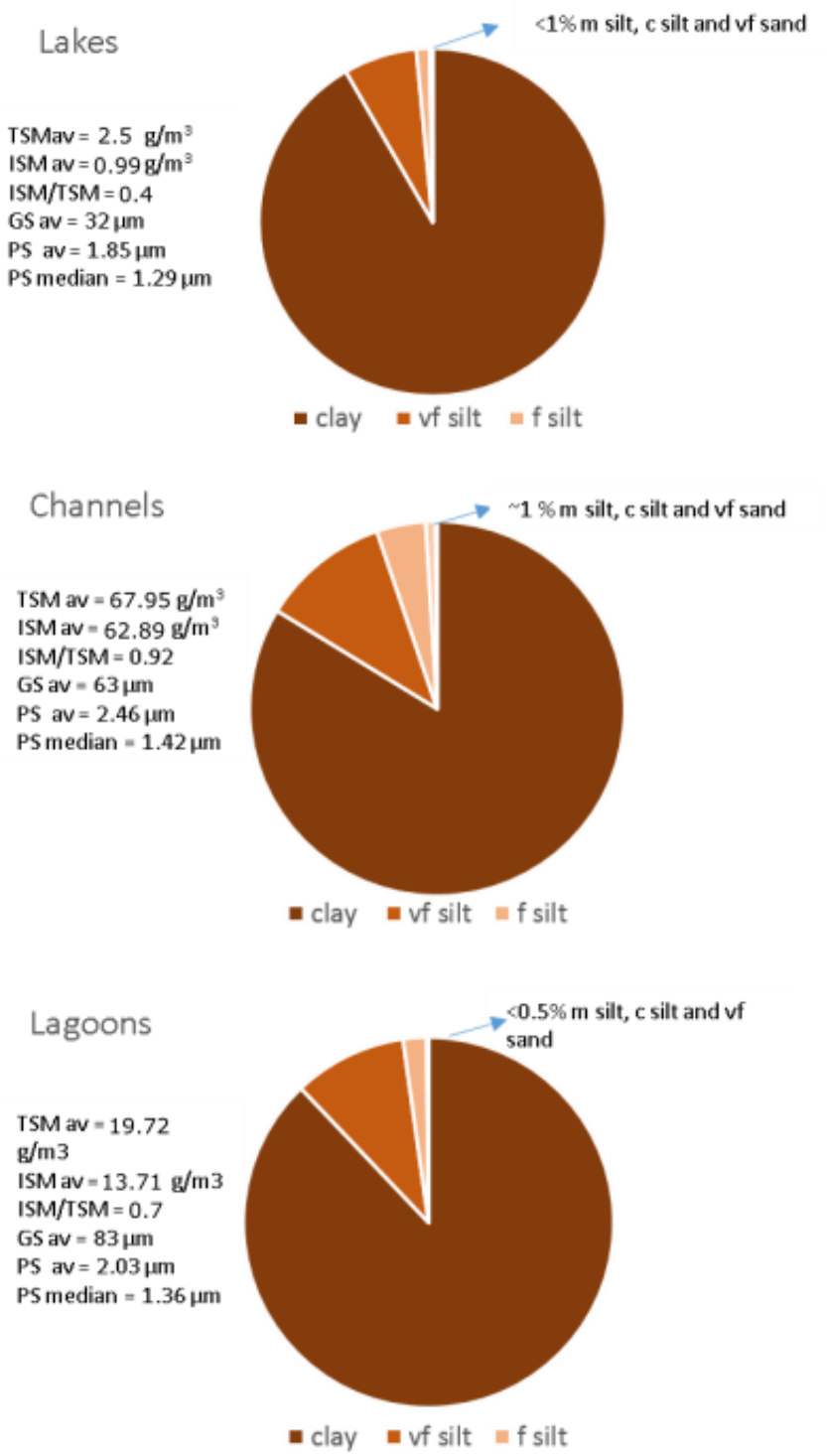

Figure 4.12. Particle size classes for various environments in the Danube Delta, presented as percentages of clay, very fine (vf) silt, fine (f) silt, medium (m) silt, coarse (c) silt and very fine (vf) and fine (f) sand. Average TSM, ISM, ISM/TSM, grain size (GS) (from sedimentary cores other published data – see Chapter 1) and average particle size (PS) as well as median particle size are given for each environment.

In order to get information about the variation of particle size range with organic and inorganic matter content, all sizes from a sampling point were plotted as a function of the ISM/TSM ratio (Fig. 4.13). In the analysed lakes and channels, particle size increases with the ISM/TSM ratio. Lake Rosu has a higher ISM/TSM than Lake Matita. The cut meanders of Sulina (‘Old Danube) and Sfantu Gheorghe (Mahmudia and Dunavat) have the lowest ISM/TSM values, below 0.905, but they are two times higher than the values of the lakes. For the main channels, with values higher than 0.905, particle size increases from Tulcea, before the Sulina and Sfantu Gheorghe channels split, to the discharging mouths, with similar values for Sulina, <0.92 and the highest value in the Sfantu Gheorghe estuary.

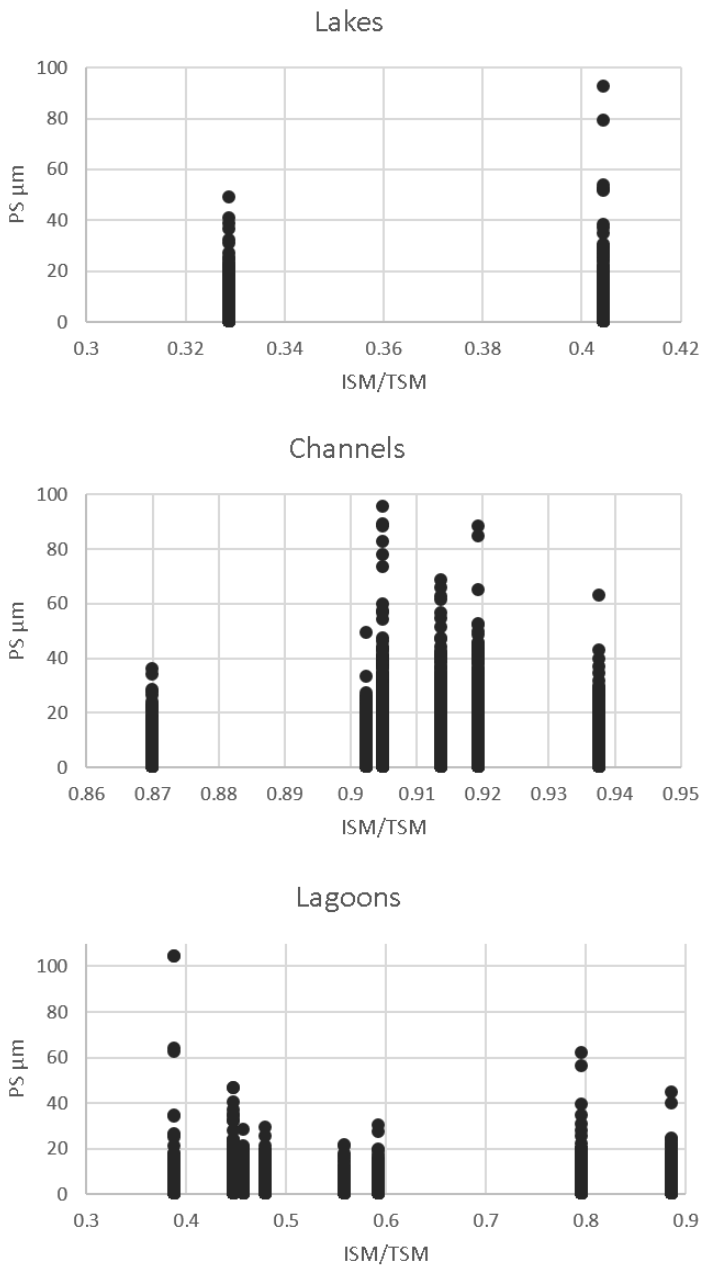

Figure 4.13. Particle size range as a function of ISM/TSM ratio for the sampled locations in the lakes, channels and lagoons of the Danube Delta

For the analysed lagoons, there are three distinct situations. The lagoons with an ISM/TSM ratio below 0.5, which are represented by the Razelm and Golovita system, show decreasing particle size values with increasing ISM/TSM ratio. The middle group, with ISM/TSM values between 0.5 and 0.6, represented by the open waters of the central areas of Musura and Sahalin, show an increase in particle size with increasing ISM/TSM, but with a very small difference. The last group, with ISM/TSM values between 0.75 and 0.9, represented by the NW of the Sahalin lagoon, where Garla Turcului reaches this area, and the proximity of the

barrier island in the Musura lagoon, show decreasing particle size with increasing ISM/TSM ratio.

4.4.2.3. Particle composition

This study is mainly based on Calcium (Ca), Iron (Fe), Titanium (Ti), Silicon (Si), Aluminium (Al) and Boron (B). It is commonly accepted that Al, Ti and Fe are related to terrigenous-siliciclastic minerals (clays, heavy minerals), while Ca mainly reflects the carbonate content (calcite and aragonite) in the sediment (Richter et al., 2006). Silicon is both an important terrigenous or productivity indicator (Rothwell et al., 2006). B was one of the elements revealed by the analysis and only found in a limited number of particles and in a certain percentage (always between 15 to 60 %). Boron is a micronutrient element required for growth and development of vascular plants, marine algae and algal flagellates, diatoms and also cyanobacteria (Brown et al., 2002). In the aquatic environments analysed here, the B bearing particles are most likely part of the zoo- and phytoplankton (diatoms, cyanobacteria and algae).

Between 80 and 130 particles were analysed for chemical composition, for each studied site. The percentage of several elements were plotted as a function of particle size, Ca and Fe for optical properties, Si, Al and the Ti/Ca ratio, as indicators of nature and provenance and B, as indicator of nature.

Lakes (Fig. 4.14)

Most suspended particles in the analysed lakes contain Ca up to 35% and Fe up to 15%. There is a low positive correlation between particle size and Ca content (r=0.246), but the highest Ca content is in particles up to 30 µm. Overall, there are less Fe bearing particles in lakes, and their sizes do not exceed 40 µm. There is no correlation with size (r~0).

Si and Al are found in most of the analysed particles, up to 36% and 15% respectively. There is a weak positive correlation between Si content and particle size (r=0.327) but most particles have a Si percentage up to 15%. There is a very low correlation between Al content and particle size (r=0.181). Most particles have a Ti/Ca value of <1. The ones with higher values, which could have a terrigenous provenance, do not exceed 40 µm. Ti/Ca ratio shows a very low negative correlation with particle size (r=-0.046).

B is only found in some of the particles, with sizes up to 20 µm, in percentages of 15 to 43 %. There is a moderate positive correlation between B percentage and particle size (r=0.418).

Channels (Fig. 4.15)

Most suspended particles in the analysed channels contain Ca, up to 60% but most of them do not exceed 25 %, higher values than the values measured in lakes. There is no correlation between particle size and Ca content (r=0.002). Most suspended particles in the analysed channels contain Fe, up to 50 %. There is a low positive correlation between Fe and particle size (r=0.191).

Si and Al are found in most of the analysed particles, up to 50 % and 15 % respectively, with higher value than the values for the lakes. There is a weak positive correlation between Si and particle size (r=0.341) and Al and particle size (r=0.348). For most suspended particles, the Ti/Ca ratio has values below 1. The higher values, 1 to 45, are for particles with sizes up to 60 µm. While these values overall, are higher than the ones from the analysed lakes, the correlation with particle size, while still negative, is stronger (r=-0.064).

B has only values of 15 to 50 %, similar to the values for the lakes, and it is only contained in a limited number of suspended particles. There is a very weak positive correlation with particle size (r=0.105).

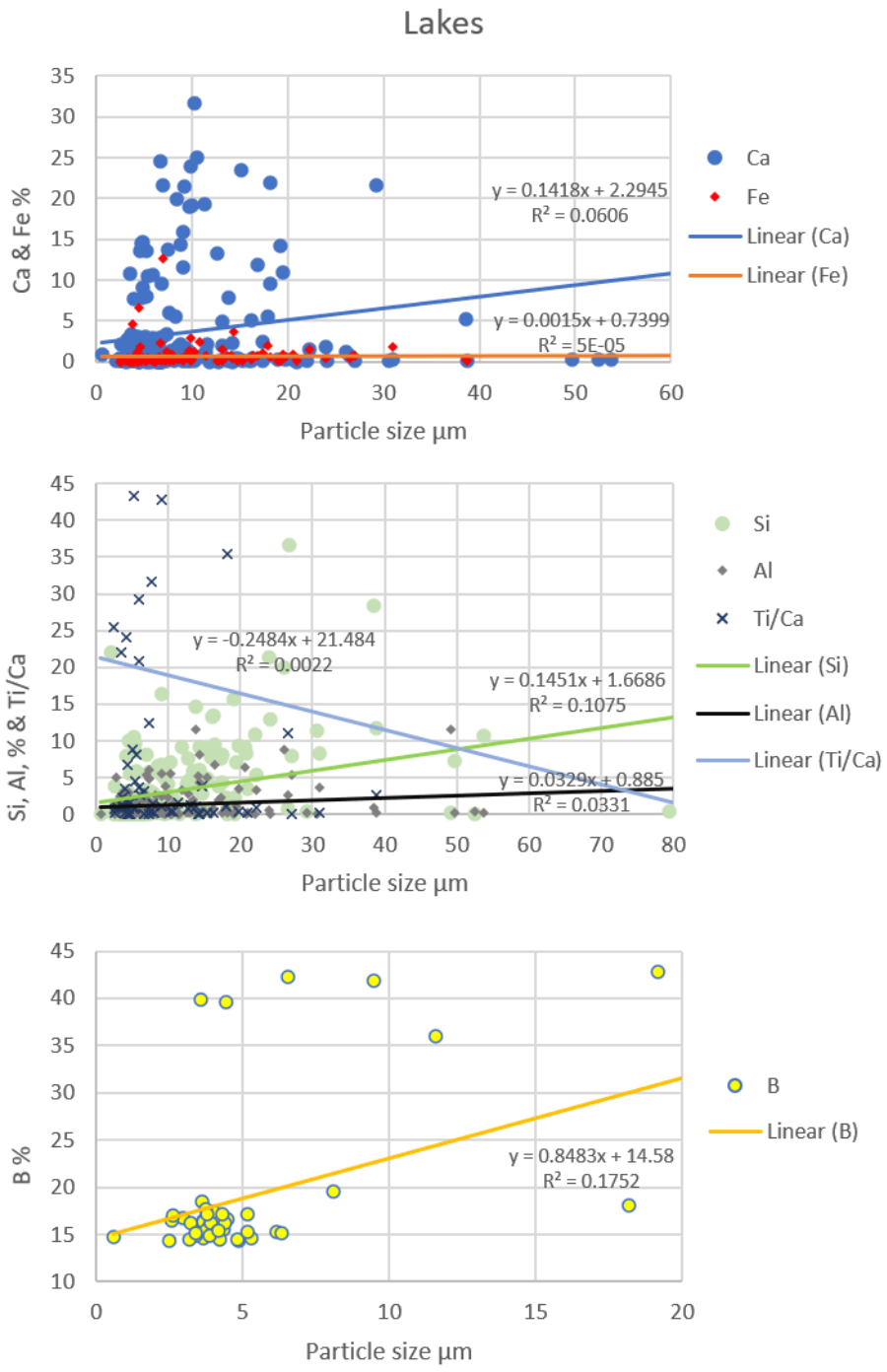

Figure 4.14. Variation of different chemical elements from the analysed suspended particles with particle size in the analysed lakes of the Danube Delta

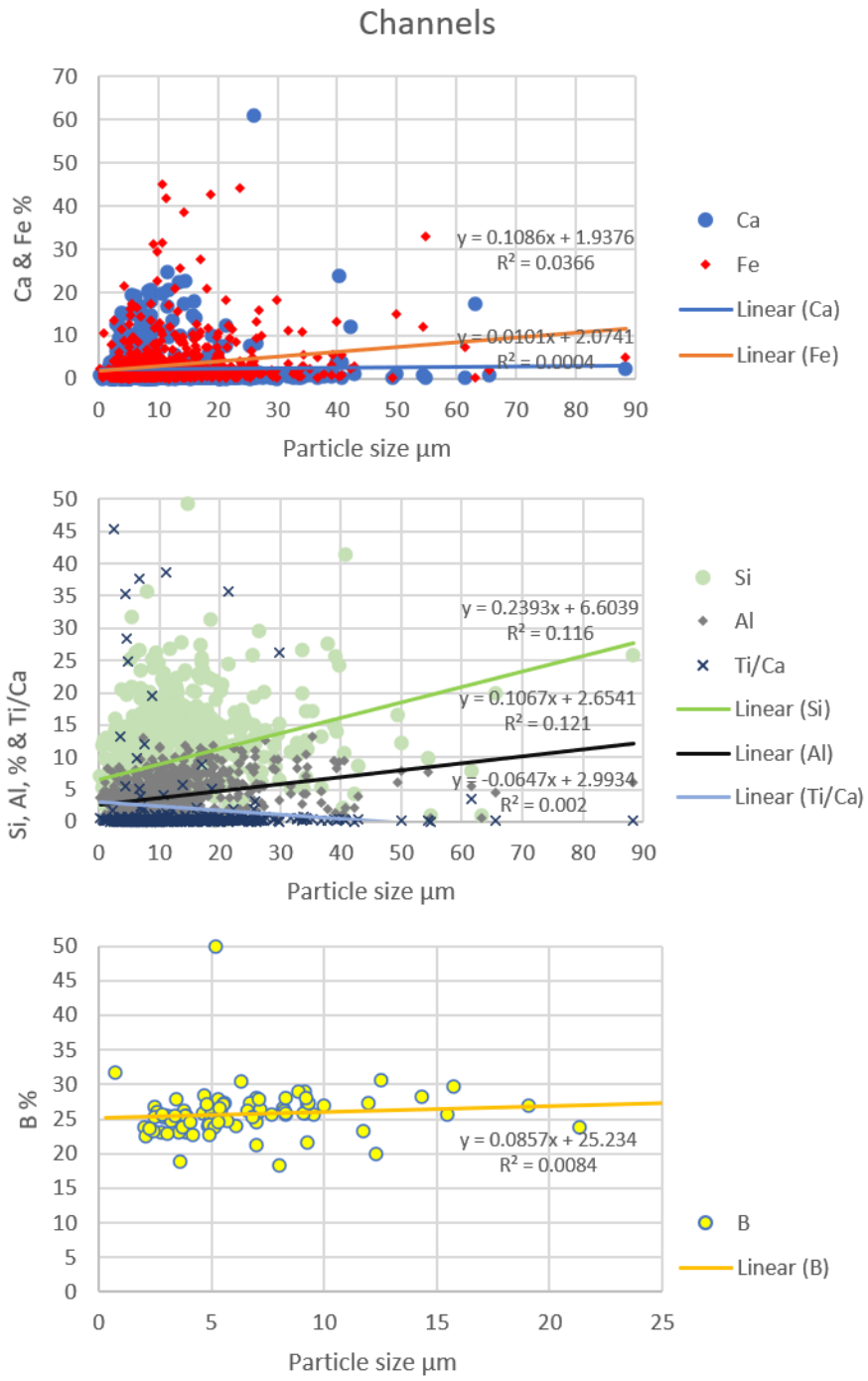

Figure 4.15. Variation of different chemical elements from the analysed suspended particles with particle size in the analysed channels of the Danube Delta

Lagoons (Fig. 4.16)

Most of the analysed particles in the lagoons contain Ca up to 40 %, which is higher than lakes or channels. There is a group of particles with very high Ca values, from 75 to ~100 %, and up to 10 µm, from the Razelm lagoon. There is very low negative correlation between Ca content and particle size (r=-0.073). Fe has values of up to 20 %, also higher than lakes or channels. There is a very low relation with particle size (r=0.191).

Most of the analysed particles in the lagoons contain Si up to 40 % and Al up to 20 %, higher than lakes, closer to the values found in the channels. Both Si and Al contents have low positive correlations with the particle size (r=0.280 and r=0.342, respectively). Most of the analysed particles have a Ti/Ca ratio of <1, but the highest value reaches 45, closer to the values found in lakes and channels. However, fewer particles have such a high ration, compared to the lakes and channels. There is a very low negative correlation with particle size (r=-0.019).

In the analysed lagoons, there are overall, more B bearing particles. The values are between 15 and 60 %, similar to the values recorded in lakes and channels. In a similar way to these environments, the B bearing particles do not exceed 20 µm in most cases, however, in the lagoons, there are more of these particles with greater sizes, and even over 100 µm. There is a very low positive correlation between B percentage and particle size (r=0.029).

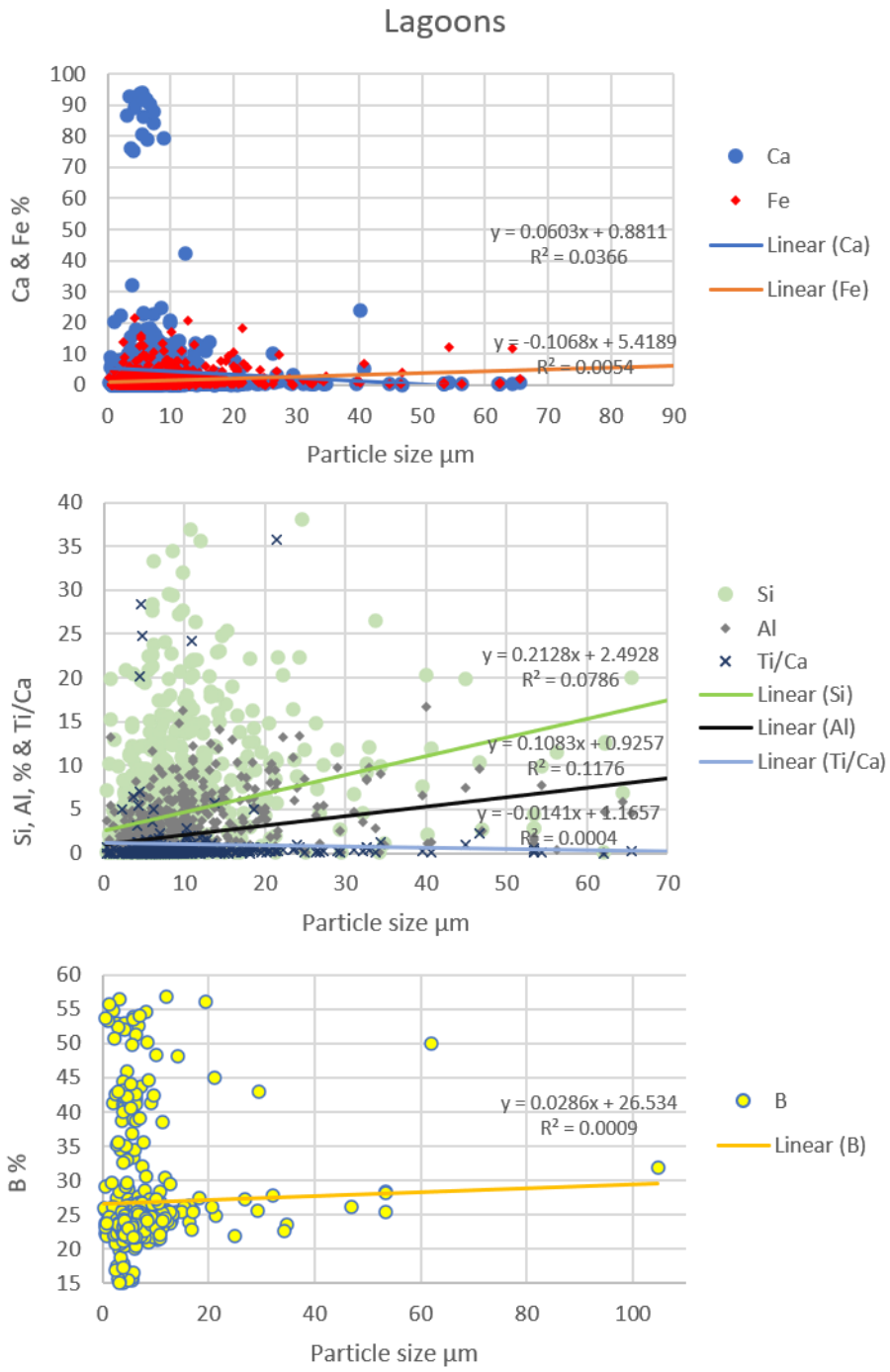

Figure 4.16. Variation of different chemical elements from the analysed suspended particles with particle size in the analysed lagoons of the Danube Delta

4.4.3. Black Sea

4.4.3.1. In situ water constituents

Total and Inorganic Suspended Matter

A total number of 26 sampling stations provide TSM and ISM data for the surface of the Black Sea, on the NW shelf (Fig. 4.17 and 4.18). The data was interpolated using SURFER (Golden Software), using the triangulation with linear interpolation method. Even if the sampling points are not always evenly distributed in the sampling area, this method does not extrapolate beyond the values of the data range.

During the sampling period of 7 days, TSM values range from 1 to 29 g/m^3, with an average of 4.7 g/m^3 and ISM values range from 0.5 to 25 g/m^3, with an average value of 3.5 g/m^3. The highest values (>10 g/m^3) are found in the close vicinity of the Danube mouths, Sulina and Sfantu Gheorghe, in the first 5 kilometres. This field of values maps the plume of the Danube at the time of sampling, in the coastal zone, with water discharge of the Danube close to annual averages and low intensity N-NE and N-NW winds. The values decrease progressively from N to S and W to E, with a very marked decrease in the first 5 kilometres from the coast, from >20 g/m^3 to 10 g/m^3, for TSM and from >15 g/m^3 to <10 g/m^3 for ISM. The area of minimum values is at 20 to 25 km from the coast. The values increase slightly eastward, 45 to 60 km from the coast.

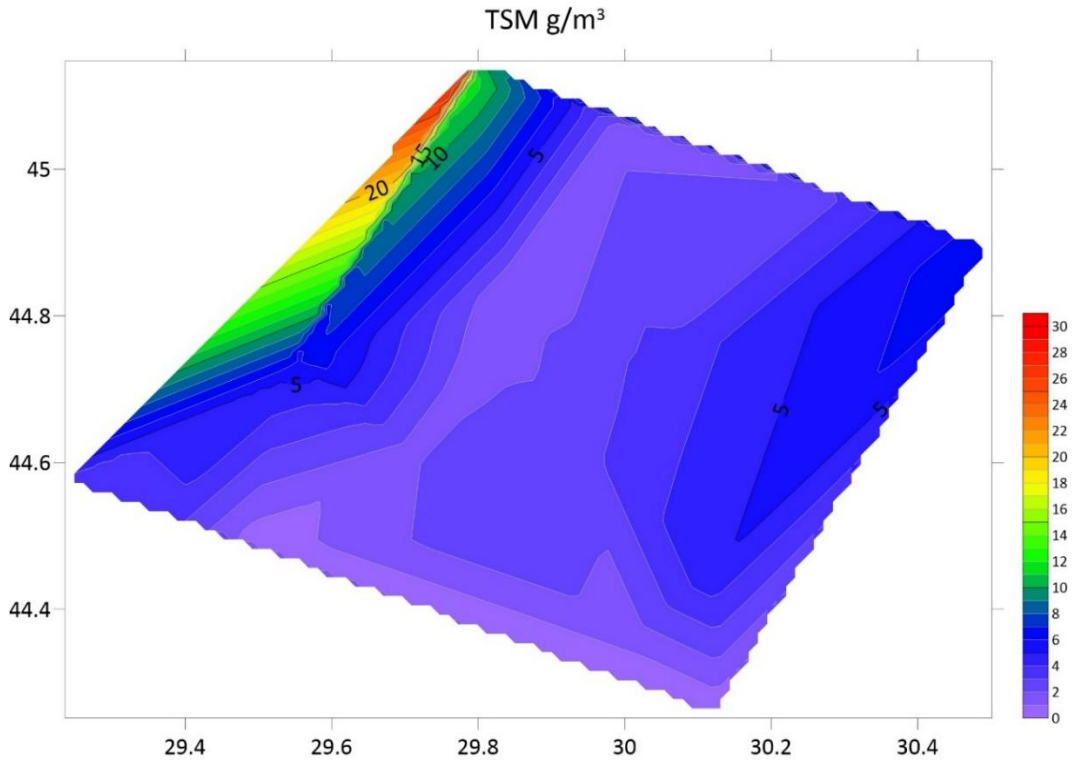

Figure 4.17. The map of Total Suspended Matter (TSM) concentration at the surface, of the Black Sea NW shelf (see Fig. 4.1 for distribution of sampling stations and table in Annex 2 for detailed description)

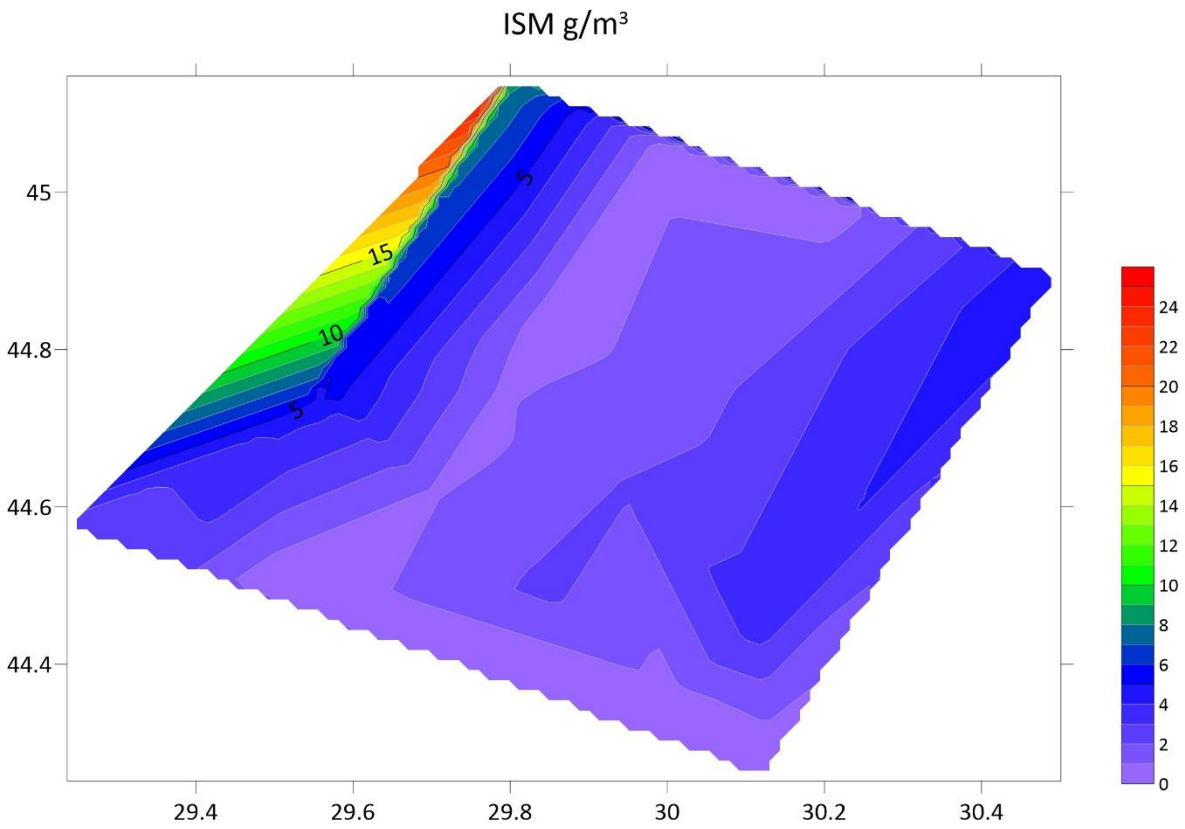

Figure 4.18. The map of Inorganic Suspended Matter (ISM) concentration at the surface, of the Black Sea NW shelf (see Fig. 4.1 for distribution of sampling stations and table in Annex 2 for detailed description)

The distribution of TSM and ISM at depth was measured in all the S stations and it is presented alongside CTD turbidity (FTU) (Figs. 4.19 – 4.21). The data is grouped according to the plume which was sampled, S007 to S010 for the northern plume, formed by Chilia and Sulina branches (Fig. 4.19), S002 to S006 for the southern plume (Fig. 4.20), formed by Sfantu Gheorghe and S001, representing the resulting effect of the Danube plume moving southward (Fig. 4.21).

In the northern plume (Fig. 4.19), TSM and ISM values have similar variations in most points. They decrease with depth, except for S008, where there is an increase in the values of both parameters at 5 m depth. The highest values of TSM and ISM, >1 g/m^3, are only recorded in the first 10 to 15 m of water depth. Below this depth, the values decrease to <1 g/m^3. While the values decrease from point to point, they stay higher in this region, showing the extent of the plume with distance from the shore and depth. The turbidity data shows a maximum at depth, from 10 to 15 m, which coincides with the highest TSM and ISM values.

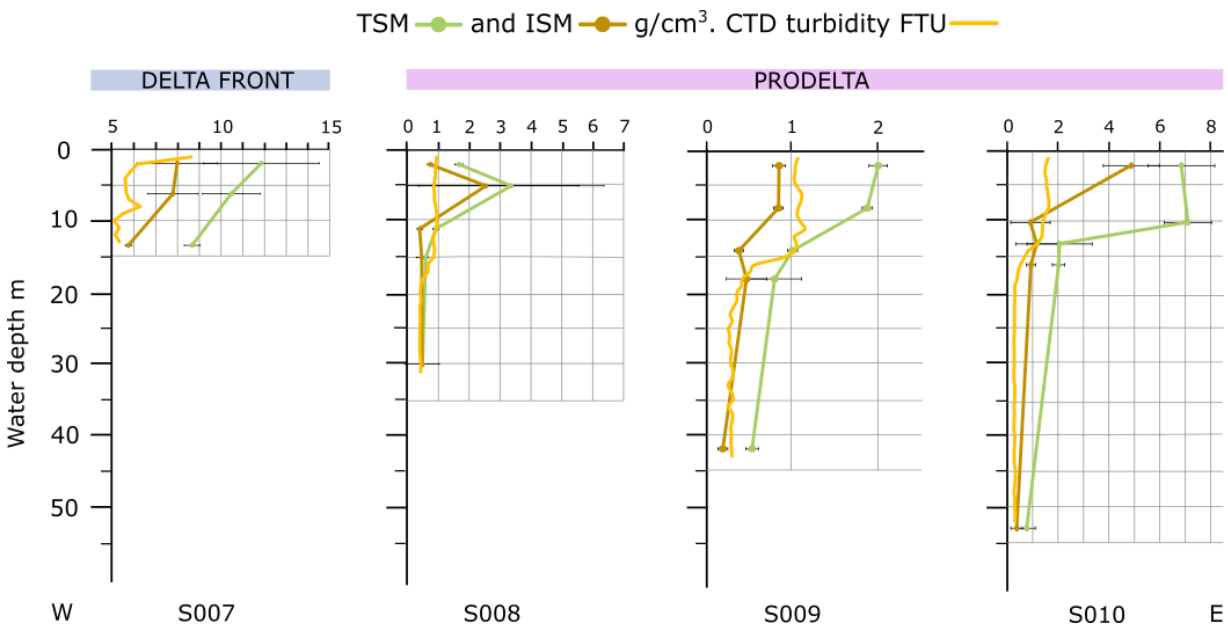

Figure 4.19. The distribution in depth of TSM, ISM and CTD turbidity for the northern plume, formed by Chilia and Sulina branches

The southern plume shows lower values of TSM and ISM, overall, than the northern plume (Fig. 4.20). Both TSM and ISM values decrease with depth in the vicinity of the estuary, at site S002. The variation is different for all the other sampling points, where maximum TSM and ISM values increase at depth, from -12 m in S003 to -24 m in S004 and -28 m in S005, showing a progressive sinking of the plume from W to E. In S004, values also stay high at the surface. This In this case, the turbidity maximum, as measured by the CTD, coincides with Maximum values of TSM and ISM for points S002 to S005, but shows a different variation in S006. This shows the extent and sinking of the plume at depth, W to E, to ~50 km offshore.

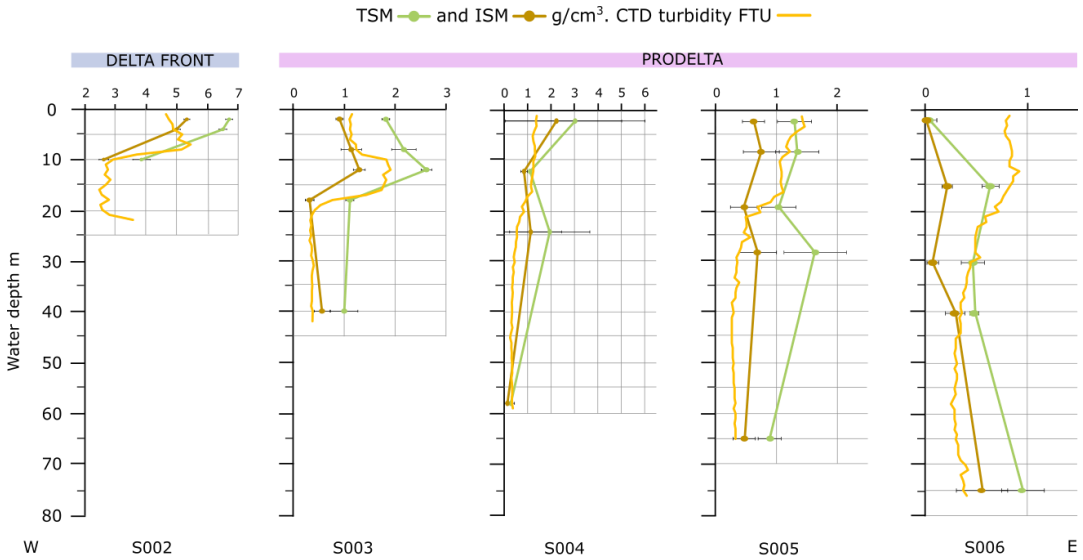

Figure 4.20. The distribution in depth of TSM, ISM and CTD turbidity for the southern plume, formed by Sfantu Gheorghe branch

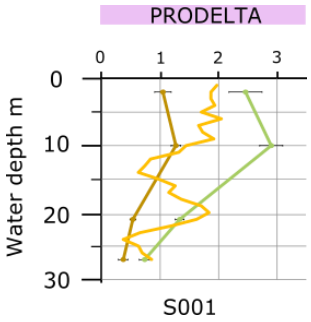

The S001 sampling point shows values of TSM and ISM increasing from the surface to 10 m depth and then a progressive decrease with depth. The CTD turbidity maximum is at the surface and it does not coincide with the TSM and ISM maximum. This sampling point reflects extent at depth the resulting Danube plume southward.

Figure 4.21. The distribution in depth of TSM, ISM and CTD turbidity for S001 sampling profile, showing the combined effect of the Danube plume

Chlorophyll-a

A total number of 26 sampling stations provide chlorophyll-a data for the surface of the Black Sea, on the NW shelf (Fig. 4.22). The distribution map was obtained the same way as it is described for TSM and ISM data.

Chl-a values range from 0.7 to 18.5 mg/m^3, with an average value of 4.5 mg/m^3, decreasing S to N and W to E. The highest values are concentrated in the NW, in the vicinity of the coast, under the direct area of influence of the Danube plume.

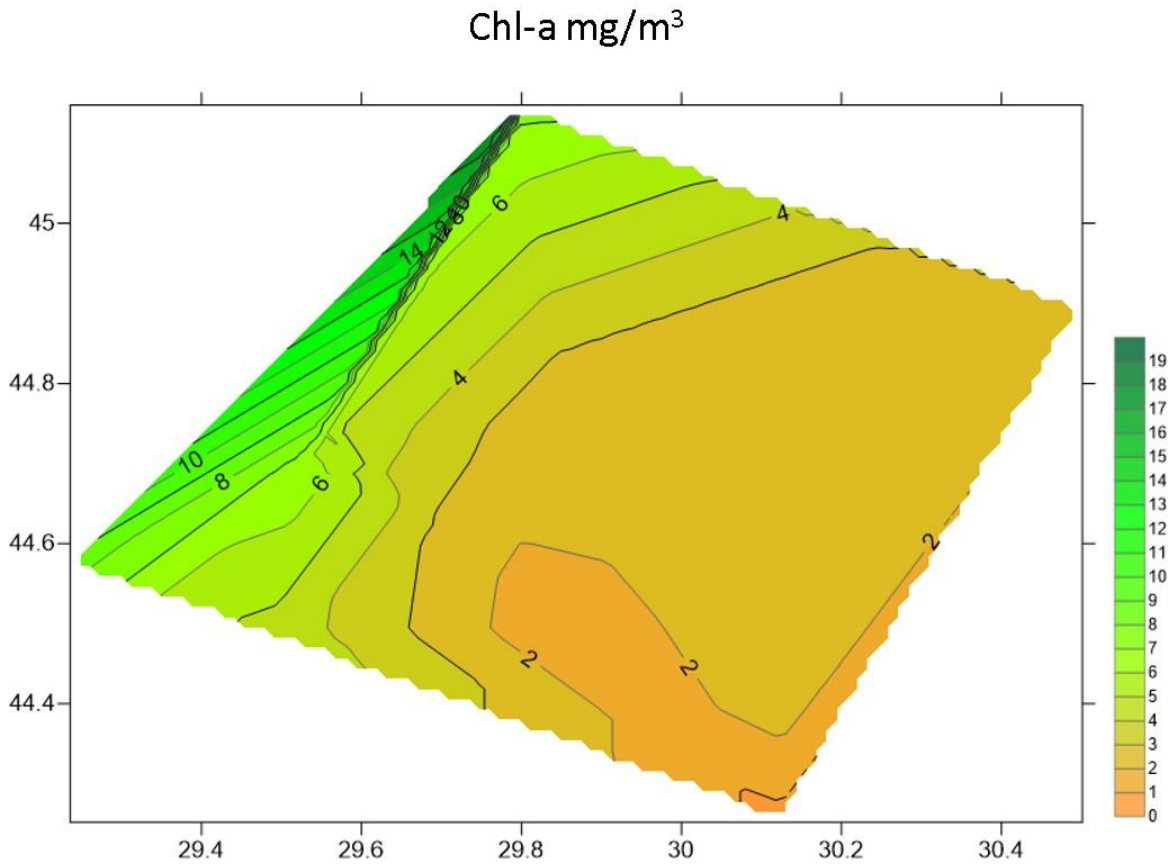

Figure 4.22. The chlorophyll-a map of the studied area of the NW shelf of the Black Sea. (see Fig. 4.1 for distribution of sampling stations and table in Annex 2 for detailed description)

The distribution of chl-a at depth was measured in all the S stations and it is presented in Figs. 4.23 to 4.25. The chl-a profiles are presented in the same way as the TSM and ISM profiles, showing the variation along two transects S007 to S010 and S002 to S006 and south of the Danube plume, in S001.

Along the northern transect, chl-a values decrease overall from S007 to S010, with very similar values for S009 and S010. In depth, chl-a values variy between stations. In S007 and S008, chl-a maximum is at the surface, while for S009 and S010 descends to 5 and 15 m water depth. At higher depths, values get close to 0, below detection limits. Both CTD chl-a and turbidity show different values and variations, compared to results of the lab analysis.

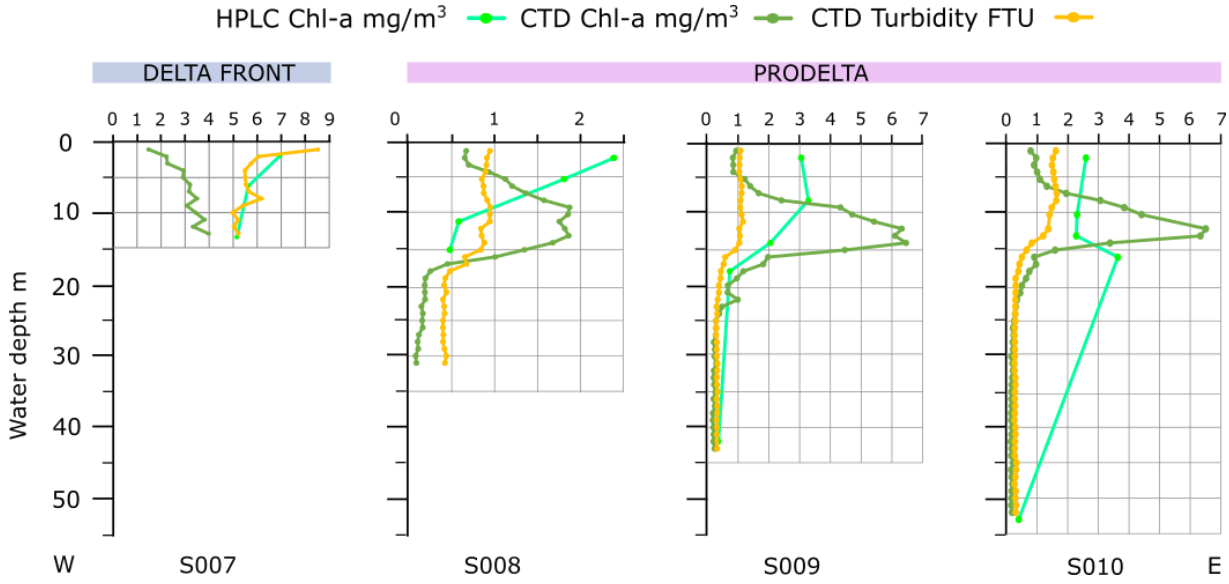

Figure 4.23. Chlorophyll-a variation at depth on the northern transect S007 to S010. See Fig. 4.1 for the location of the sampling points.

On the southern transect, chl-a values decrease from W to E, at the surface. The chl-a maximum is recorded at depth, from -5 m in S002 to -12 m in S003 and S004. In S005 and S006 Chl-a values decrease slowly with depth, with a maximum at -19 m in S005 and -31 m in S006. The bottom values for S003, S004 and S006 are very close to 0, below the limits of detection. CTD chl-a and turbidity display similar variations at depth, which correspond well with the analysed chl-a variations. In S005 and S006 CTD chl-a maximum corresponds very well with the analysed chl-a maximum at depth.

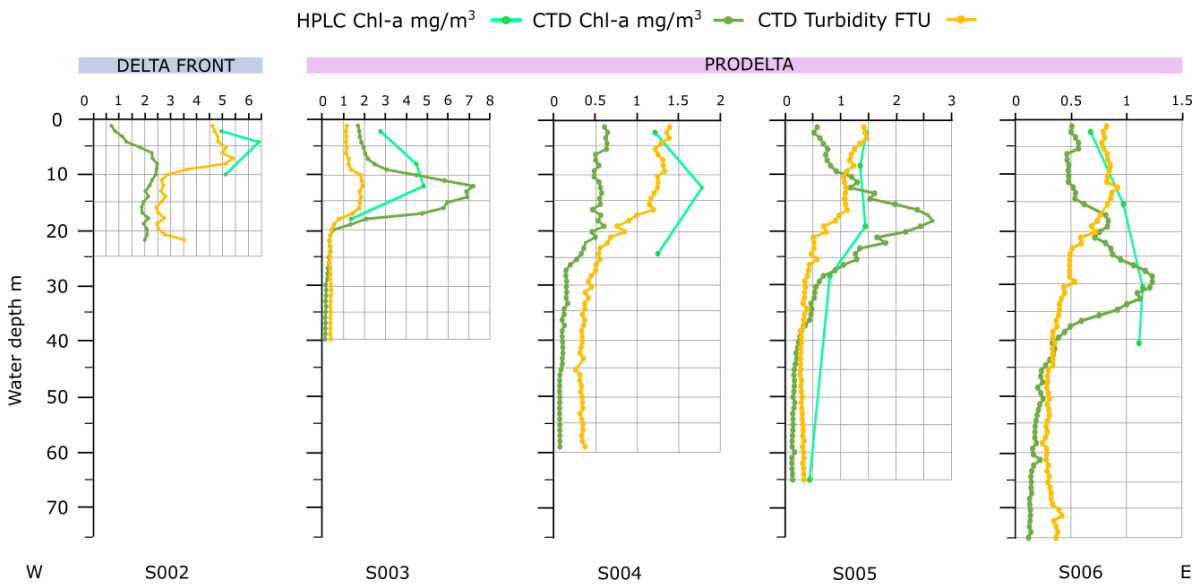

Figure 4.24. Chlorophyll-a variation at depth on the southern transect, S002 to S006. See Fig. 4.1 for the location of the sampling points.

S001 depth profile shows a very different variation of chl-a compared to all the other profiles. It records the highest value at the surface, followed by a gradual decrease at depth. CTD chl-a shows a similar variation for the first 15 m, with very similar values. CTD turbidity variation is very different from the chl-a.

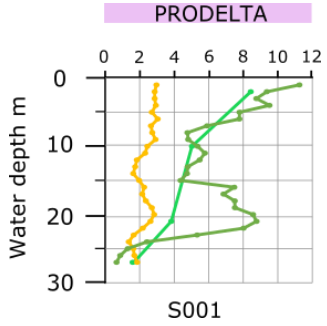

Figure 4.25 Chlorophyll-a variation at depth at S001. See Fig. 4.1 for the location of the sampling points.

4.4.3.2. Particle size

All these samples were collected during a 7 days campaign in the Black Sea, at the beginning of May 2016 (normal water level in Tulcea, Fig. 4.1).

In all the sampled sites of the NW Black Sea shelf, over 85% of the analysed suspended particles are in the size range of clays (0.06 – 3.9 µmm), according to the Udden-Wentworth scale. The amount of clay sized particles is greater in the prodelta area, further from the influence of the Danube. Very fine (3.9 – 7.8 µm) and fine silt (7.8 – 15.6 µm) sized particles represent 6.5 % and 9 % of the analysed particles in the delta front and prodelta areas,

respectively. The rest of the particles, not exceeding 0.5%, are represented by medium (15.6 – 31 µm) and coarse silt (31 – 63 µm) sized particles.

For the delta front area, there is a slight tendency of particle size decreasing with lower ISM/TSM ratio (Fig. 4.27). Also, particle size decreases with depth in this area (Fig. 2.28). However, particle sizes do not vary very much between sites, independently of ISM/TSM values or depth, not exceeding 40 µm. Overall, the northern plume (S007) has lower ISM/TSM values than the southern plume (S002).

In the prodelta area, there is no clear zonation between N and S in what concerns ISM/TSM values. Particle size decreases overall with decreasing ISM/TSM ratio (Fig. 4.27) and with depth (Fig. 4.28). It is interesting to notice that the highest ISM/TSM value, ~0.96 (S008 at -30 m depth) correlates with very low particle size, not exceeding 36 µm. The largest particle sizes correspond to ISM/TSM values between 0.28 and 0.8 and water depths between surface and -53 m.

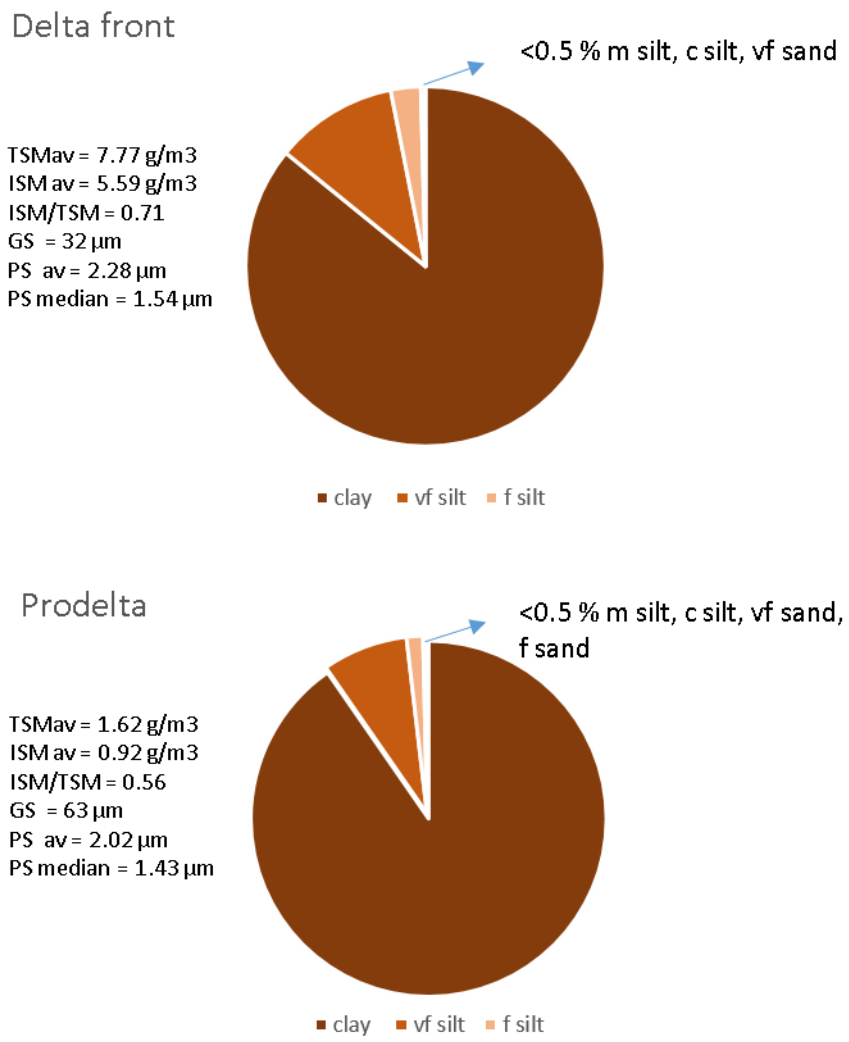

Figure 4.26. Particle size classes for the delta front and prodelta areas, presented as percentages of clay, very fine (vf) silt, fine (f) silt, medium (m) silt, coarse (c) silt and very fine (vf) and fine (f) sand. Average TSM, ISM, ISM/TSM, grain size (GS) (from sedimentary cores and literature) and average particle size (PS) as well as median particle size are given for each environment.

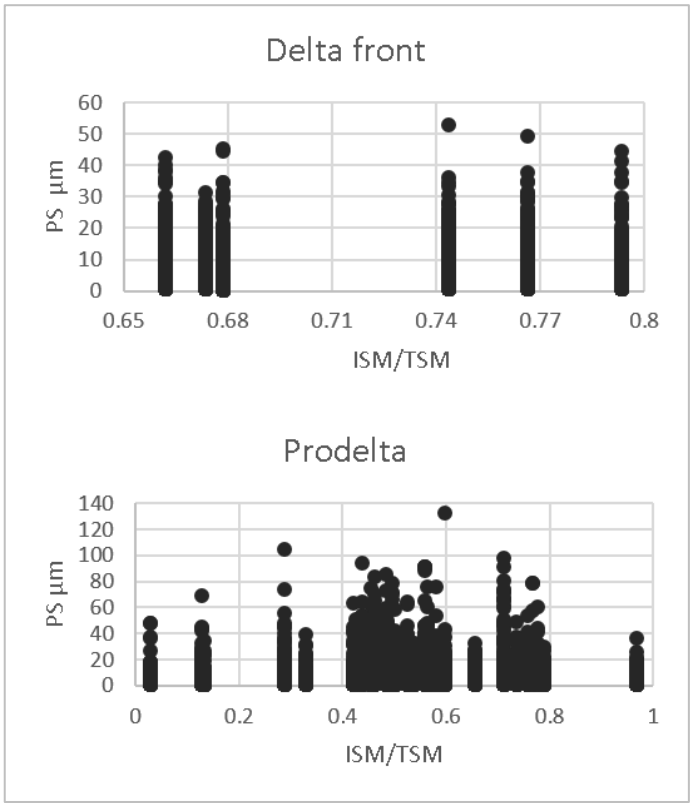

Figure 4. 27. Particle size distribution data as a function of ISM/TSM ratio for the sampled sites on the NW Black Sea shelf

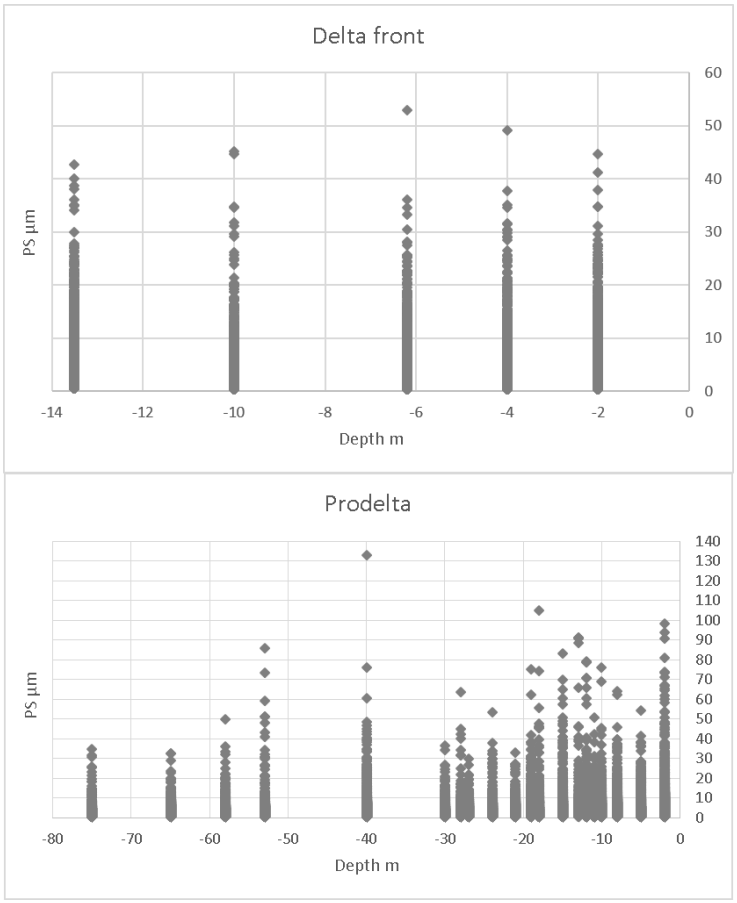

Figure 4. 28. Particle size distribution in depth for the sampled sites on the NW Black Sea shelf

4.4.3.3. Particle composition

Between 80 and 130 particles were analysed for chemical composition, for each studied site, at each sampled depth. The percentage of several elements were plotted as a function of particle size, Ca and Fe for optical properties, Si, Al and the Ti/Ca ratio, as indicators of nature and provenance and B, as indicator of nature.

The analysis was done choosing different depth intervals for the Danube delta front and prodelta: surface waters (down to 2 m depth) and below surface (where both TSM, ISM and Chl-a values vary greatly) for the delta front area and surface waters (down to 2 m depth), from 5 to 25 m depth (where TSM, ISM and CHL-a and turbidity vary greatly) and below 25 m (TSM, ISM, Chl-a and turbidity) values decrease very much, for the prodelta.

Delta front

Most of the analysed particles in the delta front area contain Ca up to 20%, in the surface waters, but most of them do not exceed 10 %. Below surface, more particles, in larger dimensions, up to 40 µm, contain higher percentages of Ca, but not exceeding 20 % as well. Fe content in particles is up to 10 % in the surface and below surface, but most particles do not exceed 5 % of Fe. There is a very low positive correlation between Ca (r=0.04) and Fe (r=0.273)

content and particle sizes for surface waters and no correlation for Ca in subsurface waters (r~0) and a very low positive correlation for Fe (r=0.008).

Si and Al are also contained in most of the analysed particles, on the entire depth profile. Si does not exceed 17 % while Al is up to 8 %. There is a weak positive correlation between the concentration of these two elements and particle size, both in surface waters (r=0.159 for Si, r=0.217 for Al) and subsurface (r=0.218 for Ca, r=0.32 for Fe). Ti is only present in a small number of particles (<50%). Ti/Ca ratio has small values, up to 2, but lower than 1 in most cases. It has no correlation with particle size for the surface waters (r~0) and a very low negative correlation for subsurface (r=-0.056).

B is only found in a small number of particles (<10 %), on the entire depth profile, with specific values ranging from ~10 to ~25 % and not exceeding 31 %. There is a very low negative correlation with particle size for surface waters (r=-0.06) and a strong positive correlation for subsurface (R^2=0.608).

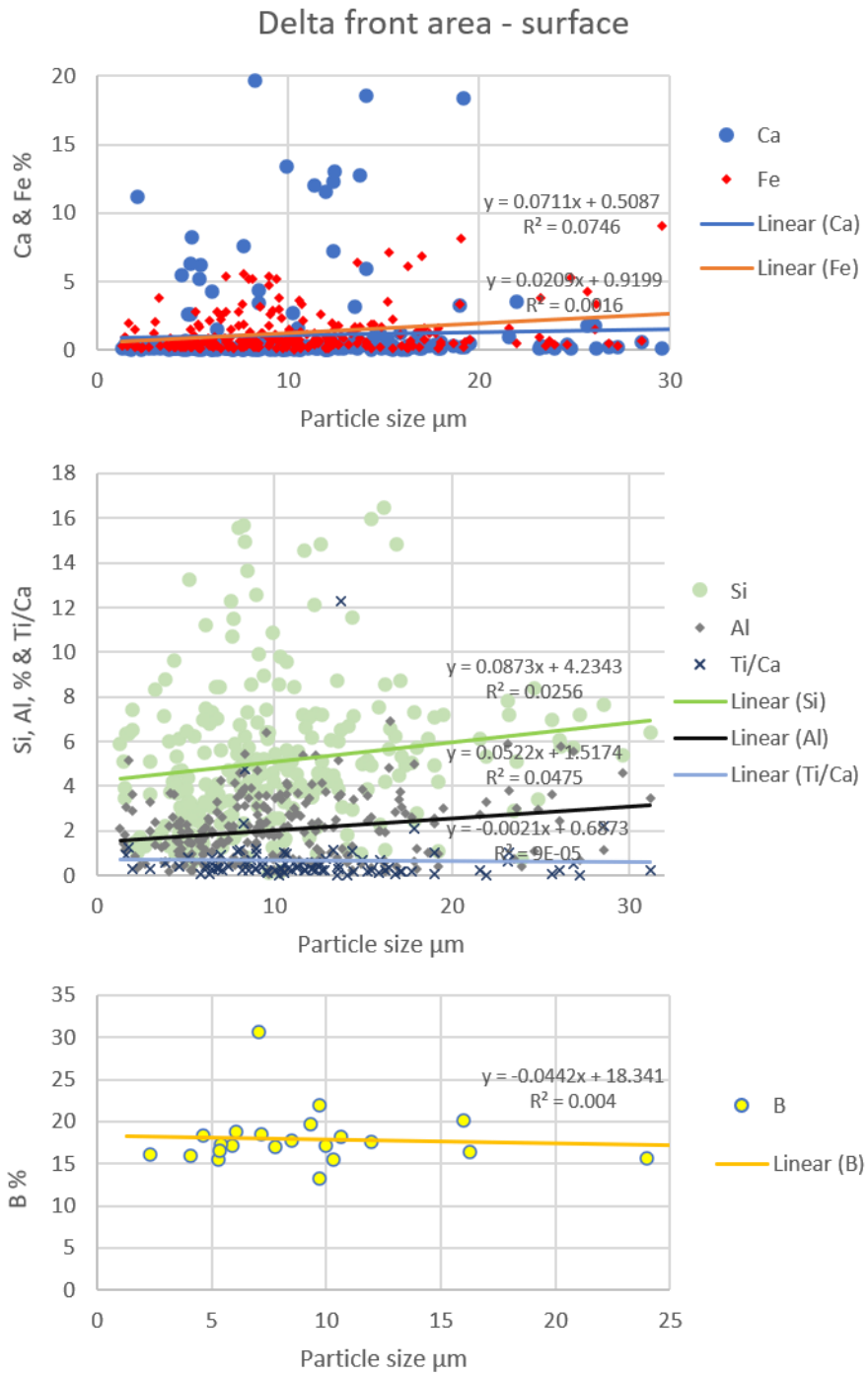

Figure 4.29. Variation of different chemical elements from the analysed suspended particles with particle size in the analysed sites of the Danube delta front, surface water

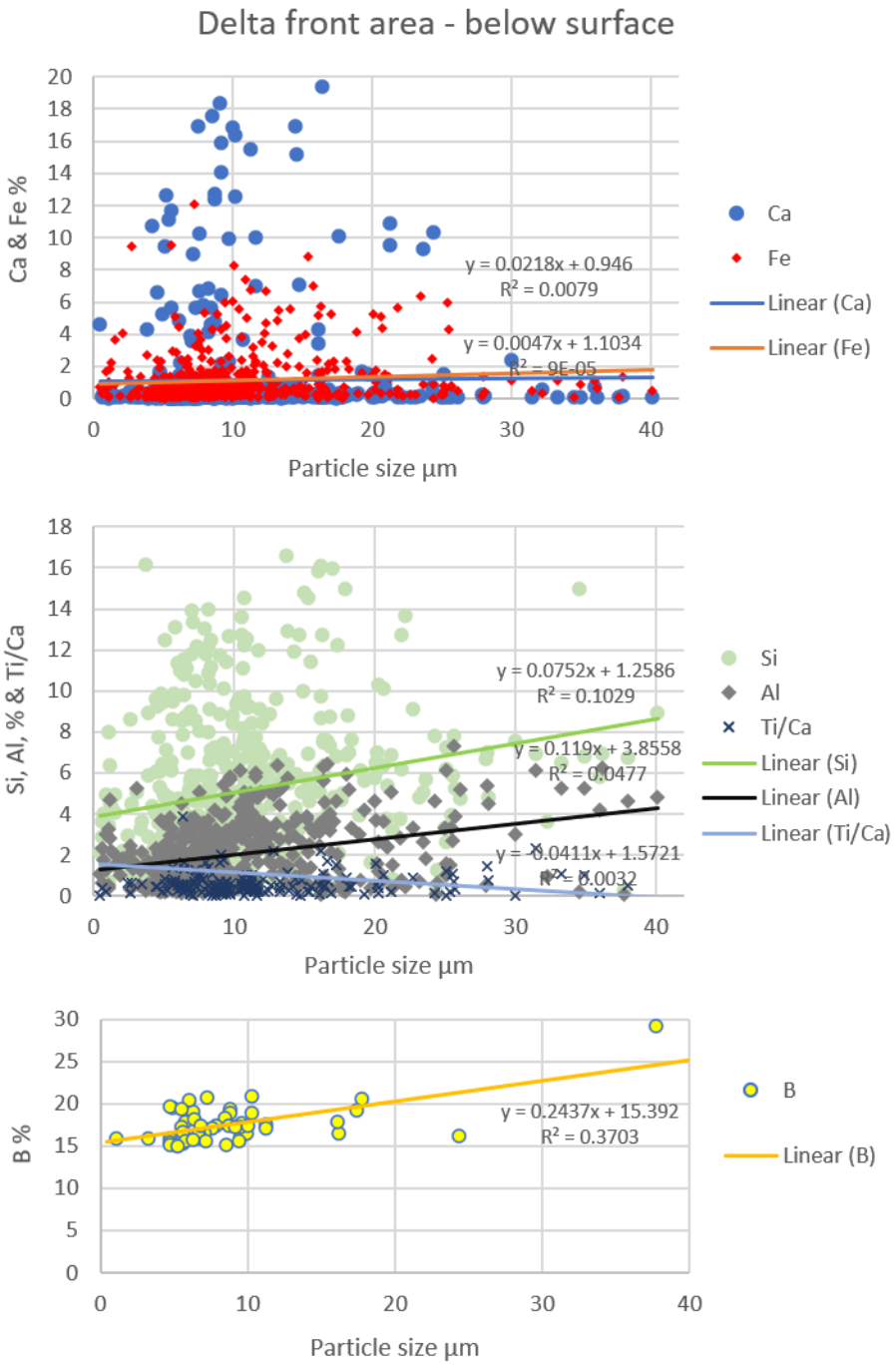

Figure 4.30. Variation of different chemical elements from the analysed suspended particles with particle size in the analysed sites of the Danube delta front, below surface

Prodelta

A large proportion of the analysed particles in the prodelta area contain both Ca and Fe. Ca content increases with depth, from a maximum of 20 % in the surface to 30 % in the intermediate layer (5 to 25 m water depth) and to 35 % below 25 m. There is a very low positive correlation with particle size (r=0.035 in the surface, r=0.240 in the intermediate layer and r=0.078 at depth). Fe content also seems to increase at depth, from a maximum of 20 % to 40 %, but most particles do not exceed 10 %. There is a low positive correlation with particle size in the surface (r=0.205) and very low positive correlations in the intermediate layer (r=0.165) and at depth (r=0.164).

Most particles analysed in the prodelta area contain both Si and Al. Si content increase with depth as well, from a maximum of 18 % to a maximum of 40 %, while the correlation with particle size is very low and positive at the surface (r=0.193), then moderate in the intermediate layer (r=0.476) and it becomes low at depth (r=0.268). Al content increases slightly with depth, from 10 to 15. Correlation with particle size is positive and low or very low, irrespective of depth (r=0.211 at the surface, r=0.125 in the intermediate layer and r^2=0.157 below 25 m). Ti is only found in a small number (~13 %) of the analysed particles, and the Ti/Ca ratio does not exceed 1 for most of them and there are not marked differences on the depth profile. These values correlate in different ways with particle size, depending on depth, with a very low negative correlation in the surface (r=-0.104), low positive for the intermediate layer (r=0.235) and very low positive at depth (r=0.165).

Less than 50 % of the analysed particles contain B. The concentrations do not change with depth, ranging from 10 to 40 %. However, most of the particle which contain B get larger at depth, not exceeding 20 µm in the surface and up to 40 µm in the intermediate layer. There is a low or very low positive correlation of B concentration with particle size, irrespective of depth (r=0.172 at the surface, r=0.235 in the intermediate layer and r=0.165 below 25 m).

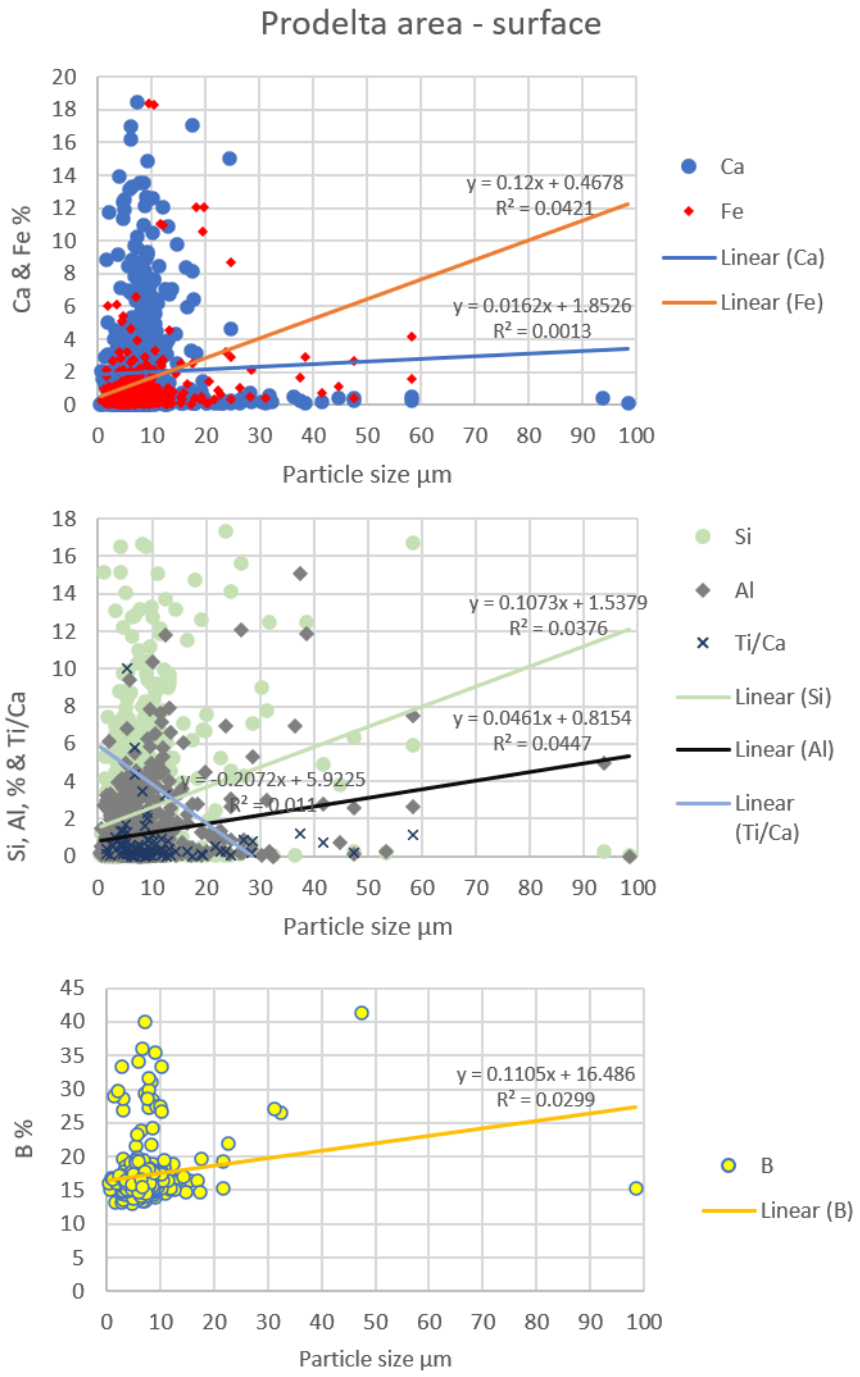

Figure 4.31. Variation of different chemical elements from the analysed suspended particles with particle size in the analysed sites of the Danube prodelta, surface water

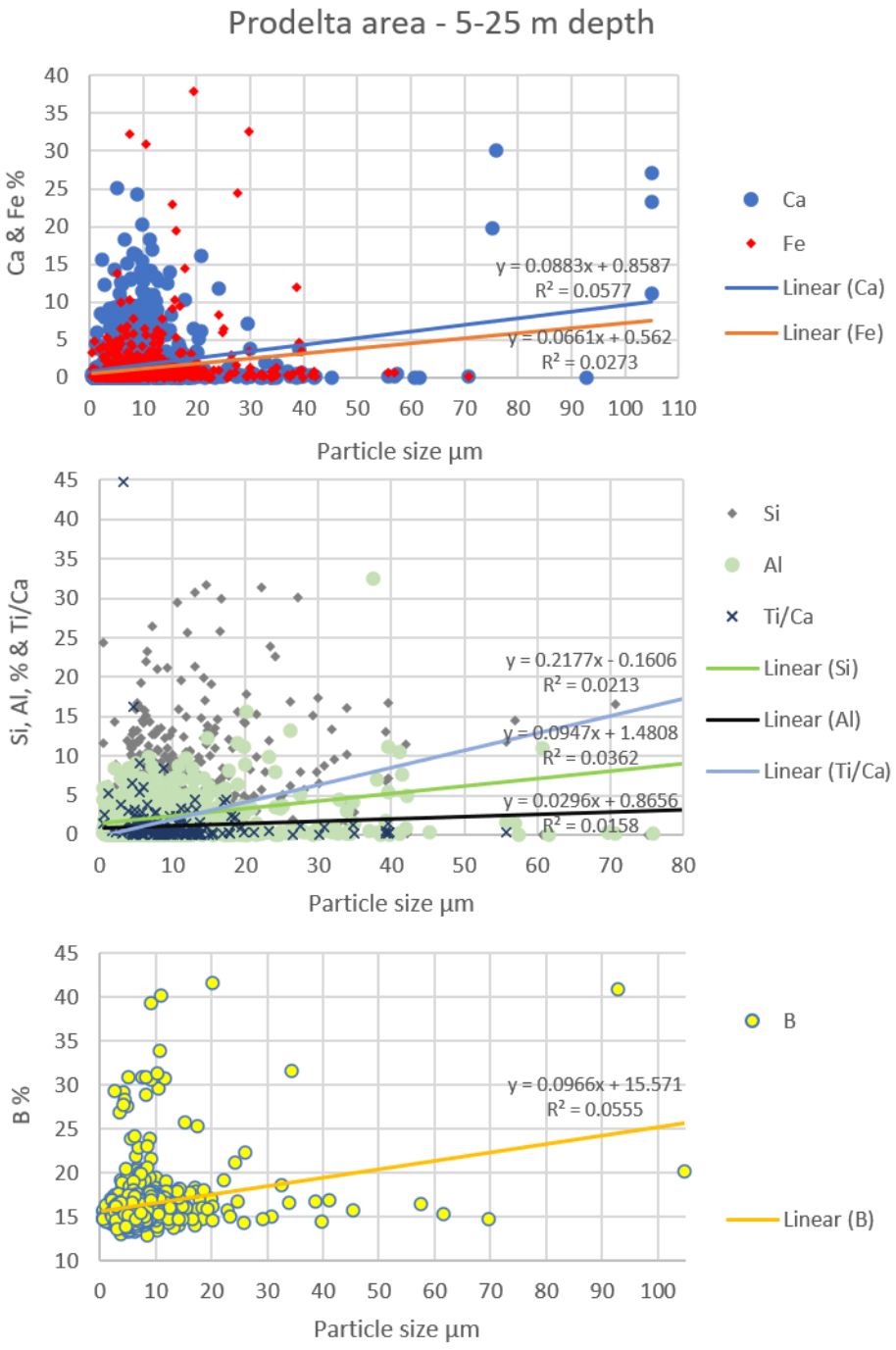

Figure 4.32. Variation of different chemical elements from the analysed suspended particles with particle size in the analysed sites of the Danube prodelta, 5 to 25 m water depth

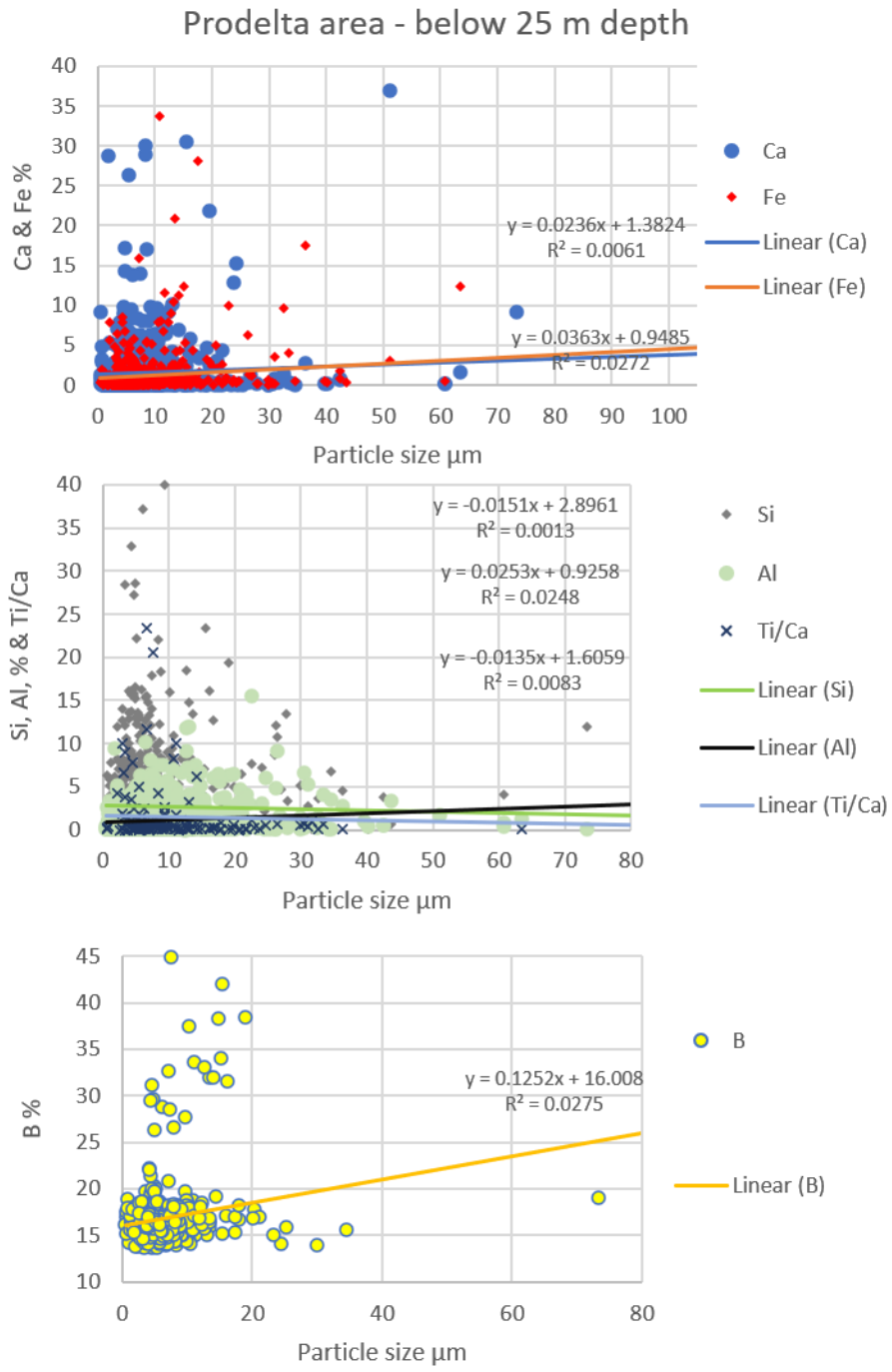

Figure 4.33. Variation of different chemical elements from the analysed suspended particles with particle size in the analysed sites of the Danube prodelta, below 25 m water depth

4.5. DISCUSSION

4.5.1. Approach

We have discussed in Chapter 2 the use of different methods to measure sediment flux, highlighting that the parameters currently measured in certain river basins tend to be either suspended sediments or total suspended solids (TSS). The comparison of these two parameters revealed that TSS underestimates the coarser fraction, usually medium and coarse sand, which might not be suitable for the case of the Danube. Our study confirms this conclusion. However, TSS or TSM are used in conjunction with satellite data, with TSM being one of the main parameters which are obtained from satellite images. This approach is used especially if the aim is to map large areas, such as river basins, deltas or coastal area (e.g. Tyler et al., 2016).

At this time, sediment fluxes cannot be estimated just from measurements of suspended particles in water – concentration, size and composition, alone. However, measuring TSM, ISM, chl-a, particle size and composition provides useful information about the quality of suspended sediments and ultimately, about the environmental status of the aquatic environments in the Danube-Black Sea area. While TSM, ISM and chl-a are more commonly measured, particle size and composition require a large amount of resources, in terms of time and technology.

Some uncertainties arise from the analysis of particle size and composition, first related to the environmental conditions sampled (hydrological, seasonal changes in primary productivity, etc) but also to the number of sampled sites. For example, only two lakes were sampled in 2016. They were chosen because they are representative for the lakes of the Danube Delta, both in terms of connectivity to the main hydrological and primary productivity processes, and they are well studied before (see further discussion of results). The timing and number of sampling sites was chosen to be optimal, considering the time frame of this research.

4.5.2. Particle size analysis

For particle size analysis and distribution in natural aquatic bodies, previous studies have concentrated on method development (Groundwater et al., 2012; Mikkelsen and Pejrup, 2001) and linking these parameters to optical properties of water, retrievable from satellite data (Peng et al., 2009; Risović, 2002). Very few studies have examined the size and composition of suspended particles in natural systems in order to describe their temporal and spatial variability (Buonassissi and Dierssen, 2010).

Our study investigates both particle size distribution and composition, for the first time in the complex area of the Danube Delta and the Black Sea, during: (i) high water discharge

during late spring in the Danube Delta and (ii) average water discharge of the Danube, no precipitations and calm, northerly winds on the Black Sea shelf. Even in different conditions of water discharge, the distribution of particle size in the main branches of the Danube Delta is very similar to the delta front area, with the highest percentage of suspended particles sizes greater than clay size. It is known that the main channels carry most of the water and suspended sediment but this data could indicate the fact that more of this suspended sediment is transferred directly in the Black Sea, together with pollutants, nutrients and plastic, for example. This leads to questioning the filtering role of the Danube Delta, as it was previously stated (Cioaca et al., 2010a).

4.5.3. Distribution of suspended sediment particles in the Danube Delta

The results show differences between the analysed lakes. They record the lowest concentration of suspended particles, overall, while recording the highest chl-a values, with the highest proportion of the smaller suspended fraction, clay size particles, >90 %. From this, more than half are biogenic, as also indicated by the analysis of composition. It is interesting to note that Lake Rosu record both a higher ISM/TSM ratio and MAR (mass accumulation rate, see Chapter 3 for details) than Lake Matita, while the grain size of the bottom sediments is very similar. The difference between these two lakes could be related to: a) a different degree of connectivity to the main branches, determining a different amount of suspended solids inputs from the main branches and b) a different contribution of organic particles to the overall suspended solids. The lakes of the delta are sinks for organic matter, which can contribute up to 85 % to the composition of bottom sediments (Catianis et al., 2014). Hence, the source of the organic suspended particles can be either from particles originating in the water column, phyto- and zooplankton or, to a certain degree, from the resuspension of bottom sediments.

On the main branches there is a longitudinal variation of concentration of suspended particles, while recording the highest concentration overall, during both low and high-water discharge. The values can vary between seasons, as much as 12 times, as shown in the Sfantu Gheorghe mouth area. Here, after a rain event at the end of May 2016, we have sampled the highest TSM and ISM values, 205.5±33.1 g/m^3 and 192±31.5 g/m^3, respectively. They also transport the highest proportion of particles larger than clay size (~17 %), and have more particles of non-biogenic origin than any other environment. Overall, the chl-a values are the lowest in the delta complex, with the exception of two secondary channels, meanders of the main branches, Old Danube, connected to Sulina and Mahmudia, connected to Sfantu Gheorghe, which also record the lowest concentration of suspended particles and the highest concentration of suspended particle of organic origin. As the main branch is deepened and maintained for navigation, it takes most of the water and sediment, with a higher current velocity,

while these meanders become partially disconnected, and they behave more like lakes, recording a decrease in water and sediment circulation (Jugaru Tiron et al., 2009; Tiron Duţu et al., 2014). The MAR calculated from cores taken from the secondary channels of the Sfantu Gheorghe delta, Garla Turcului and Canal Ciotica, show high sediment input and rapid accumulation, comparable with the terminal lagoons. This shows that smaller channels or canals, including the old meanders, such as Mahmudia (Jugaru Tiron et al., 2009) are very prone to siltation and clogging.

Lagoons record a higher concentration of suspended particles, than lakes but lower than channels. Previous studies have shown higher values of total suspended solids next to the channels that reach the lagoons (Catianis et al., 2019). The comparison done in both during low and high-water discharge of the Danube, in the Musura and Sahalin lagoons, shows similar concentrations of suspended particles, independently from water discharge variations, which indicated that resuspension plays an important role in these environments, especially in the shallow, open waters of these lagoons, further away from the main sediment supply (e.g. center of Sahalin). Both concentration and nature of suspended matter in the lagoons are mixed. While Sahalin and Musura receive an important input of water and sediment from the Danube, Razelm and Golovita are relatively isolated, and the water exchange is only done through smaller channels, such as Dunavat. Generally, in Musura and Sahalin concentration and nature of suspended particles depends on the amount brought by the Danube, as well as the in-situ primary productivity. Razelm and Golovita behave more like lakes. High MAR values in Musura and Sahalin indicated them as very active depocentres, while relatively high concentrations of suspended matter and and chl-a, as well as the composition of particles, shows an important contribution of the biogenic material to the total suspended particles.

4.5.4. Distribution of suspended sediment in the NW Black Sea area

The Danube is the largest source of freshwater and terrigenous particles in the Black Sea. For the period of our marine cruise, the Danube plume was confined to the coast, mainly controlled by Danube's water discharge (close to the annual average) and the coastal current, which should only determine minimum resuspension. In this case, we can assume that most of the analysed particle originate from the Danube's solid discharge.

The highest concentration of suspended particles in the surface waters was found in in the northern plume, formed by the Chilia and Sulina branches, two times higher than the southern plume, formed by Sfantu Gheorghe. The distribution of suspended matter at depth maps well the southern plume, as it sinks, while in the north, values decrease more rapidly eastward.

Based on the composition analysis, we estimate that in the delta front area, more than half of the suspended matter is of terrigenous origin, especially in the surface waters. Overall, there are more particles larger than clay size (~15%), very similar to what is transported in the Danube Delta channels (~17%). Particle size does not vary much with depth in the delta front area, but it decreases with depth in the prodelta area. Even if the values are very smaller overall, most of the particulate matter in the northern plume is inorganic, of larger sizes, while the organic fraction has greater values in the southern plume, and the particle size is smaller. Phytoplankton contribution to suspended solids in this area was considered more difficult to analyse, because the main productivity area overlaps the Danube turbid plume, with moderately high mineral TSM (Güttler et al., 2013).

Our results show an important contribution of biogenic particles in the total suspended particles, especially in the prodelta area, in the first 30 m of water depth. At surface chl-a values follow the same distribution as the particulate matter, with a maximum at depth. This particular situation of the chlorophyll-a maximum at depth was previously documented in the Black Sea (Chu et al., 2005). CTD turbidity maximum coinciding with the chl-a maximum in most cases. This happens especially further away from the direct influence of the Danube plume. Studies on suspended particles in this area asses that most of the sediment discharged by the Danube is being deposited in the close proximity of the discharging mouths (Karageorgis et al., 2014) and that most of the suspended sediment coming out of the delta is confined to a narrow area in the coastal zone, not reaching much of the prodelta area (Karageorgis et al., 2014, 2009). The sedimentation rates obtained from the analysed cores confirm, to a certain degree, this conclusion, with the exception of the southern part of the prodelta, where the values of recent years remain relatively high. The sedimentation rates calculated for the eastern part of the prodelta are situated not further than ~30 km offshore, and so, closer to the highest concentration of the suspended sediment discharge. Further east, lower sedimentation rates show that most of the terrigenous material does not reach this area, unless in exceptional conditions (low wind regime, very high waters).

4.5.5. Implications for mapping sediment fluxes from satellite data

Previous studies of the Danube Delta and the NW Black Sea shelf have used different parameters to study suspended sediment patterns: turbidity (Constantin et al., 2017, 2016; Güttler et al., 2013), concentration of particulate matter and particle size and distribution, related to optical properties (Karageorgis et al., 2014, 2009).

We found that an extensive study on particle size and composition brings new insights into the properties of sediment flux, together with TSM, ISM and chl-a distribution. Our results show that concentration of suspended particles, rather than size is a better indicator of higher

sedimentation rates, in most environments, in the delta and continental shelf. Our results show also that, even if the used parameters add important information for the ecological status of aquatic environments, they are not enough to describe and map sediment fluxes. In such complex systems as the Danube-Black Sea area, these parameters can vary very rapidly in both time and space, especially in areas like shallow, large lakes and lagoons, and the coastal zone.

Both nature and concentration of suspended particles, as well as the distribution of sizes in surface waters contribute to variations of optical properties which are retrievable from satellite data. This is relevant to several recent studies which are classifying both inland and coastal water types based on their optical properties (Neil et al., 2019; Spyrakos et al., 2018).

4.6. CONCLUSIONS

For this study we have defined suspended sediments as being suspended particles, of any nature, in suspension, in water at a particular time. The aim was to investigate the quality of suspended sediment particles, both in terms of nature and distribution in the Danube-Black Sea transition zone.

In the previous chapter we have shown how the supply of sediment and grain size in the different environments of the Danube Delta vary depending on the hydrological connectivity with the main branches. Largely, suspended sediment patterns follow the same distribution.

TSM, or TSS, a very commonly used parameter for assessing sediment fluxes and easily obtained from satellite data, is usually not enough, underestimating the coarser fraction. Also, TSM can vary very rapidly in both time and space. For example, the highest TSM values of the northern plume in the delta front area (Site S007 and T001 in Fig.4.2) does not necessarily mean higher sedimentation rates (Site S007 – Chapter 3), compared to the other sites. In shallow waters, such as lakes or lagoons, high TSM values may be caused by wind-driven resuspension of the bottom sediments. However, using several parameters like TSM, ISM, chl-a as a minimum brings more information of the qualitative aspect of the distribution of suspended sediment particles, rather than using just one parameter, such as turbidity. The latter is one of the most commonly measured parameter, due to accuracy of in-situ measurements (Constantin et al., 2016) and its direct relation to remote sensing reflectance (Dogliotti et al., 2015).

For assessing sediment flux from measurements of suspended sediments alone, particle size and composition bring more useful information. Suspended particles tend to have larger sizes along the main channels, as well as on the delta front. The equal amount of larger

particle sizes in the channels and the delta front may indicate that more water and sediment is transferred directly into the Black Sea, as previously thought, thus questioning the role of filtering of the delta. For the other environments, such as lakes or the prodelta, there is a much smaller amount of sediment input but there is a significant amount of particles of coarser sizes of biogenic origin.

5. SEASONAL VARIATIONS AND SPATIAL PATTERNS OF SEDIMENT FLUX INTO THE BLACK SEA

5.1. INTRODUCTION

River plumes build the delta complexes. They are the primary mechanisms for the transportation and dispersal for sediments, organic matter, carbon and nutrients for coastal ecosystems (Dagg et al., 2004; Hedges and Keil, 1995). They are also, therefore, the primary mechanism for the transportation and dispersal for pollutants, such as heavy metals, radionuclides, plastics.

Earth Observation techniques have been used to map river-sea interaction zones (e.g. Burrage et al., 2008; Doxaran et al., 2009; Gangloff et al., 2017; Petus et al., 2014) and they provide important information about the spatial and temporal variability and changes occurring in these environment trough: (i) high frequency measurements (days); (ii) ability to map these complex areas for which different spatial resolution is required (deltas, estuaries, coastal seas); (iii) retrieving parameters such as temperature, salinity, total suspended matter, turbidity and chlorophyll-a, which are good markers of the river-sea systems response to basin and climate change.

Anthropic changes in the river catchment, including changes affecting river-sea connectivity such as dams, and climate change can alter the transfer of water and sediment to the coastal zones. Plume dynamics in the river-sea interaction zone is controlled by river discharge, wind and wave resuspension, precipitations and marine currents, determining very rapid changing patterns (e.g. Gangloff et al., 2017).

In Chapter 2 we show how the dams along the Danube not only reduce the amount of sediment that feeds the Danube Delta and the Black Sea shelf, but also change the magnitude of seasonal variations. Chapter 3 and 4 provides a clearer image of the active depocentres in this area, and the effect of the reduction in sediment flux across this complex environment. The main branches carry most of the sediment, which is deposited mainly in the terminal lagoons, Musura and Sahalin and in the carrier channels of the secondary deltas of Chilia and Sfantu Gheorghe. The most active areas of deposition are in the delta front area, in the area where the two plumes form, Chlia and Sulina in the north and Sfantu Gheorghe in the south. The area with the highest deposition in the prodelta is south of Sfantu Gheorghe, while the eastern part is still receiving a very small amount of sediment. An important contribution to the overall

sediment flux is organic, more in the lakes of the delta and prodelta area, while the channels, terminal lagoons and the delta front receive more of the inorganic fraction.

Thus far, we have built an understanding of the Danube Delta – Black Sea interaction through point samples and time series analysis from historical data and sediment cores. However, this lacks the integrated spatial perspective. In this chapter, we aim to gain insight into seasonal patterns of the spatial distribution of sediment, examined in detail at selected locations of the Danube plume and link these results with the sedimentary patterns and the distribution of suspended solids in the water column.

This chapter aims to link the spatial distribution of TSM and chl-a with sediment fluxes variations, measured in the sedimentary cores (Chapter 3) and to describe the seasonal patterns in relation to the variation of both water and suspended sediment discharge of the Danube river (Chapter 2).

5.2. DANUBE – NW BLACK SEA INTERACTION ZONE

The main source of water and sediment in the NW Black Sea is the Danube River, discharging through its three arms Chlia, Sulina and Sfantu Gheorghe. (c. 60% of the total water runoff in the Black Sea basin and c. 48% of the total SPM load) (Ludwig et al., 2009; Mikhailov et al., 2008). The sediment budget, its transfer and dispersal patterns in the Danube Delta and the NW Black Sea was described in the previous chapters.

Using passive tracers, Bajo et al. (2014) observed the prevalence of Chilia's waters in the formation of the plume, while the waters of Sfantu Gheorghe follow the Sahalin spit and remain confined near the shores. The influence of Sulina is even more reduced, as it mixes with the waters of Chilia. The authors point out that instant patterns may be different, as the exact area and processes controlling the plumes should be investigated further. The plume extension is mainly restricted to the coastal waters and shelf (maximum offshore extension of 70 km as estimated by Güttler et al., 2013), with a penetration depth of 15 m near the coast (Karageorgis et al., 2009), while the influence of the Danube waters, traced through simulated inorganic N/P molar ratios at the sea surface, can extend to the Turkish coast (Tsiaras et al., 2008). The main controlling factors for the formation and extension of the plume are hydrological (solid and liquid river discharge that varies seasonally; meteorological (wind speed and direction) and the topography of the shoreline (Güttler et al., 2013; Karageorgis et al., 2009). Wind seems to be the primary factor for surface water direction of flow but the haline stratification can limit its influence in the deeper layers, especially near the delta (Bajo et al., 2014).

5.3. REMOTE SENSING STUDIES OF THE DANUBE-BLACK SEA AREA

Previous studies in the Danube – Danube Delta – Black Sea area, employing Remote Sensing techniques focused on:

(i) Thermal patterns in the Black sea (Sur and Ilyin, 1997);

(ii) Characterizing surface water optical conditions in the Black Sea and water constituents as TSM, yellow substances and Chlorophyll-a (their distribution patterns and seasonal variations), as a mean to assess environmental interactions in the Black Sea area with a particular focus on the NW zone (Barale et Murray, 1995; Barale et al., 2002; D'Allimonte et al., 2012; Karageorgis et al., 2014; Nezlin et al., 1999; Oguz et al., 2002; Tsiaras et al., 2008)

(iii) Gain insights into the Danube plume dynamics and seasonal variability. Previous research (Constantin et al., 2017; Güttler et al., 2013; Karageorgis et al., 2009) revealed that water turbidity and the redistribution of the particles in the low salinity waters in the Black Sea are controlled mainly by river discharge, wind speed and direction and sediment re-suspension. While the Danube plume extension is mainly restricted to the coast and shelf (maximum offshore extension of 70 km as estimated by Güttler et al. (2013), the influence of the Danube waters, traced through simulated inorganic N/P molar ratios at the sea surface, can extend to the Turkish coast (Tsiaras et al., 2008). The intensity of Danube discharge determines the level of eutrophication in the NW Black Sea interior shelf, as higher discharge implies higher nutrient loads. The South-Western interior shelf and the outer shelf are also affected (Nezlin et al., 1999).

5.4. METHODS AND DATA

5.4.1. Satellite data

5.4.1.1. MERIS CoastColour archive

The complete CoastColour MERIS (MEdium Resolution Imaging Spectrometer) archive (July 2002 to April 2012 for the Black Sea) was used to obtained monthly averaged distribution maps of the NW Black Sea, of TSM (Total Suspended Matter) and chl-a (chlorophyll-a) concentrations. The archive comprises the data provided by the ESA MERIS (MEdium Resolution Imaging Spectrometer) mission, which was specifically designed for coastal zone management and research.

The data was available from the MERIS CoastColour web page https://www.coastcolour.org/products.html. L2W level products, with a spatial resolution of 300 m, are available to download on demand through the Calvalus service. This level products provide water properties, such as inherent optical properties, chlorophyll and suspended matter

concentration, diffuse attenuation coefficient Kd and Secchi Disk Depth. The concentration of water constituents is calculated as follows: the chl-a concentration is calculated both with a neural network algorithm which performs best for high turbid waters and the OC4 algorithm. The blending between the two variables is done based on the TSM concentration.

The area of interest was defined within the following limits: N: 45.6582; S: 44.3582; W: 28.4582; E: 31.3, representing the coastal waters in front of the Danube Delta, comprising both the delta front and prodelta areas, as geomorphological domains.

The monthly averaged images were processed in SNAP, the software provided by the European Space Agency for processing satellite images, including those from the latest Sentinel missions. Time series data of monthly averages of both TSM (Fig. 5.1) and chl-a (Fig. 5.2) were obtained at five locations. The averaged values of 3x3 pixels was extracted from each image, at locations corresponding with the cores retrieved in the NW Black Sea: S007, S008, S002, S008 and S001 (Fig. 5.1, 5.2 and Table 3.2 in Chapter 3 for exact coordinates).

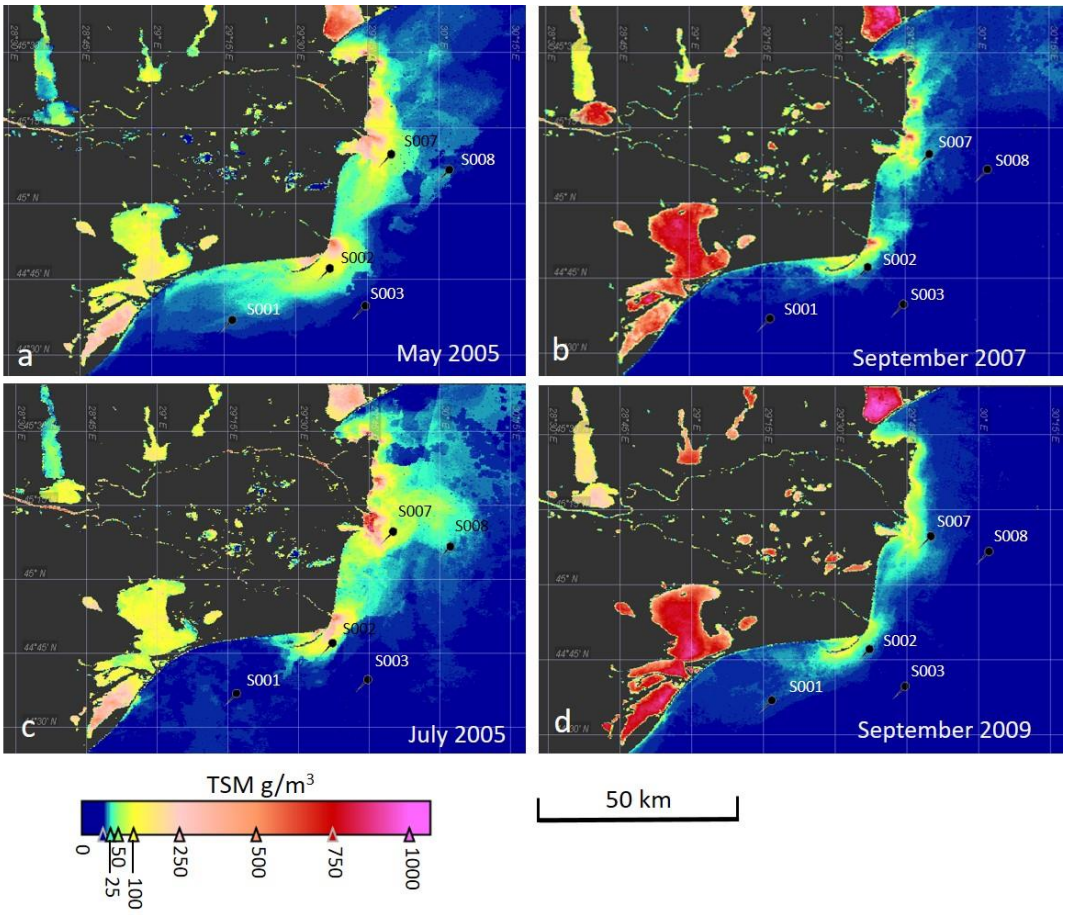

Figure 5.1. CoastColour images of monthly averages of TSM concentration in the NW Black Sea, with the location of the studied points S007, S008, S002, S003, S001, coinciding with the sediment cores of Chapter 3. The examples were chosen for the months of a maximum water discharge (a – May 2005), a minimum water discharge (b – September 2007), a maximum suspended sediment discharge (c – July 2005) and a minimum suspended sediment concentration (d – September 2009)

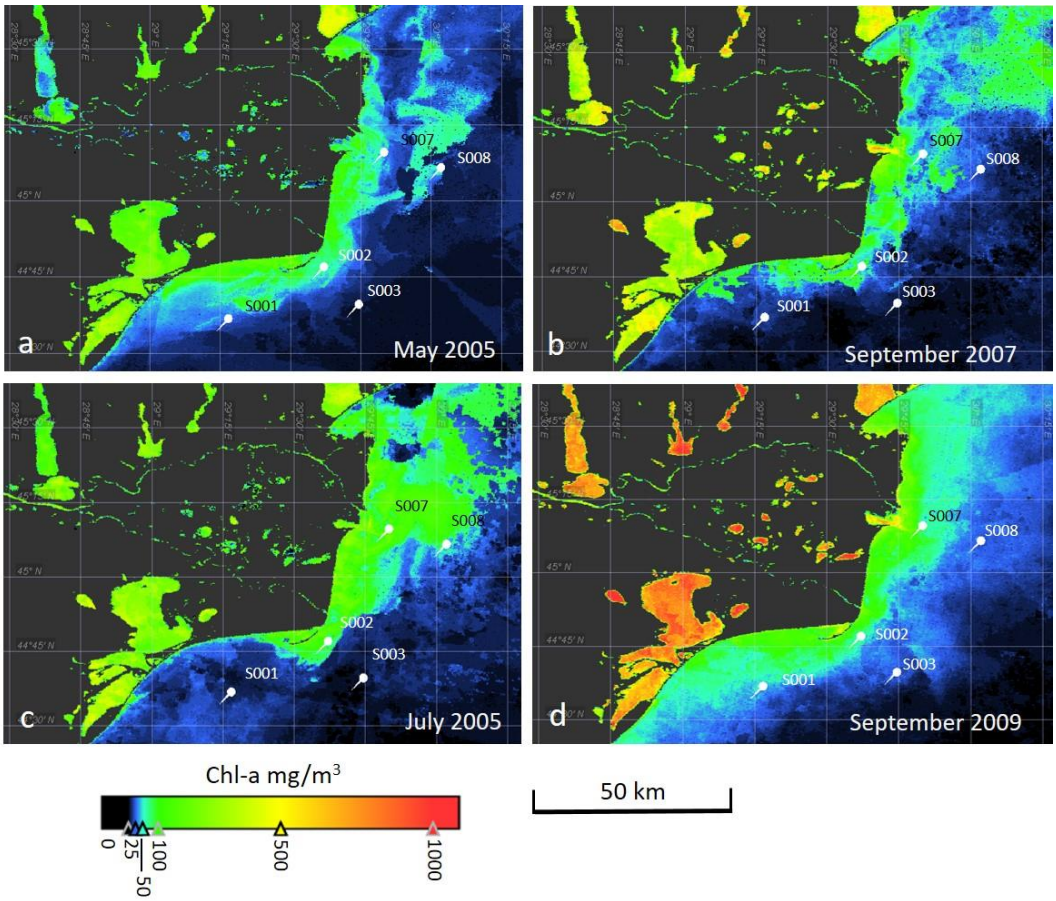

Figure 5.2. CoastColour images of monthly averages of chl-a concentration in the NW Black Sea, with the location of the studied points S007, S008, S002, S003, S001, coinciding with the sediment cores of Chapter 3. The examples were chosen to show comparison with the TSM examples (a – May 2005, b – September 2007, c – July 2005, d – September 2009).

5.4.1.2. Sentinel 3 data

The ESA Sentinel 3-OLCI data was used for comparison. A scene acquired on the 11th of May 2016 was used, validated by the data measured during the Eurofleets ReCoReD cruise mentioned in Chapter 4 (05-12th of May 2016). TSM and chl-a data measured in situ and previously presented in Chapter 4 was used to validate TSM and chl-a products obtained from the satellite image (Fig..5.15, 5.16). The image, with a spatial resolution of 250 m, was processed with the C2RCC processor, which was available at the time when the image was acquired. This C2RCC processor was trained to cover extreme ranges of scattering and absorption and is available through ESA's Sentinel toolbox SNAP. It is used in the Sentinel–3 OLCI ground segment processor of ESA for the generation of the Case–2 water products, as well as in the processor for the MERIS 4th reprocessing (Brockmann et al., 2016).

5.4.2. Statistical analysis

Linear regression was used to compare the satellite derived TSM and chl-a data, which were compared with TSM and chl-a data measured in-situ, from surface water samples. Correlation was used to assess TSM variation in station S007 with both water and suspended sediment concentration, recorded for the Sulina branch.

Time-series analysis

Both TSM and chl-a data, monthly averages obtained from the satellite data, from July 2002 to April 2012 were analysed, using time series analysis of general trends and time series decomposition. The same methods were used in Chapter 2 for water and solid discharge data and they are described in detail in section 2.3.2.

5.4.3. Hydrological data

TSM data for the studies period was compared to both water discharge and suspended sediment discharge data which was used in Chapter 2. The data is recorded at Sulina station, on the middle arm of the Danube Delta.

5.5. RESULTS

5.5.1. Validation of satellite-derived data

5.5.1.1. TSM

TSM obtained from Envisat MERIS CoastColor archive was compared with in-situ data provided by the JOINT Research Centre (JRC) for the 3rd of July 2011. Doing the validation of TSM derived from satellite data posed a very challenging problem: there is very little to none in-situ TSM data (or any other comparable parameter) for the Black Sea for the period of 2002-2012. The results of the comparison are presented below (Fig. 5.3). Only six match-ups were available for the comparison, which shows a moderate correlation (R^2=0.359). The data of the 3rd of July shows that satellite derived TSM concentration is 3 to 5 times underestimated. This is due to the mismatch in time of the satellite with the in-situ data and the lower sensitivity of the instrument.

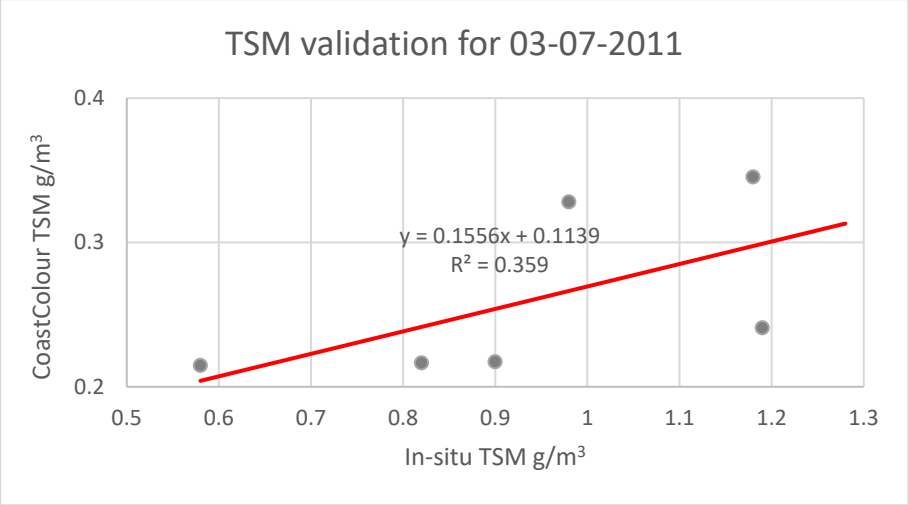

Figure 5.3. Comparison between TSM derived from satellite data (CoastColor archive) and in-situ measured TSM (point-sampling on the 3rd of July 2011, data provided by the JRC), in the coastal waters of the Black Sea

5.5.1.2. Chlorophyll-a

Doing the validation of chl-a derived from satellite data posed a very challenging problem: there is very little to no in-situ chl-a data available for the Black Sea for the period of 2002-2012. For this study we have used the chl-a data reported for the year 2009, published by Vasiliu et al., (2010), for the area around the Danube Delta. A point to point comparison was not possible at this time, as the raw data was not available. We have done a rough comparison of the intervals of variations for chl-a data retrieved from surface waters for the year 2009, in the seasons reported by the above mentioned study. The comparison is presented in Table 5.1.

Table 5.1. Comparison of chl-a data from the Black Sea

Month of 2009	In situ measured surface chl-a mg/m^3	Area of maximum in-situ chl-a	Satellite derived chl-a mg/m^3	Area of maximum satellite chl-a
February	3.19 - 9.21	S001	3.5 – 50	S001
May	2.45 – 21.92	S001	19 – 130	S007
July	0.13 - 9.94	S007, S002	10 – 150	S007
September	1.06 - 26.57	S001	20 – 200	S007

The comparison reveals a different distribution of maximum satellite retrieved chl-a in months May and September and an overall overestimation of the values, by several orders of magnitude.

5.5.2. TSM

The TSM products show the formation of the Danube plume in the coastal zone, in both low and high water and suspended sediment discharge. Irrespective of these conditions the plume forms from Chilia and Sulina in the north, partially decoupled from the southern plume,

formed in the south by Sfantu Gheorghe. The distribution of TSM values in the coastal zone decreases with distance from the Danube mouths, with higher values overall in the northern plume. This corresponds well with the sedimentary patterns on the delta front and prodelta areas, described in Chapter 3.

5.5.2.1. Linear trends

For the analysed time span, from July 2002 to April 2012, TSM shows different general trends at the analysed locations (Fig. 5.4). In the delta front area, location S007 shows a slight decrease in TSM with time, while S002 shows a slight increase, but these trends are not statistically significant at 95% confidence level (Table 5.2). In the prodelta area, all analysed locations show increasing trends of TSM. They are only statistically significant at locations S003 and S001 at 95 % confidence level (Table 5.2).

Several periods of peaks can be identified from the data, in all the analysed locations: 2005-2006, 2007, 2010 and 2012. These periods correspond largely to high water level in the Danube (for example the extreme flood of 2006 with three peaks from February until July – GeoEcoMar, unpublished data).

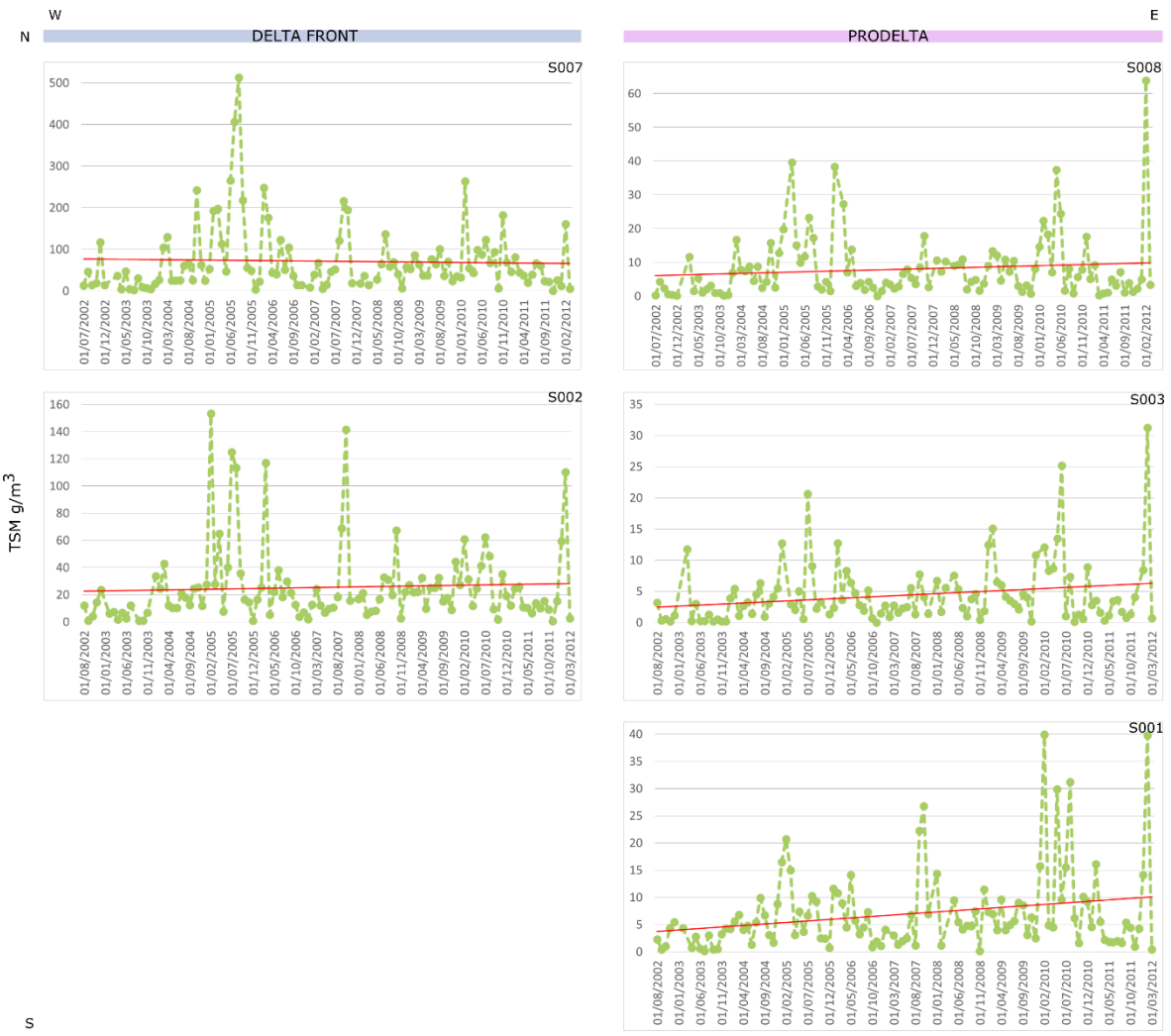

Figure 5.4 Satellite-derived TSM concentration and linear trends for the analysed period at each of the five locations

Table 5.2. Summary of statistical results of the linear regression, for TSM concentration

Site	**Statistical parameters**		
	R^2	**P value**	**Slope**
S007	0.0007	0.6008	-0.002
S002	0.004	0.6702	0.0017
S008	0.01601	0.273	0.001
S003	0.0514	0.0323	0.001
S001	0.0670	0.0122	0.0018

5.5.2.2. Evolution in time of maximum and minimum TSM

The maximum and minimum monthly TSM concentration values were plotted as functions of time, for the entire time span of the data sets (Figs. 5.5 and 5.6). This shows the seasonality of the yearly TSM variations and also changes in time of the seasonality. The maxima and minima as a function of time are represented during a hydrological year, as it was defined in section 2.3.2.1. We have used the same temporal framework as for the rivers, in

order to explore connections between water and suspended sediment discharge of the Danube (see Chapter 2) and TSM concentration. For all sites a linear and a moving average models were fitted to the data, in order to assess such changes.

For sites S007 and S002 TSM maxima can occur in any month of the year, with the exceptions of and May, but they occur most often in March and April. The peaks have a tendency of occurring later in the year in S007 and S002, by almost two and four months, respectively. However, these trends are not significant at 95% confidence level (Table 5.3). The moving average model fitted to the data shows a periodicity of the peaks' seasonality changing every two years.

At sites S008, S003 and S001 the maxima can occur almost any month of the year, with the exception of May. Trends show the tendency of the peak occurring earlier in the year, from early summer to early spring, by three months at site S008, and by almost 6 months at site S003, however, the trends are not significant at 95% confidence level (Table 5.3). At site S001, the peaks have a tendency of occurring later, with a marked shift from winter to summer, and the trend is significant at 95% confidence level (Table 5.3). The moving average model shows different periodicities of the peaks, from two years at site S008 to two to four years at site S003 and around 5 years at site S001.

For sites S007 and S002 TSM minima can occur in any month of the year, with the exceptions of May and September, but they occur most often in December and January. The minima have a tendency of occurring earlier in the year, shifting from spring to winter at S007 and later by two months at S002, winter to early spring. These trends are only significant at 94 % and 84 % confidence level, respectively (Table 5.4). The moving average model fitted to the data shows a periodicity of the seasonality of minima changing every two to four years at site S007 and every four years at site S002.

At sites S008, S003 and S001 the minima can occur almost any month of the year, but less often during summer and late autumn (October-November). Trends show different tendencies. At site S008 the minima occur mostly from autumn to spring, with a shift of two months towards the winter. At site S003, the tendency of the minima is occurring later, with a shift of two months from winter to spring. At site S001, minima are occurring mostly during winter, with a tendency of occurring earlier, from spring to winter. However, none of these trends are significant at 95 % confidence level (Table 5.4). The moving average model fitted to the data shows a periodicity of the seasonality of minima changing every two to four years.

The periodicity of seasonality for maxima and minima of TSM changes every 2 to 4 years, which is much more variable and rapid than water and sediment discharges, for which

the seasonality changes every 10 years. This is an indication that the change is only partially controlled by the hydrological regime of the Danube.

Figure 5.5. Evolution in time of maximum TSM concentration, linear and moving average trends for the studied period, in each of the five locations

Table 5.3. Summary of statistical results of the linear regression, for the evolution of maximum TSM concentration in time

Site	**Statistical parameters**		
	R^2	**P value**	**Slope**
S007	0.0242	0.6537	0.1818
S002	0.1518	0.2397	0.3818
S008	0.0986	0.3410	-0.272
S003	0.1895	0.1775	-0.4636
S001	0.5175	0.0128	0.7727

Figure 5.6 Evolution in time of minimum TSM concentration, linear and moving average trends for the studied period, in each of the five locations

Table 5.4. Summary of statistical results of the linear regression, for the evolution of minimum TSM concentration in time

Site	**Statistical parameters**		
	R^2	**P value**	**Slope**
S007	0.3180	0.0695	-0.509
S002	0.2125	0.1562	0.2272
S008	0.082	0.3892	-0.2363
S003	0.0756	0.4175	0.2454
S001	0.069	0.4312	-0.2636

5.5.2.3. Time-series decomposition

The seasonal trend decomposition reveals different tendencies for the seasonal variations and trends for TSM concentration (Fig. 5.7). In most of the studied locations, both seasonal and trend component have different magnitudes and they are small compared to the variation in the data. At S007, S008 and S003 the magnitude of the seasonal component is greater than the magnitude of the trend. Also, the amplitude of the seasonal component changes around 2008 at S007, 2008 and 2010 at S008 and S003. At S002 and S001, the magnitude of trend component is the smallest, compared to the magnitude of trend or data and the amplitude of seasonal component does not change. The seasonal component shows a period of 4 months at sites S007, S008, S002 and S003 and of 3 months at site S001.

Trends are very similar in the delta front, at sites S007 and S002, with a peak of TSM concentration in 2005 and a gradual decrease afterwards. At the prodelta sites, the trends show a TSM peak around 2005 that seems to decrease in amplitude from north to south (S008 to S001), followed by a general decrease and another peak around 2010, which seems to increase in amplitude from south to north (from S001 to S008).

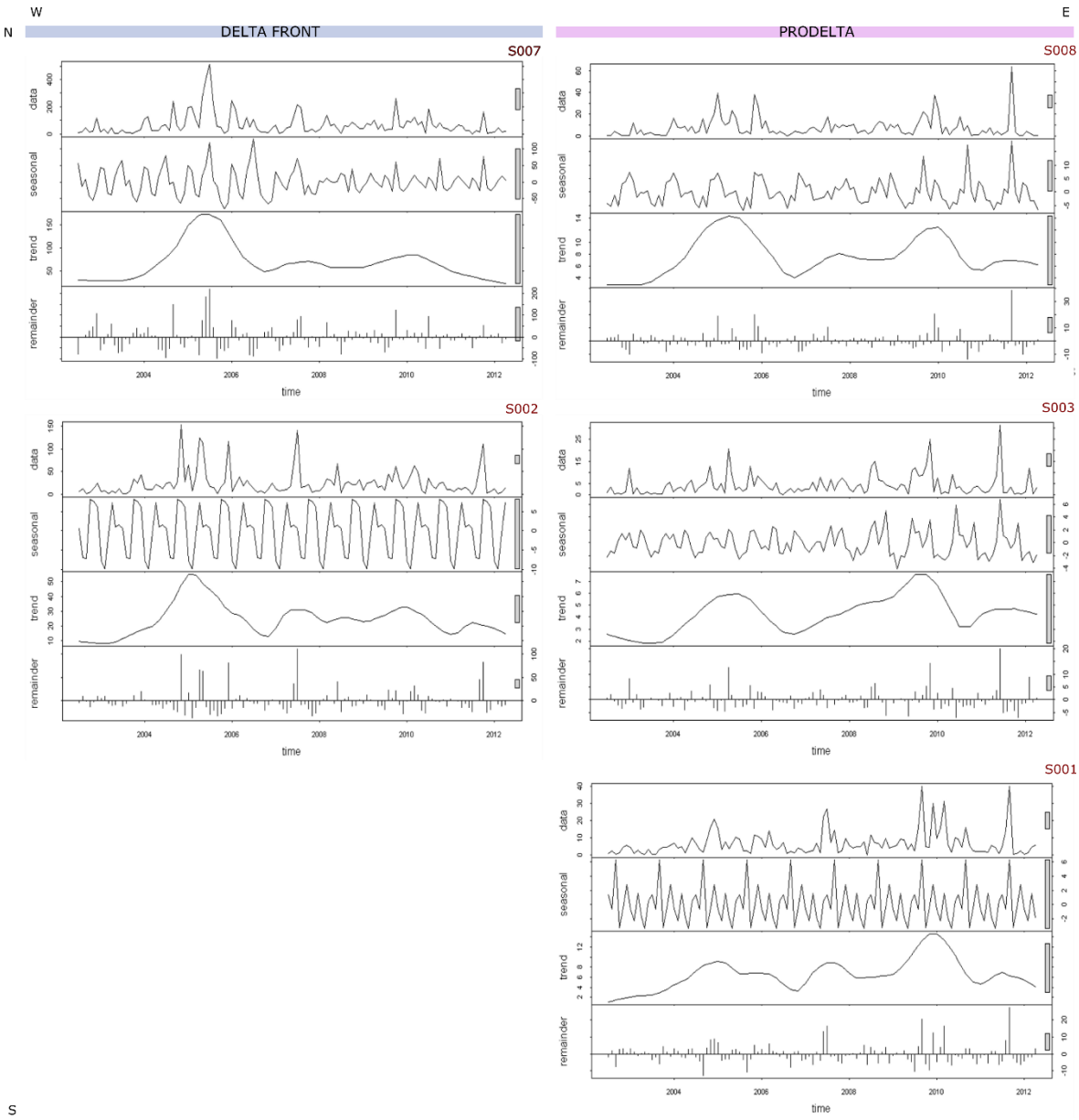

Figure 5.7. Seasonal trend decomposition (STL) analysis for satellite derived TSM data. The four panel represent the original data, the seasonal component, the trend and the remainder, for the analysed period of time (years on the horisontal axis) in the studied locations

5.5.2.4. Identifying breaks

The BFAST method was used to detect breaks in the TSM concentration trend. The results are shown below (Fig.5.8) Breakpoints were detected in the trend component of TSM concentration at sites S007, S002 and S008. At site S007 the first breakpoint, around 2004 marks a sharp increase in TSM and it is followed by another breakpoint at the end of 2005, which marks a sharp decrease. The breakpoint at site S002, from 2005 to mid-2006, marks the transition from an increasing to a decreasing trend. The breakpoint at site S008 starts in 2006 and ends in 2008, marking the change of trend from increasing to decreasing TSM concentration. There are no breakpoints at sites S003 and S001 and the trend is increasing.

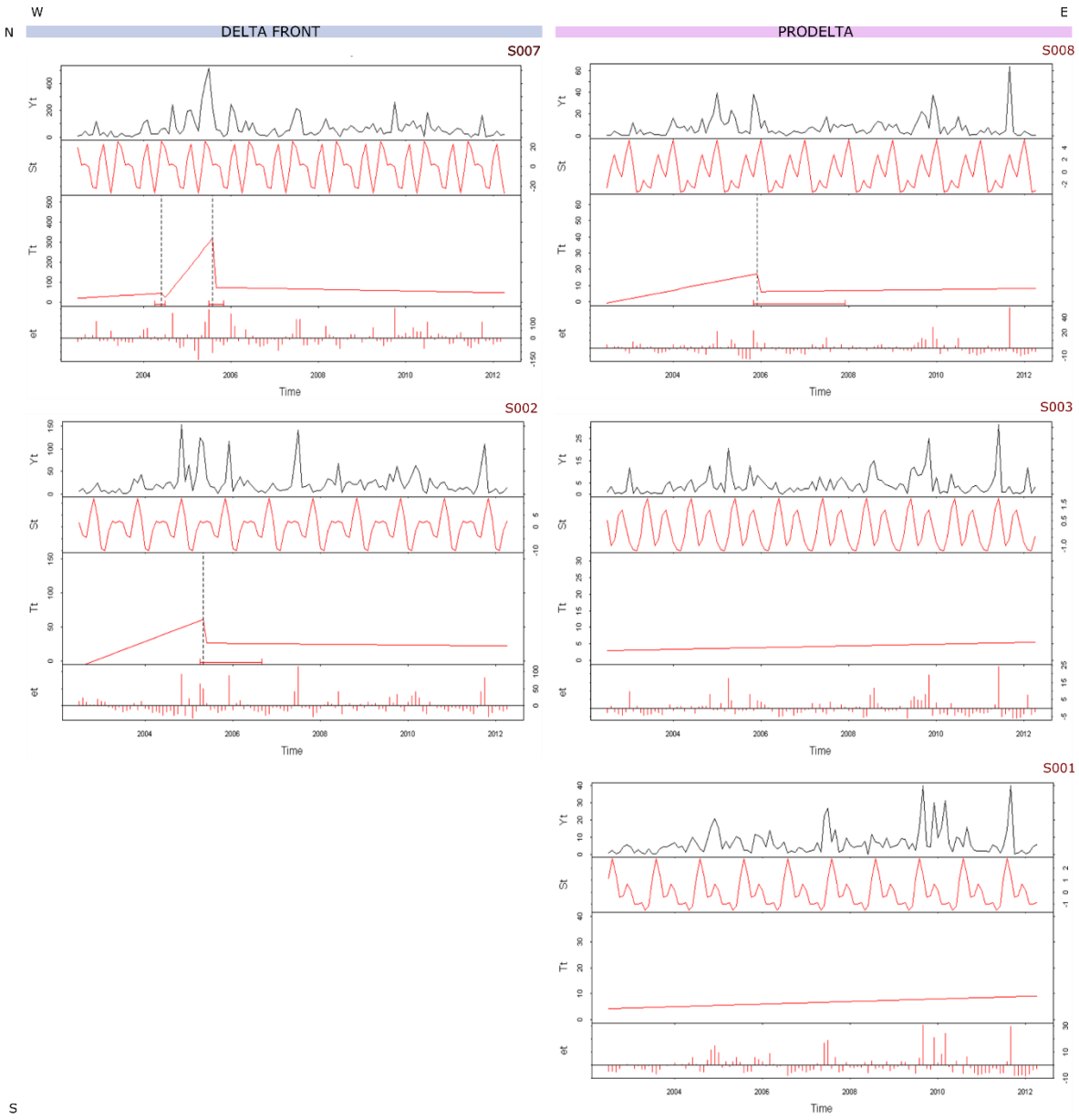

Figure 5.8 Breaks for Additive Seasonal and Trend for (BFAST) analysis for satellite-derived TSM data. The four panel represent the original data (Yt), the seasonal component (St), trend with break points (Tt) and remainder (et), in the studied period of time (years on the horizontal axis).

5.5.3. Chlorophyll-a

5.5.3.1. Linear trends

For the analysed time span, from July 2002 to April 2012, chl-a concentration data shows similar general trends at the analysed locations (Fig. 5.9). All sampled locations show an increase in chl-a over time. These trends are significant at 71 % confidence level for S007, ~90 % confidence level at S002 and S008, 94 % at S003 and 98 % confidence level at S001 (Table 5.5).

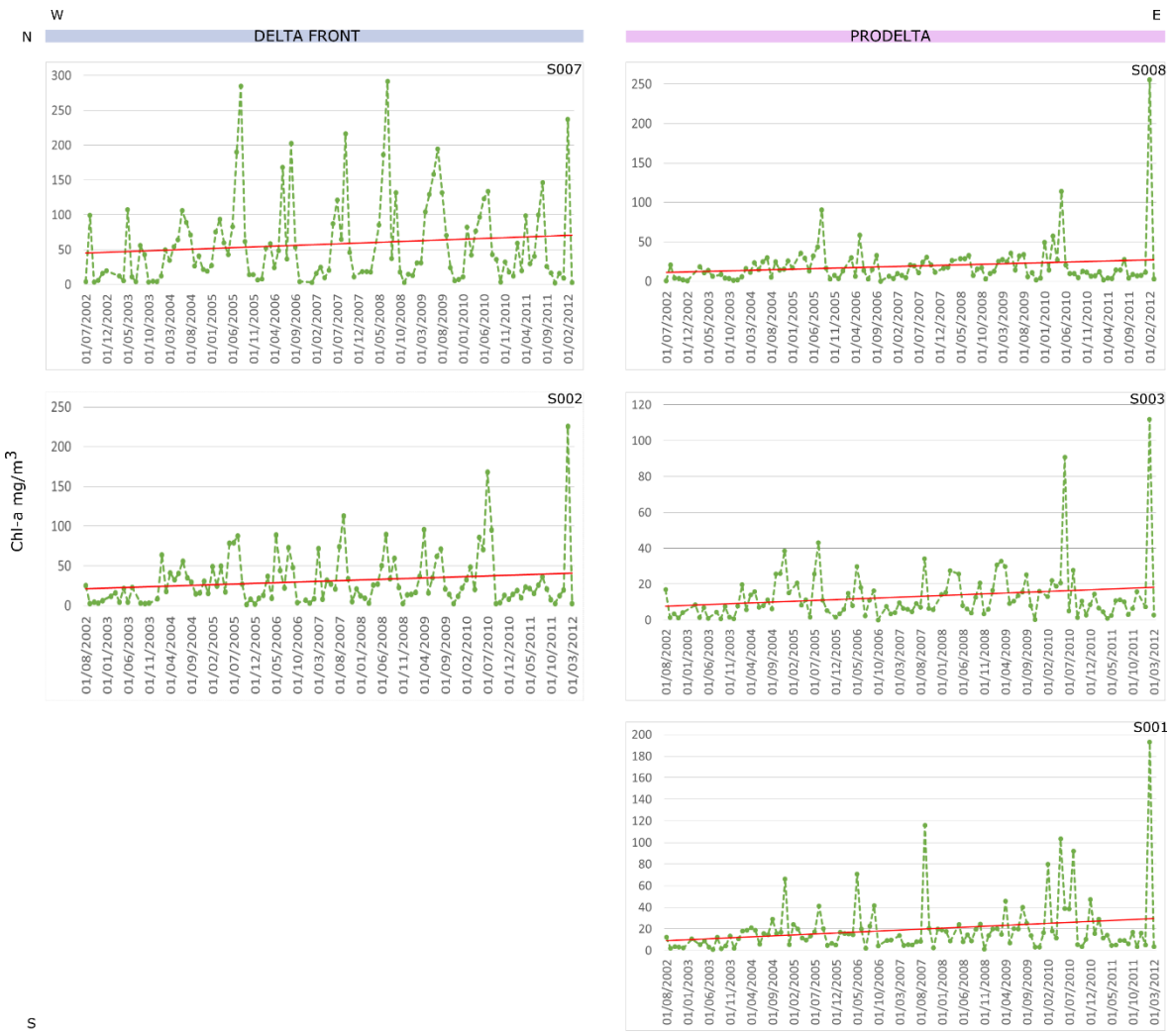

Figure 5.9 Satellite derived Chl-a concentration and linear trends at each of the five locations, for the analysed period

Table 5.5. Summary of statistical results of the linear regression, for chl-a concentration

Site	**Statistical parameters**		
	R^2	**P value**	**Slope**
S007	0.0159	0.286	0.0075
S002	0.0288	0.1207	0.0057
S008	0.0294	0.1078	0.0046
S003	0.0409	0.0622	0.0030
S001	0.0542	0.0233	0.0058

5.5.3.2. Evolution of maximum and minimum chl-a

The maximum and minimum monthly chl-a concentration values were plotted as a function of time, for the entire time span of the data sets (Figs. 5.10 and 5.11). This shows the seasonality of the yearly chl-a variations and also changes in time of the seasonality. The maxima and minima as a function of time are represented during a hydrological year, as it was defined in section 2.3.2.1 (Chapter 2). We have used the same temporal framework as for the

rivers and TSM concentration data, in order to compare with TSM data but also to have a common framework for seasonal changes. For all sites a linear and a moving average models were fitted to the data, in order to assess such changes.

For sites S007 and S002 chl-a maxima mostly occur in spring (March and May) or from June to October. They never occur in the winter time (November to February). The maxima have the tendency of occurring earlier in the year, with a shift of 2 months, from late summer to early summer. However, these trends are not significant at 95% confidence level (Table 5.6). The moving average model fitted to the data shows a periodicity of the seasonality changing every two years.

At sites S008 and S003 maxima occurs from February until November. Trends show the tendency of the maxima occurring earlier in the year, with a shift of two months, from late to early summer at site S008, and a shift of three months, from late to early spring at site S003. These trends are not significant at 95 % confidence level (Table 5.6). The moving average model fitted to the data shows a periodicity of the seasonality changing every two years.

Site S001 has a more particular character, maxima are not grouped seasonally as in the other sites, and they can occur in any season, with the exception of months February, April, July and August. The trend shows the tendency of the maximum chl-a concentration occurring later in the year, with a shift of two months, from early to late spring. The trend is not significant at 95 % confidence level (Table 5.6). The moving average model fitted to the data shows a periodicity of the seasonality changing every two years.

At sites S007 and S002 chl-a minima only occur from October to February, with one exception of Site S007, April in 2012. The trend shows a tendency of the minima occurring later in the winter, with a shift of two months at site S002 and three-four months at site S007. This trend is only significant at 94 % confidence level for S007 (Table 5.7). The moving average model shows a periodicity of the seasonality changing every four years at site S007 and every two-four years at site S002.

The chl-a minima at sites S008, S003 and S001 shows a more random distribution during the course of the year. They mostly occur from October until May at sites S008 and S003. At site S001 they occur from October to January but also in April and August. The trend shows no clear tendency of changing seasonality at site S008, a shift from early to late winter at site S008, similar to S007 and S002 and a reverse shift from late to early winter at site S001. None of these trends are significant at 95 % confidence level (Table 5.7). The moving average model shows a periodicity of the seasonality changing every two to four years.

Figure 5.10 Evolution in time of maximum chl-a concentration, linear and moving average trends for the studied period, in each of the five locations

Table 5.6. Summary of statistical results of the linear regression, for the evolution of maximum chl-a concentration in time

Site	**Statistical parameters**		
	R^2	**P value**	**Slope**
S007	0.0253	0.6303	-0.1636
S002	0.0315	0.5926	-0.1909
S008	0.0324	0.5871	-0.1818
S003	0.0756	0.4086	-0.3363
S001	0.0225	0.6648	0.1727

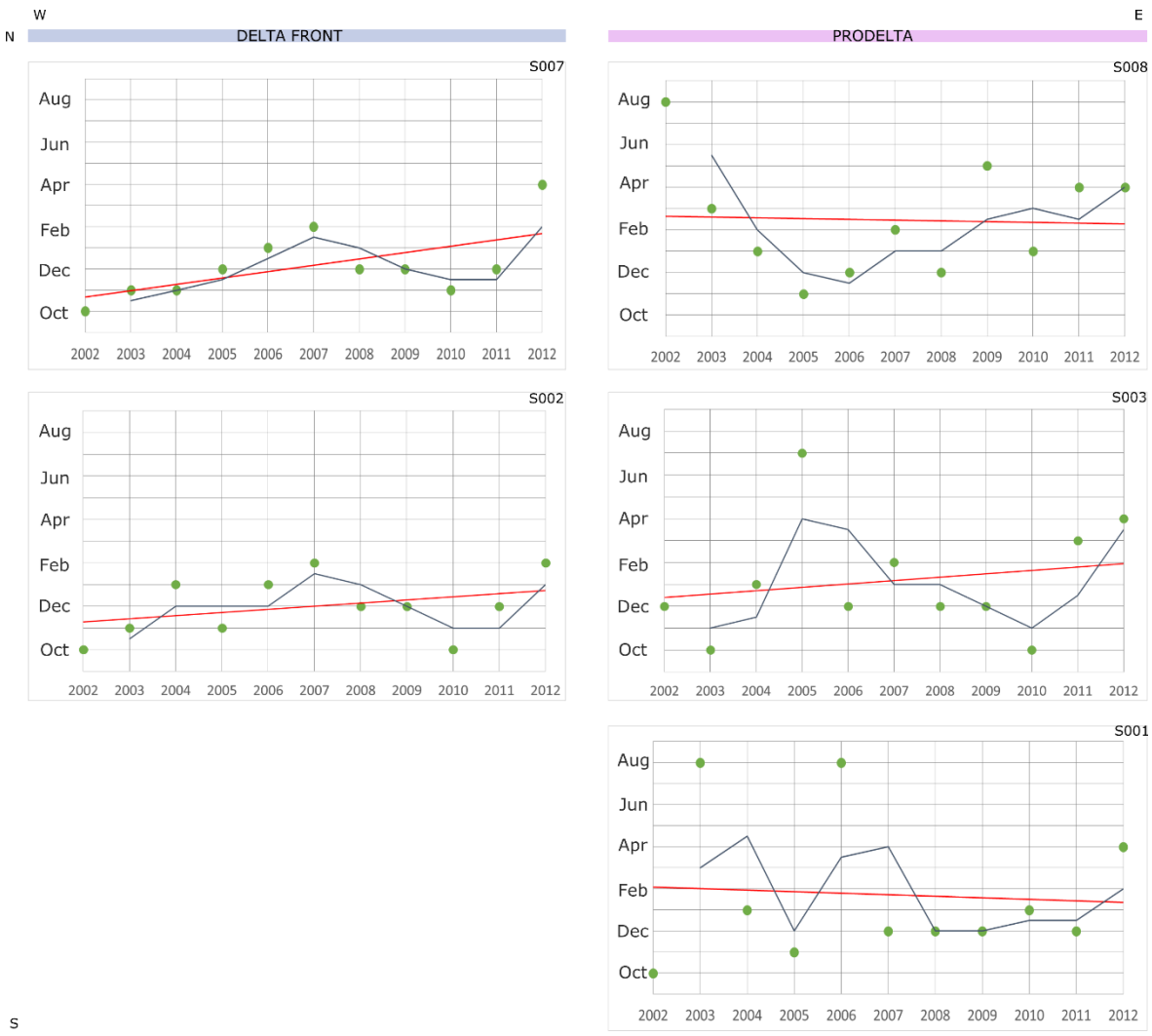

Figure 5.11 Evolution in time of minimum chl-a concentration, linear and moving average trends for the studied period, in each of the five locations

Table 5.7. Summary of statistical results of the linear regression, for the evolution of minimum chl-a concentration in time, in each of the five locations

Site	**Statistical parameters**		
	R^2	**P value**	**Slope**
S007	0.3582	0.0527	0.3
S002	0.1163	0.3093	0.1454
S008	0.0020	0.8868	-0.036
S003	0.0366	0.5777	0.1545
S001	0.0049	0.8324	-0.0727

5.5.3.3. Time series decomposition

The seasonal trend decomposition reveals different tendencies for the seasonal variations and trends for chl-a concentration (Fig. 5.12). In most of the studied locations, both seasonal and trend component have different magnitudes and they are small compared to the

variation in the data. Also, the magnitude of the seasonal component of chl-a (second panel in each figure) has a higher magnitude than the seasonal component of TSM.

The amplitude of the seasonal component changes every two years at site S007 and S002. The change in amplitude is similar at sites S008, S003 and S001, but less obvious. The seasonal component shows a period of 4 months at sites S007 and S002 and of 3 months at sites S008, S003 and S001.

At sites S007 and S002 the trend shows an increase in chl-a concentration over time, until 2010, and a general decrease afterwards. S002 shows a marked peak in the trend in 2010. Trends for S008 and S003 are very similar, with an increase in chl-a concentration from the beginning of the studied period, and a peak around 2005, followed by a decrease until 2007 and then another two peaks in 2010 and 2012. The trend of S001 is different from the other locations, with a general increase in chl-a concentration until 2010, marked by a peak and a general decrease afterwards.

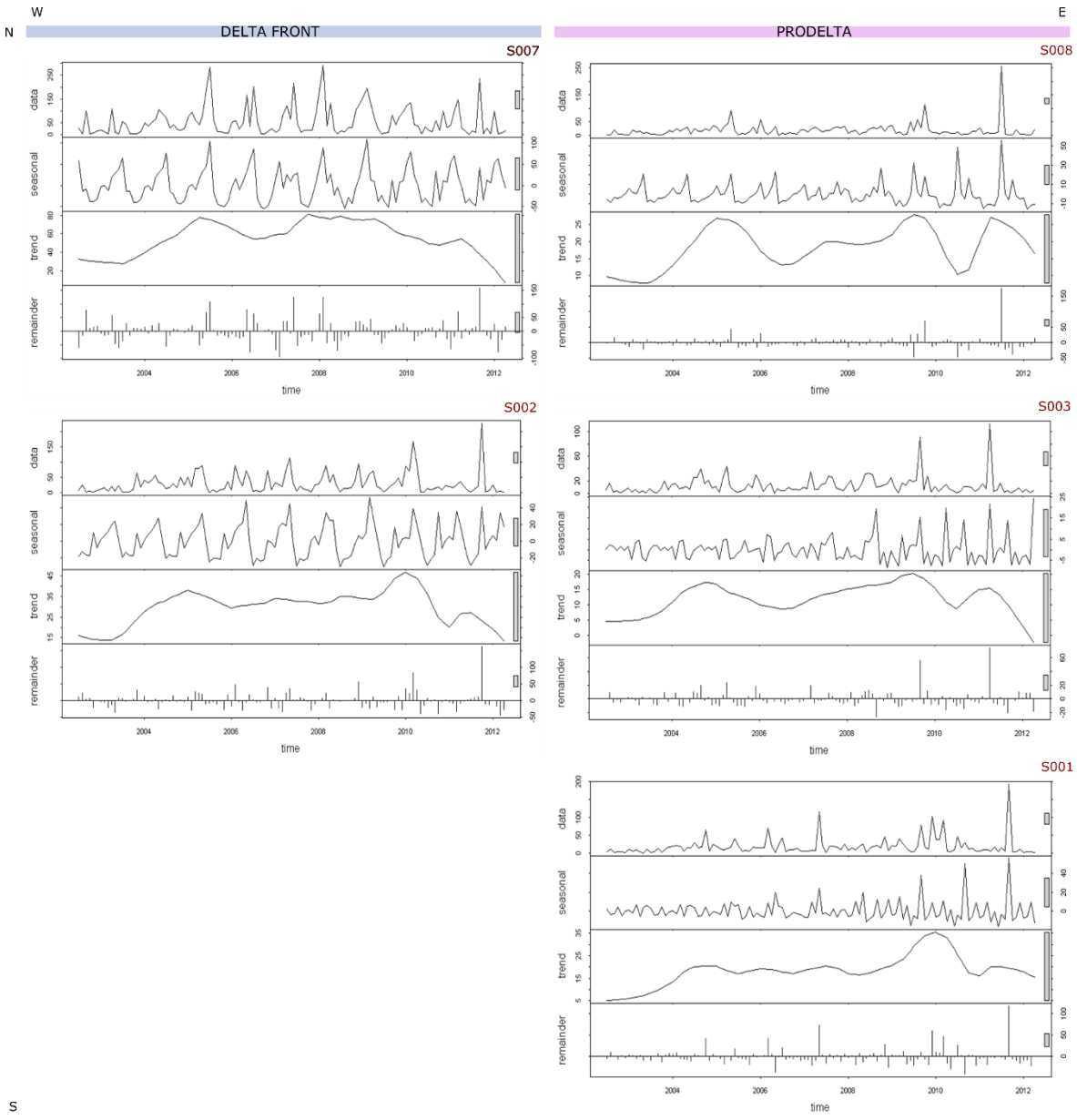

Figure 5.12 Seasonal trend decomposition (STL) analysis for satellite derived chl-a data. The four panel represent the original data, the seasonal component, the trend and the remainder, for the analysed period of time (years on the horisontal axis) in the studied locations

5.5.3.4. Identifying breaks

The BFAST method was used to detect breaks in the chl-a concentration trend. The results are shown below (Fig.5.13). No breaks were detected in the trend component of chl-a concentration in any of the studied locations. The trend only shows an increase in chl-a concentration over time.

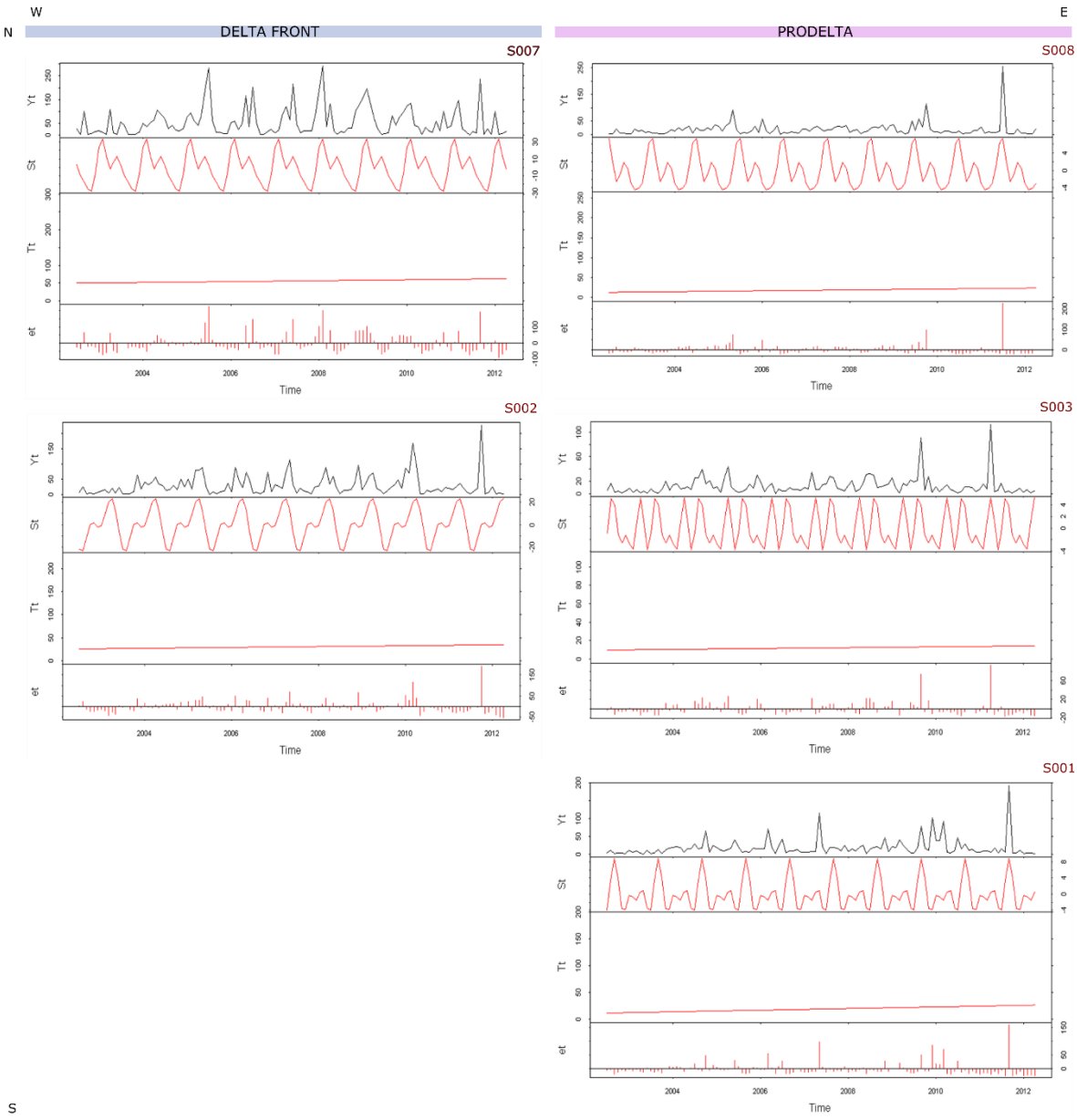

Figure 5.13 Breaks for Additive Seasonal and Trend for (BFAST) analysis for satellite-derived chl-a data. The four panel represent the original data (Yt), the seasonal component (St), trend with break points (Tt) and remainder (et), in the studied period of time (years on the horizontal axis).

5.5.4. Comparison to water and suspended sediment discharge

Total Suspended Matter (TSM), also called Particulate Suspended Matter (SPM) or Total Suspended Solids (TSS) is defined as the net weight of material collected on a GF/F by sea water filtration. It comprises the non-dissolved particles, of any origin, present at a certain time in water. Satellite derived TSM has been used previously to trace and quantify sediment fluxes (e.g. Doxaran et al., 2009; Gohin, 2011), including delineating river plumes (Gangloff et al., 2017).

This study uses monthly products of the Envisat MERIS CoastColour archive (2002-2012) to explore seasonality and evolution in time of TSM and chl-a concentrations in front of

the Danube Delta, on the NW Black Sea shelf. The ultimate aim of this study is to link sedimentation processes that happen in the delta front and prodelta area of the Danube (Chapter 3) with the distribution of sediment fluxes measured in the water column (Chapter 4) and observed (Chapter 5) at the surface.

One of the main challenges of such an approach is obtaining in-situ data for the period of the MERIS CoastColour Archive, as mentioned before. Therefore, the control of the hydrologivcal regime of the Danube on the TSM values was examined. The TSM data obtained from satellite data at site S007 was compared with the water discharge and the suspended sediment concentration data, measured in the port of Sulina, for the period of 2002-2010.

The correlation plots show low correlation (Fig. 5.12) for water discharge (r=0.3515) and suspended sediment concentration (r=0.34418).

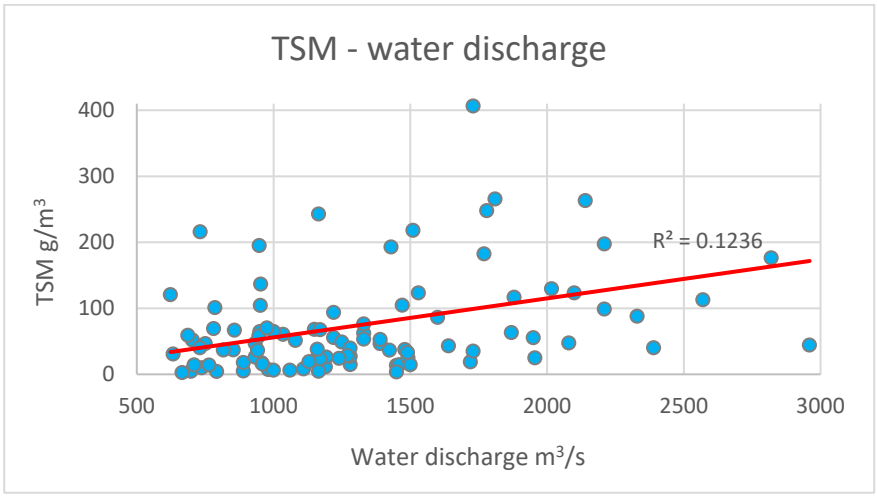

a.

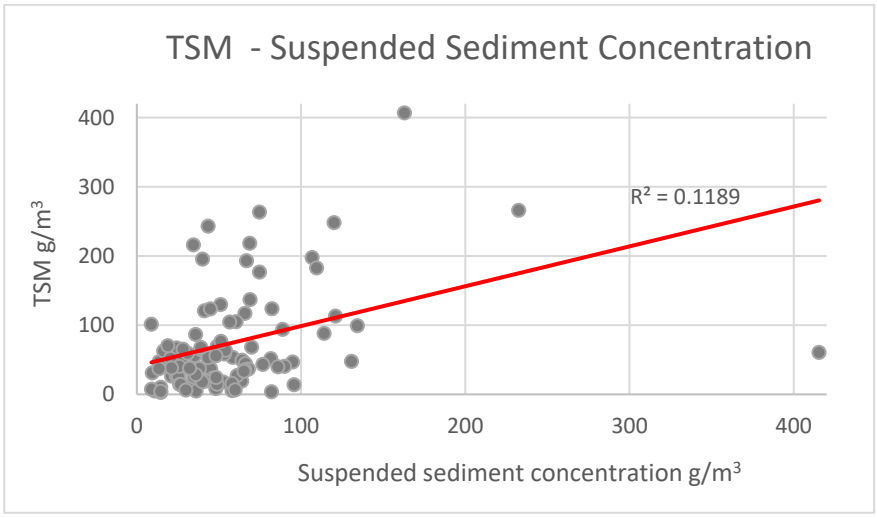

b.

Figure 5.14. Correlation plots of satellite derived TSM and a) water discharge and b) suspended sediment discharge

This correlation shows that in this case, TSM varies less with the variation in sediment concentration and more with water discharge. Previous studies in this area have identified as main controllers of turbidity, river discharge, wind speed and direction and sediment re-suspension (Constantin et al., 2017; Güttler et al., 2013; Karageorgis et al., 2009). As also seen in the seasonality of maxima and minima of both TSM and chla- concentrations, TSM values are only partially controlled the hydrological regime of the river and partially by the amount of other in-situ water constituents, like phyto or zooplankton, as shown in Chapter 4, for the NW Black Sea. The lack of in-situ chl-a data makes the assessment of the results very difficult.

5.5.5. Sentinel 3 data

The data derived from the OLCI-Sentinel 3 image shows different patterns for TSM and chl-a concentrations in the NW of the Black Sea. TSM variation follows the development of the two plumes of the Danube in the coastal zone, while chl-a variation is more evenly distributed between the N and the S areas of the Danube Delta coast. This image which was acquired during low intensity, northerly wind, shows the Danube plume forming in a 15 km distance from the coast and moving southward.

The same scale of variation as for the MERIS is given for both TSM and chl-a, for comparison. In this case, TSM ranges from 0.05 to 50 g/m^3 and chl-a from 0 to 13 mg/m^3. The comparison between the satellite derived TSM and chl-a and the in-situ measurements shows a good match, R^2=0.8098 for TSM and R^2=0.6182 for chl-a, even if the in-situ data was measured up to 6 days prior to the satellite overpass. The same hydrological and climatic conditions prevailed during the cruise. The water discharge of the Danube was at an annual average level, there were no precipitations, calm northerly winds prevailed (average speed <10 m/s), creating very small waves in the Black Sea. This shows that instant patterns of both satellite derived TSM and chl-a do not change much in stable atmospheric and hydrological conditions.

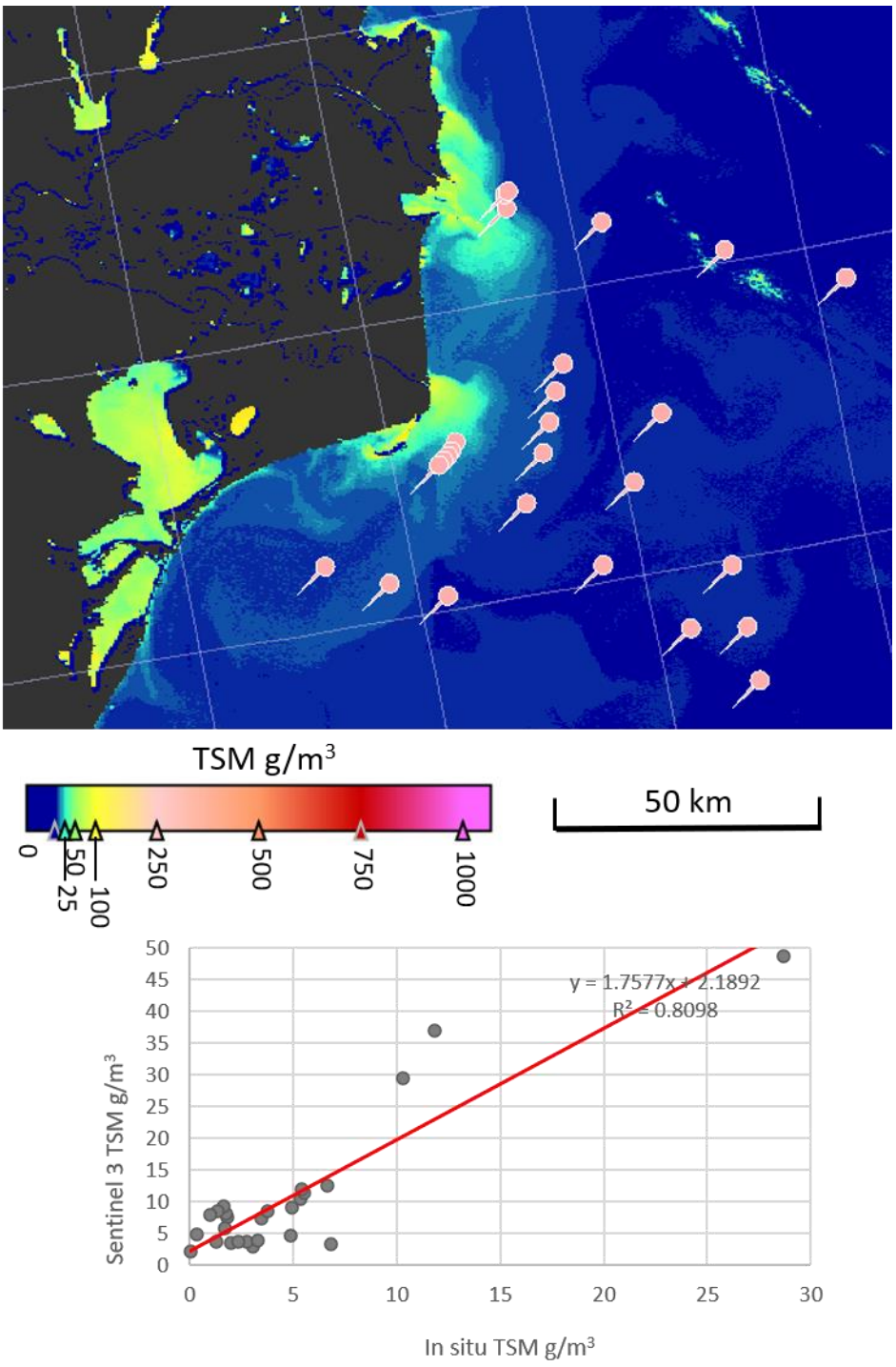

Figure 5.15 TSM variation obtained from OLCI-Sentinel 3, for the 11th of May 2016, and validation with in-situ data; 26 match-up field stations were used for validation, sampling was carried out from the 6th to 12th of May

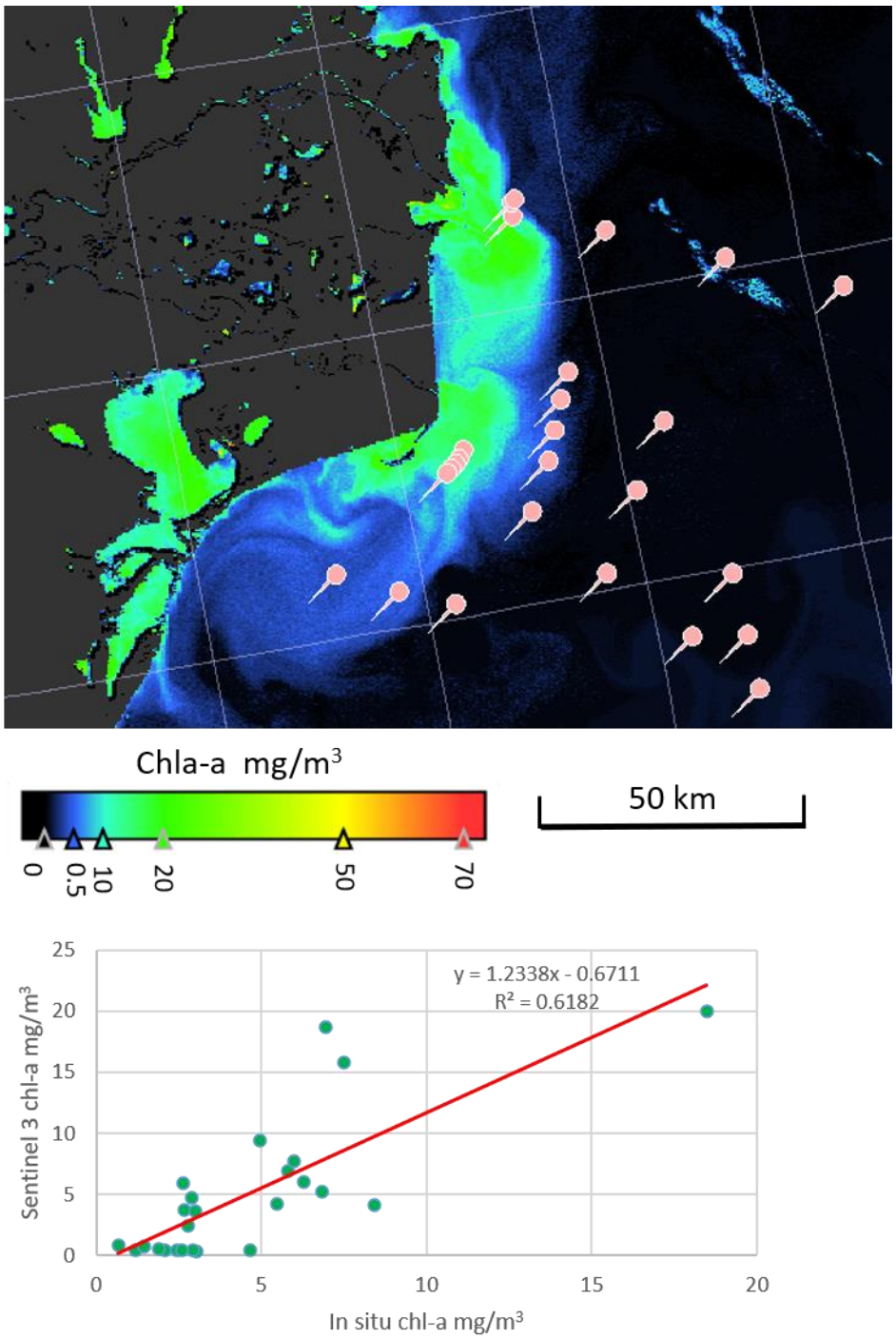

Figure 5.16 Chl-a variation obtained from OLCI-Sentinel 3, for the 11th of May 2016, and validation with in-situ data; 26 match-up field stations were used for validation, sampling was carried out from the 6th to 12th of May

5.6. DISCUSSION

5.6.1. Satellite data

The satellite data used for this study describes well the variation of both TSM and chl-a in the coastal waters of the NW Black Sea. Calibration and validation, especially for the MERIS CoastColour data, is challenging in the Black Sea, due to the lack of in-situ data. While the absolute value may not be accurate, the relative variation describes seasonal patterns, which can be linked to hydrological events, such as floods, or to in-situ seasonal variations in primary productivity of the coastal waters (Constantin et al., 2016; Güttler et al., 2013).

Parameters like water and suspended sediment discharge are routinely monitored in fixed station along rivers, only providing point data. The satellite data allows for tracking and assessing changes of these parameters on larger and more complex areas, such as deltas and coastal waters (e.g. Gangloff et al., 2017), as also shown in this study. The new Sentinel missions, launched by the European Space Agency, and especially Sentinel 2 and 3 provide new opportunities for improving the study of coastal areas from space (e.g. Petus et al., 2019; Tarpanelli et al., 2019). The results of this study show a much better match-up of the TSM and chl-a satellite derived data with the in-situ data, collected for the NW Black Sea area.

While the retrieval of water constituents is still challenging in complex environments, some definite steps are taken for a better classification of water types, based on remote sensing parameters, in order to better tune already existing algorithms (Spyrakos et al., 2018). This work is carried forward in a H2020 project, CERTO - Copernicus Evolution: Research for harmonised Transitional water Observation), which aims to address the lack of harmonisation in producing water quality data over the so-called ‘transitional environments’: deltas, estuaries, coastal lagoons and coastal waters.

5.6.2. Variation of TSM and chl-a concentrations. Relation between satellite-derived parameters and sediment fluxes and patterns

5.6.2.1. Seasonal and spatial variation

This chapter links the spatial distribution of TSM and chl-a with sediment fluxes variations retrieved from sedimentary cores (Chapter 3) and describes the seasonal patterns in relation to the variation of both water and suspended sediment discharge of the Danube river (Chapter 2).

Generally, TSM variations patterns show the formation of two distinct plumes of the Danube, one in the north, formed by Chilia and Sulina, and one in the south, formed by Sfantu Gheorghe, with different extents. Bajo et al. (2014) found that the waters of Chilia are prevalent in the north, while Sulina has a smaller contribution to the plume and the waters of Sf. Gheorghe

remain confined to the coast, around the Sahalin spit. Figures 5.1 and 5.15 support these results, in different seasons and during different meteorological conditions. The extent of plumes varies with the Danube water and sediment discharge and wind conditions (Constantin et al., 2017; Güttler et al., 2013).

The variation of Chl-a depends on several factors, generally, on nutrient input brought by the rivers and partially on the extension of the plume offshore, decreasing W to E, but the N to S variation is different. Our study indicate Chlia and Sulina discharge area (S007) as the one with the highest chl-a values, however, previous studies (Karageorgis et al., 2014; Vasiliu et al., 2010) have found the maximum chl-a concentration south of Sahalin (S001).

Both TSM and chl-a concentrations vary during the analysed period of 10 years at the study sites and in between sites. In the delta front area, there is an apparent decrease of TSM at site S007 and an increase at site S002. TSM also increases in the prodelta area, with a more significant increase in the south, at site S001. Chl-a concentration increases in time in all studied sites, with the most significant increase at site S001. The highest overall values of both TSM and chl-a concentrations from this study are found in the northern plume, at site S007. This was also observed from in-situ measurements during a week's campaign in 2016 (Chapter 4).

In the previous chapter we have shown how TSM and ISM can vary in the same way in the surface waters of the NW Black Sea, as well as in depth. We have also shown how the concentration of suspended particles, rather than the size, is a better indicator of higher sediment concentration.

More variation in the TSM trend of the Sfantu Gheorghe branch may be determined by the flow regime, which happens in natural conditions. The area of distribution of water and suspended solids is larger than for the Sulina branch, which is channelized, also, the hydrological conditions of the flow are different. A higher water discharge, lower hydrological slope, scouring and erosion of the river bed, as well as the dynamic conditions of the mixing of the Sfantu Gheorghe branch into the Black Sea, could lead to more rapid and random variations of TSM.

The southern tip of the plume, at site S001 is the furthest away from the direct supply of sediment so the increase in TSM is probably just an effect of the increase in concentration of other water constituents like phyto or zooplankton (also noticed in the increase of chkl-a concentration).

The timing of both the lowest and the highest TSM and chl-a concentrations change in the studied period, at the 5 sites, even if not significantly. The overall evolution of TSM

concentration in the delta front area depends on the hydrological regime of the Danube, for both water and suspended sediment discharge, showing the control of the river inputs on this parameter. In the prodelta area, the variation of both maximum and minimum TSM concentration is very similar with the variation of chl-a concentration, the months of the maximum and minimum coinciding in several years. The distribution of chl-a on the Black Sea shelf, in front of the Danube mouths, may also depend on variations of water discharge (Vasiliu et al., 2010) in certain cases.

The seasonal component for chl-a concentrations has a higher amplitude than the one of TSM. The period of variation of the seasonal component is of 3 or 4 months for chl-a and of 4 months for TSM, compared to 11 months for suspended sediment discharge and 12 months for water discharge of the Danube. This shows the contribution of the seasonal evolution of other water constituents (e.g. phyto or zoo-plankton) to TSM concentration, even in the areas closer to the Danube mouths.

The 2005 peak of TSM and chl-a also coincides with a peak of suspended sediment discharge of the Danube. The superposed effects may have caused the break point in the TSM concentrations at sites S007, S002 and S008, which is marked by an important increase of TSM concentration. This coincides with the exceptional floods of the years 2005-2006, with three flood peaks from February to July 2006 in the Lower Danube area, marking the 100 years (return period) flood peak (GeoEcoMar, unpublished data). The northern plume, at site S007, which has the most marked TSM breakpoints, coinciding with the 2005-2006 floods, also records these floods in a marked peak of sediment accumulation rate (SAR, Chapter3), calculated for the sedimentary core at the same location. The difference in magnitude of the breakpoints between the northern and southern plume (S007 and S002) may be explained by 1) 70 % of water and sediment are carried by the northern plume, comprising both Chilia and Sulina 2) Site S007 is reflecting the effect of the channelling of the middle branch, Sulina, restricting the area of its depocentre (see Chapter 3 for evolution of sedimentary patterns in this area).

5.6.2.2. Linking variation of TSM and chl-a concentration and sediment patterns

The distribution TSM concentration data at the studied sites, for the analysed period of time, does not generally match the sedimentary patterns identified in Chapter 3. The general trends of the TSM concentration at the studies locations show a slight increase, with the exception of S007, in the northern plume, which is characterised by a slight decrease. The sediment data shows a decrease in the sediment accumulation rate in most sites, with the exception of site S007. However, the general evolution of TSM concentration at this site is

similar to the evolution of suspended sediment concentration, measured in the port of Sulina, which is marked by a general decrease (Chapter 2). The length in time of the TSM concentration is probably not enough to establish a definite trend of variation. The data acquired by other satellite missions, like the Sentinel 3 – OLCI, can be used to cover the time gap and to identify trends and spatial variations in concentrations of water constituents.

This study is a first attempt to characterise sediment fluxes and dynamics in the NW Black Sea, using satellite-derived TSM and chl-a. Further work is needed, especially on calibrating and validating satellite data with in-situ data which is representative, both in time and space for dynamic systems with optically complex waters (Tyler et al., 2016; Zibordi et al., 2014).

So far, the main challenge lies in the fact that, in the NW Black Sea and especially, in the coastal area of the Danube Delta, the turbid plumes extents in the same area with the maximum primary productivity (Güttler et al., 2013). Most studies, so far, have linked TSM concentration with dynamics and plume extension (Güttler et al., 2013; Karageorgis et al., 2009) but not enough with sedimentation patterns. A recent study (Constantin et al., 2017) shows promising results linking turbidity with sedimentation patterns in the coastal area of the Danube Delta, where higher turbidity correlates well with coarser deposits, like sands and silty sands, while lower turbidity correlates with clay. The also find that it is mostly sediment contributing to higher turbidity, either from the Danube plumes or resuspension, especially in the delta front area. We can assume that the same factors act on TSM values, which is also shown by the results of this study.

5.7. CONCLUSIONS

This study relates concentration of water constituents retrieved from satellite data with sedimentary patterns in the NW Black Sea. The comparison and assessment are only possible to a certain extent. At this point, it is still difficult to say if TSM can be used directly to assess sedimentation patterns. In Chapter 2 we have shown that the method used to measure TSM in-situ underestimates the coarser fraction of sediment (which, in some cases, can range from silt to sand), which makes up for the bulk of deposited sediment in the studied area. However, satellite derived TSM and chl-a concentrations offer a useful tool for studying change. We have shown how extreme events, such as exceptional floods, are easy to trace in the variation of TSM concentration.

6. GENERAL DISCUSSION

6.1. INTRODUCTION

This chapter brings together the main findings of this thesis and puts them into a wider context of research and draws out the new insights into the Danube - Black Sea interaction zone.

The research undertaken for this thesis aimed first to understand sediment flux characteristics and changes in the Danube Delta and the Black Sea region, taking account of both long- (century) and short-term (seasonal and recent) change. During the time of this research, several aspects, in both data availability, monitoring methods, approaches and the use of results of research in general, were revealed as limited, incomplete or fragmented.

This thesis builds on work already undertaken in the project Horizon 2020 DANUBIUS-PP (DANUBIUS-RI Preparatory Phase), and feeds into the forthcoming work programme of H2020 CERTO (Copernicus Evolution: Research for harmonized Transitional water Observation) project.

The main challenges in managing river – sea systems, and in this case, the Danube – Black Sea System is the fragmentation between land, transitional areas, such as deltas and coastal regions, as well as the open sea, in terms of methodologies, variables used for monitoring, accessible data and management policies implemented across the system. The complex and sensitive part of the system, the delta and coastal area, is the repository for the changes in the upstream river catchment and is very vulnerable to subtle changes in climate, hydrology and geomorphology (Bianchi and Allison, 2009; Maselli and Trincardi, 2013; Renaud et al., 2013).

Our work had the following four main objectives:

1. *To understand how changes in the river basin (land use changes, dams and reservoirs, climate change) affect sediment fluxes of the Danube and some of the European rivers.* This was addressed in Chapter 2.
2. *To quantify the decrease in sediment flux of the Danube on the delta and the Black Sea shelf.* This was addressed in Chapter 3.
3. *To describe the spatial and temporal characteristics of the sediment flux in the Danube-Black Sea interaction zone.* This was addressed in Chapters 4, 5 and 6.

4. *To assess the relationship between the short-term phenomena and the long-term evolution of the Danube-Black Sea interaction zone.* This was addressed in Chapter 3 and 4 and it is addressed in the present Chapter.

6.2. LONG- AND SHORT-TERM DEVELOPMENTS IN SEDIMENTATION PATTERNS

6.2.1 Evolution of sediment flux and main factors of change

Even though it is considered that human induces changes in river basins, mostly through agricultural activities and land use, have modified sediment budgets of rivers and consequently, evolutions of river – sea transitional areas, such as deltas, for centuries, it is changes that have occurred in the last 50 years that have brought more dramatic impacts (Syvitski et al., 2005b). Extensive scientific literature shows the effect of dams on diminishing sediment loads of rivers in several systems across the world (e.g. Day et al., 2016; Panin and Jipa, 2002; Syvitski and Kettner, 2007; Wang et al., 2007; Xeidakis et al., 2010). The main effects are seen notably in the terminal areas of rivers, such as deltas or estuaries – coastal erosion, habitat loss and groundwater salinization, just to name the most obvious.

Deltas, estuaries and marshes are situated in the terminal areas of river basins, right between the land and the sea; they concentrate an important part of the world resources, being hot spots for ecosystem services: food and energy production, touristic activities, water supply, etc. The main pressures on these areas result from: local activities, local hydrotechnical interventions, climate change (especially extreme events such as flood and storms) and changes in water and sediment fluxes which feed them and support their ecosystems (Giosan et al., 2014; Palmer et al., 2008).

The results of Chapter 2 of this research show changes in both water and suspended sediment of seven European rivers, recorded in their terminal areas, either deltas (Danube, Nestos, Po and Ebro) or estuaries (Elbe, Thames and Tay). The results show that changes depend on: the size of the catchment, the degree of the sensitivity of the river basin to climate changes, the number and placement of the dams in the catchment, the natural variability of the hydrological cycle in a year. Our results show that potentially Mediterranean rivers are the most sensitive to changes in precipitation patterns, while large, complex basins, such as the Danube encompass a wider range of climate change effects. It is important to point out that from all the five rivers analysed (Danube, Elbe, Ebro, Thames and Tay) for suspended solids, all showed a significant ($p<0.05$) general decrease of suspended solids over the time periods for which data was available. Previous studies have estimated a reduction of suspended sediment arriving in the Danube Delta, of about 50-70 % (McCarney-Castle et al., 2011; Panin and Jipa,

2002), caused by the input of over 80 dams and reservoirs along the Danube (Habersack et al., 2016), among which Iron Gate I and II having the highest impact. The amount of the coarser fraction, medium to coarse sand (125 to 500 μm), is considered to be the same, even after the input of dams (Panin and Jipa, 2002), as the river regains much of the sediment in its lower reaches, due to riverbed scouring and contribution of the tributaries (Bondar, 2008).

The 90 years of data of both water and suspended sediment discharge for the Danube provide an appropriate data sets to identify the effects of dams on this major river. Dams have been also identified in this research as the main factor of decrease in suspended sediment. The data analysed for the Danube is measured on the Sulina branch, which was cut and deepened for navigation, resulting in an increase of both water and sediment flow on this branch from 7 to 20 % at the current time. It is clear that this increase due to anthropic intervention has not masked the effect of the dams in any way. Apart from a trend of increasing water flow on Sulina, the results helped identify several effects caused by the input of the two major dams along the Lower Danube: they attenuate natural variability of both water and suspended sediment discharge and they cause breaks, marked by a decrease in both water (only apparent or instant) and suspended sediment discharge. It is for the first time that evidence from time series data show more than one impact of the dams on the sediment discharge of the Danube into the Black Sea.

The analysis of the seven European rivers has shown the value of long-term monitoring of environmental parameters for identifying environmental change drivers while the lack of data makes the assessment and comparison very difficult.

6.2.2 Effects of reduced sediment delivery to the Danube Delta and the Black Sea shelf

In large and complex systems, such as the Danube Delta – NW Black Sea area, the changes in sediment load have led to increased costal erosion, as the most notable effect (Panin and Jipa, 2002; Stănică et al., 2007; Stănică and Panin, 2009). Chapter 3 of this thesis shows, for the first time, a more complete picture of these effects, across several environments: lakes, channels, lagoons, the delta front and prodelta area.

The life and evolution of the Danube Delta depends on the water and sediment flux of the Danube River. Overall, the degree of connectivity to the main hydrological network of the delta determines the evolution of sedimentation patterns. Extreme hydrological events, such as the major floods of the last century can only be traced in certain areas – larger channels, lagoons and delta front, which are directly connected to the main hydrologic network, represented by the three discharging branches.

As expected, the impact of the decrease in sedimentation rate post-dams is not evenly distributed across all environments of the delta. Within the cores sampled from the lakes, the decrease is of 30-50 %, whilst cores suggest an increase to 5-15 % in the terminal lagoons. This has broadly led to an estimated overall decrease of sediment flux in the Danube Delta of 45%. From the analysed cores, two channels in the Sfantu Gheorghe secondary delta and the northern area of the Sahalin lagoon shows an increase of sedimentation rates, after the input of dams, of 4 to 14 %, but this effect is very localized, marking the recent evolution of this particular area, rather than a general trend.

The general decrease in sedimentation is even greater in the delta front area of between 46-55 %. This contrasts with a relative increase in sedimentation rate in the Sulina area by 43 % and a marked decrease in the Sfantu Gheorghe delta front area. Results of a recent study shows that the Sfantu Gheorghe depocenter is temporary and an important part of the sediments deposited during floods are removed during storms and transported southward (Zăinescu et al., 2019). The decrease in the prodelta is of 62%, and unevenly distributed, with a strong decrease of almost 95 % in the eastern part and only 35 % in the southern area. This shows that most of the sediment carried by the Danube plume outside the delta front is transported southerward.

The overall reduction in sediment flux reaching the Danube Delta complex does not produce major changes in the distribution of depocentres. The changes are mainly represented by a decrease of sedimentation rate, while the general evolution of the delta stays the same. Both Sfantu Gheorghe and Chilia deltas remain the most active. The results of this research show only one value for the Chilia delta (core DNMU15 in the Musura lagoon), and considering the location of the sampling site, the reduction in sedimentation rate might be overestimated. The Sfantu Gheorghe delta shows an increase in sedimentation rate in the Sahalin lagoon, on the secondary channels and the area which receives their sediment supply.

Even if the Sulina discharge area records an increase in sedimentation rates, the overall value remains at least 7 times lower than the value measured for Sf. Gheorghe. This relative increase is a combined effect of the channelling of water and sediment by the Sulina jetties and a contribution from the discharging arm of Chilia.

The Sulina jetties are not the only local disturbance to change distribution of sediment flux. The canals, such as Ciotica, which were initially cut from the beginning of the 20th century to around 1980's, for access, fishing and reed harvesting (Oosterberg et al., 2000), are now clogging. The clogging of smaller channels decreases sedimentation rates locally, and the aggradation process, while increasing sediment concentration in the main channels. Smaller

channels become clogged, they either behave like lakes if there's still enough water (e.g Mahmudia meander on Sfantu Gheorghe) or they gradually fill with macrophytes – especially *Phragmitres australis*, the common reed, the most common emergent vegetation in the Danube Delta (Rudescu, 1965) (e.g. Canal Ciotica). Meander cutting on both Sulina and Sfantu Gheorghe had as main effect an increase of water and sediment flux in the main channel, while the old meanders remained elevated and partially disconnected from the main flow, dramatically enhancing deposition in these area (Jugaru Tiron et al., 2009). The poor circulation of water and sediment in these areas is adding to the poor general circulation of channels and canals, as these meanders are connected to the delta plain – to the lakes and channels or canals, being part of the main conveyor of water and sediment before the cutting. While this is a general observation for the Danube Delta, it is clear, from the results of this research, that even major hydrological events (e.g. the major, 100 years flood of 2006) are not clearly identifiable in the sediments of the delta lakes.

By examining sedimentary rates across different environments of the Danube Delta complex, this research estimates a trapping efficiency of 63% (pre-dams) and 60% (post-dams). This means that this percentage of sediment brought by the Danube in this area is deposited in the sub-aerial delta, delta front and prodelta area. The trapping efficiency of the sub-aerial delta plain is estimated at 54 % pre-dams and 52 % post dams. This is comparable to calculations performed for other river deltas around the world (e.g. 50 % trapping efficiency of the Asian rivers; Liu et al., 2009) but slightly higher.

The small difference between the trapping efficiencies pre- and post-dams may be caused by the changes in management practices in the Danube Delta, before and post-communist era (year 1989), rather than the magnitude of sediment flux. From the beginning of the 90's the Danube Delta has become a biosphere reserve, through a decision of Romania. Since then, strictly protected areas have been delineated and a policy of minimum intervention has been applied, which led to a decrease in water and sediment discharge inside the delta plain. Oher factors have to be considered as well. For example, the contribution of organic matter as sediment supply or the active role of vegetation (especially the species that provide important quantities of biomass in interactions with water and sediment fluxes, such as reed beds) in sediment dynamics are not well understood presently in the Danube Delta. The results of Chapter 4, particularly the distribution of suspended particles size in the Danube delta and the Black Sea indicate that presently, more water and sediment is transferred directly into the Black Sea, than previously thought, thus questioning the role of filtering of the delta.

On the coast, the Chlia and Sfantu Gheorghe secondary deltas remain the active depocentres, while region between Sulina and Sfantu Gheorghe is eroding. The increase in

sedimentation rate in front of the Sulina jetties reflects the local anthropic changes on the Sulina channel. In both of the active depocentres flood pulses are well recorded. The main difference of these two areas, in the near shore domain, is that while on Sulina, most of the water and sediment is channelled between the jetties, while the Sfantu Gheorghe branch flows in fairly natural conditions and feeds a secondary delta, on a much wider area than the Sulina depocentre. The main consequence is that most of the sediment on Sulina is taken out of the coastal circulation (Stănică et al., 2007), and most of the sediment of the northern plume is being trapped north from the jetties, resulting in an erosive trend of the coastal strip between Sulina and Sfantu Gheorghe, while the sediment carried by Sfantu Gheorghe branch is kept closer to the coast, feeding the Sahalin lagoon and a small area south of it (Giosan et al., 2013). The formation and extension of the Sfantu Gheorghe plume is well described in the results of Chapter 5.

6.2.3 Short-term changes in properties of suspended sediment

The results of Chapter 3 of this research show how the supply of sediment and grain size in the different environments of the Danube Delta vary depending on the hydrological connectivity with the main branches. As shown in Chapter 4, largely, suspended sediment patterns follow the same distribution. Concentration of suspended particles, rather than size is a better indicator of higher sedimentation rates, in most environments, in the delta and on the continental shelf.

In Chapter 4, the data show how the variation in the concentration of suspended matter (expressed as TSM, chl-a, particle size and distribution in this research) in different environments of the delta, depend largely on the natural variations of the river, and the degree of connectivity to the main branches. Thus, the main channels concentrate the bulk flux of the coarser particles, and their concentration decreases in lakes. Wind induced resuspension in shallow areas such as the Sahalin lagoon can increase TSM values especially, even in periods of low water discharge.

It is important to mention again that some areas in the lagoons, as well as the partially disconnected meanders behave like lakes in terms of the composition and concentration of suspended particles present in water, because of low water circulation. A recently noticed phenomenon in the Danube Delta is the early increase of water temperature in the spring season and a higher mean temperature in summer (Kovbasko et al., 2014). In these environments especially, the low water circulation, coupled with the increase in water temperature leads to regional anoxia, which has a potential negative impact on the life cycle of both flora and fauna.

The results in Chapter 3 show that Sfantu Gheorghe was a much more active depocentre than Sulina, yet sedimentation rates are very similar for both the northern and the southern areas of the delta front, for the recent years. The research has also shown that the prodelta area is still receiving some sediment. Most of the previous studies on suspended particles in this area asses that most of the sediment discharged by the Danube is being deposited in the close proximity of the discharging mouths (Karageorgis et al., 2014) and that most of the suspended sediment coming out of the delta is confined to a narrow area in the coastal zone, not reaching much of the prodelta area (Karageorgis et al., 2014, 2009). The sedimentation rates obtained from the analysed cores confirm, to a certain degree, this conclusion, with the exception of the southern part of the prodelta, where this research shows that the values of recent years remain relatively high. The sedimentation rates calculated for the eastern part of the prodelta are situated not further than ~30 km offshore, and so, closer to the highest concentration of the suspended sediment. Further east, lower sedimentation rates could be expected, as most of the terrigenous material does not reach this area, unless in exceptional conditions (low, onshore wind regime, very high river discharge).

The results of Chapter 5 show patterns of the Danube plume in the coastal area, with a norther plume, formed by Chilia and Sulina in the north and a southern plume, formed by Sfantu Gheorghe. These two plumes can be decoupled sometimes, following different orientations. However, the relatively higher deposition rates in the southern part of the prodelta show that more sediment is transported here rather than eastward, in closer proximity to the Danube mouths. This is also the case for several other delta complexes, located on high- or moderate-energy continental shelves, several studies of suspended-sediment transport indicate a stronger transport and deposition along the continental shelf, with only a minor component across-shelf e.g. Mekong, Yangtze, Amazon, Po, Ebro, Eel, Columbia, (Liu et al., 2009; Wright and Nittrouer, 1995; Driscoll and Karner, 1999; Cattaneo et al., 2004).

6.3. DATA NEEDS, LIMITATIONS AND REQUIREMENTS

During the work undertaken for this thesis, the need of reliable time series data for several parameters was obvious. Hence water and suspended sediment discharge for the Danube and for each branch, in situ measured water parameters used with Earth Observation data (TSM, Chl-a), especially for the Black Sea area were hard to find. All these parameters are necessary for a better understanding of the sediment flux distribution and change in the Danube Delta and the Black Sea area.

Generally, data is inconsistent in:

a) Methodological approach. TSM, TSS or suspended sediment data can be measured to express the amount of suspended loads carried by a river. Suspended sediment is one of the most commonly and routinely measure parameter in river-sea systems, alongside TSM (Total Suspended Matter) or TSS (Total Suspended Solids), for sediment management practices and scientific studies. However, it does not always provide a clear picture of the sediment distribution and dynamics, especially in complex areas, such as deltas. Bed load, as additional parameter, is not currently measured because it is difficult to measure, at best (Milliman and Farnsworth, 2011). A comparison between suspended sediment and TSS reveals that TSS underestimates the coarser fraction, usually sand (Gray et al., 2000; Qizhong (George) Guo, 2006), approach which might not be suitable in the case of the Danube. This research confirms this conclusion. However, TSS or TSM are used in conjunction with satellite data, easily obtainable and useful for mapping large areas (e.g. Tyler et al., 2016).

b) Time. Time series data is available at certain location in a river basin but it can lack completely in others. In certain river basin parameters such as suspended sediment is not routinely measured or only point measurements are available. This is a problem especially in river basins with major anthropic interventions, such as dams, which have a marked effect on sediment flux. Data measured before and after the input of dams, flood embankments, etc give indications about the magnitude and timing of changes in sediment flux, as well as about the possible solutions.

c) Space. The sediment flux carried by a river varies on longitudinal and lateral scales within a basin, as well as in depth (bed load, suspended sediment load or TSM). Most measurements fail to capture this variation at basin scale and even on smaller areas such as deltas, estuaries, coastal lagoons or coastal seas.

Routinely monitoring and assessing sediment fluxes in a river – sea continuum is vital for sediment management practices, for sediment sufficiency and dredging activities, as well as for mitigating their effects (coastal erosion and habitat loss, ‘mudding the waters’ and their effect on aquatic fauna and flora) (H2020 DANUBIUS-PP Consortium, 2019). This should include mapping and understanding deposition and erosion patterns, general circulation of water and sediment in channels, canal, lakes and lagoons.

The results of this research show how reliable data sets are crucial for understanding both long term and short-term phenomena which affect the sediment flux in a river-sea interaction zone.

6.4. METHODS DEVELOPMENT FROM IN-SITU TO EARTH OBSERVATION, CONSISTENCY, STANDARDS, PROTOCOLS, COMPLEXITY OF THE OPTICAL PROPERTIES, OPTICAL WATER TYPES

Previous studies of the Danube Delta and the NW Black Sea shelf have used different parameters to investigate suspended sediment patterns: turbidity (Constantin et al., 2017, 2016; Güttler et al., 2013), concentration of particulate matter and particle size and distribution, related to optical properties (Karageorgis et al., 2014, 2009).

The findings from the research on particle size and composition brought new insights into the properties of sediment flux, together with TSM, ISM and chl-a distribution. Our results show that concentration of suspended particles, rather than size is a better indicator of higher sedimentation rates, in most environments, in the delta and continental shelf.

Our results show also that, even if the used parameters add important information for the ecological status of aquatic environments, they are not enough to describe and map sediment fluxes. In such complex systems as the Danube-Black Sea area, these parameters can vary very rapidly in both time and space, especially in areas like shallow, large lakes and lagoons, and the coastal zone.

Both nature and concentration of suspended particles, as well as the distribution of sizes in surface waters contribute to variations of optical properties which are retrievable from satellite data. This is relevant to several recent studies which are classifying both inland and coastal water types based on their optical properties (Neil et al., 2019; Spyrakos et al., 2018).

Earth Observation data (from both ESA MERIS CoastColour archive and ESA Sentinel 3 – OLCI) is used in this research to describe and map the variation of both TSM and chl-a in the coastal waters of the NW Black Sea. Calibration and validation, especially for the MERIS CoastColour data, is challenging in the Black Sea, due to the lack of in-situ data. The comparison with existing in situ data call into question the calibration viability associated with these EO products. However, while the absolute value may not be accurate, the relative variation in concentrations should still provide valuable insights into describing the phenology of events and patters, which can be linked to hydrological events, such as floods and droughts, or to in-situ seasonal variations in primary productivity of the coastal waters.

Parameters like water and suspended sediment discharge are routinely monitored in fixed station along rivers, but they only provide point data. Satellite data allows for tracking and assessing changes over larger and more complex areas, such as deltas and coastal waters, as shown in this research.

While the retrieval of water constituents is still challenging in complex environments, some definite steps need to be taken to deliver a better framework for the applications of validated algorithms for these dynamic and complex environments. The classification of these optically complex waters into optical water types, based on remote sensing reflectance provides a robust framework for deployment of an assemble of algorithms for EO (Spyrakos et al., 2018). By tuning algorithms to specific relevant optical water types (Neil et al., 2019), more accurate in water constituent retrieval can be achieved, as applied in lake environments within the GloboLakes project. This work is now being taken forward through the Horizon 2020 project, CERTO - Copernicus Evolution: Research for harmonised Transitional water Observation), which aims to address the lack of harmonisation in producing water quality data over the so-called 'transitional environments: deltas, estuaries, coastal lagoons and coastal waters. To date, the separation between inland and oceanic water bodies still exists in remote sensing studies and applications, due to the lack of suitable sensors and regional processing algorithms for optically complex waters (H2020 CERTO proposal).

6.5. THE FUTURE – IMPLICATIONS FOR MANAGEMENT OF RIVER-SEA SYSTEMS

Sediment and soil management is a key priority in many river-sea systems around the world, and it is related to several of the UN Development Goals, such as 15 Life on land, 14 Life below water, 6 Clean water and sanitation and 13 Climate action. Sediment is an intricate part of river-sea systems. Both its quality and quantity play an important role in maintaining a good water quality status for rivers, deltas, estuaries and coastal areas. There is a need for integration of both strategies and methodologies for maintaining a good quality and quantity of water at basin level, from the headwaters to the coastal sea, as emphasised by the Water Framework Directive.

The variations in sediment supply, which is the main focus of this research, for the terminal areas of river-sea systems determines both short and long-term effects on the evolution of these environments. All the analysed river-sea systems in this research show disturbances in their water and sediment discharge, mainly due to human activities in the catchment and some of them show obvious effects of climate change.

An improved management plan for deltas and coastal areas of river-sea systems should take into account the overall water and sediment supply; the overall sediment distribution in relation to hydrological connectivity; the effects of climate change on the seasonality of both water and sediment discharge and the impact of extreme events; the role of vegetation in sediment trapping and attenuating erosion; the effect of so-called 'filter' of deltas.

Many studies on river-sea systems around the world (Falkenmark et al., 2019; Palmer et al., 2008; Syvitski et al., 2009), as well as the results of the present study show that the more engineered and controlled river basins and transitional areas are, the more they are sensitive to adverse effects – degradation of habitats and loss of biodiversity, erosion, low buffering of extreme events like floods or droughts.

Longitudinal, lateral, vertical and time connectivity are a pre-requisite for healthy river-sea systems (H2020 DANUBIUS-PP, 2019). Globally, source-to-sea connections have been lost in 77% of very long rivers (>1,000 km), including the Danube, and in 54% of long rivers (500–1,000 km) (Grill et al., 2019). The need to address the loss of connectivity and improve management of transitional areas, in particular, is recognized globally (e.g. Giosan et al., 2014). The results of the present study show how water and sediment fluxes vary longitudinally, laterally and in time, in a heavily managed delta (Renaud et al., 2013) and they can contribute to a better management of water and sediment fluxes in deltas around the world.

Lateral connectivity is very important for both aggradation and progradation of deltas, and, in the case of the Danube Delta, it may be attenuated by natural processes - silting and vegetation growth. Maintaining longitudinal connectivity of the river, and not enough of the lateral connectivity, as it is the case in the Danube Delta - dredging on the main Danube branches and not of the lateral channels and canals, may cause environmental disturbances in adjacent meanders, as it is shown in our results. Lakes, lagoons or meanders becoming disconnected from the main hydrographical network or the sea, may lead to local eutrophication and hypoxia, with adverse effects on medium- and long-term. This process also decreases the role of 'physical filter' of the delta and the aggradation process in the sub-aerial delta, conveying more of the sediment in the coastal zone, where it is reworked by waves and dispersed by coastal currents.

One key aspect which is not being discussed in detail about the Danube Delta is the change of policies on delta management and exploitation, from the 19th century, when Sulina channel was opened for maritime navigation, to the 'policy on non-intervention' of the last 30 years. The main periods for intensive anthropic interventions in the delta were: the beginning

of the 20th century, with cutting and dredging of several canals; the embankment of Sulina, but which was gradual, as it took over 100 years (from 1860 to present day) for this channel to reach 20 % of water and sediment discharge of the Danube; the period of 1950-1990 with several interventions – creating polders for agriculture and cutting of numerous canals; 1980's for the cutting of the meanders of Sfantu Gheorghe (see section 1.2.3. for a detailed description). This fragmentation in time of interventions and policies may have allowed the delta to have more time to adapt to changes, while the decrease in sediment flux happened gradually, over 20 years, as it is also shown by the variation in sediment accumulation rates over several environments, presented here. Allowing deltas and wetlands time to adjust to anthropic environmental and climate change may prove to be a better solution and less costly, especially on mid and long-term (Palmer et al., 2008). However, we consider that, even if the effects of sediment depletion are not as dangerous in the Danube Delta, as in other deltas, this is the time to reconsider the monitoring and management strategies in this area.

Re-establishing a higher sediment supply in deltas and estuaries to compensate for the general loss, may be proven more difficult, however. At the moment, dams are recognized as the main trapping system for sediment, with adverse consequences on the river bed and evolution of transitional areas – deltas, estuaries, coastal lagoons (e.g. Latrubesse et al., 2017; Wu et al., 2020), and their numbers will only increase in the future (Zarfl et al., 2014). One solution may be dam-removal, to increase connectivity at the scale of river basins (Magilligan et al., 2016) and to potentially restore coastal habitats (Warrick et al., 2015).

While the role of an adequate supply of sediment, and especially sand, is a pre-requisite for maintaining deltas above se-level rise, some other strategies can enhance sediment deposition and stability of deltas and coastal area. Maintaining coastal wetlands and the role of vegetation in decreasing erosion has been proven efficient in mitigating the effects of storm surges and even tsunamis (Gedan et al., 2011; Kourafalou and Stanev, 2001; Temmerman et al., 2013; van Wesenbeeck et al., 2017), increasing the stability of shores in deltas and estuaries.

The results of this research show, once more, the importance of understanding water and sediment fluxes at the scale of river-sea systems, and considering all acting factors for improved management strategies.

7. CONCLUSIONS

This research assesses the change of sediment flux from the Danube Delta into the Black Sea for the last century, under the influence of dams and climate change.

The long-term patterns are assessed through time series analysis of 90 years of both water and suspended sediment discharge data, measured in the port of Sulina; radiogenic dating of sediment cores and grain size analysis. It is for the first time that sediment cores from such a wide range of environments of the Danube Delta are used to quantify the effect of the reduction of sediment fluxes in this area. It is also for the first time that sedimentation rates are produced for the Danube delta front and prodelta, on such a large scale.

The short-term patterns are described through analysis of water constituents, retrieved from both satellite data or in-situ, suspended particle size and composition, analysis of time series TSM and chl-a concentration, retrieved from satellite data. It is for the first time that an investigation on the size and composition of suspended particles from both surface water and in-depth profiles is done on such a wide area.

In addition, the research compares, for the first time, changes in both water and suspended sediment discharge of another 6 European rivers: Nestos, Po, Ebro, Elbe, Thames, Tay. For all the analysed rivers, changes in trends of both water and suspended solids were identified. These changes depend on: the size of the catchment, the degree of the sensitivity of the river basin to climate changes, the number and placement of the dams in the catchment, the natural variability of the hydrological cycle in a year.

Some of the controls of the changes need further investigation. Apart from the obvious effects of coastal erosion, other potential effects are not yet well described in the terminal areas of the analysed rivers. While it is easier to quantify long-term changes in water and suspended solids pre and post dam input, the understanding of seasonal changes, under different climate change scenarios, need a more refined temporal and spatial investigation.

For the Danube River, the major dams in the catchment (Iron Gate I and II) determine both a general reduction of overall sediment flux and a decrease in magnitude of water and sediment peaks. The main identified effect of climate change is a change in the seasonality of the hydrological regime of the river, with early spring peaks.

Based on the last century evolution of the Danube-Black Sea interaction zone, a reduction of sediment flux is estimated, of around 46% for the delta, 46-55% for the delta front area and of 62% for the prodelta.

The impact over the various environments of the delta – lakes, channels and lagoons, delta front and prodelta are different. The overall reduction in sediment flux does not produce major changes in the depocentre in the delta or the shelf areas. The changes are mainly represented by a decrease of sedimentation rate, while the general evolution stays the same. This is mainly controlled by the degree of connectivity to the main branches or by local anthropic interventions in the area. The changes of water and sediment flux on the Sulina channel and a channeling effect of the jetties increase sediment supply in this area of the delta front. The extreme hydrological events, such as the major floods of the last century can only be traced in certain areas – bigger channels, lagoons and delta front, which are directly connected to the main hydrologic network, represented by the three discharging branches.

Largely, suspended sediment patterns follow the same distribution. For assessing sediment flux from measurements of suspended sediments alone, particle size and composition bring additional information. Suspended particles tend to have larger sizes along the main channels, as well as on the delta front. The equal amount of larger particle sizes in the channels and the delta front may indicate that more water and sediment is transferred directly into the Black Sea, than previously thought, thus questioning the role of filtering of the delta. For the other environments, such as lakes or the prodelta, there is a much smaller amount of sediment input but there is a significant amount of particles of coarser sizes of biogenic origin.

The present research improves greatly our understanding on the effect of reduction of sediment fluxes in the Danube – Black Sea interaction zone. The effects are identified both on a long-term scale (one century) and on a short-term scale (seasonal variations). The results of this research could be used for a better management of the Danube Delta and its coastal zone, whilst also providing evidence for those responsible for changes occurring within the catchment on the likely consequences of their interventions. This has the potential for improving land use and remediation practices and contributing to future development of methodologies for monitoring environmental changes not only in this area, but also in other similar environments around the world.

8. ANNEXES

8.1. ANNEX 1. R CODE FOR THE STATISTICAL ANALYSIS, EXAMPLE FOR THE DANUBE RIVER

```
#River data analysis water Adriana 20/09/2017

# clear R of all objects

rm(list=ls())

#set work space

setwd ("D:/Data analysis/River data")

#create monthly averages for all files if not already done

#Convert to date if not already

#df1$X1 <- as.Date(df1$X1)

#  Get months

#df1$Month <- months(df1$X1)

#  Get years

#df1$Year <- format(df1$X1,format="%y")

#  Aggregate 'X2' on months and year and get mean

#aggregate( X2 ~ Month + Year , df1 , mean )

#calculate monthly averages

dat$month <- months(dat$date)

dat$year <- format(dat$date, format="%Y")

mean<-aggregate( Discharge1 ~ month + year , dat , mean)

#export dat

write.csv(mean, file='Elba mean.csv')

#quick plot of the entire data set

#names(df1)

#plot(df1[,2], type="l",lwd=2, col="red", xlab="date", ylab="water discharge")

#plot


.libPaths() # get library location
```

```
library()   # see all packages installed
search()    # see packages currently loaded
#load packages
library(bfast)
library(zoo)
library(forecast)
library(xts)
#import dataset
d1 <- read.csv("Danube_water_discharge.csv", header=TRUE, sep=",")
#create ts for sediment data
water <- ts(d1$Water,start=c(1921,1),end=c(2010,12),deltat=1/12)
#quick plots of data
plot(water)
abline(h=mean(d1$Water), col='Red', lwd=2)
#decomposition using stl
fit1<-stl(water, s.window="periodic")
plot(fit1)
monthplot(fit1)
#decomposition using bfast
fit3 <- bfast(water, h=0.13, season="harmonic", max.iter = 10)
plot(fit3)
plot(fit3,type="all")
fit3$output[[2]]$St
#find month of annual peak
#format date using xts
d2 <- as.xts(sediment)
from <- as.Date("1921-01-01")
to <- as.Date("2010-12-01")
myDates <- seq.Date(from=from,to=to,by="month")
```

```
#split data by calender year
myList <- tapply(d2, format(myDates, "%Y"), c)
#plot a given year
plot(myList$`1921`)
#find the date of the sediment peak
sedmax <- do.call(rbind, lapply(split(d2,"years"), function(x) x[which.max(x)]))
sedmax <- data.frame(date=index(sedmax), coredata(sedmax))
#convert to Julian day and bind data
tmp <- as.POSIXlt(sedmax$date, format = "%d%b%y")
years <- seq.Date(from=as.Date("1921","%Y"), to=as.Date("2010","%Y"), by="year")
sedmax <- cbind(sedmax,tmp$yday, years
#plot data and fit linear and lowess models
plot(sedmax$years, sedmax$`tmp$yday`,
    ylab="Day of Year",
    xlab="Time")
mod1 <- lm(sedmax$`tmp$yday` ~ sedmax$years)
summary(mod1)
abline(mod1)
lines(lowess(sedmax$years, sedmax$`tmp$yday`, f=0.2), col="red")
```

8.2. ANNEX 2. LOCATIONS OF SAMPLED POINTS IN CHAPTER 4

Point ID	Month/Year	Location
Danube Delta		
Lakes		
DN006	July 2015	Lake Matita
DN007	July 2015	Lake Matita
DN011	July 2015	Lake Rosu
DN012	July 2015	Lake Rosu
DN013	July 2015	Lake Rosu
DN014	July 2015	Lake Rosu
DN031	May 2016	Lake Fortuna
DN032	May 2016	Lake Matita
DN033	May 2016	Lake Matita
DN034	May 2016	Lake Matita
DN035	May 2016	Lake Matita
DN042	May 2016	Lake Rosulet
DN043	May 2016	Lake Rosulet

DN044	May 2016	Lake Rosu
DN045	May 2016	Lake Rosu
DN046	May 2016	Lake Rosu
DN047	May 2016	Lake Rosu
DN048	May 2016	Lake Rosu
Channels/canals		
DN001	July 2015	Sfantu Gheorghe branch
DN002	July 2015	Tulcea branch
DN003	July 2015	Sulina branch
DN004	July 2015	Sulina branch Crisan
DN005	July 2015	Sulina branch Old Danube
DN008	July 2015	Sulina branch Old Danube
DN009	July 2015	Sulina branch Old Danube
DN010	July 2015	Canal Magistral
DN017	July 2015	Sfantu Gheorghe branch, Mahmudia meander
DN018	August 2015	Sfantu Gheorghe branch Dunavatul de Sus
DN019	August 2015	Sfantu Gheorghe branch
DN021	August 2015	Garla Turcului
DN022	August 2015	Canal Ciotica
DN023	August 2015	Sfantu Gheorghe branch mouth
DN026	May 2016	Tulcea branch
DN027	May 2016	Sulina branch Partizani
DN028	May 2016	Sulina branch Old Danube Mile 23
DN029	May 2016	Sontea Channel
DN030	May 2016	Sontea Channel
DN036	May 2016	Sulina branch Crisan
DN054	May 2016	Sfantu Gheorghe branch mouth
DN055	May 2016	Sfantu Gheorghe branch mouth
DN056	May 2016	Sfantu Gheorghe branch mouth
DN057	May 2016	Sfantu Gheorghe branch Dunavat
DN077	June 2016	Sfantu Gheorghe branch Dunavatul de Sus
DN078	June 2016	Sfantu Gheorghe branch Mahmudia meander
DN079	June 2016	Sfantu Gheorghe branch Ceatal
Lagoons		
DN015	July 2015	Musura Lagoon
DN016	July 2015	Musura Lagoon
DN020	August 2015	Musura Lagoon
DN024	August 2015	Sahalin Lagoon north
DN025	August 2015	Sahalin Lagoon centre
DN037	May 2016	Musura Lagoon
DN038	May 2016	Musura Lagoon
DN039	May 2016	Musura Lagoon
DN040	May 2016	Musura Lagoon
DN041	May 2016	Musura Lagoon
DN049	May 2016	Sahalin Lagoon
DN050	May 2016	Sahalin Lagoon
DN051	May 2016	Sahalin Lagoon
DN052	May 2016	Sahalin Lagoon
DN053	May 2016	Sahalin Lagoon
DN058	May 2016	Razelm Lagoon

DN059	May 2016	Razelm Lagoon
DN060	May 2016	Razelm Lagoon
DN061	May 2016	Razelm Lagoon
DN062	May 2016	Razelm Lagoon
DN063	May 2016	Razelm Lagoon
DN064	May 2016	Razelm Lagoon
DN065	May 2016	Razelm Lagoon
DN066	May 2016	Razelm Lagoon
DN067	May 2016	Razelm Lagoon
DN068	May 2016	Razelm Lagoon
DN069	May 2016	Razelm Lagoon
DN070	May 2016	Razelm Lagoon
DN071	May 2016	Razelm Lagoon
DN073	June 2016	Golovita Lagoon
DN074	June 2016	Golovita Lagoon
DN075	June 2016	Golovita Lagoon
DN076	June 2016	Golovita Lagoon
Black Sea Shelf		
Danube Delta front		
S002	May 2016	Depth profiles
S007	May 2016	Depth profiles
T001	May 2016	Surface sample
T002	May 2016	Surface sample
T003	May 2016	Surface sample
T004	May 2016	Surface sample
T005	May 2016	Surface sample
T006	May 2016	Surface sample
Danube Prodelta		
S001	May 2016	Depth profiles
S003	May 2016	Depth profiles
S004	May 2016	Depth profiles
S005	May 2016	Depth profiles
S006	May 2016	Depth profiles
S008	May 2016	Depth profiles
S009	May 2016	Depth profiles
S010	May 2016	Depth profiles
T007	May 2016	Surface sample
T008	May 2016	Surface sample
T009	May 2016	Surface sample
T010	May 2016	Surface sample
T011	May 2016	Surface sample
T012	May 2016	Surface sample
T013	May 2016	Surface sample
T014	May 2016	Surface sample
T015	May 2016	Surface sample
T016	May 2016	Surface sample
T017	May 2016	Surface sample
T018	May 2016	Surface sample

9. BIBLIOGRAPHY

Acker, J., Ouillon, S., Gould, R., Arnone, R. 2005. Measuring Marine Suspended Sediment Concentrations from Space: History and Potential. Presented at the 8th International Conference on Remote Sensing for Marine and Coastal Environments, Halifax, NS, Canada, May 17-19, 2005.

Allison, M.A., Kineke, G.C., Gordon, E.S., Goñi, M.G. 2000. Development and reworking of a seasonal flood deposit on the inner continental shelf off the Atchafalaya River. Continental Shelf Research 20: 2267-2294.

Appleby, P.G., 2008. Three decades of dating recent sediments by fallout radionuclides: A review. Holocene 18, 83–93. https://doi.org/10.1177/0959683607085598

Appleby, P.G., Oldfield, F., 1978. The calculation of lead-210 dates assuming a constant rate of supply of unsupported210Pb to the sediment. Catena 5, 1–8. https://doi.org/10.1016/S0341-8162(78)80002-2

Arnell, N.W., Gosling, S.N., 2013. The impacts of climate change on river flow regimes at the global scale. J. Hydrol. 486, 351–364. https://doi.org/10.1016/j.jhydrol.2013.02.010

Ayçik, G., Çetaku, D., Erten, H., Salihoglu, I., 2004. Dating of Black Sea sediments from Romanian coast using natural 210Pb and fallout 137Cs. J. Radioanal. Nucl. Chem. 259, 177–180.

Bai, J., & Perron, P. (2003). Computation and analysis of multiple structural change models. Journal of Applied Econometrics, 18(1), 1−22.

Bajo, M., Ferrarin, C., Dinu, I., Umgiesser, G., Stanica, A., 2014. The water circulation near the Danube Delta and the Romanian coast modelled with finite elements. Cont. Shelf Res. 78, 62–74. https://doi.org/10.1016/j.csr.2014.02.006

Barale, V., Cipollini, P., Davidov, A., Melin, F., 2002. Water constituents in the north-western Black Sea from optical remote sensing and in situ data. Estuar. Coast. Shelf Sci. 54, 309–320. https://doi.org/10.1006/ecss.2000.0649

Begy, R.C., Simon, H., Kelemen, S., Preoteasa, L., 2018. Investigation of sedimentation rates and sediment dynamics in Danube Delta lake system (Romania) by 210Pb dating method. J. Environ. Radioact. 192, 95–104. https://doi.org/10.1016/j.jenvrad.2018.06.010

Bentley, S.J., Nittrouer, C.A. 2003. Emplacement, modification, and preservation of event strata on a flood dominated continental shelf: Eel shelf, Northern California. Continental Shelf Research 23: 1465-1493.

Bianchi, T.S., Allison, M.A., 2009. Large-river delta-front estuaries as natural “recorders” of global environmental change. Proc. Natl. Acad. Sci. U. S. A. 106, 8085–8092. https://doi.org/10.1073/pnas.0812878106

Black, A.R., Hardie, A.M., 2000. Construction and interpretation of a 60-year flow record for the river tay at Kenmore. Scottish Geogr. J. 116, 93–109. https://doi.org/10.1080/00369220018737084

Boldrin, A., Langone, L., Miserocchi, S., Turchetto, M., Acri, F., 2005. Po River plume on the Adriatic continental shelf: Dispersion and sedimentation of dissolved and suspended matter during different river discharge rates. Mar. Geol. 222–223, 135–158. https://doi.org/10.1016/j.margeo.2005.06.010

Bondar, C., 1998. HYDROMORPHOLOGICAL RELATION RIVER MOUTHS THE DANUBE AND THE COASTAL ZONE IN FRONT OF THE DANUBE DELTA. Geo-Eco-Marina 3, 99–102.

Bondar, C., 1996. Aspects hydrologiques dans “L’etude de cas” du Delta du Danube. Geo-Eco-Marina 1, 48–52.

Bondar, C., 1998. HYDROMORPHOLOGICAL RELATION RIVER MOUTHS THE DANUBE AND THE COASTAL ZONE IN FRONT OF THE DANUBE DELTA. Geo-Eco-Marina 3,

99–102.
Bondar, C., Panin, N., 2001. The Danube Delta hydrologic database and modelling. Geo-Eco-Marina 5–6, 5–52.
Bondar, C., Roventa, V., State, I., 1973. La Mer Noire dans la zone du littoral Roumain. Monographie hydrologique. Editura Tehnica, Bucharest, Romania (p. 516) (in French).
Bondar, C., 1983. New data on big alluvia discharge on the Sulina arm. Studii de Hidrologie 37: 155-162.
Bondar, C., State, I., Cernea, D. & Harabagiu, E. 1991 Water flow and sediment transport of the Danube at its outlet into the Black Sea. Meteorology and Hydrology 21: 21–25.
Bondar, C. 1994. Referitor la alimentarea si tranzitul apelor Dunarii prin interiorul deltei. Scientific Annals of DDI, Volume 3(2): 259-261. (In Romanian)
Bondar, C., 2003. The high floods along the Danube River. Scientific Annals of the Danube Delta Institute for Research and Development, Volume IX: 1-9. Tulcea-Romania.
Bondar, C. 2008. Hydromorphological balance of the Danube River Channel on the Sector between Bazias (km 1072.2) and Danube Delta Inlet (km 80.5). International Expert Conference on 'The Safety of Navigation and Environmental Security in a Transboundary Context in the Black Sea Basin, Odessa, Ukraine, 24-26 June 2008
Bondar, C., Iordache, G., 2012. Extinderea pe trecut (pana in anul 1840) ale nivelelor si debitelor de apa zilnice ale Dunarii la posturile si sectiunile hidrometrice din sectorul romanesc de granita. Conferinta stiintifica internationala a INHGA din 8-10 octombrie 2012. Abstract p. 43-44. Bucuresti – in Romanian.
Brockmann, C., Doerffer, R., Marco, P., Stelzer, K., Embacher, S., Ruescas, A., 2016. Evolution Of The C2RCC Neural Network For Sentinel 2 and 3 For The Retrieval of Ocean. Proc. 'Living Planet Symp. 2016', Prague, Czech Republic, 9–13 May 2016 (ESA SP-740, August 2016) 2016, 9–13.
Broecker, W.S., Peng, T.-H., 1983. Tracers in the sea, LAMONT-DOHERTY GEOLOGICAL OBSERVATORY, COLUMBIA UNIVERSITY, PALISADES, NEW YORK 10964. https://doi.org/10.1016/0016-7037(83)90075-3
Brown, P.H., Bellaloui, N., Wimmer, M.A., Bassil, E.S., Ruiz, J., Hu, H., Pfeffer, H., Dannel, F., Römheld, V., 2002. Boron in plant biology. Plant Biol. 4, 205–223. https://doi.org/10.1055/s-2002-25740
Buonassissi, C.J., Dierssen, H.M., 2010. A regional comparison of particle size distributions and the power law approximation in oceanic and estuarine surface waters. J. Geophys. Res. Ocean. 115, 1–12. https://doi.org/10.1029/2010JC006256
Buesseler, K.O., Livingston, H.D., 1996. Natural and man-made radionuclides in the Black Sea. In: Radionuclides in the Ocean: Inputs and Inventories. IPSN, France, pp. 199-217.
Burrage, D., Wesson, J., Martinez, C., Pérez, T., Möller, O., Piola, A., 2008. Patos Lagoon outflow within the Río de la Plata plume using an airborne salinity mapper: Observing an embedded plume. Cont. Shelf Res. 28, 1625–1638. https://doi.org/10.1016/j.csr.2007.02.014
Bussi, G., Dadson, S.J., Prudhomme, C., Whitehead, P.G., 2016. Modelling the future impacts of climate and land-use change on suspended sediment transport in the River Thames (UK). J. Hydrol. 542, 357–372. https://doi.org/10.1016/j.jhydrol.2016.09.010
Catianis, I., Rădan, S., Grosu, D., 2014. Loss of ignition as a proxy indicator for assessing the lithological composition of the recent sediments accumulated in some freshwater lakes from the Danube Delta , Romania. Int. J. Innov. Appl. Stud. 9, 260–278.
Catianis, I., Vasiliu, D., Constantinescu, A.M., Pojar, I., Grosu, D., 2019. WATER QUALITY ASSESSMENT IN A RIVER-SEA TRANSITION ZONE . RECENT RESULTS FROM DISTINCT AQUATIC ENVIRONMENTS OF THE DANUBE DELTA BIOSPHERE RESERVE AREA , ROMANIA. Geo-Eco-Marina 25, 99–118.

Cattaneo, A., Correggiari, A., Marsset, T., Thomas, Y., Marsset, B., Trincardi, F., 2004. Seafloor undulation pattern on the Adriatic shelf and comparison to deep-water sediment waves. Mar. Geol. 213, 121–148. https://doi.org/10.1016/j.margeo.2004.10.004

Chapman, P.M., Wang, F., 2001. Assessing sediment contamination in estuaries. Environ. Toxicol. Chem. 20, 3–22. https://doi.org/10.1002/etc.5620200102

Charmasson, S., Radakovitch, O., Arnaud, M., Bouisset, P., Pruchon, A.-S., 1998. Long-core profiles of 137Cs, 134Cs, 60Co and 210Pb in sediment near the Rhône River (northwestern Mediterranean Sea). Estuaries 21, 367–378.

Chu, P.C., Ivanov, L.M., Margolina, T.M., 2005. Seasonal variability of the Black Sea chlorophyll- a concentration. J. Mar. Syst. 56, 243–261. https://doi.org/10.1016/j.jmarsys.2005.01.001

Cioaca, E., Bondar, C., Borcia, C., 2009. Danube Delta Biosphere Reserve hydrographic network morphological dynamics. Sci. Ann. Danube Delta Inst. 15, 137–148.

Cioaca, E., Bondar, C., Borcia, C., Marian, M., 2010a. Mathematical model of the Danube Delta Hydrographical Network Morphological Dynamics. Sci. Ann. Danube Delta Inst. 16, 57–64.

Cioaca, E., Bondar, C., Borcia, C., Mierla, M., 2010b. Mathematical model of the Danube Delta Hydrographical Network Morphological Dynamics. Sc. Ann. DDI, Tulcea, Rom. 16, 57–64.

Cleveland, R.B., Cleveland, W.S., McRae, J.E., Terpenning, I., 1990. STL: A Seasonal-Trend Decomposition Procedure Based on Loess. J. Off. Stat. 6, 3–73.

Constantin, S., Constantinescu, Ștefan, Doxaran, D., 2017. Long-term analysis of turbidity patterns in Danube Delta coastal area based on MODIS satellite data. J. Mar. Syst. 170, 10–21. https://doi.org/10.1016/j.jmarsys.2017.01.016

Constantin, S., Doxaran, D., Constantinescu, S., 2016. Estimation of water turbidity and analysis of its spatio-temporal variability in the Danube River plume (Black Sea) using MODIS satellite data. Cont. Shelf Res. 112, 14–30. https://doi.org/10.1016/j.csr.2015.11.009

Constantinescu, A.M., Toucanne, S., Dennielou, B., Jorry, S.J., Mulder, T., Lericolais, G., 2015. Evolution of the Danube Deep-Sea Fan since the Last Glacial Maximum: new insights into Black Sea water-level fluctuations. Mar. Geol. 367, 50–68. https://doi.org/10.1016/j.margeo.2015.05.007

Constantinescu, S., Achim, D., Rusu, I., Giosan, L. 2015. Embanking the Lower Danube: From Natural to Engineered Floodplains and Back. Book Chapter in Geomorphic Approaches to Integrated Floodplain, Management of Lowland Fluvial Systems in North America and Europe, P. Hudson, H. Middelkoop (eds). Springer New York 2015

Coops, H., Hanganu, J., Tudor, M., Oosterberg, W., 1999. Classification of Danube Delta lakes based on aquatic vegetation and turbidity. Hydrobiologia 415, 187–191. https://doi.org/10.1023/A:1003856927865

Corcoran, M.K., Kelley, J.R., 2006. Sediment-Tracing Technology : An Overview.

Cristofor, S., Vadineanu, A., Sarbu, A., Postolache, C., Dobre, R., Adamescu, M., 2003. Long-term changes of submerged macrophytes in the Lower Danube Wetland System. Hydrobiologia 506–509, 625–634. https://doi.org/10.1023/B:HYDR.0000008601.16757.35

Croitoru, A.E., Minea, I., 2015. The impact of climate changes on rivers discharge in Eastern Romania. Theor. Appl. Climatol. 120, 563–573. https://doi.org/10.1007/s00704-014-1194-z

Croitoru, A.E., Piticar, A., Burada, D.C., 2016. Changes in precipitation extremes in Romania. Quat. Int. 415, 325–335. https://doi.org/10.1016/j.quaint.2015.07.028

Dagg, M., Benner, R., Lohrenz, S., Lawrence, D., 2004. Transformation of dissolved and particulate materials on continental shelves influenced by large rivers: Plume processes. Cont. Shelf Res. 24, 833–858. https://doi.org/10.1016/j.csr.2004.02.003

Dan, S., Stive, M., Walstra, D.J., Sabatier, F., 2007. Sediment budget of the Danube Delta coastal zone. Coast. sediments 2007 ASCe 1–14.
Dan, S., Stive, M.J.F., Walstra, D.-J.R., Panin, N., 2009. Wave climate, coastal sediment budget and shoreline changes for the Danube Delta. Mar. Geol. 262, 39–49. https://doi.org/10.1016/j.margeo.2009.03.003
Dan, S., Walstra, D.-J.R., Stive, M.J.F., Panin, N., 2011. Processes controlling the development of a river mouth spit. Mar. Geol. 280, 116–129. https://doi.org/10.1016/j.margeo.2010.12.005
Darakas, E., 2002. The transboundary River Nestos and its water quality assessment: Cross-border cooperation between Greece and Bulgaria. Environmentalist 22, 367–375. https://doi.org/10.1023/A:1020771015365
Day, J.W., Agboola, J., Chen, Z., Elia, C.D., Forbes, D.L., Giosan, L., Kemp, P., Kuenzer, C., Lane, R.R., Ramachandran, R., Syvitski, J., Ya, A., 2016. Estuarine , Coastal and Shelf Science Approaches to de fi ning deltaic sustainability in the 21st century. Estuar. Coast. Shelf Sci. 183, 275–291. https://doi.org/10.1016/j.ecss.2016.06.018
Diaconu, C., Nichiforov, I. D., (Eds).1963. The Danube Emptying Zone. A Hydrological Monograph. Water State Committee, Bucharest. 78 pp (in Romanian)
Dinu, I., Bajo, M., Umgiesser, G., Stănică, A., 2011. Influence of wind and freshwater on the current circulation along the Romanian Black Sea coast. Geo-Eco-Marina 17, 13–26.
Dogliotti, A.I., Ruddick, K.G., Nechad, B., Doxaran, D., Knaeps, E., 2015. A single algorithm to retrieve turbidity from remotely-sensed data in all coastal and estuarine waters. Remote Sens. Environ. 156, 157–168. https://doi.org/10.1016/j.rse.2014.09.020
Doxaran, D., Froidefond, J.M., Castaing, P., Babin, M., 2009. Dynamics of the turbidity maximum zone in a macrotidal estuary (the Gironde, France): Observations from field and MODIS satellite data. Estuar. Coast. Shelf Sci. 81, 321–332. https://doi.org/10.1016/j.ecss.2008.11.013
Doxaran, D., Froidefond, J.M., Castaing, P. 2003. Remote sensing reflectance of turbid sediment-dominated waters. Reduction of sediment type variations and changing illumination conditions effects using reflectance ratios. Applied Optics 42: 2623–2634.
Duck, R.W., 2005. 14. Evolving Understanding of the Tay Estuary, Scotland: Exploring the Linkages Between Frontal Systems and Bedforms. High Resolut. Morphodynamics Sediment. Evol. Estuaries 299–313.
Duliu, O., Dinescu, L., Dinescu, M., Dorcioman, R., Mihailescu, N., Vanghelie, I., 1996. Some considerations concerning 137Cs vertical profile in the Danube Delta: Matita Lake core. Sci. Total Environ. 188, 9–14. https://doi.org/10.1016/0048-9697(96)05130-3
Dunn, F.E., 2017. Multidecadal Fluvial Sediment Fluxes to Major Deltas Under Environmental Change Scenarios: Projections and Their Implications. Thesis. UNIVERSITY OF SOUTHAMPTON. https://doi.org/10.1016/j.jsv.2010.04.020
Engström, P., Dalsgaard, T., Hulth, S., Aller, R.C., 2005. Anaerobic ammonium oxidation by nitrite (anammox): Implications for N2 production in coastal marine sediments. Geochim. Cosmochim. Acta 69, 2057–2065. https://doi.org/10.1016/j.gca.2004.09.032
Estournel, C., Kondrachoff, V., Marsaleix, P., Vehil, R., 1997. The plume of the Rhone: Numerical simulation and remote sensing. Cont. Shelf Res. 17, 899–924. https://doi.org/10.1016/S0278-4343(96)00064-7
Falkenmark, M., Wang-Erlandsson, L., Rockström, J., 2019. Understanding of water resilience in the Anthropocene. J. Hydrol. X 2, 100009. https://doi.org/10.1016/j.hydroa.2018.100009
Filip, F., Giosan, L., 2014. Evolution of Chilia lobes of the Danube delta: Reorganization of deltaic processes under cultural pressures. Anthropocene 5, 65–70. https://doi.org/10.1016/j.ancene.2014.07.003
Frignani, M., Sorgente, D., Langone, L., Albertazzi, S., Ravaioli, M., 2004. Behavior of Chernobyl radiocesium in sediments of the Adriatic Sea off the Po River delta and the Emilia-Romagna coast. J. Environ. Radioact. 71, 299–312.

https://doi.org/10.1016/S0265-931X(03)00175-9
Gangloff, A., Verney, R., Doxaran, D., Ody, A., Estournel, C., 2017. Investigating Rhône River plume (Gulf of Lions, France) dynamics using metrics analysis from the MERIS 300m Ocean Color archive (2002–2012). Cont. Shelf Res. 144, 98–111. https://doi.org/10.1016/j.csr.2017.06.024
Gastescu, P., Driga, B., Anghel, C., 1983. Caracteristici morfohidrografice ale Deltei Dunarii, Hidrobiologia, 17. Academia Romana, Bucuresti – in Romanian.
Gastescu, P., Driga, B., Anghel, C., 1986. Alterations of the Romanian Shore of the Black Sea. University of Bucharest Publishing House.
Gedan, K.B., Kirwan, M.L., Wolanski, E., Barbier, E.B., Silliman, B.R., 2011. The present and future role of coastal wetland vegetation in protecting shorelines: Answering recent challenges to the paradigm. Clim. Change 106, 7–29. https://doi.org/10.1007/s10584-010-0003-7
Gilvear, D.J., Black, A.R., 1999. Flood-induced embankment failures on the river tay: Implications of climatically induced hydrological change in Scotland. Hydrol. Sci. J. 44, 345–362. https://doi.org/10.1080/02626669909492231
Giorgi, F.: Climate change hot-spots, Geophys. Res. Lett., 33, L08707, doi:10.1029/2006GL025734, 2006.
Giosan, L., Bokuniewicz, H., Panin, N., Postolache, I., 1999. Longshore Sediment Transport Pattern Along the Romanian Danube Delta Coast. J. Coast. Res. 15, 859–871.
Giosan, L., Bokuniewicz, H., Panin, N., Postolache, I., 1997. Longshore sediment transport pattern along Romanian Danube delta coast. Geo-Eco-Marina 2, 11–24.
Giosan, L., Constantinescu, S., Filip, F., Deng, B., 2013. Maintenance of large deltas through channelization: Nature vs. humans in the Danube delta. Anthropocene 1, 35–45. https://doi.org/10.1016/j.ancene.2013.09.001
Giosan, L., Coolen, M.J.L., Kaplan, J.O., Constantinescu, S., Filip, F., Filipova-Marinova, M., Kettner, A.J., Thom, N., 2012. Early Anthropogenic Transformation of the Danube-Black Sea System. Sci. Rep. 2, 1–6. https://doi.org/10.1038/srep00582
Giosan, L., Syvitski, J., Constantinescu, S., Day, J., 2014. Protect the world's deltas. Nature 516, 31–33. https://doi.org/10.1038/516031a
Gohin, F., 2011. Annual cycles of chlorophyll-a, non-algal suspended particulate matter, and turbidity observed from space and in-situ in coastal waters. Ocean Sci. 7, 705–732. https://doi.org/10.5194/os-7-705-2011
Gohin, F., Druon, J. N., & Lampert, L. 2002. A five channel chlorophyll concentration algorithm applied to SeaWiFS data processed by SeaDAS in coastal waters. International Journal of Remote Sensing, 23: 1639-1661.
Goldberg, E. D. 1963. Geochronology with 210Pb. In Radioactive Dating. Proceedings of the Symposium on Radioactive Dating Held by the International Atomic Energy Agency in Co-operation with the Joint Commission on Applied Radioactivity, Athens, November 19–23, 1962, pp. 121–131.
Gomoiu, M.T., Secrieru, D., Oaie, G., Cristescu, M., Nicolescu, N., Marinescu, V. 1998. Ecological state of the river Danube ecosystems in 1995. Geo-Eco-Marina 3: 37-88.
Gray, B.J.R., Glysson, G.D., Turcios, L.M., Schwarz, G.E., 2000. Comparability of Suspended-Sediment Concentration and Total Suspended Solids Data. Water-Resources Investigations Report 00-4191. USGS WRI 4191, 20p. https://doi.org/Report 00-4191
Grill, G., Lehner, B., Thieme, M., Geenen, B., Tickner, D., Antonelli, F., Babu, S., Borrelli, P., Cheng, L., Crochetiere, H., Ehalt Macedo, H., Filgueiras, R., Goichot, M., Higgins, J., Hogan, Z., Lip, B., McClain, M.E., Meng, J., Mulligan, M., Nilsson, C., Olden, J.D., Opperman, J.J., Petry, P., Reidy Liermann, C., Sáenz, L., Salinas-Rodríguez, S., Schelle, P., Schmitt, R.J.P., Snider, J., Tan, F., Tockner, K., Valdujo, P.H., van

Soesbergen, A., Zarfl, C., 2019. Mapping the world's free-flowing rivers. Nature 569, 215–221. https://doi.org/10.1038/s41586-019-1111-9

Gracia, V., A. Sánchez-Arcilla, and G. Anfuso: 2013c, 'Spain'. In: E. Pranzini and A. WIlliams (eds.): Coastal Erosion and Protection in Europe, Coastal erosion and protection in Europe. Oxon: Routledge, pp. 254–274. 1, 1.1, 2.3.1, 2.4.1, 2.4.4.1, 7.6

Groundwater, H., Twardowski, M.S., Dierssen, H.M., Sciandra, A., Freeman, S.A., 2012. Determining size distributions and composition of particles suspended in water: A new SEM-EDS protocol with validation and comparison to other methods. J. Atmos. Ocean. Technol. 29, 433–449. https://doi.org/10.1175/JTECH-D-11-00026.1

Gulin, S.B., Mirzoyeva, N.Y., Egorov, V.N., Polikarpov, G.G., Sidorov, I.G., Proskurnin, V.Y., 2013. Secondary radioactive contamination of the Black Sea after Chernobyl accident: Recent levels, pathways and trends. J. Environ. Radioact. 124, 50–56. https://doi.org/10.1016/j.jenvrad.2013.04.001

Gulin, S.B., Polikarpov, G.G., Egorov, V.N., Martin, J.M., Korotkov, A. a., Stokozov, N. a., 2002. Radioactive Contamination of the North-western Black Sea Sediments. Estuar. Coast. Shelf Sci. 54, 541–549. https://doi.org/10.1006/ecss.2000.0663

Güttler, F.N., Niculescu, S., Gohin, F., 2013. Turbidity retrieval and monitoring of Danube Delta waters using multi-sensor optical remote sensing data: An integrated view from the delta plain lakes to the western–northwestern Black Sea coastal zone. Remote Sens. Environ. 132, 86–101. https://doi.org/10.1016/j.rse.2013.01.009

Habersack, H., Hein, T., Stanica, A., Liska, I., Mair, R., Jäger, E., Hauer, C., Bradley, C., 2016. Challenges of river basin management: Current status of, and prospects for, the River Danube from a river engineering perspective. Sci. Total Environ. 543, 828–845. https://doi.org/10.1016/j.scitotenv.2015.10.123

Hanganu, J., Doroftei, M., Stefan, N., 2008. ASSESMENT OF ECOLOGICAL STATUS OF DANUBE DELTA LAKES USING INDICATOR MACROPHYTES SPECIES. Analele Stiint. ale Universtatii "Al. I. Cuza" Iasi LIV, 103–108.

Haywood, B.J., White, J.R., Cook, R.L., 2018. Investigation of an early season river flood pulse: Carbon cycling in a subtropical estuary. Sci. Total Environ. 635, 867–877. https://doi.org/10.1016/j.scitotenv.2018.03.379

Hedges, J.I., Keil, R.G., 1995. Sedimentary organic matter preservation: an assessment and speculative synthesis. Mar. Chem. 49, 81–115. https://doi.org/10.1016/0304-4203(95)00008-F

Hein, T., Schwarz, U., Habersack, H., Nichersu, I., Preiner, S., Willby, N., Weigelhofer, G., 2016. Current status and restoration options for floodplains along the Danube River. Sci. Total Environ. 543, 778–790. https://doi.org/10.1016/j.scitotenv.2015.09.073

Hillebrand, G., Hardenbicker, P., Fisher, H., Otto, W., Vollmer, S., 2018. Dynamics of total suspended matter and phytoplankton loads in the river Elbe. J. Soils Sediments PHYSICAL A, 10.

Hu, G., Li, A., Liu, J., Xu, G., Mei, X., Kong, X. 2014. High resolution records of flood deposition in the mud area off the Changjiang River mouth during the past century. Chinese Journal of Oceanology and Limnology, 32(4): 909-920.

Hudson, P.F., Hans Middelkoop, 2015. Geomorphic Approaches to Integrated Floodplain Management of Lowland Fluvial Systems in North America and Europe. Springer New York 2015.

H2020 DANUBIUS-PP Consortium.2019. Science and Innovation Agenda of DANUBIUS-RI - the International Centre for Advances Studies on River-Sea Systems

Ibàñez, C., Prat, N., Canicio, A., 1996. Changes in the hydrology and sediment transport produced by large dams on the lower Ebro River and its estuary. Regul. Rivers Res. Manag. 12, 51–62. https://doi.org/10.1002/(SICI)1099-1646(199601)12:1<51::AID-RRR376>3.0.CO;2-I

ICPDR 2009. Annex 8 of the DRBM Plan - Pressures and impacts related to quantity and quality aspects of sediments. Source: www.icpdr.org

Ionita, M., Badaluta, C.A., Scholz, P., Chelcea, S., 2018. Vanishing river ice cover in the lower part of the Danube basin-signs of a changing climate. Sci. Rep. 8, 1–12. https://doi.org/10.1038/s41598-018-26357-w

Jones, P.D., Jonsson, T., Wheeler, D., 1997. Extension to the North Atlantic oscillation using early instrumental pressure observations from Gibraltar and south-west Iceland. Int. J. Climatol. 17, 1433–1450. https://doi.org/10.1002/(SICI)1097-0088(19971115)17:13<1433::AID-JOC203>3.0.CO;2-P

Jugaru Tiron, L., Le Coz, J., Provansal, M., Panin, N., Raccasi, G., Dramais, G., Dussouillez, P., 2009. Flow and sediment processes in a cutoff meander of the Danube Delta during episodic flooding. Geomorphology 106, 186–197. https://doi.org/10.1016/j.geomorph.2008.10.016

Karageorgis, a. P., Gardner, W.D., Mikkelsen, O. a., Georgopoulos, D., Ogston, A.S., Assimakopoulou, G., Krasakopoulou, E., Oaie, G., Secrieru, D., Kanellopoulos, T.D., Pagou, K., Anagnostou, C., Papathanassiou, E., 2014. Particle sources over the Danube River delta, Black Sea based on distribution, composition and size using optics, imaging and bulk analyses. J. Mar. Syst. 131, 74–90. https://doi.org/10.1016/j.jmarsys.2013.11.013

Karageorgis, a. P., Kourafalou, V.H., Anagnostou, C., Tsiaras, K.P., Raitsos, D.E., Papadopoulos, V., Papadopoulos, A., 2009. River-induced particle distribution in the northwestern Black Sea (September 2002 and 2004). J. Geophys. Res. 114, 16 p. https://doi.org/10.1029/2009JC005460

Kinniburgh, J.H., Barnett, M., 2010. Orthophosphate concentrations in the River Thames: Reductions in the past decade. Water Environ. J. 24, 107–115. https://doi.org/10.1111/j.1747-6593.2008.00161.x

Kolker, A.S., Li, C., Walker, N.D., Pilley, C., Ameen, A.D., Boxer, G., Ramatchandirane, C., Ullah, M., Williams, K. a., 2014. The impacts of the great Mississippi/Atchafalaya River flood on the oceanography of the Atchafalaya Shelf. Cont. Shelf Res. 86, 1–17. https://doi.org/10.1016/j.csr.2014.04.023

Kondolf, G.M., Schmitt, R.J.P., Carling, P., Darby, S., Arias, M., Bizzi, S., Castelletti, A., Cochrane, T.A., Gibson, S., Kummu, M., Oeurng, C., Rubin, Z., Wild, T., 2018. Changing sediment budget of the Mekong: Cumulative threats and management strategies for a large river basin. Sci. Total Environ. 625, 114–134. https://doi.org/10.1016/j.scitotenv.2017.11.361

Kourafalou, V.H., Stanev, E. V, 2001. Annales Geophysicae Modeling the impact of atmospheric and terrestrial inputs on the Black Sea coastal dynamics. Ann. Geophys. 245–256.

Kovbasko, O., Ionescu, C., Saaf, E.J., Nesterenko, M., Dyakov, O., Drumea, D., Doroftei, M., 2014. Adapting to change: Climate Change Adaptation Strategy and Action Plan for Danube Delta Region Romania-Ukraine-Moldova. https://doi.org/10.1038/nphoton.2010.302

Latrubesse, E.M., Arima, E.Y., Dunne, T., Park, E., Baker, V.R., D'Horta, F.M., Wight, C., Wittmann, F., Zuanon, J., Baker, P.A., Ribas, C.C., Norgaard, R.B., Filizola, N., Ansar, A., Flyvbjerg, B., Stevaux, J.C., 2017. Damming the rivers of the Amazon basin. Nature 546, 363–369. https://doi.org/10.1038/nature22333

Lechner, A., Keckeis, H., Lumesberger-Loisl, F., Zens, B., Krusch, R., Tritthart, M., Glas, M., Schludermann, E., 2014. The Danube so colourful: A potpourri of plastic litter outnumbers fish larvae in Europe's second largest river. Environ. Pollut. 188, 177–181. https://doi.org/10.1016/j.envpol.2014.02.006

Lericolais, G., Bulois, C., Gillet, H., Guichard, F., 2009. High frequency sea level fluctuations recorded in the Black Sea since the LGM. Global and Planetary Change, 66: 65-75.

Lericolais, G., Guichard, F., Morigi, C., Minereau, A., Popescu, I., Radan, S., 2010. A post Younger Dryas Black Sea regression identified from sequence stratigraphy correlated to core analysis and dating. Quaternary International, 225: 199-209.

Lericolais, G., Guichard, F., Morigi, C., Popescu, I., Bulois, C., Gillet, H., Ryan, W.B.F., 2011. Assesment of Black Sea water-level fluctuations since the Last Glacial Maximum. The Geological Society of America, Special Paper, 473: 1-18.

Lericolais, G., Popescu, I., Guichard, F., Popescu, S.M., 2007. A Black Sea lowstand at 8500 yr B.P. indicated by a relict coastal dune system at a depth of 90 m below sea level. The Geological Society of America, Special Paper, 426: 171-188.

Livingston, H.D., Buesseler, K.O., Izdar, E., Konuk, T., 1988. Characteristics of Chernobyl fallout in the southern Black Sea. In: Guary, J.C., Guéguéniat, P., Pentreath, R.J. (Eds.), Radionuclides: A Tool for Oceanography. Elsevier Applied Science, London & New York, pp. 204e216.

Liu, J.P., Xue, Z., Ross, K., Wang, H.J., Yang, Z.S., Li, A.C., Gao, S., 2009. Fate of sediments delivered to the sea by Asian large rivers: Long-distance transport and formation of remote alongshore clinothems. Sediment. Rec. 7, 4–9. https://doi.org/10.2110/sedred.2009.4.4

Ludwig, W., Dumont, E., Meybeck, M., Heussner, S., 2009. River discharges of water and nutrients to the Mediterranean and Black Sea: Major drivers for ecosystem changes during past and future decades? Prog. Oceanogr. 80, 199–217. https://doi.org/10.1016/j.pocean.2009.02.001

Magilligan, F.J., Graber, B.E., Nislow, K.H., Chipman, J.W., Sneddon, C.S., Fox, C.A., 2016. River restoration by dam removal: Enhancing connectivity at watershed scales. Elementa 2016, 1–14. https://doi.org/10.12952/journal.elementa.000108

Manieri, F., 2016. The Po River Basin : Managing a Complex System. Lessons from the Past, Recommendations for the Future. Master's thesis Glob. Environ. Hist. Uppsala, Dep. Archaeol. Anc. Hist. 79.

Marchetti, M., 2002. Environmental changes in the central Po Plain (northern Italy) due to f luvial modifications and anthropogenic activities. Geomorphology 44, 361–373. https://doi.org/10.1016/S0169-555X(01)00183-0

Marion, C., Dufois, F., Arnaud, M., Vella, C., 2010. In situ record of sedimentary processes near the Rhone River mouth during winter events (Gulf of Lions, Mediterranean Sea). Cont. Shelf Res. 30, 1095–1107. https://doi.org/10.1016/j.csr.2010.02.015

Maselli, V., Trincardi, F., 2013. Man made deltas. Sci. Rep. 3, 1–7. https://doi.org/10.1038/srep01926

McCarney-Castle, K., Voulgaris, G., Kettner, A.J., Giosan, L., 2011. Simulating fluvial fluxes in the Danube watershed: The "Little Ice Age" versus modern day. The Holocene 22, 91–105. https://doi.org/10.1177/0959683611409778

McManus, J. 1998. Mixing of sediments in estuaries. In: Cracknell, A.P and Rowan, E.S. (Eds) *Physical processes in the Coastal Zone: Computer Modelling and Remote Sensing*, 281-298, SUSSP Publications and Institute of Physics.

Merchand, M., Guchte, C. van de (Eds.), 2010. Comparative assessment of the vulnerability and resilience of 10 deltas.

Merrett S. The Thames catchment: a river basin at the tipping point. Water Policy 2007; 9:393–404.

Mikhailov, V.N., Morozov, V.N., Cheroy, N.I., Mikhailova, M. V., Zav'yalova, Y.F., 2008. Extreme flood on the Danube River in 2006. Russ. Meteorol. Hydrol. 33, 48–54. https://doi.org/10.3103/S1068373908010081

Mikhailov, V.N., Morozov, V.N., Cheroy, N.I., Mikhailova, M. V., Zav'yalova, Y.F., 2008. Extreme flood on the Danube River in 2006. Russ. Meteorol. Hydrol. 33, 48–54.

https://doi.org/10.3103/S1068373908010081
Mikhailova, M. V., Mikhailov, V.N., Morozov, V.N., 2012. Extreme hydrological events in the Danube River basin over the last decades. Water Resour. 39, 161–179. https://doi.org/10.1134/S0097807812010095
Mikhailova, M. V., Mikhailov, V.N., Morozov, V.N., 2012. Extreme hydrological events in the Danube River basin over the last decades. Water Resour. 39, 161–179. https://doi.org/10.1134/S0097807812010095
Mihailescu, N. 1981. Lower Danube recent alluvia: sediment and sedimentary factors. 12th Congress of the Carpatho-Balkan Geological Association, 8-13 September, Bucharest, Romania.
Mihailescu, N., Radan, S., Costea, C., Vanghelie, I., Radan, S.C., Radan, M., Gyongy, R. 1996. Geoecological researches on the Danube-Danube Delta-Black Sea littoral-Black Sea system. Assessment of data for developing the conception regarding the protection of the characteristic ecosystems. Anuarul Institutului Geologic al Romaniei, Volum 90, Partea 1, Bucuresti.
Mikkelsen, O.A., Pejrup, M., 2001. The use of a LISST-100 laser particle sizer for in-situ estimates of floc size, density and settling velocity. Geo-Marine Lett. 20, 187–195. https://doi.org/10.1007/s003670100064
Milligan, T.G., Hill, P.S., Law, B.A., 2007. Flocculation and the loss of sediment from the Po River plume. Cont. Shelf Res. 27, 309–321. https://doi.org/10.1016/j.csr.2006.11.008
Milliman, J.D., Farnsworth, K.L. (Eds.), 2011. River Discharge to the Coastal Ocean. A Global Synthesis. Cambridge University Press.
Mimides, T., Kotsovinos, N., Rizos, S., Soulis, C., Karakatsoulis, P., Stavropoulos, D., 2007. Integrated runoff and balance analysis concerning Greek-Bulgarian transboundary hydrological basin of River Nestos/Mesta. Desalination 213, 174–181. https://doi.org/10.1016/j.desal.2006.04.086
Neil, C., Spyrakos, E., Hunter, P.D., Tyler, A.N., 2019. A global approach for chlorophyll-a retrieval across optically complex inland waters based on optical water types. Remote Sens. Environ. 229, 159–178. https://doi.org/10.1016/j.rse.2019.04.027
Nezlin, N.P., Kostianoy, a. G., Gregoire, M., 1999. Patterns of seasonal and interannual changes of surface chlorophyll concentration in the Black Sea revealed from the remote sensed data. Remote Sens. Environ. 69, 43–55. https://doi.org/10.1016/S0034-4257(99)00007-3
Noakes, J.E. and Hertz, N. 1983. University of Georgia. Radiocarbon dates VII, Radiocarbon, 25: 919-929.
Oaie, G., Secrieru, D., Shimkus, K., 2004. Black Sea Basin : Sediment Types And Distribution , Sedimentation Processes. Geo-Eco-Marina 9–10.
Oaie, G., Secrieru, D., Szobotka, Ş., Fulga, C., Stănică, A., 2005. Danube River : sedimentological , mineralogical and geochemical characteristics of the bottom sediments. Geo-Eco-Marina 11, 77–85.
Oaie, G., Secrieru, D., Szobotka, S., Stanica, A., Soare, R., 1999. Pollution state of sediments dredged from the Sulina distributary and their influence on the Danube Delta front area. Geo-Eco-Marina 4, 37–41. https://doi.org/10.1073/pnas.0703993104
Oguz, T., Deshpande, A.G., Malanotte-Rizzoli, P. 2002. The role of mesoscale processes controlling biological variability in the Black Sea coastal waters: inferences from SeaWIFS-derived surface chlorophyll field. Continental Shelf Research 22: 1477–1492.
Oguz, T., Malanotte-Rizzoli, P. & Aubrey, D. 1995 Wind and thermohaline circulation of the Black Sea driven by yearly mean climatological forcing. Journal of Geophysical Research 100: 6845– 6863.
Oosterberg, W., Buijse, A.D., Coops, H., Ibelings, B.W., Menting, G.A.M., Staras, M.,

Bogdan, L., Constantinescu, A., Hanganu, J., Navodaru, I., Torok, L., 2000. Ecological gradients in the Danube Delta lakes. RIZA Rapp. 2000.015, 168 p. https://doi.org/90.369.5309x

O'Reilly, J. E., Maritorena, S., Mitchell, B. G., Siegel, D. A., Carder, K. L., Garver, S. A., Kahru, M., McClain C. 1998. Ocean color chlorophyll algorithms for SeaWiFS, Journal of Geophysical Research 103: 24,937 – 24,953, doi:10.1029/98JC02160.

Opreanu, G., Oaie, G., Paun, F., 2007. The dynamic significance of the grain size of sediments transported and deposited by the Danube. Geo-Eco-Marina 13, 111–119.

Palinkas, C.M., Nittrouer, C.A., Wheatcroft, R.A., Langone, L., 2005. The use of ^{7}Be to identify event and seasonal sedimentation near the Po River delta, Adriatic Sea. Marine Geology 222–223: 95–112.

Palmer, M.A., Reidy Liermann, C.A., Nilsson, C., Flörke, M., Alcamo, J., Lake, P.S., Bond, N., 2008. Climate change and the world's river basins: Anticipating management options. Front. Ecol. Environ. 6, 81–89. https://doi.org/10.1890/060148

Panin, N., 1999. Global changes, sea level rising and the Danube Delta: risk and responses. Geo-Eco-Marina 4, 19–29.

Panin, N., 1997. On the geomorphologic and geologic evolution of the River Danube - Black sea interaction zone. Geo-Eco-Marina 2, 31–40.

Panin, N., 1996. Danube Delta. Genesis, Evolution, Geological Setting and Sedimentology. Geo-Eco-Marina 1, 7–23.

Panin, N., Jipa, D., 2002. Danube River Sediment Input and its Interaction with the North-western Black Sea. Estuar. Coast. Shelf Sci. 54, 551–562. https://doi.org/10.1006/ecss.2000.0664

Panin, N., Jipa, D., 1998. Danube river sediment input and its interaction with the north-western Black Sea: results of EROS-2000 and EROS-21 projects. Geo-Eco-Marina 3.

Panin, N., Jipa, D. C., Gomoiu, M. T. & Secrieru, D. 1998. Importance of sedimentary processes in environmental changes: lower river Danube–Danube delta–western Black Sea system. In *Environmental Degradation of the Black Sea: Challenges and Remedies* (Unluata, U., ed.). Kluwer Academic Publishers, Dordrecht, pp. 23–41.

Panin, N., Overmars, W., 2012. The Danube Delta evolution during the Holocene : reconstruction attempt using geomorphological and geological data, and some of the existing cartographic documents. Geo-Eco-Marina 18, 75–104.

Pekárová, P., 2009. MULTIANNUAL RUNOFF VARIABILITY IN THE UPPER DANUBE REGION. Slavak Academy of sciences.

Pekárová, P., Halmová, D., Mitková, V.B., Miklánek, P., Pekár, J., Škoda, P., 2013. Historic flood marks and flood frequency analysis of the Danube River at Bratislava, Slovakia. J. Hydrol. Hydromechanics 61, 326–333. https://doi.org/10.2478/johh-2013-0041

Pekárová, P., Miklánek, P., Pekár, J., 2003. Spatial and temporal runoff oscillation analysis of the main rivers of the world during the 19th-20th centuries. J. Hydrol. 274, 62–79. https://doi.org/10.1016/S0022-1694(02)00397-9

Pekarova, P., Pekar, J., 2006. Long-term discharge prediction for the Turnu Severin station (the Danube) using a linear autoregressive model. Hydrol. Process. 20, 1217–1228. https://doi.org/10.1002/hyp.5939

Peng, F., Effler, S.W., O'Donnell, D., Weidemann, A.D., Auer, M.T., 2009. Characterizations of minerogenic particles in support of modeling light scattering in Lake Superior through a two-component approach. Limnol. Oceanogr. 54, 1369–1381. https://doi.org/10.4319/lo.2009.54.4.1369

Petts, G.E., Gurnell, A.M., 2005. Dams and geomorphology: Research progress and future directions. Geomorphology 71, 27–47. https://doi.org/10.1016/j.geomorph.2004.02.015

Petus, C., Marieu, V., Novoa, S., Chust, G., Bruneau, N., Froidefond, J.M., 2014. Monitoring spatio-temporal variability of the Adour River turbid plume (Bay of Biscay, France) with MODIS 250-m imagery. Cont. Shelf Res. 74, 35–49.

https://doi.org/10.1016/j.csr.2013.11.011
Petus, C., Waterhouse, J., Lewis, S., Vacher, M., Tracey, D., Devlin, M., 2019. A flood of information: Using Sentinel-3 water colour products to assure continuity in the monitoring of water quality trends in the Great Barrier Reef (Australia). J. Environ. Manage. 248, 109255. https://doi.org/10.1016/j.jenvman.2019.07.026
PN0302 report 2016 – Romanian Core Program for Research
Poncos, V., Teleaga, D., Bondar, C., Oaie, G., 2013. A new insight on the water level dynamics of the Danube Delta using a high spatial density of SAR measurements. J. Hydrol. 482, 79–91. https://doi.org/10.1016/j.jhydrol.2012.12.037
Qizhong (George) Guo, P.I., 2006. Correlation of Total Suspended Solids (TSS) and Suspended Sediment Concentration (SSC) Test Methods. Final Report. Final Report, New Jersey Dep. Environ. Prot.
Renaud, F.G., Syvitski, J.P., Sebesvari, Z., Werners, S.E., Kremer, H., Kuenzer, C., Ramesh, R., Jeuken, A., Friedrich, J., 2013. Tipping from the Holocene to the Anthropocene: How threatened are major world deltas? Curr. Opin. Environ. Sustain. 5, 644–654. https://doi.org/10.1016/j.cosust.2013.11.007
Richter, T.O., van der Gaast, S., Koster, B., Vaars, A., Gieles, R., de Stigter, H.C., De Haas, H., van Weering, T.C.E., 2006. The Avaatech XRF Core Scanner: technical description and applications to NE Atlantic sediments. Geol. Soc. London, Spec. Publ. 267, 39–50. https://doi.org/10.1144/GSL.SP.2006.267.01.03
Risović, D., 2002. Effect of suspended particulate-size distribution on the backscattering ratio in the remote sensing of seawater. Appl. Opt. 41, 7092. https://doi.org/10.1364/ao.41.007092
Romanescu, G., 2013. Alluvial transport processes and the impact of Anthropogenic intervention on the Romanian littoral of the Danube Delta. Ocean Coast. Manag. 73, 31–43. https://doi.org/10.1016/j.ocecoaman.2012.11.010
Rong, Z., Hetland, R.D., Zhang, W., Zhang, X., 2014. Current–wave interaction in the Mississippi–Atchafalaya river plume on the Texas–Louisiana shelf. Ocean Model. 84, 67–83. https://doi.org/10.1016/j.ocemod.2014.09.008
Rothwell, R.G., Hoogakker, B., Thomson, J., Croudace, I.W., Frenz, M., 2006. Turbidite emplacement on the southern Balearic Abyssal Plain (western Mediterranean Sea) during Marine Isotope Stages 1–3: an application of ITRAX XRF scanning of sediment cores to lithostratigraphic analysis. Geol. Soc. London, Spec. Publ. 267, 79–98. https://doi.org/10.1144/gsl.sp.2006.267.01.06
Routschek, A., Schmidt, J., Kreienkamp, F., 2014. Impact of climate change on soil erosion - A high-resolution projection on catchment scale until 2100 in Saxony/Germany. Catena 121, 99–109. https://doi.org/10.1016/j.catena.2014.04.019
Rovira, A., Ibáñez, C., Martín-Vide, J.P., 2015. Suspended sediment load at the lowermost Ebro River (Catalonia, Spain). Quat. Int. 388, 188–198. https://doi.org/10.1016/j.quaint.2015.05.035
Rudescu, L., Niculescu, C., Chivu, L.P. editors. 1965. Monografia stufului din Delta Dunarii. Editura Academiei Republicii Socialiste Romania. 542 p. (in Romanian).
Samaras, A.G., Koutitas, C.G., 2008. Modelling the impact on coastal morphology of the water management in transboundary river basins: The case of River Nestos. Manag. Environ. Qual. An Int. J. 19, 455–466. https://doi.org/10.1108/14777830810878641
Santschi, P.H., 1988. Santschi, 1988 - Factors controlling the biogeochemical cycles of trace elements in fresh and coastal marine waters as revealed by artificial radioisotopes. Limnol. Oceanogr. 33, 848–866.
Schiller, H., Miklós, D., 2010. Hydrological Processes of the Danube River Basin, in: M. Brilly (Ed.), Hydrological Processes of the Danube River Basin. Springer Science+Business Media B.V. 2010, pp. 25–77. https://doi.org/10.1007/978-90-481-3423-6
Schillereff, D.N., Chiverrell, R.C., Macdonald, N., Hooke, J.M. 2014. Flood stratigraphies in lake sediments: A review. Earth-Science Reviews 135: 17-37.

Schmidt, M., Glasson, J., Emmelin, L., Helbron, H., 2008. Standards and Thresholds for Impact Assessment. https://doi.org/10.1007/978-3-540-31141-6

Schneider, C., Laizé, C.L.R., Acreman, M.C., Flörke, M., 2013. How will climate change modify river flow regimes in Europe? Hydrol. Earth Syst. Sci. 17, 325–339. https://doi.org/10.5194/hess-17-325-2013

Schwarz, U., 2008. Assessment of the Balance and Management of Sediments of the Danube. XXIVth Conf. Danubian Ctries. Hydrol. Forecast. Hydrol. Bases Water Manag. Bled, Slov. 2-4 June, 2008.

Sommerfield, C.K., Nittrouer, C.A., 1999. Modern accumulation rates and a sediment budget for the Eel shelf: a flood-dominated depositional environment. Marine Geology 154: 227–241.

Sommerfield, C.K., Nittrouer, C.A., Alexander, C.K., 1999. 7Be as a tracer of flood sedimentation on the northern California continental margin. Continental Shelf Research 19: 335–361.

Spyrakos, E., O'Donnell, R., Hunter, P.D., Miller, C., Scott, M., Simis, S.G.H., Neil, C., Barbosa, C.C.F., Binding, C.E., Bradt, S., Bresciani, M., Dall'Olmo, G., Giardino, C., Gitelson, A.A., Kutser, T., Li, L., Matsushita, B., Martinez-Vicente, V., Matthews, M.W., Ogashawara, I., Ruiz-Verdú, A., Schalles, J.F., Tebbs, E., Zhang, Y., Tyler, A.N., 2018. Optical types of inland and coastal waters. Limnol. Oceanogr. 63, 846–870. https://doi.org/10.1002/lno.10674

Stanev, E.V., Kandilarov, R., 2012. Sediment dynamics in the Black Sea: Numerical modelling and remote sensing observations. Ocean Dyn. 62, 533–553. https://doi.org/10.1007/s10236-012-0520-1

Staras, M. 2000. Restoration programme in the Danube Delta: Achievements, benefits and constraints. Proceeding of the IInd ECRR International Conference on River Restoration in Europe 2000, NIJLAND, H. J. & CALS, M. J. R. (Ed.), Institute for Inland Water Management and Waste Water Treatment/RIZA Lelystad (Pub.). Wageningen (Netherlands), pp. 95-101.

Stănică, A. 2003. "Evolutia geodinamica a litoralului romanesc in sectorul Sulina – Sf. Gheorghe si posibilitati de predictie", *Biblioteca Universitatii Bucuresti, Facultatea de Geologie si Geofizica*, Bucharest (unpublished Ph. D. Thesys, in Romanian).

Stanica A., Panin N., Caraivan G., 2013. Romanian shore and coastal protection. Chapter 20 of the volume „Coastal Erosion and Protection in Europe". A. Williams and E. Pranzini Editors. Pp. 396-412, Earthscan Publishing House, Taylor and Francis Group. ISBN 978-1-84971-339-9.

Stănică, A., Dan, S., Jiménez, J. a., Ungureanu, G. V., 2011. Dealing with erosion along the Danube Delta coast. The CONSCIENCE experience towards a sustainable coastline management. Ocean Coast. Manag. 54, 898–906. https://doi.org/10.1016/j.ocecoaman.2011.06.006

Stănică, A., Dan, S., Ungureanu, V.G., 2007. Coastal changes at the Sulina mouth of the Danube River as a result of human activities. Mar. Pollut. Bull. 55, 555–563. https://doi.org/10.1016/j.marpolbul.2007.09.015

Stănică, A., Panin, N., 2009. Present evolution and future predictions for the deltaic coastal zone between the Sulina and Sf. Gheorghe Danube river mouths (Romania). Geomorphology 107, 41–46. https://doi.org/10.1016/j.geomorph.2007.04.041

Sur, H., Ozsoy, E., Ilyin, Y.P., Unluata, U., 1996. Coastal / deep ocean interactions in the Black Sea and their ecological / environmental impacts. J. Mar. Syst. 7, 293–320.

Sur, H.I., Ilyin, Y.P., 1997. Evolution of satellite derived mesoscale thermal patterns in the Black Sea. Prog. Oceanogr. 39, 109–151.

Swarzenski, P.W., 2014. 210Pb Dating. Encycl. Sci. Dating Methods 1–11.

https://doi.org/10.1007/978-94-007-6326-5_236-1
Sylaios, G.K., Kamidis, N., Tsihrintzis, V.A., 2010. Impact of river damming on coastal stratification-mixing processes: The cases of Strymon and Nestos Rivers, N. Greece. Desalination 250, 302–312. https://doi.org/10.1016/j.desal.2009.09.047
Syvitski, J.P.M., 2011. Global sediment fluxes to the Earth's coastal ocean. Appl. Geochemistry 26, S373–S374. https://doi.org/10.1016/j.apgeochem.2011.03.064
Syvitski, J.P.M., Kettner, A.J., 2007. On the flux of water and sediment into the Northern Adriatic Sea. Cont. Shelf Res. 27, 296–308. https://doi.org/10.1016/j.csr.2005.08.029
Syvitski, J.P.M., Kettner, A.J., Correggiari, A., Nelson, B.W., 2005a. Distributary channels and their impact on sediment dispersal. Mar. Geol. 222–223, 75–94. https://doi.org/10.1016/j.margeo.2005.06.030
Syvitski, J.P.M., Kettner, A.J., Overeem, I., Giosan, L., Brakenridge, G.R., Hannon, M., Bilham, R., 2013. Anthropocene metamorphosis of the Indus Delta and lower floodplain. Anthropocene 3, 24–35. https://doi.org/10.1016/j.ancene.2014.02.003
Syvitski, J.P.M., Kettner, A.J., Overeem, I., Hutton, E.W.H., Hannon, M.T., Brakenridge, G.R., Day, J., Vörösmarty, C., Saito, Y., Giosan, L., Nicholls, R.J., 2009. Sinking deltas due to human activities. Nat. Geosci. 2, 681–686. https://doi.org/10.1038/ngeo629
Syvitski, J.P.M., Milliman, J.D., 2007. Geology, Geography, and Humans Battle for Dominance over the Delivery of Fluvial Sediment to the Coastal Ocean. J. Geol. 115, 1–19. https://doi.org/10.1086/509246
Syvitski, J.P.M., Vorosmarty, C.J., Kettner, A.J., Green, P., 2005b. Impact of Humans on the Flux of Terrestrial Sediment to the Global Coastal Ocean. Science (80-.). 308.
Tarpanelli, A., Camici, S., Nielsen, K., Brocca, L., Moramarco, T., Benveniste, J., 2019. Potentials and limitations of Sentinel-3 for river discharge assessment. Adv. Sp. Res. https://doi.org/10.1016/j.asr.2019.08.005
Temmerman, S., Meire, P., Bouma, T.J., Herman, P.M.J., Ysebaert, T., De Vriend, H.J., 2013. Ecosystem-based coastal defence in the face of global change. Nature 504, 79–83. https://doi.org/10.1038/nature12859
Tena, A., Batalla, R.J., Vericat, D., López-Tarazón, J.A., 2011. Suspended sediment dynamics in a large regulated river over a 10-year period (the lower Ebro, NE Iberian Peninsula). Geomorphology 125, 73–84. https://doi.org/10.1016/j.geomorph.2010.07.029
Tesi, T., Miserocchi, S., Acri, F., Langone, L., Boldrin, A., Hatten, J.A., Albertazzi, S., 2013. Flood-driven transport of sediment, particulate organic matter, and nutrients from the Po River watershed to the Mediterranean Sea. J. Hydrol. 498, 144–152. https://doi.org/10.1016/j.jhydrol.2013.06.001
Tessler, Z.D., Vorosmarty, C.J., Grossberg, M., Gladkova, I., Aizenman, H., Syvitski, J.P., Foufoula-Georgiou, E., 2015. Profiling Risk and Sustainability in Coastal Deltas of the World. Science (80-.). in press. https://doi.org/10.1126/science.aab3574
Tiron Duţu, L., Provansal, M., Le Coz, J., Duţu, F., 2014. Contrasted sediment processes and morphological adjustments in three successive cutoff meanders of the Danube delta. Geomorphology 204, 154–164. https://doi.org/10.1016/j.geomorph.2013.07.035
Tsiaras, K.P., Kourafalou, V.H., Davidov, A., Staneva, J., 2008. A three-dimensional coupled model of the western Black Sea plankton dynamics: Seasonal variability and comparison to SeaWiFS data. J. Geophys. Res. 113. https://doi.org/10.1029/2006JC003959
Tyler, A.N., Hunter, P.D., Spyrakos, E., Groom, S., Constantinescu, A.M., Kitchen, J., 2016. Developments in Earth observation for the assessment and monitoring of inland, transitional, coastal and shelf-sea waters. Sci. Total Environ. https://doi.org/10.1016/j.scitotenv.2016.01.020
Ungureanu, V.G., Stanica, A., 2000. Impact of human activities on the evolution of the Romanian Black Sea beaches. Lakes Reserv. Res. Manag. 5, 111–115.
Vadineanu, A., Adamescu, M., Vadineanu, R., Cristofor, S., Negrei, C., 2003. Past and Future Management of Lower Danube Wetlands System : A Bioeconomic Appraisal. J.

Interdiscip. Econ. 14, 415–447.
Vadineanu, A., S. Cristofor & G. Ignat, 1992. Phytoplankton and submerged macrophytes in the aquatic ecosystems of the Danube Delta during the last decade. Hydrobiologia 243/244: 141–146.
van Wesenbeeck, B.K., de Boer, W., Narayan, S., van der Star, W.R.L., de Vries, M.B., 2017. Coastal and riverine ecosystems as adaptive flood defenses under a changing climate. Mitig. Adapt. Strateg. Glob. Chang. 22, 1087–1094. https://doi.org/10.1007/s11027-016-9714-z
Vasiliu, D., Gomoiu, M.T., Boicenco, L., Lazar, L., Timofte, F.., 2010. Chlorophyll a distribution in the Romanian Black Sea inner shelf waters in 2009. Geo-Eco-Marina 16, 19–28.
Verbesselt, J., Hyndman, R., Newnham, G., Culvenor, D., 2010a. Remote Sensing of Environment Detecting trend and seasonal changes in satellite image time series. Remote Sens. Environ. 114, 106–115. https://doi.org/10.1016/j.rse.2009.08.014
Verbesselt, J., Hyndman, R., Zeileis, A., Culvenor, D., 2010b. Phenological change detection while accounting for abrupt and gradual trends in satellite image time series. Remote Sens. Environ. 114, 2970–2980. https://doi.org/10.1016/j.rse.2010.08.003
Verbesselt, J., Zeileis, A., Herold, M., 2012. Near real-time disturbance detection using satellite image time series. Remote Sens. Environ. 123, 98–108. https://doi.org/10.1016/j.rse.2012.02.022
Vespremeanu-Stroe, A., Constantinescu, S., Tatui, F., Giosan, L., 2007. Multi-decadal Evolution and North Atlantic Oscillation Influences on the Dynamics of the Danube Delta Shoreline. J. Coast. Res. ICS2007 Pr, 157–162.
Vörösmarty, C.J., Meybeck, M., Fekete, B., Sharma, K., Green, P., Syvitski, J.P.M., 2003. Anthropogenic sediment retention: Major global impact from registered river impoundments. Glob. Planet. Change 39, 169–190. https://doi.org/10.1016/S0921-8181(03)00023-7
Walling, D.E., Fang, D., 2003. The changing sediment loads of the world's rivers. Glob. Planet. Change 39, 111–126. https://doi.org/10.2478/v10060-008-0001-x
Wang, H., Ge, Z., Yuan, L., Zhang, L., 2014. Evaluation of the combined threat from sea-level rise and sedimentation reduction to the coastal wetlands in the Yangtze Estuary, China. Ecol. Eng. 71, 346–354. https://doi.org/10.1016/j.ecoleng.2014.07.058
Wang, H., Yang, Z., Saito, Y., Liu, J.P., Sun, X., Wang, Y., 2007. Stepwise decreases of the Huanghe (Yellow River) sediment load (1950–2005): Impacts of climate change and human activities. Glob. Planet. Change 57, 331–354. https://doi.org/10.1016/j.gloplacha.2007.01.003
Warrick, J.A., Bountry, J.A., East, A.E., Magirl, C.S., Randle, T.J., Gelfenbaum, G., Ritchie, A.C., Pess, G.R., Leung, V., Duda, J.J., 2015. Large-scale dam removal on the Elwha River, Washington, USA: Source-to-sink sediment budget and synthesis. Geomorphology 246, 729–750. https://doi.org/10.1016/j.geomorph.2015.01.010
Whitehead, P.G., Crossman, J., Balana, B.B., Futter, M.N., Comber, C., Jin, L., Skuras, K., Wade, A.J., Bowes, M.J., Read, D.S., 2013. A cost-effectiveness analysis of water security and water quality: impacts of climate and land-use change on the River Thames system. Philos. Trans. R. Soc. A Math. Phys. Eng. Sci. https://doi.org/10.1098/rsta.2012.0413
Wu, B., Amelung, W., Xing, Y., Bol, R., Berns, A.E., 2018. Iron cycling and isotope fractionation in terrestrial ecosystems. Earth-Science Rev. 190, 323–352. https://doi.org/10.1016/j.earscirev.2018.12.012
Wu, Z., Zhao, D., Syvitski, J.P.M., Saito, Y., Zhou, J., Wang, M., 2020. Science of the Total Environment Anthropogenic impacts on the decreasing sediment loads of nine major rivers in China , 1954 – 2015. Sci. Total Environ. 739, 139653. https://doi.org/10.1016/j.scitotenv.2020.139653
Xeidakis, G.S., Georgoulas, A., Kotsovinos, N., Varagouli, E., 2010. Human interventions and

degradation of the coastal zone of Nestos River Delta , North Aegean Sea , N . Greece 2002, 797–804.
Yang, S.L., Xu, K.H., Milliman, J.D., Yang, H.F., Wu, C.S., 2015. Decline of Yangtze River water and sediment discharge: Impact from natural and anthropogenic changes. Sci. Rep. 5, 1–14. https://doi.org/10.1038/srep12581
Zăinescu, F., Vespremeanu-Stroe, A., Anthony, E., Tătui, F., Preoteasa, L., Mateescu, R., 2019. Flood deposition and storm removal of sediments in front of a deltaic wave-influenced river mouth. Mar. Geol. 417. https://doi.org/10.1016/j.margeo.2019.106015
Zarfl, C., Lumsdon, A.E., Berlekamp, J., Tydecks, L., Tockner, K., 2014. A global boom in hydropower dam construction. Aquat. Sci. 77, 161–170. https://doi.org/10.1007/s00027-014-0377-0
Zibordi, G., Mélin, F., Berthon, J.-F., Talone, M., 2014. In situ autonomous optical radiometry measurements for satellite ocean color validation in the Western Black Sea. Ocean Sci. Discuss. 11, 3003–3034. https://doi.org/10.5194/osd-11-3003-2014
Zeileis, A. (2005). A unified approach to structural change tests based on ML scores, F statistics, and OLS residuals. Econometric Reviews, 24(4), 445−466

The R Project for Statistical Computing, available at https://www.r-project.org/